# Investigating The Role Of Alzheimer's Risk Genes PLCγ2 And PLD3 In Glial Engulfment Using *Drosophila*


Presented

By

**Freya E.T. Storer**

A thesis submitted for the degree of

Doctor of Philosophy

At

Cardiff University

School of Medicine

August 2022

Primary Supervisor: Dr Gaynor Smith

Secondary Supervisor: Prof Julie Williams

Additional Supervisor: Prof Yves-Allain Bardes

This work is dedicated to Toby Panatti for being my rock these past few years, and to my family, Andy Storer, Helen Thomas and Felix Storer for their unconditional support.

## Acknowledgements

I would like to express my humble appreciation to my primary supervisor, Gaynor Smith, who has been an incredible role model, and mentor and provided unprecedented support throughout my project. I would also like to extend my thanks to my adopted supervisor Owen Peters, who has made many invaluable contributions and has always been happy to talk about music. I would equally like to thank my secondary supervisor Julie Williams for her continual support and refreshing insight into my work. I would like to offer special thanks to collaborators Eilish Mackinnon, Rajini Chandrasegaram and Hannah Clarke for their contributions to my thesis in Chapters 3 and 5. My sincere thanks are also extended to past and present members of the UK Dementia Research Institute (UK DRI) fly group, including Leonardo Amadio, Bilal Malik, Daniel Maddison, Dina Fathalla, Freja Sadler, Andrew Lloyd, Louise Townsend, Uroosa Chughtai, Peta Greer, Jasmine Reese, Tim Johnston, Meredith Graham and Lainey Williams. This group has provided a dynamic and welcoming environment to share ideas, expertise and protocols and will remain one of my favourite work experiences. I am also very grateful to my progress monitoring panellists Kerry Thomas and Meng Li for their kind feedback and meaningful suggestions. It has been a pleasure to belong to the wider DRI community and I would like to thank all my colleagues and mentors for their guidance, including Cerys Ballard, Lauren Thorburn, Elena Simonazzi, Emily Maguire, Megan Torvell and Dayne Beccano-Kelly amongst many others. Finally, I would like to thank friends and family, including Toby Panatti, África Fernández, Rosie Harman, Sorcha Sheehy Williams, Fiona Fessey, Jack Pickering, Sinead Morrison, Jasmie Donaldson and many others for their kindness, enthusiasm and endless support on my journey.

## Abstract

Microglial dysfunction is likely to play an important role in the pathogenesis of Alzheimer's disease (AD). Dysregulated glial cells can excessively eliminate neuronal synapses of AD-affected brains and this loss correlates strongly with cognitive decline. Phagocytosis by glia is also important for the efficient clearance of amyloid beta (Aβ) aggregates, which characteristically accumulate during AD progression. Failure to clear aggregates can also negatively impact neuronal survival. Genome-Wide Association Studies (GWAS) and Meta-analyses have identified multiple genetic variants associated with AD progression risk, some of which are enriched in microglia. However, little is known about the function of risk genes in microglia and how they may promote disease. The present project aims to investigate a potential role for these genes in glial engulfment pathways using *Drosophila melanogaster* as a model. My first aim was to complete a reverse candidate knockdown (KD) screen using a robust injury-induced engulfment system. Here, maxillary palps are surgically removed, causing GFP-labelled neurons to degenerate, thereby triggering glial engulfment of neuronal debris, a process which takes up to 5 days. A significant change in the rate at day 1 was recorded as a hit. Knocking down small wing (*sl*) and phospholipase D family member 3 (*Pld3*) saw a significant delay in the rate of engulfment after day 1 and further investigation over multiple time points confirmed a significant partial delay over time. *sl* and *Pld3* are likely to affect glial engulfment through changes in Phosphatidylinositol 4,5-bisphosphate (PIP2) levels, which were found to be significantly decreased in glia after antennal injury. Inversely, Phosphatidylinositol (3,4,5)-trisphosphate (PIP3) levels appeared significantly increased in response to injury. Individual gene KD in PIP reporters saw stark changes in general PIP levels as well as a change in the response after injury, suggesting that the phospholipid pathway has an important part to play in engulfment function. Finally, epistatic experiments revealed that knocking down *PTEN* in *sl* KD flies led to a rescue of the engulfment deficit observed in our initial data. Overall, the present project has identified new elements to be considered in existing pathways known to regulate glial engulfment and sheds light on how AD risk variants could be involved in microglial dysfunction in dementia.

## Contents


**1 Introduction ..... 23**

1.1 Introduction Summary ..... 24

1.2 The Importance of Researching Alzheimer's Disease ..... 25

1.2.1 Treating Alzheimer's Disease ..... 26

1.3 Alzheimer's Disease Pathology: The Story so Far ..... 27

1.3.1 Pathology Manifestation ..... 28

1.3.2 Amyloid Hypothesis ..... 30

1.3.3 Tau Hypothesis ..... 33

1.3.4 Cholinergic Hypothesis ..... 35

1.3.5 Vascular Hypothesis ..... 36

1.3.6 Cellular Phase Hypothesis ..... 37

1.3.7 Risk Gene Hypothesis ..... 38

1.4 Immunity in Alzheimer's Disease Pathology ..... 41

1.4.1 Microglia and Neuroinflammation ..... 42

1.4.2 Neuroinflammation and Cytokine Storms ..... 43

1.4.3 Neuroinflammation and Alzheimer's Risk Genes ..... 44

1.5 Engulfment in Alzheimer's Disease Pathology ..... 46

1.5.1 Synaptic Pruning ..... 46

1.5.2 Dying Cell Removal ..... 48

1.5.3 Aβ Clearance ..... 49

1.6 Lipids in Alzheimer's Disease Pathology ..... 50

1.7 Modelling Alzheimer's Disease ..... 52

1.7.1 Transgenic Mouse Models ..... 52

1.7.2 Cell Culture Models ..... 54

1.7.3 Invertebrate Models ..... 54

1.8 The *Drosophila melanogaster* model ..... 55

1.8.1 *Drosophila* Genetic Tools ..... 56

1.8.2 The *Drosophila* Nervous System ..... 57

1.8.3 Modelling Alzheimer's Disease in *Drosophila* ..... 59

1.8.4 Investigating Alzheimer's risk genes in *Drosophila* ..... 59

1.8.5 *Drosophila* Glial Engulfment Model ..... 60
1.8.6 Engulfment Receptor Intracellular Signalling Pathway ..... 62
1.9 Aims and Objectives ..... 64
**2 Materials & Methods ..... 65**
2.1 Fly Stocks and Husbandry ..... 66
2.2 Genetic Crosses ..... 67
2.3 Neuronal Axotomy ..... 72
2.4 Brain Dissections ..... 73
2.5 Immunohistochemistry ..... 73
2.6 Slide Mounting ..... 74
2.7 Confocal Microscopy ..... 74
2.8 Fluorescence Measurements ..... 75
2.8.1 Olfactory Neuron GFP Analysis ..... 75
2.8.2 Antennal Lobe Analysis ..... 76
2.8.3 Imaging Statistical Analysis ..... 77
2.9 Molecular Biology ..... 78
2.9.1 DNA Extraction ..... 78
2.9.2 Polymerase Chain Reaction ..... 78
2.9.3 Gel Electrophoresis ..... 79
2.9.4 Snap Freezing ..... 80
2.9.5 RNA Extraction ..... 80
2.9.6 cDNA Synthesis ..... 80
2.9.7 Real-time qPCR ..... 82
2.9.8 qPCR Analysis ..... 83
2.9.9 Protein Extraction & Quantification ..... 83
2.9.10 Western Blotting ..... 85
2.9.11 SCope Analysis ..... 86
**3 Biological and Environmental Variability on the Rate of Glial Engulfment 87**
3.1 Introduction ..... 88
3.1.1 Sexual Dimorphism in Glial Biology ..... 88

3.1.2 Temperature Control of Glial Phenotypes ..... 90
3.1.3 Age and Glial Dysfunction ..... 91
3.2 Aims and Objectives ..... 93
3.3 Experimental Design ..... 94
3.4 Results ..... 96
3.4.1 The Rate of Glial Engulfment of Injured Neurons is not Differentially Affected by Sex ..... 96
3.4.2 The Rate of Glial Engulfment of Injured Neurons is not Affected by Temperature ..... 99
3.4.3 The Rate of Glial Engulfment of Injured Neurons Decreases with Age 102
3.5 Discussion ..... 108
3.5.1 Sex Does Not Impact The Rate Of Engulfment ..... 108
3.5.2 Rearing Temperature has a Negligible Impact on Glial Function ..... 109
3.5.3 Glial Engulfment Rate is Highly Dependent on Age ..... 110
3.6 Summary of Key Findings ..... 112
**4 Screening for AD Risk Genes for Roles in Engulfment ..... 113**
4.1 Introduction ..... 114
4.1.1 Alzheimer's Risk Genes ..... 114
4.1.2 Microglia in Alzheimer's Disease ..... 116
4.1.3 Conserved AD Risk Gene Orthologs ..... 117
4.2 Aims and Objectives ..... 119
4.3 Experimental Design ..... 120
4.4 Results ..... 127
4.4.1 Expressing Some AD Risk Gene Orthologues Led to Developmental Phenotypes ..... 127
4.4.2 Knocking Down AD Risk Gene Orthologs Led to Multiple Engulfment Phenotypes ..... 129
4.4.3 Verifying Screen Candidates Yielded Similar Phenotypes ..... 138
4.5 Discussion ..... 141
4.5.1 Several AD Risk Genes are Involved in Glial Engulfment ..... 141

4.5.2 Reverse Candidate Screening ..... 145
4.6 Summary of Key Findings ..... 146
**5 sl and Pld3 Help Regulate Engulfment of Neuronal Debris ..... 147**
5.1 Introduction ..... 148
5.1.1 PLCγ2 Variants Confer Reduced Risk of AD ..... 148
5.1.2 PLD3 May Play A Role In Amyloid Processing And Endosomal Trafficking ... 150
5.2 Aims and Objectives ..... 153
5.3 Experimental Design ..... 154
5.4 Results ..... 155
5.4.1 sl and Pld3 are Enriched in *Drosophila* Primary Phagocytes ..... 155
5.4.2 Knocking down Draper Causes a Glial Engulfment Deficit ..... 157
5.4.3 Knocking Down sl Leads To A Partial Engulfment Deficit ..... 159
5.4.4 Knocking Down Pld3 Leads to a Partial Glial Engulfment Deficit ..... 161
5.5 Discussion ..... 163
5.5.1 Co-Expression Of AD Risk Gene Orthologs In Glia ..... 163
5.5.2 PLD3 and PLCγ2 as Modulators of Phagocytosis ..... 164
5.5.3 Phagocytosis and the Phosphoinositide Pathway ..... 165
5.6 Summary of Key Findings ..... 168
**6 Draper and Phosphoinositide Signalling Converge to Mediate Engulfment 169**
6.1 Introduction ..... 170
6.1.1 Phosphoinositide Signalling ..... 170
6.1.2 Draper and the Phosphoinositide Pathway ..... 172
6.1.3 Models of the Phosphoinositide Pathway ..... 173
6.2 Aims and Objectives ..... 175
6.3 Experimental Design ..... 176
6.4 Results ..... 178
6.4.1 Knocking Down sl May Impact Draper Upregulation In Response To Injury 178
6.4.2 Knocking Down PTEN Rescues sl KD Engulfment Phenotype ..... 180

6.4.3 Phosphoinositide Dynamics Change In Response To Injury ..... 182
6.4.4 Phosphoinositide Changes In Response To Injury Are Modified By Draper And sl ..... 184
6.4.5 Calcium Dynamics Change In Response To Injury ..... 186
6.4.6 Cytosolic $Ca^{2+}$ Elevation In Response to Injury May be Regulated By sl 187
6.5 Discussion ..... 189
6.5.1 Draper Upregulation Is Modified By Small Wing ..... 189
6.5.2 Crossovers Between Draper And Phosphoinositide Signalling ..... 190
6.5.3 Phosphoinositide Dynamics May be Required For Engulfment ..... 191
6.5.4 Calcium Dynamics In Response to Injury ..... 192
6.6 Summary of Key Findings ..... 195
**7 Discussion ..... 196**
7.1 Conclusions and Hypothesis ..... 208
**8 Supplementary Data ..... 210**
8.1 Confirmation of qPCR Primers ..... 211
8.2 Tubulin-driven Pld3 RNAi Expression Led To Significant Gene Knockdown ..... 212
8.3 Tubulin-driven sl RNAi Expression Led To Significant Wing Size Reduction. ..... 214
8.4 Knocking Down shark Leads to an Engulfment Deficit ..... 216
8.5 Calcium Dynamics in LacZ-expressing Flies ..... 218
8.6 Novel Model System to Investigate Amyloid Engulfment in Drosophila ..... 219
**Bibliography ..... 221**

## List of Tables

***Table 1:*** *Treatment of Alzheimer's Disease*……...27
***Table 2:*** *List of ingredients used to prepare fly food*……..67
***Table 3:*** *List of all stocks used in thesis experiments*……..72
***Table 4:*** *List of antibodies used in immunohistochemistry protocols*……75
***Table 5:*** *Confocal imaging settings*……76
***Table 6:*** *Tracing methods for antennal lobe analysis*……...78
***Table 7:*** *Reagents used in PCR reaction*……...79
***Table 8:*** *PCR incubation times and temperatures*……80
***Table 9:*** *List of primers used in PCR reactions*…….....80
***Table 10:*** *List of reagents added to eliminate genomic DNA*……..82
***Table 11:*** *List of reagents added for reverse transcription*……..82
***Table 12:*** *List of reagents added to make SYBR master mix for qPCR*……83
***Table 13:*** *Summary of incubation temperatures and times used at each qPCR stage*……84
***Table 14:*** *Dilution scheme for standard test tube protocol and microplate procedure*……....85
***Table 15:*** *Secondary antibodies used in western blot protocols*……....86
***Table 16:*** *List of stocks used in Chapter 3*…….....96
***Table 17:*** *List of stocks used in Chapter 4*……...127
***Table 18:*** *List of stocks used in Chapter 5*……...155
***Table 19:*** *List of stocks used in Chapter 6*……...178

## List of Figures

***Fig. 1.*** *The Amyloidogenic and Nonamyloidogenic Pathways of APP Processing…*32
***Fig. 2.*** *The Pathological "Tangling" of Tau Protein in Alzheimer's Disease……..…...*35
***Fig. 3.*** *The Frequency and Predicted Function of AD Risk Genes……..…*41
***Fig. 4.*** *Microglia Employ Phagocytic/Endocytic Mechanisms to Perform Essential Homeostatic Functions……..*46
***Fig. 5.*** *The GAL4 tool Allows for Transgene Expression to be Regulated in Time and Space……...*57
***Fig. 6.*** *Drosophila Brains Contain Glial Subtypes with Specific Functions…….……....*58
***Fig. 7.*** *Ablation of GFP-labelled Neurons Triggers Engulfment of Debris……..…*61
***Fig. 8.*** *Mechanistic Diagram of Draper Pathway……....*63
***Fig. 9.*** *Injuring Different Olfactory Organs Triggers the Degeneration of Various Neuronal Networks……*72
***Fig. 10.*** *Example Tracing of Neuronal Structures…….……*76
***Fig. 11.*** *Outline of Chapter 3 experimental design……*94
***Fig. 12.*** *Engulfment Rate Is Unaffected By The Sex……*98
***Fig. 13.*** *Engulfment Rate Is Unaffected By Rearing Temperature……....*101
***Fig. 14.*** *Less neuronal Debris is Cleared with Age…….…*104
***Fig. 15.*** *Knocking down Draper Led to a Delay After 7 Days of Age……..…...*106
***Fig. 16.*** *AD Risk Gene Orthologs…….……..*118
***Fig. 17.*** *Knocking down AD Risk Genes Sometimes Yielded Lethal Phenotypes....*128
***Fig. 18.*** *Knocking down AD Risk Genes Led to LOF/GOF Phenotypes…….…*130
***Fig. 19.*** *Knocking down AD Risk Genes Led to Various Engulfment Phenotypes....*135
***Fig. 20.*** *Verifying Screen Hits Led to Some Repeatable Phenotypes……..…*138
***Fig. 21.*** *Knocking down AD Risk Genes Led to Various Engulfment Phenotypes....*139
***Fig. 22.*** *Schematic of sl and Pld3 Roles in Phospholipid Pathway……..…..*152
***Fig. 23.*** *SCope Analysis of Gene Expression in Glia……....…..*156
***Fig. 24.*** *Knocking Down Draper Causes A Significant Delay In Engulfment….……..*158
***Fig. 25.*** *Knocking Down sl Causes A Delay In Engulfment…….……...*160
***Fig. 26.*** *Knocking Down Pld3 Causes A Delay In Engulfment…….……..*162
***Fig. 27.*** *Knocking Down sl Prevents The Upregulation Of Draper After Injury……...*179

***Fig. 28.*** *Knocking Down Various Factors Alongside sl Led to Multiple Phenotypes..*181
***Fig. 29.*** *Phosphoinositide Dynamics Alter In Response to Injury…….……*183
***Fig. 30.*** *Draper And sl May Mediate PI Dynamics After Injury…….……..*185
***Fig. 31.*** *Cytosolic Calcium increases Immediately After Injury…….……*187
***Fig. 32.*** *Knocking Down sl Prevents $Ca^{2+}$ in Response to Injury…….……*188
***Fig. 33.*** *Proposed Mechanistic Diagram…….……..*209

***Fig. S1.*** *Exon-Spanning Primers Successfully Amplified Target Gene….……...*211
***Fig. S2.*** *qPCR Revealed Significant Knockdown of Pld3…….……..*212
***Fig. S3.*** *Knocking Down sl using RNAi Successfully Reduced Wing Size….……*215
***Fig. S4.*** *Knocking Down shark alongside LacZ Led to an Engulfment Deficit.……*217
***Fig. S5.*** *Cytosolic Calcium Changes in LacZ-expressing Flies…….…....*218
***Fig. S6.*** *QF2-driven Aβ Expression Led to Quantifiable Pathology……...…..…..*219

## List of Abbreviations

***A****a – amino acids*

*Aβ – amyloid beta protein*

*ABCA7 – ATP-binding cassette sub-family A member 7*

*Abi – Abelson interacting protein*

*ABI3 – Abi gene family member 3*

*AC – apoptotic cell*

*ACE – angiotensin-converting enzyme*

*Ach – acetylcholine*

*AD – Alzheimer's Disease*

*ADAM10 – ADAM Metallopeptidase Domain 10*

*ADAMTS4 – a disintegrin and metalloproteinase with thrombospondin motifs 4*

*ADI – Alzheimer's Disease International*

*AICD – APP intracellular domain*

*AKT1 – PKB/Protein Kinase B*

*ALPK2 – Alpha Kinase 2*

*Amph – Amphiphysin*

*ANK1 – ankyrin 1*

*AP-1 – adaptor protein complex 1*

*APH1B – Aph-1 Homolog B*

*APOE – apolipoprotein*

*APOE-ε4 – apolipoprotein epsilon 4 isoform*

*APP – Amyloid precursor protein*

*APP-CTF83, αCTF - APP at the C-terminal fragment 83*

*ARF6 – GTPase ADP ribosylation factor 6*

*ASD – autism spectrum disorders*

*ATP – adenosine-triphosphate*

*Atg1 – Autophagy related 1*

*AXL – AXL Receptor Tyrosine Kinase*

***B****ACE1 – beta-site APP-cleaving enzyme 1*

*BAI1 – brain-specific angiogenesis inhibitor 1*

*BBB – the blood-brain barrier*

*BCA – Bicinchoninic Acid*

*BCR – B cell receptor*

*BDNF – brain-derived neurotrophic factor*

*BDSC – Bloomington Drosophila stock centre*

*BIN1 – Bridging integrator-1*

*BLNK – B Cell Linker*

*Bru1 – Bruno 1*

*BSA – Bovine serum albumin*

*Bsk – Basket*

*BTK – Bruton's tyrosine kinase*

***C****1q – complement component 1q*

*C3 – complement component 3*

*C3a – complement component 3a*

*C3b – complement component 3b*

*CAA – cerebral amyloid angiopathy*

*Cas9 - CRISPR-associated protein 9*

*CASS4 – Cas scaffolding protein family member 4*

*CBF – cerebral blood flow*

*CCH – chronic cerebral hypoperfusion*

*CD11b – cluster of differentiation molecule 11b*

*CD2AP – CD2-associated protein*

*CD33 – Cluster of differentiation 33, also known as SIGLEC3*

*CDE – clathrin-dependent endocytosis*

*cDNA – complementary DNA*

*ced-6 – adaptor protein*

*CELF1 – CUGBP ELav-like family member 1*

*ChAT – choline acetyltransferase*

*CIE – clathrin-independent endocytosis*

*CIN85 – Cbl interacting protein of 85kDa*

*cindr – CIN85 and CD2AP related*

*CLNK – Cytokine Dependent Hematopoietic Cell Linker*

*CLU – Clusterin precursor*

*CNS – central nervous system*

*CNTNAP2 – contactin-associated protein 2*

*COVID-19 – Coronavirus disease 2019*

*CR1 – Complement receptor 1*

*CR3 – complement receptor 3*

*CRISPR – Clustered regularly interspaced short palindromic repeats*

*CUGBP – CUG triplet repeat, RNAi binding protein*

*CSMD3 – CUB and Sushi multiple domains 3*

*Csw – corkscrew*

***D**AG – Diacylglycerol*

*DAMP – danger-associated molecular patterns*

*dAP-1 – Drosophila adaptor protein complex 1*

*DIOPT – DRSC Integrative Orthologue Prediction Tool*

*DGK – DG-kinase*

*dk – donkey*

*Dm – Drosophila melanogaster*

*DOR – Diabetes and obesity regulated*

*DNA – Deoxyribonucleic acid*

*dNTPs – Deoxynucleotide triphosphates*

*DPA – day(s) post-ablation*

*dJNK – Drosophila Jun N-terminal kinases*

*drk* – downstream receptor kinase

*DRSC – Drosophila RNAi screening database*

*DSHB – Developmental studies hybridoma bank*

***E**DTA – Ethylenediaminetetraacetic acid*

*EGQO – End-labelled Fluorescence-Quenched Oligonucleotide*

*EGF – Epidermal Growth Factor*

*ELISA - enzyme-linked immunosorbent assay*

*EPHA1 – Eph receptor A1*

*Eph – Eph receptor tyrosine kinase*

*EOAD – Early-onset Alzheimer's disease*

*eQTL - expression quantitative trait loci*

*ER – endoplasmic reticulum*

*ERK – extracellular signal-regulated kinases*

*ESCRT – endosomal sorting complexes required for transport*

*Esr1 - Estrogen Receptor 1*

*EtOH – ethanol*

*Ets98B – Ets at 98B*

*EWAS – Epigenome-wide associated studies*

***F**AD – Familial Alzheimer's disease*

*Fak – Focal adhesion kinase*

*FAM47E – family with sequence similarity 47 member E*

*FcR – immunoglobulin-like receptor*

*FcγR – immunoglobulin-like receptor γ*

*FDA - Food and Drug Administration*

*FERMT2 – Fermitin family member 2*

*Fit1 – Fermitin 1*

*FTD – frontotemporal dementia*

*fwe - flower*

***G**ABA - Gamma-aminobutyric acid*

*GAL4 – galactokinase 4*

*GD – VDRC P-element RNAi stocks*

*gDNA – genomic DNA*

*GDP – Gross domestic product*

*GEF – guanine-nucleotide exchange factor*

*GFP – Green fluorescent protein*

*GOF – fain-of-function*

*GOI – gene of interest*

*GPCR – G-protein-coupled receptors*

*Grp1 – general receptor for phosphoinositides, isoform 1*

*GSK3β – glycogen synthase kinase 3β*

*gt – goat*

*GWAS – Genome-wide association studies*

***H**asp – Hig-anchoring scaffold protein*

*hbs – hibris*

*HESX1 – homeobox 1*

*HLA – Human leukocyte antigen*

*HLA-DRB1/5 – HLA class II histocompatibility antigen, DRB1-5 beta chain*

*hr – hour*

*HS3ST1 – Heparan sulfate glucosamine 3-O-sulfotransferase 1*

*Hs3st-A – Heparan sulfate 3-O sulfotransferase-A*

*h-Tau – hyperphosphorylated Tau*

***I**FN-1 – interferon type 1*

*IL1RAP – Interleukin-1 receptor accessory protein precursor*

*INPP5D – Phosphatidylinositol 3,4,5-trisphosphate 5-phosphatase 1*

*InR – Insulin-like receptor*

*IP3 – Inositol trisphosphate*

*IP3R – IP3 receptor*

*iPSC - Induced pluripotent stem cells*

*IQCK - IQ Motif Containing K*

*IRF3 – Interferon regulatory factor 3*

*ITAM – Immunoreceptior tyrosine-based activation motif*

***J**NK – Janus kinase*

*Jra – Jun-related antigen*

***K**AT8 – K(lysine) acetyltransferase 8*

*Kay - Kayak*

*KD – knockdown*

*KK – VDRC phiC31 RNAi Stocks*

*KO – knockout*

***O**crl – Oculocerebrorenal syndrome of Lowe*

*OR2B2 – Olfactory Receptor Family 2 Subfamily B Member 2*

*OR85e – odour receptor 85e*

*ORN – olfactory receptor neurons*

***L****AMP1 – Lysosomal-associated membrane protein 1*

*lap – like-AP180*

*LD – linkage disequilibrium*

*LOF – loss-of-function*

*LpR2 – lipophorin receptor 2*

*LPS – lipopolysaccharide*

*LOAD – Late-onset Alzheimer's disease*

***M****AP – microtubule-associated protein*

*MAP1 – microtubule-associated protein 1*

*MAP2 – microtubule-associated protein 2*

*MAPT – microtubule-associated phosphoprotein Tau*

*Mbc – myoblast city*

*MC – multiple comparisons*

*mCD8 – mouse cluster of differentiation 8*

*MCI – mild cognitive impairment*

*MEGF10 – Multiple epidermal growth factor-like domains protein 10*

*MEK/MAPK – Mitogen-activated protein kinase kinase*

*MerTK – MER Proto-Oncogene, Tyrosine Kinase*

*Mg – magnesium*

*MKK – mitogen-activating kinase kinase 4*

*MM – master mix*

*mTor – mammalian target of rapamycin*

*MRI – Magnetic resonance imaging*

*mRNA – messenger RNA*

*ms – mouse*

*MS4A6A – Membrane-spanning 4-domains subfamily A member 6A*

*MSA – Multiple system atrophy*

*MSN – misshapen*

*MTM – myotubularin-1*

***N****aCl – Sodium chloride*

*NC – nitrocellulose*

*NF – nuclease-free*

*NF-kB – Nuclear factor kappa B*

*NFTs - neurofibrillary tangles*

*NK – natural killer cells*

*NMDA - N-methyl-D-aspartate receptor*

*NME8 – NME family member 8*

*NMJ – the neuromuscular junction*

*NOTCH – Neurogenic locus notch homolog protein*

*NPC – neural progenitor cells*

*NXPY - NXPY (Asparagine, X, Proline, Tyrosine)*

***O**R85e – odour receptor 85e*

*ORN – olfactory receptor neuron*

***P**A – phosphatidic acid*

*PAGE – Polyacrylamide gel electrophoresis*

*PAMP – pathogen-associated molecular patterns*

*PBS – phosphate Buffered Saline*

*PC – phosphatidylcholine*

*PCR – polymerase chain reaction*

*PDK1 – phosphoinositide-dependent kinase 1*

*PFA – paraformaldehyde*

*PH – pleckstrin homology*

*PHF – paired helical filaments*

*PH-GFP – pleckstrin homology domain-green fluorescent protein*

*PI – phosphatidylinositols*

*PI3K - phosphoinositide 3-kinase*

*PICALM – Phosphatidylinositol binding clathrin assembly protein*

*PIP2 - Phosphatidylinositol 4,5-bisphosphate*

*PIP3 - Phosphatidylinositol (3,4,5)-trisphosphate*

*PKC – Protein kinase C*

*PLCγ2 – 1-Phosphatidylinositol-4,5-bisphosphate phosphodiesterase gamma-2*

*PLD1 – Phospholipase D1*

*PLD2 – Phospholipase D2*

*PLD3 – Phospholipase D3*

*PLD4 – Phospholipase D4*

*PNS – peripheral  nervous system*

*PRR – pattern recognition receptors*

*PRS – polygenic risk scores*

*PS – polystyrene*

*PSEN 1 – Presenilin 1*

*PSEN 2 – Presenilin 2*

*PTB – phosphotyrosine-binding domain*

*PTEN – Phosphatase and tensin homolog*

*PTK2B - Protein Tyrosine Kinase 2 Beta*

*PTMs – post-translational modifications*

*PTx – phosphate-buffered saline-triton Xion 10x*

*Puc – puckered*

***q**PCR – real-time polymerase chain reaction*

***R**ac1 – Ras-related C3 botulinum toxin substrate 1*

*Raf – rapidly accelerated fibrosarcoma*

*Ras – Rat sarcoma virus*

*Ras-MAPK – Ras/mitogen-activated protein kinase*

*rb – rabbit*

*repo – reversed polarity*

*RNA – ribonucleic acid*

*RNAi – ribonucleic acid interference*

*RNAse – ribonuclease*

*RNAseq – RNA sequencing*

*ROS – reactive oxygen species*

*rRNA – ribosomal RNA*

*RT – room temperature*

*RTK – receptor tyrosine kinase*

*Rya-r44F – ryanodine receptor 44F*

***s**APP-α – Soluble APP fragment cleaved by α-secretase*

*sAPP-β – Soluble APP fragment cleaved by β-secretase*

*SB – squishing buffer*

*SF - straight filaments*

*SH2 - Src Homology 2*

*SHIP1 – Src homology 2 (SH2) domain-containing inositol polyphosphate 5-phosphatase 1*

*SF – straight filaments*

*SGZ – subgranular zone*

*shark – SH2 ankyrin repeat kinase (syk family)*

*sl – small wing*

*SLC24A4 - Solute Carrier Family 24 Member 4*

*SNP – single nucleotide polymorphism*

*SOCE – store-operated $Ca^{2+}$ entry*

*SORL1 – Sortilin Related Receptor 1*

*Src – protein kinase*

*STAT92E – Signal transducer and transcription activator 92E*

*SVEP1 – sushi, von Willebrand factor type A, EGF and pentraxin domain containing 1*

*SVZ – subventricular zone*

*Syk - Spleen tyrosine kinase*

***T**ACE – TNF-α converting enzyme*

*TBK1 – Tank-binding kinase 1*

*TBS – TRIS-buffered saline*

*TBS-T - 0.1% Tween-20 in TBS*

*TIM-4 – T-cell immunoglobulin mucin protein 4*

*TLR – toll-like receptor*

*TLR4 – toll-like receptor 4*

*TOR – Target of Rapamycin*

*TORC1 – Tor complex 1*

*TNF-α – tumour necrosis factor-α*

*TP53Np1 – Tumor protein p53-induced nuclear protein 1*

*TRAF4 – TNF receptor-associated factor 4*

*TREM2 – Triggering receptor expressed on myeloid cells 2*

*TRiP – Transgenic RNAi Project*

*TRIP4 – Thyroid Hormone Receptor Interactor 4*
*TYK – tyrosine kinase*
*TYROBP – tyrosine kinase binding protein*

***U**AS – upstream activation sequence*
*UAS-RNAi - UAS-Ribonucleic acid interference*
*UK DRI – United Kingdom Dementia Research Institute*

***V**DRC – Vienna Drosophila Resource Centre*
*VHAD – Vascular Hypothesis of Alzheimer's Disease*

***W**B – Western blot*
*WD – Wallerian degeneration*
*WHO – World Health Organisation*
*WWOX – WW domain-containing oxidoreductase*

***Y**XXI – Tyrosine, X, X, Isoleucine*
*YXXL – Tyrosine, X, X, Leucine*

***Z**CWPW1 – Zinc finger CW-type PWWP domain protein 1*
*zyd – zydeco*

*2D – two-dimensional*
*3D – three-dimensional*

# 1 Introduction

## 1.1 Introduction Summary

Alzheimer's Disease (AD) is characterised by widespread atrophy, neuroinflammation and an accumulation of misfolded proteins in the brain. With disease progression, neurodegeneration exacerbates, resulting in cognitive decline and disabling dementia. Familial early-onset AD (EOAD) and "sporadic" late-onset AD (LOAD) constitute the 2 main forms of AD. EOAD is an autosomal dominant disorder resulting from a mutation in a few known genes, however, the genetics of LOAD is more complicated. To date, LOAD research has focused on the amyloid (Hardy and Allsop 1991) and Tau (Hernández and Avila 2007) hypotheses, but with a growth in new technologies, researchers have made further contributions to the genetic underpinnings of LOAD. Since 1993, scientists have identified genetic risk factors associated with disease onset (Corder et al. 1993). Various institutions have collaborated to identify >40 genetic loci in which single nucleotide polymorphisms (SNPs) alter an individual's risk of developing AD (Jonsson et al. 2013; Lambert et al. 2013; Cruchaga et al. 2014; Sims et al. 2017; Aikawa et al. 2018; Bertram and Tanzi 2019; Kunkle et al. 2019; Zhao et al. 2019; Bellenguez et al. 2022). Moreover, rarer genetic variants involved in lipid metabolism have also been identified. Some SNPs confer with reduced risk of disease progression, including the inheritance of the *PLCγ2-P522R* variant (Sims et al. 2017). Interestingly, risk gene expression is enriched in microglia, including that of *PLCγ2*. Such convergence of AD-associated genes with glial lineages is common, promoting microglia as prominent regulators of disease (Sims et al. 2017). However, the specific role of AD risk variants in microglial function is currently being investigated (Hansen et al. 2018; Gabandé-Rodríguez et al. 2020).

Microglia are innate immune cells of the central nervous system (CNS), performing key functions such as engulfment of pathogens, neuronal debris and misfolded proteins (Fu et al. 2014; Heneka et al. 2015; Gabandé-Rodríguez et al. 2020). Microglia in the context of AD are considered both "friend and foe" with both protective and damaging phenotypes recorded (Mandrekar-Colucci and Landreth 2010). Phagocytic mechanisms appear altered in AD (Fiala et al. 2005; Fu et al. 2014), leading to the reduced clearance of amyloid (Aβ) plaques or damaged neurons (D'Andrea et al. 2004; Pan et al. 2011) and the over-elimination of synapses (Hong et al. 2016; Rajendran and Paolicelli 2018). *Drosophila melanogaster* is an excellent

model to investigate the cellular and molecular foundations of disease and has glial cells (Freeman and Doherty 2006) analogous to microglia known as ensheathing glia (Logan and Freeman 2007; Doherty et al. 2009). Ensheathing glial phagocytosis is regulated by the Draper pathway (MacDonald et al. 2006; Ziegenfuss et al. 2008; MacDonald et al. 2013; Evans et al. 2015; Fullard and Baker 2015; Lu et al. 2017; Purice et al. 2017; Hilu-Dadia et al. 2018), homologous to human MEGF10, mouse Megf10 and *C-Elegans* Ced-1, which have all been implicated in phagocytosis (Zhou et al. 2001; Scheib et al. 2012; Iram et al. 2016). The present project harnesses the powerful genetics of *Drosophila* to investigate the overlap between GWAS-identified risk genes and glial function in a disease context, to further our knowledge in the field and inform novel therapeutic practices.

## 1.2 The Importance of Researching Alzheimer's Disease

AD is an irreversible, neurodegenerative disorder which was first identified by Alois Alzheimer in 1906 and is one of the most financially demanding diseases in the Western world with an estimated global annual cost of US$ 1 trillion (Hippius and Neundörfer 2003; Breijyeh and Karaman 2020). It is the leading cause of dementia, causing up to 70% of cases, alongside vascular dementia, and frontotemporal dementia. As of 2020, approximately 50 million people worldwide have suffered from AD (Breijyeh and Karaman 2020). In the UK alone, 1 in 14 people over the age of 65 are likely to be affected, increasing to 1 in 6 people over the age of 80 (Dementia UK report | Alzheimer's Society 2022). More than 520,000 patients currently suffer from this disorder in the UK, contributing to ca. 35 million patients worldwide, with roughly 7 million new cases each year. Due to improved healthcare and demographic ageing, AD is not restricted to Western populations – in fact over 50% of dementia cases are being reported in low- and middle-income countries, according to a World Alzheimer report from 2021. This is set to rise at an exponential rate compared to high-income countries. Even the COVID-19 pandemic is believed to have influenced the prevalence of dementia due to the shortage of frontline workers and carers (World Alzheimer Report 2021 | Alzheimer's Disease International (ADI)). The total number of cases is predicted to rise to 60 million by 2030 and with it, a vast economic burden. The worldwide estimated cost of dementia in 2015 was $818 billion, representing 1.09% of global GDP – the cost considers informal, social, and medical care. And in 2015, funding for research amounted to only a 13$^{th}$ of the funding raised for cancer research

(World Alzheimer Report 2015 | Alzheimer's Disease International (ADI)). Although awareness of dementia is growing and more resources are being directed to the cause, our understanding of dementia, in particular AD, is still young. Early diagnosis is near impossible and current methods rely on specific symptoms, a cognitive assessment and invasive blood tests to rule out other causes. A definite diagnosis is only possible in a post-mortem examination of the brain tissue and treatments are scarce. Further research needs to be made to establish effective methods of diagnosis, therapies, and a basic understanding of pathology.

### 1.2.1 Treating Alzheimer's Disease

Treatments of AD and other dementias are very limited, with no existing cure. It is considered beneficial to maintain healthy lifestyle choices, consume a balanced diet and engage in mental and physical exercises, helping to prevent disease (Dhana et al. 2020). Such changes may reduce the risk of AD, however, there is still little evidence supporting it and most research points to genetics being a major driver of pathology (Bellenguez et al. 2022). Current medications cannot stop or reverse the progress of disease, however, some treatments improve symptoms with available drugs targeting different aspects of disease presentation (**Table 1**). Common solutions counteract neurotransmitter disturbances, such as cholinesterase inhibitors which improve symptoms of confusion and memory loss (Yiannopoulou and Papageorgiou 2020). However, more recent treatments have been designed to target Aβ aggregation and plaques. In June 2021, Aducanumab (Aduhelm™) received accelerated approval from The Food and Drug Administration (FDA), the first treatment to address disease hallmarks. Having reached clinical trials the treatment proves promising, the antibody demonstrates the successful removal of Aβ plaques in some patients and is likely to improve symptoms (Sevigny et al. 2016). Further studies are being pursued before the drug reaches the open market to validate its efficacy in relieving symptoms (Sevigny et al. 2016). Although current treatments are sparse, our growing understanding of disease pathology helps to inform novel therapies such as Aducanumab and may pave the way for potential individualised therapeutic frameworks in the future (Yiannopoulou and Papageorgiou 2020).

| Treatment Name: | Details: | Function: |
|---|---|---|
| Aducanumab | *Anti-Aβ Antibody* | *Reduces Aβ plaques.* |
| Donepezil | *Cholinesterase Inhibitor* | *Improves symptoms of confusion and memory loss.* |
| Memantine | *NMDA Receptor Antagonist* | *Improves symptoms of confusion and cognition.* |
| Galantamine | *Acetylcholinesterase Inhibitor* | *Improves symptoms of cognition and memory loss.* |
| Rivastigmine | *Cholinesterase Inhibitor* | *Improves symptoms of movement and memory loss.* |
| Antipsychotics | *Various* | *Improves symptoms of psychosis.* |
| Mental Health Counselling | *Psychological Support* | *Improves symptoms of mental health.* |
| Music and Art Therapy | *Memory Stimulation* | *Improves symptoms of depression, anxiety, and memory loss.* |
| Speech and Language Therapy | *Speech Therapy* | *Improves symptoms of speech and swallowing difficulties.* |

***Table 1. Drugs and Therapies Approved for the Treatment of Alzheimer's Patients.*** *Medication references:* (Donepezil: MedlinePlus Drug Information; Memantine: MedlinePlus Drug Information; Galantamine: MedlinePlus Drug Information; Rivastigmine: MedlinePlus Drug Information; Dementia | SLT | Expert providers of speech and language therapy throughout the UK.; Aducanumab-avwa Injection: MedlinePlus Drug Information).

## 1.3 Alzheimer's Disease Pathology: The Story so Far

AD can be divided into 2 types, based largely on genetic characteristics and the age of disease presentation. Familial or EOAD, responsible for 1-5% of cases, is largely driven by the inheritance of certain genetic factors. Affected individuals often develop symptoms before the age of 60, however, some patients exhibit them as young as 30 years old (Reitz et al. 2020). EOAD is defined as an autosomal dominant familial form of AD and attributed to mutations in amyloid precursor protein (APP) and/or presenilin 1 and 2 (PSEN1/2) (Waring and Rosenberg 2008; Burns and Iliffe 2009; Ballard et al. 2011). Mutations in these genes generally lead to the production of Aβ protein, which

may accumulate and aggregate to form extracellular plaques (Turner et al. 2003; Stokin et al. 2008). Sporadic or LOAD (hereafter referred to as AD) accounts for the remaining 95% of AD diagnoses and does not exhibit autosomal-dominant inheritance (Reitz et al. 2020). However, thanks to GWAS, common genetic risk factors continue to be identified (Bellenguez et al. 2020). A principal genetic factor includes the inheritance of the epsilon 4 allele of apolipoprotein (APOE-ε4) (Strittmatter et al. 1993; Mahley et al. 2006). APOE-ε4, and other associated genes, are collectively described as AD risk genes, with variant inheritance conferring an increased or decreased likelihood of developing the disease (Lambert et al. 2013). Moreover, AD has also been attributed to changes in the epigenome, with several independent epigenome-wide association studies (EWAS) of separate cohorts suggesting overlapping methylation signals in loci such as *ANK1, RPL13, RHBDF2 and CDH23* (de Jager et al. 2014; Lord and Cruchaga 2014; Lunnon et al. 2014; CT et al. 2016; Lardenoije et al. 2019; Li et al. 2020). Environmental risk factors are also important, with an increased risk associated with traumatic head injuries (Ramos-Cejudo et al. 2018), mental health disorders (Richmond-Rakerd et al. 2022) and hypertension (Lennon et al. 2019). Overall, AD presents as a complex, multi-factorial condition merging both genetic and environmental factors, proving it a genuine challenge to grasp and interpret.

### 1.3.1 Pathology Manifestation

AD is characterised by a progressive decline in cognitive ability, leading to the loss of core brain functions such as memory and comprehension (Huang and Mucke 2012). Post-mortem AD brains reveal widespread atrophy and the deposit of cytotoxic proteins, accompanied by excessive synapse loss, inflammatory markers and oxidative stress (Yasojima et al. 1999; Smith 2002; Tönnies and Trushina 2017). As the disorder progresses patients are known to suffer from aberrant memory loss, confusion, severe cognitive impairment, linguistic disability and mental health problems such as anxiety and depression (Backman et al. 2004; Burns and Iliffe 2009; Ballard et al. 2011). Physical functions, such as hand-eye coordination, are gradually lost, ultimately leading to an individual's inability to self-care. Ageing patients become increasingly vulnerable and usually die as a result of external factors, such as infection

and not due to AD itself. Depending on the severity of symptoms, a patient's life expectancy is predicted to be 3-9 years after diagnosis. A patient's quality of life is severely impacted and symptoms can have a devastating effect on them and their family.

The trajectory of disease is often divided into four stages based on specific symptoms, with a progressive decline of cognitive functions. Stage 1 (or pre-dementia) presents with milder symptoms such as forgetfulness, which are often misinterpreted as general signs of ageing and stress (Waldemar et al. 2007). Such difficulties can be observed up to 8 years in advance of clinical diagnosis. Short-term memory loss and emotion-associated symptoms such as apathy are collectively termed mild cognitive impairment (MCI) and transition the divide between ageing and dementia (Morris et al. 2001). Memory is particularly affected since brain regions such as the hippocampus are heavily targeted during disease progression (Rao et al. 2022). Stage 2 or early dementia is more discernible, often leading to some degree of diagnosis. Symptoms include further memory complications and language difficulties, characterised by declining fluency and a shrunken vocabulary (Förstl and Kurz 1999). In rarer cases, this is supplemented with perception issues (agnosia) or difficulty in executing movements (apraxia) (Yesavage et al. 1993). These symptoms already impact the independence of the patient, however, at Stage 3 or moderate AD, the effect is far more severe. Oral communication diminishes with a limited vocabulary and reading and writing skills curtail (Woodward 2013). Long-term memory becomes affected, defined by an inability to recognise close friends or family members. Other symptoms include neuropsychiatric changes, such as outbursts of emotion and aggression (Lyketsos et al. 2011). This combined with an existing decline in fine motor skills and confusion can put the patient at substantial risk. In the final Stage 4 or advanced AD, the patient is heavily reliant on external care, from either family or professional staff. Individuals often lose the ability to communicate, forming short sentences with simple, unrelated words (Woodward 2013). Their ability to move is severely inhibited, condemning them to bed, unable to care for themselves, leading to loss of independence, and the exacerbation existing of mental health conditions such as depression. Despite external care, the patient is increasingly vulnerable and can die as a result of infection or self-neglect (Förstl and Kurz 1999). This 4-stage process describes a gradual and brutal decline of function, resulting in pain and suffering for

the patient and their family (Smith 2002). Defining the cause(s) of AD is an ongoing ambition, however, some competing hypotheses exist that explain the cause and progression of the disease.

### 1.3.2 Amyloid Hypothesis

AD is often referred to as a proteopathy, or protein misfolding disease, due in part to a prominent hypothesis in the field. A large body of literature suggests that abnormally folded extracellular Aβ plaques are a central event in AD aetiology (Musiek and Holtzman 2015). The amyloid theory is strongly supported by data from rare autosomal dominant forms of AD and postulates that specific modulators of Aβ synthesis result in the secretion of abnormally folded Aβ proteins, giving rise to neurodegeneration and other symptoms (Selkoe and Hardy 2016). APP is a transmembrane protein found in healthy neurons, with functions in neuronal growth, survival and post-injury repair (Turner et al. 2003). It is encoded by the *APP* gene, which exists as multiple isoforms ranging in length from 639 to 770 amino acids in humans (Matsui et al. 2007). The Aβ region of the protein, located in the membrane-spanning domain is exposed after APP is cleaved (Zheng and Koo 2006). APP can be processed in nonamyloidogenic (neuroprotective) and amyloidogenic (neurodegenerative) pathways, dependent on the secretase enzymes engaged in the reaction. In the nonamyloidogenic pathway, proteolytic enzyme α-secretase cleaves APP in the middle, clipping the Aβ region and releasing soluble APP-fragments (sAPP-α). Activated γ-secretase then cleaves APP at the C-terminal fragment 83 (APP-CTF83, αCTF), releasing the APP intracellular domain (AICD) and P3 into the extracellular space. In the amyloidogenic pathway, β-secretase cleaves APP to produce the soluble fragment sAPP-β, thereafter cleaved by γ-secretase to produce Aβ40, Aβ42, and AICD (**Fig. 1**) (Pająk et al. 2016). In AD, proteolytic β- and γ-secretase (of which PSEN1/2 are two subunits) act together to cleave APP into “stickier” fragments, 39-43 amino acids (aa) in length. Abnormal Aβ fragments are released and aggregate, forming plaques composed of oligomeric or fibrillary Aβ peptides. These can interfere with normal signalling processes and promote the degeneration in neurons (Hardy and Allsop 1991; Turner et al. 2003; Hooper 2005). Aβ plaques in AD brains consist primarily of Aβ42, which has two extra

residues at the C-terminus compared to Aβ40 (Gu and Guo 2013). Aggregation of the longer peptide can lead to earlier and more severe cognitive decline (Findeis 2007).

Most familial forms of AD can be attributed to mutations in APP and presenilins 1 and 2 (Hooper 2005; Waring and Rosenberg 2008). The amyloid hypothesis was cemented when early evidence correlated the location of the APP gene on chromosome 21 with AD-like symptoms in trisomy 21 (Down Syndrome) patients (Lott and Head 2005). Sequencing the APP locus in familial early-onset AD patients identified common and rare missense mutations that indeed led to AD (Hooli et al. 2012). The rare inheritance of a mutant APP gene virtually guarantees the development of AD in affected individuals according to some research (Bekris et al. 2010; TCW and Goate 2017). Certain mutations merely affect the balance of Aβ42 levels compared to levels of Aβ40, which alters the levels of plaque formation (Borchelt et al. 1996). Equally, recent findings discovered a coding variant APP A673T, which reduces the risk of disease progression (Kokawa et al. 2015). Furthermore, inheriting the apolipoprotein epsilon 4 isoform (APOE-ε4) is considered a significant genetic risk factor, further supporting the Aβ hypothesis (Strittmatter et al. 1993; Pearson et al. 2007). APOE-ε4 is an isoform of APOE family proteins that traditionally promote Aβ breakdown which is ineffective compared to other alleles. Inheritance further contributes to the build-up of Aβ aggregates (Polvikoski et al. 1995). It is also known that Aβ may selectively build up in the mitochondria of AD neurons, which can lead to metabolic dysfunction and oxidative stress in neurons (Chen and Yan 2006). Finally, the recent development and approval of Aducanumab (Aduhelm™), a therapeutic antibody which targets Aβ plaques, promotes the importance of the amyloid hypothesis in treatment design (Sevigny et al. 2016). However, the relevance of the hypothesis is increasingly questioned with advances in disease-related knowledge (Morris et al. 2014). Post-mortems show the presence of Aβ plaques in cognitively normal individuals, suggesting a weaker correlation between protein deposition and cognition (Price et al. 2009). The role of Aβ in non-diseased brains remains a mystery and continues to be studied, questioning the biochemical resonance of the hypothesis (Chen et al. 2017). Importantly, the hypothesis has driven a bias in preclinical modelling of AD, with poorly explained pathological heterogeneity and comorbidities associated with the disorder. Although a prominent hypothesis for 25 years, how the

Aβ peptide exactly contributes to disease is still not certain and it is essential to invite novel theories and extend our research beyond Aβ.

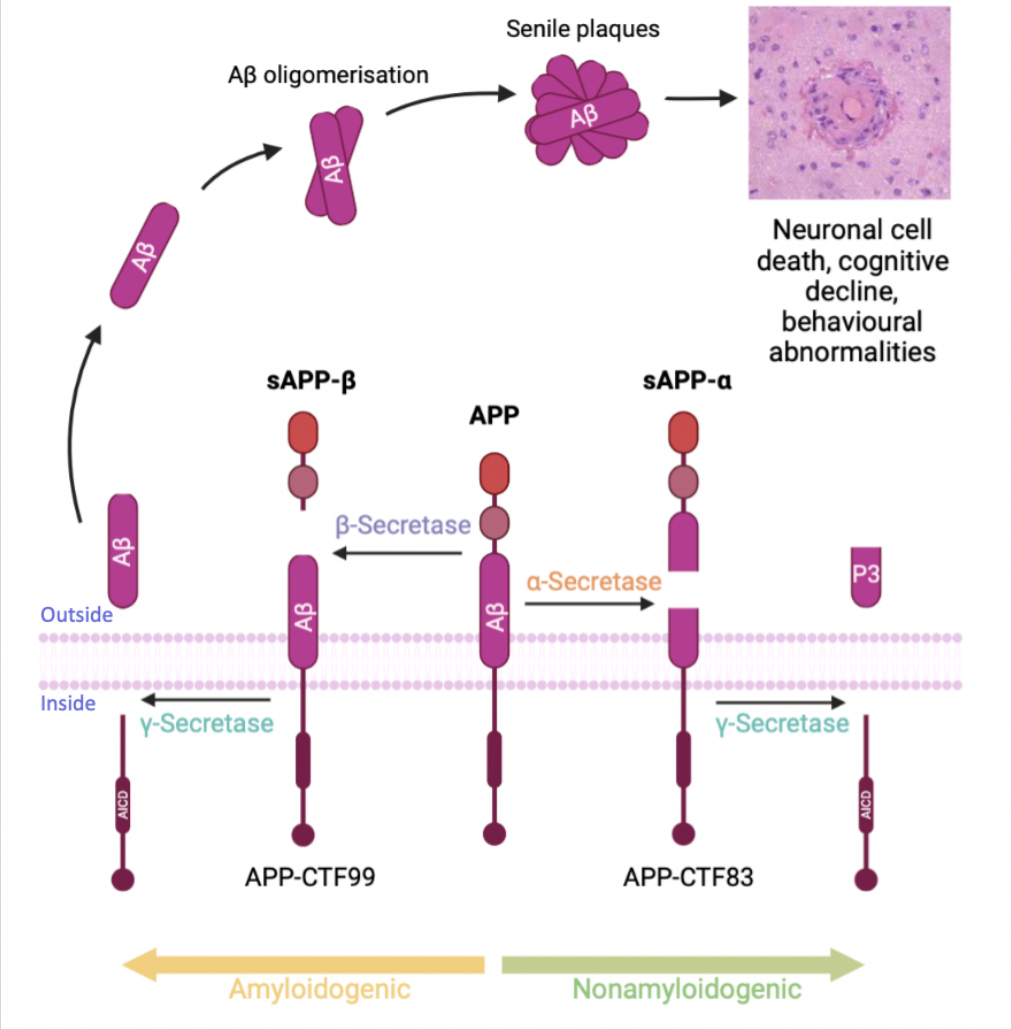


***Fig. 1. The Amyloidogenic and Nonamyloidogenic Pathways of APP Processing.*** *A diagram representing the different mechanisms in which APP is processed and senile plaques are formed. APP crosses the plasma membrane (light pink) and is processed by two distinct pathways determined by the type of secretases engaged. In the nonamyloidogenic pathway (green arrow), α-secretase cleaves the Aβ region (dark pink) of APP, releasing sAPP-α. γ-secretase then cleaves the C-terminus APP-CTF83, producing AICD (dark purple) and P3 fragments (dark pink). In the amyloidogenic pathway (yellow arrow), β-secretase cleaves APP, releasing Aβ from soluble fragment sAPP-β. γ-secretase then cleaves APP-CTF99, generating AICD and Aβ40/42. Aβ42 oligomers aggregate to form senile plaques leading to Aβ deposition in the brain. Histology image credit:* (Wong et al. 2006)*, made in ©BioRender - biorender.com.*

### 1.3.3 Tau Hypothesis

An additional factor that gives AD the label of proteopathy is the observed hyperphosphorylation and misfunction of Tau protein in various cells (Brunden et al. 2009). Tauopathy is characterised by the hyperphosphorylation of Tau leading to prominent intracellular accumulations which are proposed to initiate disease (Lee et al. 2001; Hernández and Avila 2007). Hyperphosphorylated Tau (h-Tau) pairs more readily with other Tau proteins forming threads and eventually long neurofibrillary or gliofibrillary tangles in neuronal cell bodies and glia respectively (Goedert et al. 1991; Goedert and Jakes 2005). Tau is a microtubule-associated phosphoprotein (MAP) coded by a single gene on chromosome 17, with isoforms generated through alternative splicing of its pre-mRNA (A et al. 1989; M et al. 1989). Usually highly soluble, Tau's primary function when phosphorylated is to promote the assembly of tubulin to form microtubules, essential for protein and nutrient transport in healthy neurons (Wang and Mandelkow 2015). The structure of the neuron is dependent on cytoskeletal proteins, with the shape and function of the axon particularly dependent on microtubule maintenance. Normal adult Tau contains 2-3 moles phosphate per mole of Tau protein, an amount 3-4 times higher in hyperphosphorylated versions, which depresses its biological activity. The "stickier" Tau polymerises into paired helical filaments (PHF) which can mix with straight filaments (SF) forming insoluble aggregates (A et al. 1989; M et al. 1989). Tau protein interacts with tubulin through a site located at the C-terminal end, which is highly acidic. Phosphorylation can neutralise the positively charged terminus, leading to a conformation change and detachment (Fischer et al. 2009; Jho et al. 2010). H-Tau readily dissociates from microtubules in axons, causing microtubule disintegration and freeing misfolded Tau to form neurofibrillary tangles (NFTs) (**Fig. 2**). The combination of tangles and destabilised microtubules leads to the disruption of essential processes, affecting nutrient and molecular transport in the cell (Wang and Mandelkow 2015). This can first result in abnormal neuronal communication and eventually neuronal cell death (Guo et al. 2017).

Transient h-Tau exists in normal brains during development, anaesthesia and hypothermia, however, in AD, h-Tau can sequester normal Tau and other microtubule-associated proteins 1 and 2 (MAP1 and MAP2) resulting in detrimental consequences (MD et al. 1975; I et al. 1986). Tauopathies are often caused by dysregulation of messenger RNA (mRNA) splicing and the resulting accumulation of a particular isoform of Tau, or by a genetic mutation (Goedert and Jakes 2005). Equally, post-translational modifications (PTMs) other than phosphorylation, such as methylation, ubiquitination and acetylation can impact Tau's binding affinity (Iba et al. 2013; Park et al. 2018b). High levels of ubiquitinated Tau and aggregation promoted by lysine acetylation have been recorded in AD studies (Spillantini and Goedert 2013). Tau pathology is also associated with aberrant activation and mobilisation of transposable elements, contributing to the genomic instability of neurons (Guo et al. 2018). Overall, Tauopathy is intrinsically associated with AD patients and models and is a leading cause of dementia however, similarly to Aβ, Tau does not appear wholly causative, therefore exploring other avenues which could contribute to pathology is essential (Iqbal et al. 2010).

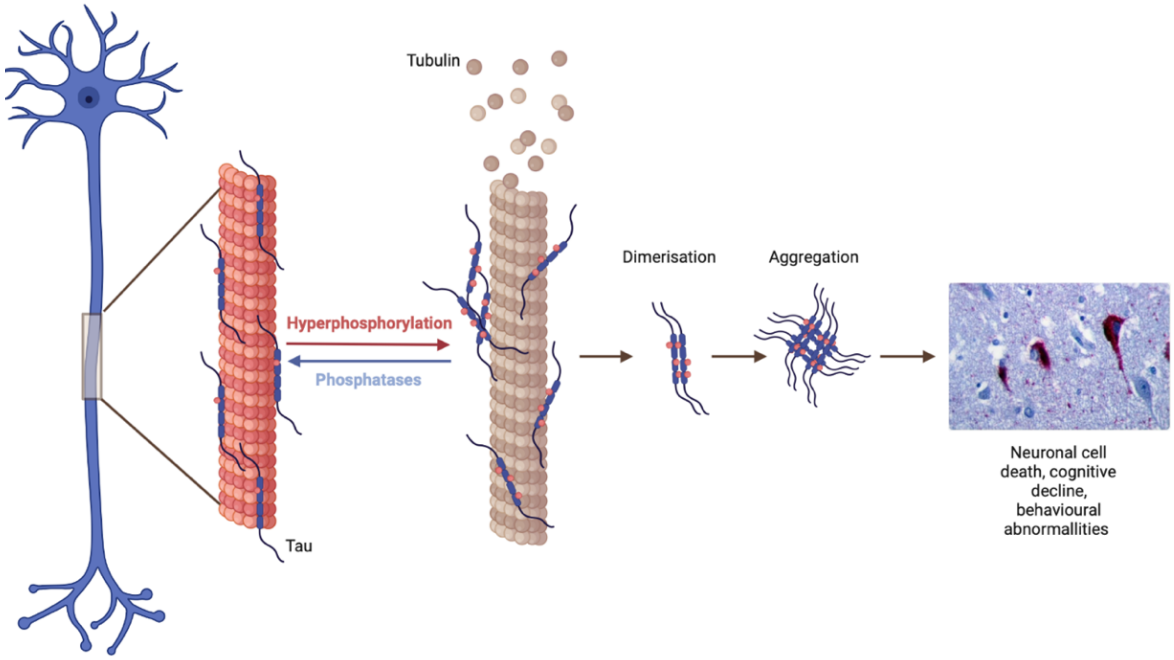

***Fig. 2. The Pathological "Tangling" of Tau Protein in Alzheimer's Disease.*** *A diagram representing the build-up of hyperphosphorylated Tau leading to aggregation and the formation of NFTs. The phosphorylation (represented by a pink spot) of Tau protein (dark blue) leads to Tau's dissociation from microtubules leading to the destabilisation of the microtubule-Tau complex. Hyperphosphorylated Tau protein into dimers and higher-order aggregates. Image credit: Patho [CC BY-SA 3.0], made in ©BioRender - biorender.com.*

### 1.3.4 Cholinergic Hypothesis

An old, although often overlooked hypothesis is the cholinergic hypothesis (Francis et al. 1999). It proposes that elements of pathology are caused by reduced acetylcholine synthesis. Disrupting this process can lead to the degeneration of cholinergic neurons in the forebrain resulting in the loss of synapses and neurotransmission in various brain areas, including the cerebral cortex (Ferreira-Vieira et al. 2016). This is supported by biochemical investigations of AD patient biopsy tissue. These show that neurotransmitter pathologies occur early in the course of the disease, with the uniform reduction of presynaptic markers of the cholinergic system (Francis et al. 1993). Post-mortem and antemortem studies have identified a distinct reduction in acetylcholine (Ach) production, and a reduction of choline acetyltransferase (ChAT) in AD patients of advanced age (Perry et al. 1978; Wilcock et al. 1982; Sims et al. 1983; Francis et al. 1993; DeKosky et al. 1996). Some serotonergic and noradrenergic markers are affected, however, markers of dopamine gamma-aminobutyric acid (GABA), or somatostatin are not altered. Post-mortem studies at later stages of disease see the involvement of other neurotransmitter systems including GABA and others above (Rossor et al. 1982; Rossor and Iversen 1986; Francis et al. 1987; Lowe et al. 1990). Brain dissections have shown the resulting atrophy of the brain extending to multiple regions, including the cholinergic nucleus basalis of Meynert (DeKosky et al. 1996).

Cholinergic abnormalities investigated using animal models include alterations to choline transport, acetylcholine synthesis and release, nicotinic and muscarinic receptor expression, and even axonal transport, all advancing cognitive impairments of the brain (Caccamo et al. 2006; Castro et al. 2009; Shirey et al. 2009). Some research also links cholinergic abnormalities to behavioural defects such as depression (Palmer et al. 1988; Chen et al. 1996). Evidence suggests that cholinergic abnormalities arise early in disease progression, leading to initial cognitive decline, however, it is unclear whether there is a causal relation (Neary et al. 1986). The hypothesis defines a major contributing process to the deterioration in cognitive function seen in patients with AD and highlights a pathway with the potential for therapeutic intervention. Most current therapies indeed target this process by substituting levels of acetylcholine or inhibiting cholinesterases have been mediocre, only able to treat disease symptoms, instead of inhibiting its progress (Hunter et al. 1989; Thompsem et al. 1991; Massoulié 2002; Pohanka 2011).

### 1.3.5 Vascular Hypothesis

Some epidemiological studies reveal that pre-existing cardiovascular conditions could be important contributors to the onset of AD, a notion referred to as the Vascular Hypothesis of Alzheimer's Disease (VHAD) (Love and Miners 2016; Scheffer et al. 2021). VHAD was proposed after a study subjected ageing rodents to chronic brain hypoperfusion and recorded the aggravations of AD-related pathology (Sopala and Danysz 2001; Paris et al. 2004). The hypothesis was supported by obvious changes in cerebral perfusion and metabolic deficits in AD patients (Verfaillie et al. 2015). Findings elaborate that hypertension, diabetes and obesity (which disrupt normal cerebral hemodynamics) can increase the risk of developing AD by 6% according to the Lancet report (Torre 2004). Sustained vascular disruption can bring about local ischemia, hypoxia and chronic cerebral hypoperfusion (CCH). In turn, this can exacerbate elements of AD pathology such as inflammation, oxidative stress, Aβ and Tau accumulation (Torre 2004; Kapasi and Schneider 2016; Love and Miners 2016; Francula-Zalinovic and Iskra 2018; Scheffer et al. 2021). Over time this builds a significant impact on neuronal health, eventually leading to widespread neurodegeneration and atrophy, implying an additive or even synergistic effect.

To disrupt cerebral blood flow, VHAD can provoke the dysfunction of the neurovascular unit – the blood-brain barrier (BBB), a wall of specialised endothelial cells supported by glial cells, such as microglia and astrocytes (Sweeney et al. 2018). The BBB is essential to maintaining brain homeostasis, by regulating the entrance of neurotoxins and pathogens as well as enabling the supply of nutrients. Damage to the brain vasculature or BBB breakdown is associated with early cognitive decline and these can serve as early markers of disease (Montagne et al. 2015; de Wit et al. 2017; Torre et al. 2018; Scheffer et al. 2021). Cerebral hemodynamics have attracted the attention of neuroradiologists as disturbed cerebral blood flow (CBF) could serve as a valuable prediction tool for the onset of AD, enabling the stratification of patients' risk (Kapasi and Schneider 2016; Torre 2018; Livingston et al. 2020; Scheffer et al. 2021). The most apparent anatomical signs include cerebral amyloid angiopathy (CAA) and vascular morphological changes and degenerative changes in affected parts of the brain (Miyakawa 2010). VHAD may help to prevent the early onset of disease, by adopting a healthier and more balanced lifestyle however newer insights imply its potential for therapeutic interventions (Torre 2004; Love and Miners 2016; Francula-Zaninovic and Nola 2018; Livingston et al. 2020; Scheffer et al. 2021). As much as the vascular hypothesis stands on its own, it is also relevant to other contemporary theories.

### 1.3.6 Cellular Phase Hypothesis

So far, hypotheses propose a linear, neuron-centric cascade of events which lead to AD pathology, however, emerging evidence implicates the importance of other cells of the brain (Benarroch 2013; Jones et al. 2015; Shi and Holtzman 2018; Heneka 2020). The relatively new cellular phase hypothesis posits a complex phase of cellular interactions, choreographed by feedback and feedforward responses between microglia, astrocytes and vasculature (de Strooper and Karran 2016). It tears away from backbone hypotheses and questions how initially benign processes such as inflammation can ultimately become chronic, resulting in disease. A ‘biochemical’ phase initiates the process, characterised by the accumulation and aggregation of misfolded proteins, including Aβ and h-Tau (Walker and Jucker 2015). Proteopathic

stress triggers local cells of the brain, eliciting responses in neurons and recruiting immune cells (Labbadia and Morimoto 2015), beginning the initial cellular phase. Proteopathies are reversible and manageable, sometimes going unnoticed for years, however, the theory proposes that defective clearance of aggregates or Tau could result in irreversible damage (de Strooper and Karran 2016). Many clearance mechanisms have been identified as potential targets, with genetic risk factors such as APOE-ε4, PICALM and CLU believed to affect Aβ clearance (Verghese et al. 2013; Zhao et al. 2015). Similar mechanisms, such as synaptic pruning are also likely to become dysfunctional leading to disruptions in neuronal circuitry and synaptic plasticity – the main cellular phase of AD (Palop and Mucke 2010; de Strooper and Karran 2016). Diverse evidence exists to support many changes in neuronal circuitry during AD and that this is mediated by hyperactive glia which over-eliminate synapses and can directly induce neuronal apoptosis (Bossers et al. 2010; Salter and Beggs 2014). Central players of the cellular phase include astrocytes (responsible for synapse maintenance in the hippocampus) (Bushong et al. 2002) and microglia (plaques clearance and proinflammatory cytokines) (Lawson et al. 1990). However, oligodendrocytes are likely to contribute to neuropathology, unable to support neurons in remyelination processes (Pelvig et al. 2008). Although very promising, the theory is in its infancy and requires modern approaches to cement core concepts. Progress has already been achieved using single-cell sequencing methods which have mapped transcriptional changes in different cell types of the mouse hippocampus (Zeisel et al. 2015) and the human cortex (Darmanis et al. 2015), contributing to a growing body of research addressing the underlying genetic mechanisms and causal relationships in disease progression.

### 1.3.7 Risk Gene Hypothesis

Since >95% of idiopathic AD cases do not exhibit autosomal-dominant inheritance, many efforts have been made to find common genetic variants. The heritability of non-Mendelian AD is estimated at around 60-80% with the inheritance of ε4 polymorphism in the *APOE* locus being the most common risk factor, possessed by 40-80% of patients (Gatz et al. 2006; Lambert et al. 2013). Individuals carrying one *APOE-ε4* allele are three times more likely to develop symptoms, increasing to 8- to 12-fold in

homozygous carriers (Corder et al. 1993). Technical advances in genetic research and the recruitment of larger sample sizes have enabled the discovery of new variants and susceptibility loci (Lambert et al. 2013; Cuyvers and Sleegers 2016). GWAS have uncovered gene variants with considerable population frequency, but low disease penetrance. Such studies typically use microarray genotyping to test the association of a single trait such as disease diagnosis, or biometric phenotypes (e.g., height), with the frequency of common single nucleotide polymorphisms (SNPs), across the entire genome (Novikova et al. 2021b). These SNPs are selected because they represent a group of genetic variants frequently inherited together as a haplotype block of high linkage disequilibrium (LD), spanning over a specific region of the genome. Conclusively, SNPs associated with traits by GWAS, inform us of regions, or haplotypes associated with the disease (Uffelmann et al. 2021). Intriguingly, most SNPs are non-coding, with predicted small effect sizes of the identified associations, except for the *APOE* locus (Novikova et al. 2021b). Post-GWAS annotation allows for the selection of causal variants, largely based on the proximity of SNPs to functional genes (Watanabe et al. 2017). Predictions accommodate positional and expression quantitative trait loci (eQTLs), and sometimes chromatin interaction mappings, which provide gene-based, expression and pathway information (Watanabe et al. 2017).

To date, large GWA studies, investigating diverse AD patient cohorts, have identified common genetic variants that modulate disease susceptibility in >40 genomic loci implicated in several functional pathways (**Fig. 3**) (Jonsson et al. 2013; Lambert et al. 2013; Sims et al. 2017; Aikawa et al. 2018; Hansen et al. 2018; Bertram and Tanzi 2019; Jansen et al. 2019; Kunkle et al. 2019; Sleegers and van Broeckhoven 2019; Sims et al. 2020; Bellenguez et al. 2022; Mol et al. 2022). Some are associated with increased risk (e.g., *BIN1, CR1*) whilst others confer decreased risk (e.g., *PLCγ2, CLU*) of AD pathology (Zhao et al. 2019; Sims et al. 2020). Equally, next-generation sequencing has revealed rare variants with higher penetrance such as *TREM2* (Korvatska et al. 2015). Some genes such as *SORL1* and *ABCA7*, are found to harbour both common and rare variants associated with risk (Bellenguez et al. 2017; de Roeck et al. 2019).

Growing evidence from EWAS also implicates epigenetic modifications could play a role in AD. Most studies utilised methylation arrays to assess levels of DNA methylation in cortical brain tissue from donors with varying degrees of AD pathology. Independently these studies have identified >30 genomic loci that show robust differential DNA methylation in disease. Loci such as *ANK1, RHBDF2, HOXA3, CDH23* and *RPL13* have been consistently reported as an overlap between studies (de Jager et al. 2014; Lunnon et al. 2014; Watson et al. 2016; Gasparoni et al. 2018; Smith et al. 2018; Lardenoije et al. 2019; Smith et al. 2019; Li et al. 2020a).

Overall, GWAS and EWAS gradually reveal the complex genetic architecture of AD. Identifying common genetic variants has paved the way for prediction tools such as polygenic risk scoring (PRS), which calculates the risk of disease progression in AD patient cohorts based on their genetics, enabling early detection and the accurate triaging of relevant risk genes (Baker and Escott-Price 2020). Pathway-enrichment analyses also allow us to confirm the involvement of amyloid/Tau pathways emphasising the crosstalk between different theories (Bellenguez et al. 2020). Although these findings are rich in novel information, a large part of genetic risk and functional implications remains unexplained. Functional mapping, from the identification of specific genes to causal cell types, is critical to further our understanding of disease aetiology and the production of disease-modifying treatments. Extending GWAS studies to multiple ancestries and coupling this with follow-up functional studies will help deepen our understanding of AD and provide mechanistic insight. Already, some studies have identified enrichment of AD risk alleles in myeloid cells. eQTLs and RNAseq data have revealed a selective expression pattern of many genes in macrophages, such as microglia (Raj et al. 2014; Huang et al. 2017; Finucane et al. 2018; Novikova et al. 2021a; Novikova et al. 2021b). This has been formative in the growing interest in the role of the immune system in AD and nominated multiple candidate causal genes which function within the endolysosomal compartment of these cells (Novikova et al. 2021a).

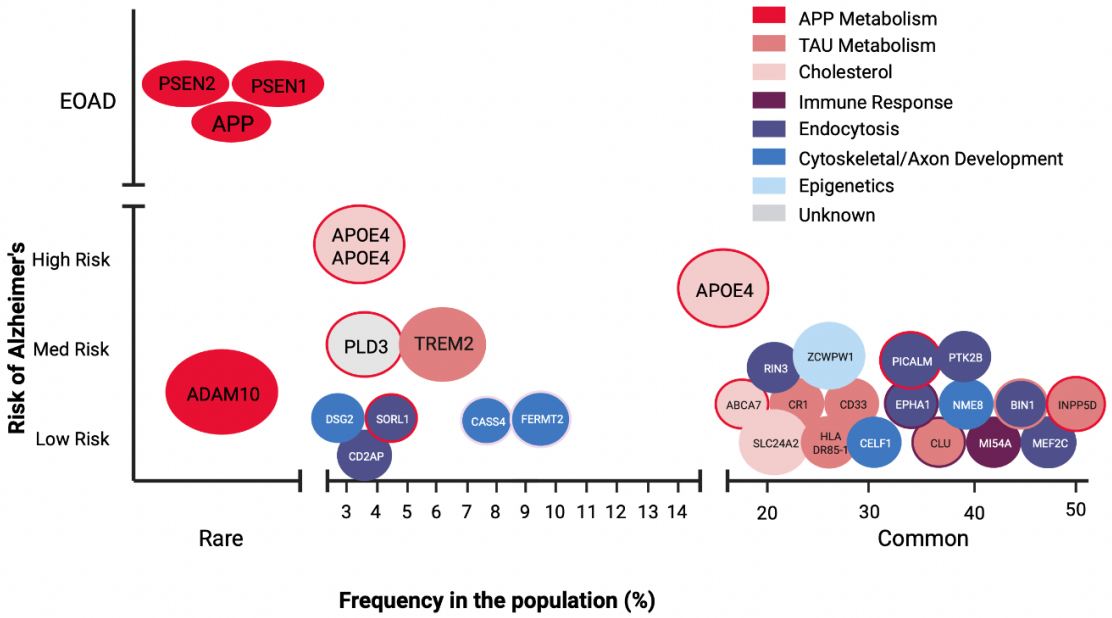


***Fig. 3. The Frequency and Predicted Function of AD Risk Genes.***

*A plot representing the frequency and predicted function of GWA identified genes associated with AD risk. Predicted functions are denoted by colour, with the potential for genes to behave in APP metabolism (red), TAU metabolism (medium pink), cholesterol maintenance (light pink), immune response (purple), endocytosis (dark blue), cytoskeletal and axon development (medium blue), epigenetics (light blue) and unknown functions (grey). Some genes are predicted to be involved in more than one process therefore are outlined with a second colour. Adapted from* (Karch and Goate 2015)*, made in ©BioRender - biorender.com.*

## 1.4 Immunity in Alzheimer's Disease Pathology

Current research into the role of novel AD risk genes is largely limited to their function in neuronal networks of the brain (Karch and Goate 2015). Primary research comprises genetic manipulations in mono-cell cultures and mouse models, however, contemporary approaches aim to address the cumulative effects of multiple risk genes in a wider range of CNS cells.

### 1.4.1 Microglia and Neuroinflammation

An important cell group, recently attributed to the progression of AD and other neurodegenerative disorders, is known as neuroglia; non-neuronal cells, forming a large fraction of the mammalian brain and found in the CNS and peripheral nervous system (PNS) (Jäkel and Dimou 2017). Consisting of microglia, astrocytes and oligodendrocytes, these lineage cells provide physical and metabolic support to neuronal networks (Jäkel and Dimou 2017). With recent developments, microglia have become a significant research focus and therapeutic target in dementia (Rajendran and Paolicelli 2018). Microglia are important immune cells of the CNS, and are especially concentrated in areas such as the hippocampus, basal ganglia, substantia nigra, and olfactory cortex (Benarroch 2013). These surveying macrophages play crucial roles in CNS tissue maintenance, injury response and defence against infection (Rajendran and Paolicelli 2018). The microglial membrane is home to many receptors, including neurotransmitter receptors, cytokine, and chemokine receptors amongst others (Helmut et al. 2011), which sit at the top of diverse signalling pathways. Even at rest, highly motile microglia scan their environment, searching for pathogens, cellular debris and misfolded proteins (Nayak et al. 2014). Most microglial functions are inhibited in AD and presumed protective, however, some research suggests that they could be harmful, accelerating neurodegeneration (Perry and Teeling 2013; Kempuraj et al. 2016). In addition, transcriptional profiling of microglial gene expression implies that they may switch between states during AD, pertaining to the discussion that the microglial pro-inflammatory state correlates with increased neurodegeneration (Block et al. 2007; von Bernhardi 2007; Mandrekar-Colucci and Landreth 2010; Joshi et al. 2014; Lopategui Cabezas et al. 2014; Li and Barres 2017; Hansen et al. 2018; Vilalta and Brown 2018; Whitelaw 2018). Depletion or dysfunction of microglia could therefore contribute to pathologies observed in neurodegenerative disorders, including AD.

### 1.4.2 Neuroinflammation and Cytokine Storms

Inflammation is often a consequence of changes to CNS homeostasis, from local neuronal death to an accumulation of misfolded proteins (Rock and Kono 2008). Microglia are highly sensitive, with a diversity of pattern recognition receptors (PRRs) at the membrane, including scavenger receptors and toll-like receptors (TLRs). These bind numerous ligands, such as danger-associated molecular patterns (DAMP) and pathogen-associated molecular patterns (PAMP) (Kigerl et al. 2014). During the progression of AD, microglial activation results in the production of proinflammatory cytokines, including tumour necrosis factor-alpha (TNF-α), interleukin (IL)-1, -6, -12 and -18 and subsequent phagocytic function (Wang et al. 2018). Chronic exposure to inflammation induces the conversion of microglial phenotypes from proinflammatory (M1) to anti-inflammatory (M2). Recent evidence demonstrates the upregulation of pro-inflammatory cytokines may promote both neuroprotection and neurodegeneration (Wang et al. 2015b; Kinney et al. 2018). IL-1β, released by microglia is suggested to protect against AD, since it promotes phagocytic mechanisms to clear Aβ and simultaneously enhances α-cleavage of APP, through the upregulation of the TNF-α converting enzyme (TACE) (Tachida et al. 2008). TNF-α is a multifunctional proinflammatory cytokine responsive to both intrinsic and extrinsic signals (Gruss and Dower 1995). Many lines of evidence already suggest an association between TNF-α and the onset of AD, with a significant rise in the cytokine levels in AD post-mortem brains and cerebrospinal fluid (McGeer and McGeer 2002). Crucially, TNF-α mRNA transcripts have been observed to significantly increase before the accumulation of Aβ in mouse model brains (Janelsins et al. 2008) and found in excess around Aβ plaques (Wang et al. 2015b). Furthermore, pro-inflammatory cytokines; IL-6, IL-12/IL-23 and IL-18 have also been associated with AD phenotypes. Increased levels of cytokines have been observed in the cerebrospinal fluid of AD-affected individuals (Chen et al. 2018) and appear to reduce amyloid pathology when knocked down (Wang et al. 2015b).

Conversely, elevated levels of anti-inflammatory cytokines such as IL-10 were recorded in APP mouse brains and suggested to exacerbate Aβ accumulation (Chakrabarty et al. 2015). In addition, IL-10 deficiency in microglia alleviates Aβ deposition in APP/PSEN1 mice, additionally rescuing synaptic toxicity and memory impairment (Guillot-Sestier et al. 2015). The immediate and prolonged inflammatory response observed in recent studies suggests a compelling hypothesis for the role of innate immunity in promoting and preventing AD progression, however further evidence exists that correlates other pathways with disease.

### 1.4.3 Neuroinflammation and Alzheimer's Risk Genes

AD-associated risk genes appear selectively expressed in microglia relative to other brain cells, which remains a major supporting argument for the involvement of immunity in AD (Srinivasan *et al.*, 2016; Hansen, Hanson and Sheng, 2018). Genes with a high enrichment score include *ABI3, INPP5D, MAF, PILRA, PLCγ2, RIN3,* and *TREM2*, particularly in microglia of hippocampal tissue (Darmanis et al. 2015; Zhang et al. 2016b; Hodges et al. 2021). Ongoing work suggests that risk genes overlap in important microglial pathways as immune receptors (*TREM2, MS4A4A, HLA-DGA1 & CD33*), signalling intermediates (*PLCγ2, PLD3, PTK2B & IPP5D*) or effectors (*ABI3 & EPHA1*) (Hodges et al. 2021). Some genes are already linked to core pathogenic immune responses and cell mechanisms such as complement components (*CR1 & CLU*) or cytoskeletal machinery (*ABI3, EPHA1 and FERMT2*) (Hodges et al. 2021). Among well-studied receptors, Triggering Receptor Expressed On Myeloid Cells 2 (*TREM2)* is highly expressed in microglia, particularly when confronted with inflammatory stimuli (Sims *et al.*, 2017). Multiple studies have shown that *TREM2* inhibits the production and secretion of inflammatory cytokines released by microglia, suppressing an inflammatory response usually observed in AD (Heneka et al. 2014). TREM2 is activated by damage-associated signals, such as sphingomyelin, phosphatidylserine and phosphatidylethanolamine, which are often presented by damaged or dying cells (Daws et al. 2003; Wang et al. 2015c; Shirotani et al. 2019). Studies have revealed a functional variant of R47H in the *TREM2* locus, resulting in reduced TREM2 activity coupled with increased AD susceptibility (Korvatska et al. 2015; Cheng-Hathaway et al. 2018). Loss of TREM2 function in microglia may

therefore lead to systemic inflammation and neuronal death. Equally, *Cluster of differentiation 33 (CD33),* belonging to a family of immunoglobulin-like lectins are expressed among macrophages and myeloid progenitor cells and is also thought to modulate cell-cell interactions and cytokine secretion in AD pathogenesis (Crocker and Redelinghuys 2008).

Crucially, consolidating knowledge about microglia and AD risk genes has presented novel therapeutic possibilities, through the manipulation of microglia to promote a protective response to AD. TREM2 activating antibodies (agonistic monoclonal antibodies) AL002c are entering Phase I clinical studies with some successful results (Wang et al. 2020). Ongoing research aims to understand the role of risk genes and their respective variants in immune function, with many already suggested to operate in phagocytic and/or endocytic mechanisms.

## 1.5 Engulfment in Alzheimer's Disease Pathology

Originally, the presumed function of microglia in the CNS was to eliminate infectious agents, however, their role in tissue maintenance extends to the sculpting of neuronal circuits by engulfment and removal of unwanted neurons, synapses or cytotoxic proteins (Li and Barres 2017; Herzog et al. 2019). The dysregulation of phagocytic and/or endocytic mechanisms in microglia is likely one of the major drivers of disease (**Fig. 4**).

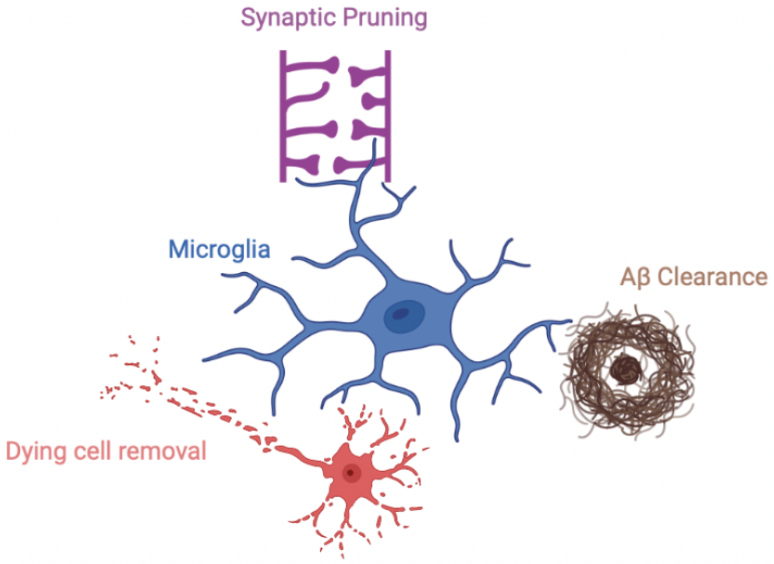


***Fig. 4. Microglia Employ Phagocytic/Endocytic Mechanisms to Perform Essential Homeostatic Functions.*** *A diagram representing the essential functions involving engulfment pathways that can go unregulated during AD. Microglia (blue), can adopt hyperactive phenotypes where synapse elimination (purple) is dysregulated, and hypoactive phenotypes where the removal of dying/dead neurons (red) and Aβ plaque clearance (brown) is affected. Adapted from* (Brown and Neher 2014), *made in ©BioRender - biorender.com*

### 1.5.1 Synaptic Pruning

During CNS development, microglial phagocytosis is essential for the pruning of excessive synapses and refining of neuronal networks, contributing to learning and memory (Lichtman and Colman 2000; Schafer and Stevens 2013; Galloway et al.

2019). Microglia employ multiple signalling pathways including complement pathways to effectively prune synaptic connections (Stephan et al. 2012). Complement-mediated synapse loss is likely to occur in AD through initiated phagocytic mechanisms (Hong et al. 2016). Briefly, the classical complement system labels targets with complement component 1q (C1q), which catalyses the production of C3 convertase, subsequently cleaving C3 to produce proinflammatory mediators C3a, C3b (Stevens et al. 2007; Noris and Remuzzi 2013). Opsonin C3b thereafter initiates phagocytic mechanisms via complement receptors on macrophage membranes, such as the CR1. Incidentally, CR1 variants are also associated with AD risk (Craig et al. 2005; Zhu et al. 2020). The presence of complement activation in AD has been well established, however, the genetic drivers of this pathology have only recently been identified (Afagh et al. 1996; Yasojima et al. 1999; Harold et al. 2009; Lambert et al. 2013; Morgan 2018).

Synapse loss is an early occurrence in AD progression and correlates strongly with cognitive decline (Terry et al. 1991; Jack et al. 2010). Inhibition of complement components such as C1q, C3 and CR3 has demonstrated reduced synapse loss in mammalian AD models (Fonseca et al. 2004; Hong et al. 2016; Shi et al. 2017). Equally, TREM2 is required for microglial-mediated synaptic elimination during development according to a mammalian study (Filipello et al. 2018). Other immune cells, such as astrocytes have also been known to perform important phagocytic functions in circuit refinement (Chung et al. 2015; Allen and Eroglu 2017). Crucially, astrocytes were reported to mediate phagocytosis of synapses through Multiple epidermal growth factor-like domains protein 10 (MEGF10) signalling at the membrane, such that genetic ablation led to a lack of synaptic refinement in the developing visual system (Chung et al. 2013). Astrocytes are likely to prune synapses in the adult CNS as well, due to discoveries made in dissociated cultures and cerebral organoids (Zhang et al. 2016b; Sloan et al. 2017). AD risk genes also confer functional roles in astrocytes, such that APOE-mediated phagocytosis is determined by C1q accumulation at the synapse (Chung et al. 2016). Taken together, excessive synapse elimination is likely mediated by brain macrophages and complement activation, and this significantly accelerates cognitive symptoms (Stephan et al. 2013).

### 1.5.2 Dying Cell Removal

As tissue develops, microglia are also required to remove apoptotic neurons and oligodendrocytes that are often overproduced (Galloway et al. 2019). Dying cells are continuously produced during development and tissue homeostasis (Trapp et al. 1997; Marín-Teva et al. 2004; Takahashi et al. 2005). Here, numerous receptors have been identified as being required for apoptotic cell clearance, including TREM2, CD11b, BAI1 and TIM-4 (Takahashi et al. 2005; Peri and Nüsslein-Volhard 2008; Wakselman et al. 2008; Mazaheri et al. 2014). Recent work has also identified a novel microglia subtype specifically employed during the removal of dying cells and oligodendrocytes in white matter, leading to the hypothesis that microglia acquire distinct phenotypes required for region-specific phagocytosis (Li et al. 2019c). Later in adulthood, microglia equally continue to survey the brain, promoting synaptic plasticity and phagocytosing invading pathogens and apoptotic cells (Nimmerjahn et al. 2005). Clearance of neural progenitor cells (NPC) debris is reliant on TAM family receptors such as MER Proto-Oncogene Tyrosine Kinase (MerTK) and AXL Receptor Tyrosine Kinase (AXL) (Fourgeaud et al. 2016). With age, microglia undergo senescence, exhibiting dysfunction, either through impaired debris clearance or excessive synaptic elimination (Greenwood and Brown 2021). Increased levels of complement protein C1q have been observed in aged brains, with cognitive decline inhibited in C1q KO mice (Stephan et al. 2013). Moreover, C1q is a ligand for scavenger protein Megf10 which mediates the clearance of apoptotic cells by astrocytes in the developing mammalian brain (Iram et al. 2016). The invertebrate ortholog of MEGF10 (Draper) is also studied in the context of engulfment, with research proposing that related mechanisms generate molecular memory that primes macrophages in an inflammatory response (Weavers et al. 2016). In mammals, neurons are more prone to damage with age as myelin sheaths degenerate, further contributing to cognitive decline (Peters et al. 2000; Morrison and Baxter 2012). Higher amounts of myelin debris have been evidenced in mouse brains and are normally cleared by resident microglia, however with age microglia become less able to engulf material, resulting in the accumulation of insoluble lipofuscin granules (Peters 2002; Hill et al. 2018). Equally, neuronal death can be initiated by immune cells through the production of neurotoxic cytokines (Kempuraj et al. 2016).

### 1.5.3 Aβ Clearance

AD post-mortem and mammalian studies have consistently found concentrated rosettes of active and proliferating microglia around Aβ plaques (von Bernhardi 2007; Joshi et al. 2014; Hopperton et al. 2017). In AD, microglial dysfunction can lead to the Aβ clearance impairment, which has been argued to have a greater impact on disease than Aβ accumulation alone (Mawuenyega et al. 2010). The resident macrophages are responsible for the effective clearance of neurotoxic proteins through phagocytic mechanisms, but also the production of intra- and extracellular degrading enzymes (Ries and Sastre 2016). In addition to promoting neuroprotection through apoptotic cell clearance, microglia help to form a barrier around Aβ plaques which restricts their growth and diffusion of synaptotoxic oligomers (Bolmont et al. 2008; Lee and Landreth 2010; Condello et al. 2015). However, long-term exposure to aggregates can induce reactive microgliosis, which results in the continuous secretion of pro-inflammatory cytokines, leading to compromised phagocytosis and further neuronal damage (Pan et al. 2011; Hellwig et al. 2015; Heneka et al. 2015).

AD risk gene TREM2 may equally be implicated in the microglia-mediated clearance of insoluble Aβ aggregates in AD (Gratuze et al. 2018). When stimulated, the TREM2 receptor initiates signal transduction pathways that promote microglial chemotaxis, phagocytosis, survival, and proliferation (Hsieh *et al.*, 2009; Kleinberger *et al.*, 2014; Sims *et al.*, 2017). Studies have found that TREM2-deficient microglia are less able to engulf Aβ aggregates in mouse models (Wang *et al.*, 2015; Yeh *et al.*, 2016) and that loss of TREM2 demonstrated reduced membrane ruffling, contributing to reduced phagocytic ability (Phillips et al. 2018). Crucially, APOE is an endogenous TREM2 ligand (Atagi et al. 2015; Yeh et al. 2016) and can bind both Aβ and apoptotic cells, presumably marking them for phagocytosis by TREM2-expressing microglia (Kim et al. 2009; Atagi et al. 2015). This TREM2-APOE signalling pathway has been reported to induce a shift in microglia promoting neurodegenerative phenotypes, which implies a role for the pathway regulating both beneficial and detrimental microglial functions (Krasemann et al. 2017). Being the most significant AD genetic risk factors, APOE and TREM2 interactions occur at the microglial membrane demonstrating the relevance of immunity in disease. Furthermore, TREM2 is likely to signal through another risk candidate PLCγ2 (Magno et al. 2021). Investigations found that the protective

hypermorphic allele *PLCγ2-P522R* yielded enhanced phagocytic function in BV2-microglial lines, complementing other research in the field (Maguire et al. 2020; Takalo et al. 2020; Tsai et al. 2022). While microglial phagocytosis appears to be a key function contributing to the ageing brain and dementia progression, pathway analysis uncovers the importance of other mechanisms such as lipid metabolism.

## 1.6 Lipids in Alzheimer's Disease Pathology

Lipids constitute a large proportion of the brain's dry mass with important functions in health and disease. The process of lipid metabolism, crucial to the recycling of lipids at the cell membrane, is considered a major contributor to AD with the most common risk gene *APOE-ε4* being involved (Husain et al. 2021). Beyond metabolism, lipids are important in BBB maintenance, myelination and inflammation among other functions (Chew et al. 2020). Much of the brain is composed of different types of lipids, grouped as sphingolipids, glycerophospholipids, and cholesterol (Dawson 2015; Hussain et al. 2019). Cholesterol forms lipoproteins, which are molecules containing a hydrophobic lipid core and a hydrophilic exterior of phospholipids, free cholesterol and apolipoproteins (Linton et al. 2019; Feingold and Grunfeld 2021). The most abundant apolipoprotein, APOE is responsible for phospholipid and cholesterol transport, with notable alleles involved in APP processing (Kim et al. 2009). Expressed mainly in astrocytes and microglia, APOE-ε4 demonstrates a lower affinity for lipids compared to other isoforms, limiting lipid transport throughout the CNS for neuronal remodelling and repair (Fernandez et al. 2019). Apolipoproteins are likely to be involved in lipid metabolism as key regulators of plasma and tissue lipid content, leading to altered synaptogenesis and neural plasticity when affected (Huang and Mahley 2014; Chew et al. 2020). Equally, increased levels of APOE-ε4 receptors directly correlate with Aβ clearance, which could serve as the basis for new AD treatments (Zhao et al. 2018).

Cell membranes are composed of multiple lipid classes, which secure membrane-bound receptors enabling them to interface with cellular organelles and extracellular signals. The BBB is composed of a lipid bilayer and forms the largest semipermeable membrane barrier of the CNS. It performs the crucial function of carefully regulating the exchange of solutes between the blood and the brain, blocking the entry of pathogens and toxins (Dotiwala et al. 2022). This delicate operation is highly

dependent on the membrane's integrity, which can be lost with the release of BBB tight junctions, pericyte and endothelial degeneration and brain capillary leakages (Halliday et al. 2016; Hussain et al. 2021). In AD, BBB breakdown can have devastating effects leading to damaged vasculature and brain parenchyma and eventually neurodegeneration (Hussain et al. 2021). Recent evidence also suggests that membrane lipids and downstream processes are highly important in immune cell function (Hubler and Kennedy 2016; Barnett and Kagan 2020; Liao et al. 2021). It is common for immune receptors such as TREM2 and CD33 to signal via the phosphoinositide pathway, a signalling cascade involving important lipid sensing messengers known as phosphoinositides (PIs). PIs regulate numerous cell processes reliant on cytoskeletal dynamics, from adhesion and motility to cell division and phagocytosis (Hubler and Kennedy 2016; Liao et al. 2021). The most notable events in the pathway are the conversion of phosphatidylinositol 4,5-bisphosphate (PIP2) to secondary messengers; inositol 1,4,5-trisphosphate (IP3) and diacylglycerol (DAG) by PLC enzymes, and the conversion of PIP2 to Phosphatidylinositol (3,4,5)-trisphosphate (PIP3) by phosphoinositide 3-kinase (PI3K) (Falkenburger et al. 2010). TREM2 signalling has been shown to trigger downstream events of phosphoinositide signalling, leading to calcium mobilisation, mammalian target of rapamycin (mTOR) and MAPK signalling and cytoskeletal rearrangement via Syk and is considered protective against AD pathology (Zou et al. 2008).

PLCγ2, encoded by the AD risk gene *PLCγ2,* is likely to function in this pathway, enabling phagocytic mechanisms. The discovery of the *PLCγ2-P522R* variant is one of few SNPs which confers a reduced risk of AD progression and has attracted a lot of attention in recent years (Sims et al. 2017). Its main function is to hydrolyse PIP2, producing secondary messengers, with IP3 releasing $Ca^{2+}$ from the endoplasmic reticulum (ER) (Magno et al. 2019). Recent evidence evokes that *PLCγ2-P522R* may promote certain phagocytic functions such as the clearance of Aβ, converging with existing evidence that lipid metabolism is central to immune function (Maguire et al. 2020; Maguire et al. 2021). Equally, PI3K activation via Syk is hypothesised to operate downstream of TREM2, expected to convert PIP2 to PIP3, promoting cell membrane extensions from lamellipodia (Peng et al. 2010; Li et al. 2019a). PI3K activity can be inhibited by the AD risk gene *INPP5D*, which cooperates with factor SHIP-1 to prevent immune receptor signalling (Fu et al. 2019). *Phospholipase D3 (PLD3)* is another risk

gene, likely to promote disease progression through lipid metabolism (Blanco-Luquin et al. 2018). Studies have only scraped the surface of the gene's role with identified roles in APP processing and mTOR signalling (Fazzari et al. 2017; Mukadam et al. 2018; Nackenoff et al. 2021). However, growing evidence suggests it could behave downstream of PI3K helping to regulate immune functions (Jiao et al. 2014; Satoh et al. 2014; Wang et al. 2015a). The wide variance of lipid disturbances associated with brain dysfunction suggests a promising hypothesis for AD, with lipid metabolism likely functioning in pathological processes associated with immunity. The complexity of the phospholipid pathway is well established, with ongoing research aiming to understand the overlap between lipids, immunity, and AD risk genes.

## 1.7 Modelling Alzheimer's Disease

Although we recognise the patterns of disease progression and the morphological changes that happen in AD-affected brains, the aetiology of idiopathic AD is generally unknown. Animal models continue to be used extensively to understand the cellular and genetic mechanisms underlying the condition, whilst circumventing general and ethical limitations in human studies. Some of the most popular models used in neurodegenerative research include yeast (*Saccharomyces cerevisiae*), worms (*Caenorhabditis elegans*), fruit flies (*Drosophila melanogaster)*, zebrafish (*Danio reriomice*), mice (*Mus musculus*) and *in vitro* cell lines, including models of neuronal and microglial cells (Drummond and Wisniewski 2017). No single system has recapitulated all the aspects of AD pathology, however, most have enabled the investigation of individual components of the disease.

### 1.7.1 Transgenic Mouse Models

Most AD research is carried out in transgenic mice, where often human genes associated with familial AD are overexpressed (le Bras 2021). Some are designed to produce excessive, mutant APP, with the PD-APP transgenic mouse being the first APP-based model to reproduce amyloid pathologies (Murrell et al. 1991). Since then, numerous mouse models have been characterised, with a focus on different genetic components. The widely used Tg2576 mouse model carries a mutant *APP (APP$_{695}$SWE)*, which has vastly progressed research and highlighted the importance

of core concepts, such as Aβ peptide length in pathogenesis (Hsiao et al. 1996; LaFerla and Green 2012). Researchers observed that shorter Aβ40 correlated with reduced AD and that longer Aβ42 exacerbated disease, (McGowan et al. 2005). APP-transgenic mouse models have been instrumental in demonstrating the relevance of the amyloid hypothesis and upstream elements, including ubiquitin and alpha-synuclein (Yang et al. 2000; Billings et al. 2005; Blurton-Jones and LaFerla 2006). Early research shows the expression of mutant human APP in transgenic mice leads to Aβ deposits in the brain, along with AD-like symptoms (Games et al. 1995; Hsiao et al. 1996; Masliah et al. 1996). Crucially, Aβ accumulation in the form of extracellular plaques occurs in a similar pattern to post-mortem, AD brains (LaFerla and Green 2012). APP-overexpressing models have also taught us about other hallmarks of pathology, including h-Tau within cells. Some predict the amyloid cascade to instigate Tau hyperphosphorylation, since some Tg2576 mice show increased hyperphosphorylated Tau, drawing connections between the two main competing hypotheses (Lewis et al. 2001; Götz et al. 2007). NFTs have been observed in other mouse models, which were designed with either a mutated human Tau (Oddo et al. 2003) or the removal of nitric oxide synthase 2 (Wilcock et al. 2008). These transgenic mice can also have mutated APP, creating multigenic AD models, such as 3xTg-AD mice (Oddo et al. 2003). Inflammatory pathologies have equally been modelled in mice, with an important study implicating the phagocytic role of microglia in Aβ plaque clearance (Wyss-Coray and Mucke 2002).

In addition to carrying hallmark mutations, transgenic mouse models have been designed to elucidate genetic risk mechanisms (Kitazawa et al. 2012). APP mice with *APOE* knockout have significantly reduced Aβ deposits and increased neuroinflammation (Bales et al. 1997; Bales et al. 1999). Intriguingly these mice are not relieved of behavioural symptoms, with some cases presenting with declined abilities (Dodart et al. 2000). *APOE* is better studied than most, however, other risk genes such as *ABCA1*, *TREM2* and *PLCγ2* are well studied using transgenic mouse models (Hirsch-Reinshagen et al. 2005; Song et al. 2018; Claes et al. 2022). Although murine studies have contributed valuable insights into disease mechanisms, new models must be constructed to mimic modern theories such as the cellular hypothesis (Oddo et al. 2004; Herzig et al. 2006; Meyer-Luehmann et al. 2008).

### 1.7.2 Cell Culture Models

Bridging the gap between animal and human studies, cell culture models continue to be developed to study potential therapies and investigate findings from other models in the field (Slanzi et al. 2020). Cell models have become increasingly advanced, enabling researchers to mimic neuronal and glial cell interactions in complex environments. Many research groups have developed 2D models based on induced pluripotent stem cells (iPSC) (Yagi et al. 2011; Israel et al. 2012; Mohamet et al. 2014; Li et al. 2016). Some iPSCs are prepared from fibroblast of EOAD patients with mutations in *PSEN1* and *PSEN2*, with differentiated neurons replicating amyloid and Tau pathologies (Yagi et al. 2011; Israel et al. 2012). CRISPR/Cas9 technology has been essential in generating genetic iPSC models such as knock-in human neurons carrying $APP^{swe}$ and $PSEN1^{M146V}$ mutations, helping to further model amyloid-based pathologies (Paquet et al. 2016). More complex models, such as tricultures have been used to study interactions between neurons, astrocytes and microglia, in addition to tools such as microfluidics platform to mimic blood flow (Park et al. 2018a). These 3D-engineered human neural progenitor cells have replicated key features of AD, such as the Aβ and Tau accumulation, and neuroinflammation. Interestingly, the authors demonstrated physiologically relevant interactions such as the release of pro-inflammatory cytokines and chemokines (TNFα, and IFNγ), microglial recruitment, and microglial neurotoxic activation contributing to neurodegeneration (Park et al. 2018a). However, the biggest limitation in culture modelling is that investigations can only take place in developing cells as opposed to adult or aged cells, a caveat yet to be overcome.

### 1.7.3 Invertebrate Models

Invertebrate animal models (such as worms and *Drosophila*) and lower-order vertebrates (such as zebrafish) have been instrumental in modelling AD and dementia (Paquet et al. 2009; Alexander et al. 2014; Fernandez-Funez et al. 2015). Although sequence homology is restricted, the ease of genetic manipulation is a considerable advantage when studying genetic disorders. *Drosophila, C.elegans* and zebrafish all express orthologs of the major EOAD-associated genes, including *APP, PSEN1* and

*PSEN2*, with some varying homology between species. *C.elegans*, with a short lifespan of 2-3 weeks, have a neuronal network and basic immune system and display complex behaviours, such as pathogen avoidance (Hobert 2010; Melo and Ruvkun 2012; Singh and Aballay 2020). Studies have used them to investigate neuronal cell death, implicating proteins that closely relate to mammalian calpains and cathepsins (Alexander et al. 2014). MEGF10/Draper/Ced-1 was originally discovered to mediate cell corpse engulfment in *C.elegans,* catalysing numerous advances in the field of glial cell biology (Zhou et al. 2001). Although Aβ is not naturally expressed in *C.elegans* or *Drosophila,* numerous models have been designed, where humanised mutant APP, Aβ and/or Tau are overexpressed, replicating pathologies observed in higher organisms (Fernandez-Funez et al. 2015; O'Keefe and Denton 2018). They have served in several genetic and drug screens revealing new insights to be verified using other model systems (Pandey and Nichols 2011; Su 2019). *Drosophila* has been central in identifying modifiers of Tau toxicity and amyloid pathology, and more recently in brain inflammation (Arora and Ligoxygakis 2020). Despite promising pre-clinical data, several neuroprotective drugs have failed during clinical trials, highlighting the complexity of AD and modelling it. There are caveats to all modelling systems, however, collectively they build a detailed image of AD (Blurton-Jones and LaFerla 2006).

## 1.8 The *Drosophila melanogaster* model

Many models exist to study human disease, however, at the heart of many genetic discoveries we have the common "fruit fly". Investigating genetics in a disease context is highly complex and near impossible to study in humans without encountering genetic and ethical constraints. *Drosophila melanogaster* enable us to bypass these restrictions, providing a simple, elegant model for genetic studies. Their diploid, 139.5 million base pair genome is condensed into 4 chromosomes – an X/Y pair and three autosomes labelled 2, 3 and 4, with low genetic redundancy (Roote and Prokop 2013). The genome was sequenced in 2001, and curated at the FlyBase database, providing accessible data on specific genes, including homology with other organisms (Fernández-Moreno et al. 2007). Approximately 75% of known human disease-causing genes have a recognisable match in *Drosophila,* and orthologs can be identified using various accessible tools including the DRSC Integrative Orthologue

Prediction Tool (DIOPT), (Roote and Prokop 2013). The development of the fruit fly is 10 days from egg to adult at 25$^{o}$C, which means that genetic manipulation by crossbreeding is very cost and time effective. A female fly lays up to 100 eggs per day, which allows large sample sizes to be generated in specific experiments. In addition to public databases, information and stocks are generously shared in the scientific community, providing extensive access to genetics tools, RNA interference (RNAi) and mutants, relevant to almost any gene. This provides a model, which is easy to manipulate, giving rise to opportunities to identify proteins and signalling pathways that may play a role in higher organisms (Roote and Prokop 2013).

### 1.8.1 *Drosophila* Genetic Tools

One of the primary benefits of using *Drosophila* as a model is the variety of genetic tools available to manipulate genes and/or pathways. A tool known as the GAL4 system is commonly used in *Drosophila* studies. GAL4 is a yeast-derived transcription factor, inserted downstream of a promoter in the fly genome, referred to as a driver. Adjacent to a transgene of choice, an Upstream Activation Sequence (UAS) is introduced. *GAL4* is expressed in a tissue-specific manner and binds to the UAS site, initiating the expression of the transgene (**Fig. 5**) (Brand and Perrimon 1993). This simple and elegant mechanism enables us to regulate transgene expression spatially and temporally. When regulating important genes, breeding can often lead to non-viable progeny; thus, bypassing developmental defects through temporal control can be useful. GAL80$^{ts}$ is a temperature-sensitive repressor of GAL4. It is active at 18$^{o}$C, binding GAL4 and preventing it from binding to the UAS, blocking expression of the adjacent transgene. A simple shift of the flies to a higher temperature (29$^{o}$C), causes Gal80$^{ts}$ to dissociate from GAL4, allowing binding to UAS and thus promoting expression of the gene of interest (GOI) (**Fig. 5**) (McGuire et al. 2004). This mechanism is also very useful when modelling age-related diseases as we can mediate when certain genes are ON/OFF and test whether the impact occurs after long- or short-term expression. Furthermore, we can genetically encode fluorophores downstream of tissue-enriched promoters, to label certain cells (Keppler et al. 2003). We can also label cells endogenously, using Mouse-derived cluster of differentiation 8 (mCD8), a membrane protein often found on immune cells which is fused with a GFP

molecule, symbolised as mCD8::GFP (Burr et al. 2014). These systems are some of many useful genetic tools that are available and due to their extensive use, we can be sure that they are robust. The powerful genetics of the fruit fly might help us to interpret the results of GWAS of AD patients, enabling us to triage genetics before testing them in mammals and cell lines.

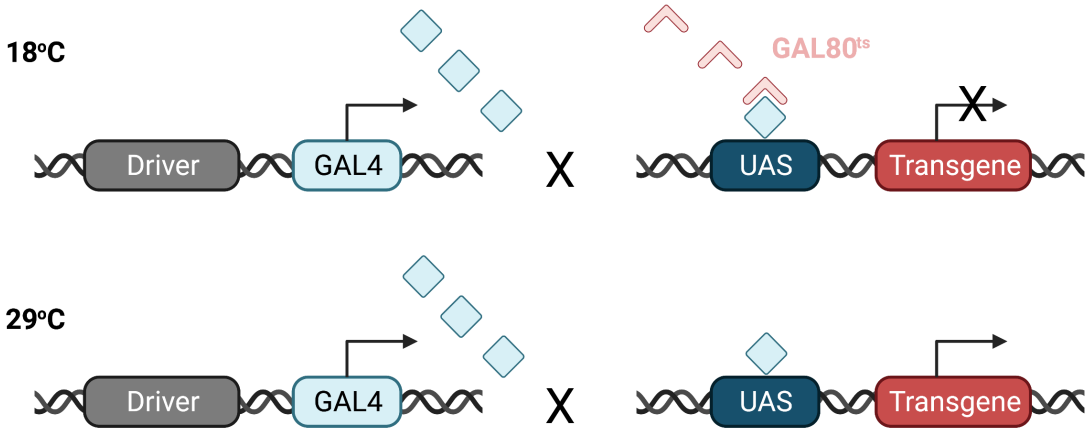


***Fig. 5. The GAL4 tool Allows for Transgene Expression to be Regulated in Time and Space.*** *A diagram to represent the mechanism of the GAL4 expression tool. A tissue-specific promoter (grey) drives the expression of GAL4 (light blue), which then binds and activates a UAS (dark blue), enabling transgene expression (red). GAL80$^{ts}$ (pink) is a temperature-sensitive inhibitor of GAL4 that operates at lower temperatures (18°C). Image made in ©BioRender - biorender.com.*

### 1.8.2 The *Drosophila* Nervous System

Composed of the brain and PNS, the *Drosophila* nervous system shares many similarities with humans and mammalian counterparts, performing analogous functions, from movement to memory. The brain houses a series of neuronal networks, composed of approximately 200,000-300,000 neurons, which localise in two main regions – the central brain, and optic lobes (Freeman 2015). Networks bundle to form the visual, auditory, gustatory, and olfactory systems (Gordon et al. 2008; Greenspan et al. 2010). *Drosophila* have functional glia, which share characteristics with their mammalian counterparts, these include: i) reciprocal trophic support between neurons and glia, ii) recycling pathways of synaptic neurotransmitters, iii) morphological and

functional similarities and iv) immune protection (Stork et al. 2012; Freeman 2015). The main classes of glia include i) surface-associated glia (which are found in the outermost regions of the nervous system), ii) cortex glia (which tightly envelop neuronal cell bodies) and iii) neuropil-associated glia. The latter consists of 3 subtypes, wrapping, ensheathing and astrocytic glia, which share many morphological and functional similarities with microglia and astrocytes respectively (**Fig. 6**). Despite *Drosophila* having a modest brain compared to humans, they have sufficient specificity in cell types and functions to be a plausible model for neurobiological research.

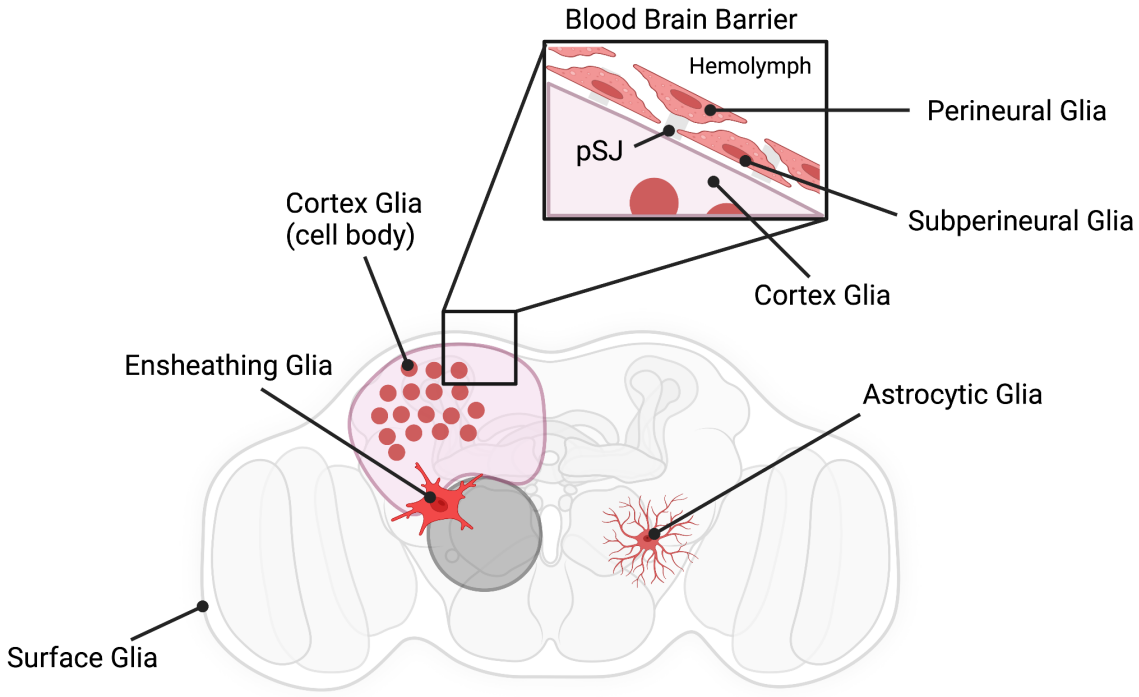


***Fig. 6. Drosophila Brains Contain Glial Subtypes with Specific Functions.***

*A schematic cross-section highlighting the major glial subtypes of the Drosophila brain, including ensheathing glia and astrocytic glia, analogous to microglia and astrocytes respectively. The insert displays subtypes of surface glia, which closely associate with cortex glia helping to form the BBB. Pleated septate junctions (pSJs) between subperieneural glia are in grey. Adapted from* (Ou et al. 2014)*, made in ©BioRender - biorender.com.*

### 1.8.3 Modelling Alzheimer's Disease in *Drosophila*

*Drosophila* genetics have been deployed against significant neurodegenerative diseases, resulting in the generation of models for AD based on current theories of pathology. A widely used model of Aβ toxicity combines *GAL4*-driven constructs encoding human APP and human beta-site APP-cleaving enzyme 1 (BACE1). Expressing these human genes in the fly brain, along with the secondary cleavage by endogenously produced γ-secretase, leads to the generation of the Aβ peptide (Greeve 2004). This model has been important in assessing the modulators of amyloid pathology, through BACE1 and APP metabolism. Other models have been generated by which the Aβ sequence is fused downstream of a secretion signal peptide. Here, the signal peptide is cleaved as Aβ enters the secretory pathway, allowing a portion of the peptide to be secreted by the cell (Finelli et al. 2004; Stokin et al. 2008). Effects in immunohistochemistry and cognitive behaviours result from intracellular Aβ accumulation, which localises to the ER, Golgi and lysosomes, specifically (Crowther et al. 2005). Other fly models exist to investigate Tau-related hypotheses of AD, which focus on the overexpression of human wild-type Tau protein. Previous research has identified neurotoxic effects from Tau overexpression, as to be expected, however, more severe phenotypes in various assays have been found when expressing disease variants of Tau (Iijima-Ando and Iijima 2010; Beharry et al. 2013; Scarpelli et al. 2019). Another Tau model sees the formation of intracellular inclusions similar to neurofibrillary tangles when increasing the activity of glycogen synthase kinase 3β (GSK3β) (Wittmann et al. 2001; Jackson et al. 2002). These represent the main models of AD, however, through the increased understanding of the disorder, further models are being constructed based on more modern theories of AD pathology (Bilen and Bonini 2005; Moloney et al. 2010; Younan et al. 2018).

### 1.8.4 Investigating Alzheimer's risk genes in *Drosophila*

*Drosophila* screening techniques have allowed for the systematic dissection of important genes in dementia, with *PTEN-induced kinase 1* (Pink1) and Parkin being notable examples in Parkinson's disease research (Deng et al. 2008). Similar tools have been employed to understand the role of AD-associated risk genes. Shulman

and colleagues have identified *CD2AP, FERMT2* and *CELF1* orthologs as Tau modifiers (Shulman et al. 2014). Other studies have generated risk gene mutants and characterised their role, such as loss of *CD2AP Drosophila* ortholog *cindr* enhancing the neurotoxicity of human Tau, promoting AD-like pathology (Ojelade et al. 2019). Equally the study identified new functions including roles in synapse maturation, synaptic vesicle recycling and release (Ojelade et al. 2019). Despite there not being a *Drosophila* homolog for *TREM2*, a recent study confirmed a glial phenotype when expressing human *TREM2* or human tyrosine kinase binding protein (*TYROBP*), which encodes the intracellular adaptor of TREM2. Intriguingly, flies expressing neuronal TREM2 in tandem with Aβ42 did not yield any AD-like phenotypes, however, glial expression of TREM2 did modify molecular signatures induced by Aβ42 (Sekiya et al. 2018; Jeon et al. 2020). These studies highlight the versatility of reverse candidate screening and mutant generation in *Drosophila* research, providing valuable insights into certain aspects of AD pathogenesis and its modulators. With relatively few studies investigating the role of AD risk genes in *Drosophila*, researchers are returning to the model to understand their role in glial function.

### 1.8.5 *Drosophila* Glial Engulfment Model

Previous literature describes a well-characterised system to assess glial engulfment function in *Drosophila* (MacDonald et al. 2006; Doherty et al. 2009; Logan et al. 2012; MacDonald et al. 2013; Doherty et al. 2014; Tasdemir-Yilmaz and Freeman 2014; Musashe et al. 2016; Purice et al. 2016). A subset of olfactory receptor neurons (ORNs), expressing a putative odour receptor OR85e, have cell bodies in an olfactory organ known as the maxillary palp (Couto et al. 2005). The axons of the neurons project into the olfactory cavity of the *Drosophila* brain and converge at synaptic junctions in a cluster known as glomeruli (a total of 51) found in the antennal lobes (**Fig. 7**). Several labs have adopted this system to investigate neurons and glia alike. Neurons are tagged using an mCD8::GFP construct, introduced adjacent to the OR85e promoter, leading to GFP expression in a single population of ORN membranes. Tagging enables visualisation, revealing beautiful axons and glomeruli. Macdonald and colleagues found that by surgically ablating maxillary palps, thereby removing the cell bodies, they instigatedneurodegeneration analogous to Wallerian

degeneration (WD) in the ORNs (MacDonald et al. 2006). Neuronal ablation triggers reactive gliosis, where glia undergo morphological and genetic changes, initiating many pro-inflammatory mechanisms. Over time GFP-labelled neurons begin to disappear due to the engulfment of axonal debris by resident ensheathing glia. Neuronal fluorescence, measured using confocal microscopy, provides a robust readout for glial phagocytosis. In recent years, the system has been deployed to identify key regulators of the engulfment pathway including *Draper* (considered the major upstream regulator) and serves as an excellent model to study modifiers of glial function and phagocytosis (MacDonald et al. 2006; MacDonald et al. 2013; Lu et al. 2017).

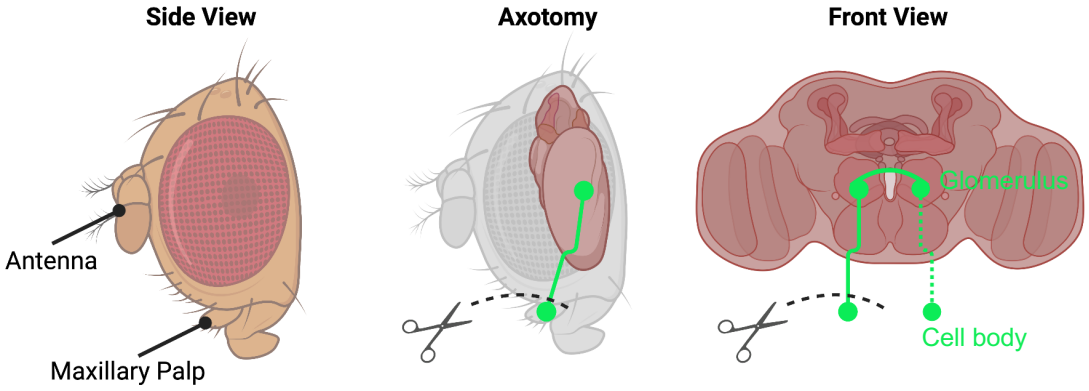


***Fig. 7. Ablation of GFP-labelled Neurons Triggers Engulfment of Debris.*** *Side-view and front view schematics of the Drosophila head and brain. GFP-tagged neurons project into the olfactory cavity of the Drosophila brain, overlapping at synaptic junctions known as glomeruli. Axotomy results from the non-lethal surgical removal of cell bodies in the maxillary palp, causing the degeneration of axons, in turn leading to the engulfment of axonal debris. Image made in ©BioRender - biorender.com.*

### 1.8.6 Engulfment Receptor Intracellular Signalling Pathway

Glial clearance of cellular debris after ablation requires the highly conserved Draper receptor, which initiates a tyrosine kinase-signalling cascade when binding to its respective ligand(s) (MacDonald et al. 2006). It is also required in the engulfment of neuronal projections in early development in flies and the adult CNS (Williamson and Vale 2018). Enrichment of the receptor was first identified in 2006, using the same model system described above (MacDonald et al. 2006). Since then, each component of the highly conserved pathway has been identified (MacDonald et al. 2006; Doherty et al. 2009; Logan et al. 2012; MacDonald et al. 2013; Doherty et al. 2014; Tasdemir-Yilmaz and Freeman 2014; Musashe et al. 2016; Purice et al. 2016; Ray et al. 2017).

*Draper* is enriched in activated glia after axotomy and is necessary for debris clearance (MacDonald et al. 2006). Draper signals through a cascade which drives cytoskeletal remodelling and promotes the expression of other genes involved in phagocytic activity, including *Draper* itself. The receptor contains an Immunoreceptor tyrosine-based activation motif (ITAM) where pathway components Shark and Ced-6 bind (Ziegenfuss et al. 2008). Phosphorylation of the ITAM activates downstream components including the *Drosophila* Janus kinase (dJNK) signalling pathway, through TNF receptor-associated factor 4 (TRAF4) associated with misshapen (MSN) (Lu et al. 2017). Eventually, adaptor protein complex 1 (AP-1) is activated and promotes the expression of engulfment machinery (Hilu-Dadia et al. 2018). Recent evidence suggests an overlap between the Draper pathway and phospholipid pathway through the knockdown of PI3K leading to a partial engulfment deficit (Purice et al. 2016). Other research identified links between injury response mechanisms during *Drosophila* embryonic wound healing with calcium-induced dJNK signalling, leading to the upregulation of Draper after injury (Weavers et al. 2016; Weavers et al. 2019). Most pathway components were identified using the engulfment model described above, with knockdown of each component leading to either the delay or complete inhibition of glial phagocytosis (**Fig. 8**). The vertebrate ortholog MEGF10 is also implicated in glial activity in the context of debris engulfment as well as sharing conserved components (Chung et al. 2013; Iram et al. 2016). More recently, Draper has been observed rescuing Aβ toxicity in *Drosophila* AD models (Ray et al. 2017). However, the role of Draper/MEGF10 in AD pathology is rarely explored and there are

still many unknowns associated with the pathway. It is conceivable that genes associated with AD risk may also link to the engulfment pathway.

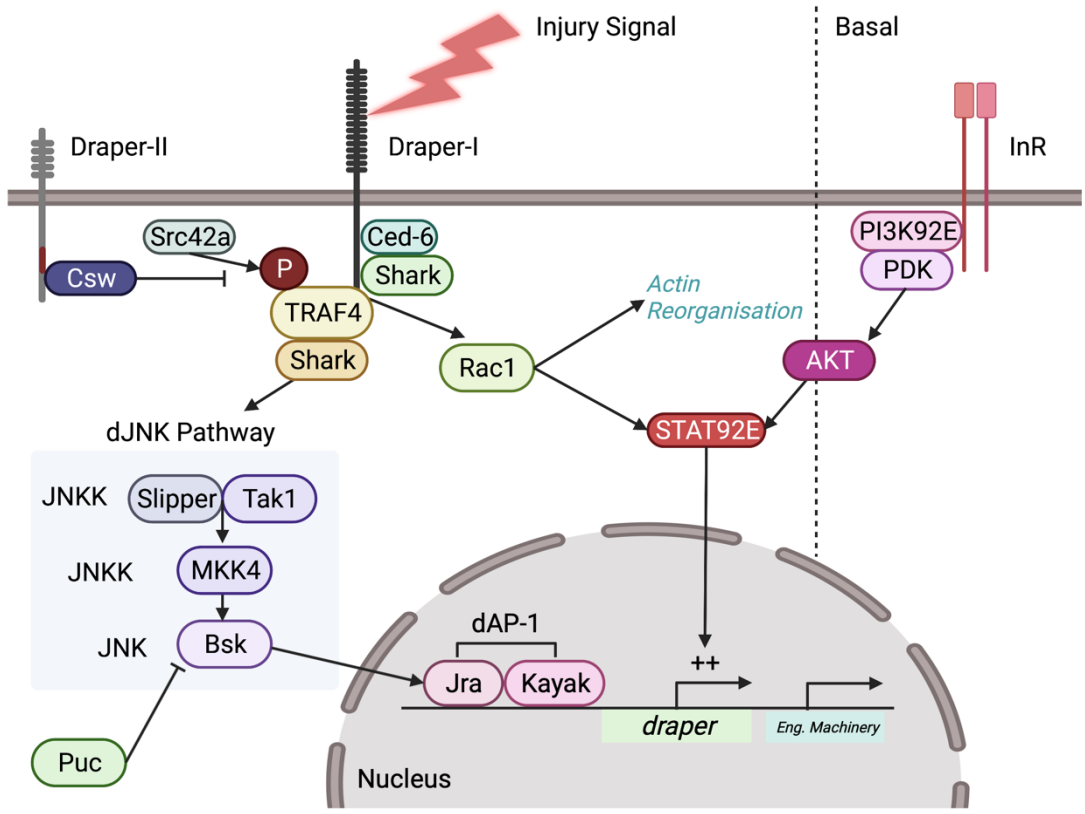


***Fig. 8. Mechanistic Diagram of Draper Pathway.*** *At the glial membrane, Draper-I is activated by neuronal injury leading to the recruitment of Ced-6, TRAF4 and shark. Upon phosphorylation of TRAF4 by Src42a, the dJNK pathway is activated. Thereafter Basket (Bsk) activates the dAP-1 complex, composed of Jun-related antigen (Jra) and Kayak, promoting the expression of target genes, including engulfment machinery and Draper-I itself. Inhibitory Draper-II prevents engulfment by recruiting corkscrew (Csw) and inhibiting TRAF4 phosphorylation, however, engulfment is also inhibited through Puckered (Puc) which prevents Bsk activity. Downstream of Draper, shark activates Rac1 which is hypothesised to regulate cytoskeletal changes and STAT92E activity. At basal levels, the engulfment pathway is proposed to be regulated by the insulin pathway and PI3K, overlapping with the Draper pathway through STAT92E. Image made in ©BioRender - biorender.com.*

## 1.9 Aims and Objectives

The present project aims to identify novel modulators of *Drosophila* glial engulfment and contribute to research in the field of AD risk genes. We hypothesise that glial phenotypes will present due to overlaps between tested genetic factors and the Draper pathway.

- Experimental variables including sex, rearing temperature and age will be investigated in the injury response model to optimise conditions for further experiments.
- With existing knowledge of genes associated with AD onset risk, a reverse candidate screen will be performed, employing genetic tools such as GAL4 and RNAi, to decipher the potential roles of *Drosophila* orthologs in glial engulfment function.
- Novel modulators will then be verified and characterised using quantitative and qualitative methods to clarify the significance of any given phenotype.
- To further our understanding of genetic mechanisms, candidate genes will be investigated using epistasis approaches and downstream pathways will be assessed using GFP-tagged PIP2, PIP3 and GCAMP models.

# 2 Materials & Methods

## 2.1 Fly Stocks and Husbandry

*Drosophila* were kept and bred following standard practice (Roote and Prokop 2013). Stocks were maintained in wide vials (*Drosophila* tubes 25X95mm (PS), Regina), using cotton wool stoppers, on food sourced and manufactured on-site. The recipe used to prepare food was adapted from a molasses medium recipe described by the Bloomington *Drosophila* Stock Centre (BDSC), using ingredients outlined in **Table 2**. Most stocks were kept at room temperature (ca. 21ºC, RT) and passed on to fresh food every 3.5 weeks. Genotype was assessed based on chromosomal markers, where specimens were tipped onto a $CO_2$ pad (Diffuser Pad, Genese Scientific) and inspected under a dissection microscope (Stemi 508, Zeiss).

| **Ingredient** | **Manufacturer** | **Amount** | **Units** |
|---|---|---|---|
| Agar | MIN GEL 920, BTP DREWITT | 300* | g |
| Brewer's Yeast | 903312, MP biomedical | 1000 | g |
| Cornmeal | 901411, MP biomedical | 2500 | g |
| Molasses | 62-118, FLYSTUFF SLS | 2.5 | l |
| Acid mix | | 168 | ml |
| Propionic Acid | 220130025, ACROS ORGANIC | 250 | ml |
| Phosphoric Acid | 201140010, ACROS ORGANIC | 25 | ml |
| Deionised Water | | 325 | ml |
| Methyl-p-Hydroxybenzoate (Tegosept) | 102341, MP biomedical | 56 | g |
| Ethanol | E/0600DF/21, Fisher Scientific | 280 | ml |

***Table 2:*** *Outlines ingredient information to produce fly food according to our protocols.*
** Adjust amount depending on gel strength.*

## 2.2 Genetic Crosses

All flies were bred in narrow vials (*Drosophila* tubes 20x95 mm (PS), Regina), with food prepared as described above. Crosses were designed and maintained accordingly, with conditions optimised for each experiment (See **Chapters 3-6** for details on cross design). Generally, crosses were prepared with a minimum of 10 males and 20 females, placed at 25$^{o}$C and flipped into new tubes every 3 days. A list of all fly stocks can be found in **Table 3**.

| Chapter | Stock Name | *Genotype* | Stock Number |
|---|---|---|---|
| **3,4,5** | Virgin Line 1 | *w-;OR85e-mCD8::GFP/+;repo-GAL4/TM3, Sb, e-* | 7415 |
| **4** | Virgin Line 2 | *w-;OR85e-mCD8::GFP/+;repo-GAL4, UAS-mcherry/TM3, Sb, e-* | 7415 |
| **5** | Virgin Line 3 | *w-;+/+;P{w[+mC]=tubP-GAL4}LL7/TM6b, Hu, Tb* | 90974 |
| **6** | Virgin Line 4 | *w-;+/+;repo-GAL4/TM6b, Hu, Tb* | 7415 |
| **6** | Virgin Line PIP2 | *w-;repo]/CyO; UAS-PLCdelta-PH-EGFP}3/TM6B, Hu, Tb* | 39693 |
| **6** | Virgin Line PIP3 | *w-; P{w[+mC]=tGPH}2; repo-GAL4/ TM3, Sb, e-* | 8163 |
| **6** | Virgin Line GCAMP | *w-;20XUAS-IVS-GCaMP6f}attP40;repo-GAL4/TM6b, Hu, Tb* | 42747 |
| **3,4,5,6** | w- | *w-;+/+;+/+* | Lab |
| **4,5** | UAS-GFPvallium | *y,v; P{y[+t7.7] v[+t1.8]=UAS-GFP.VALIUM10}attP2* | 35786 |
| **4** | attP40 | *y,v;p(caryP)attP40* | 36304 |
| **4** | attP2 | *y,v;;p(caryP)attP2* | 36303 |
| **4** | KK | *P{attP,y+,w3'}VIE-260B* | 60101 |
| **6** | LacZ | *w-;;P{w[+mC]=UAS-lacZ.Exel}/TM6b* | 8530 |
| **4** | Draper RNAi (I) | *w1118; P{GD2628}v4833* | 4833 |
| **4** | **Draper RNAi (II)** | *w1118; P{GD14423}v27086* | 27086 |
| **4, 5, 6** | Abi RNAi (I) | *y1 v1; P{TRiP.HMC03190}attP40* | 51455 |
| **4** | Abi RNAi (II) | *y1 sc* v1 sev21; P{TRiP.HMS01597}attP2* | 36707 |
| **4** | Abi RNAi (III) | *P{KK108071}VIE-260B* | 100714 |

| | | | |
|---|---|---|---|
| **4** | Ance RNAi (I) | *y1 sc* v1 sev21; P{TRiP.HMS03009}attP2* | 36749 |
| **4** | Ance RNAi (I) | *y1 sc* v1 sev21; P{TRiP.GLC01369}attP2* | 51394 |
| **4** | Amph RNAi (I) | *w1118; P{GD1311}v7190* | 7190 |
| **4** | Amph RNAi (II) | *w1118; P{GD1311}v9264* | 9264 |
| **4** | ApolPP RNAi | *y1 v1; P{TRiP.HM05157}attP2* | 28946 |
| **4** | bru1 RNAi (I) | *y1 v1; P{TRiP.HMS01899}attP40* | 38983 |
| **4** | bru1 RNAI (II) | *y1 sc* v1 sev21; P{TRiP.GL00314}attP2* | 35394 |
| **4** | bru1 RNAi (III) | *y1 v1; P{TRiP.HMJ21531}attP40* | 54812 |
| **4** | bru1 RNAi (IV) | *w1118; P{GD8699}v41567* | 41567 |
| **4** | bru1 RNAi (V) | *w1118; P{GD8699}v41568* | 41568 |
| **4** | bru1 RNAi (VI) | *w1118; P{GD17093}v48237/TM3* | 48237 |
| **4** | bru1 RNAi (VII) | *P{KK110026}VIE-260B* | 107459 |
| **4** | cindr RNAi (I) | *w1118; P{GD8679}v38854* | 38854 |
| **4** | cindr RNAi (II) | *P{VSH330422}attP40* | 330422 |
| **4** | CG11710 RNAi (I) | *P{KK102304}VIE-260B* | 109760 |
| **4** | CG11710 RNAi (II) | *y1 sc* v1 sev21; P{TRiP.HMC05087}attP40* | 60093 |
| **4** | CG17600 RNAi (I) | *w1118; P{GD3716}v51085* | 51085 |
| **4** | CG17600 RNAi (II) | *y1 sc* v1; P{TRiP.HMS01812}attP2* | 38345 |
| **4** | CG17600 RNAi (III) | *P{KK105222}VIE-260B* | 102833 |
| **4** | CG34120 RNAi (I) | *P{KK104441}VIE-260B* | 100472 |
| **4** | CG34120 RNAi (II) | *$w^{1118}$; P{GD3704}v11673/TM3* | 11673 |
| **4** | CG34120 RNAi (III) | *$w^{1118}$; P{GD15895}v48377* | 48377 |
| **4** | CG34120 RNAi (IV) | *P{KK106128}VIE-260B* | 100384 |
| **4** | CG34120 RNAi (V) | *P{KK105495}VIE-260B* | 101700 |

| | | | |
|---|---|---|---|
| **4** | CHMP2B RNAi (I) | *y1 v1; P{TRiP.HMJ21039}attP40* | 50942 |
| **4** | CHMP2B RNAi (II) | *y1 v1; P{TRiP.HMS01844}attP40* | 38375 |
| **4** | DOR RNAi (I) | *w1118; P{GD5124}v41186* | 41186 |
| **4** | DOR RNAi (II) | *y1 v1; P{TRiP.HMJ22607}attP40* | 60389 |
| **4** | DOR RNAi (III) | *P{KK111208}VIE-260B* | 105330 |
| **4** | Eph RNAi (I) | *w1118; P{GD14481}v27236* | 27236 |
| **4** | Eph RNAi (II) | *P{KK101831}VIE-260B* | 110448 |
| **4** | Eph RNAi (III) | *w1118; P{GD2535}v4771* | 4771 |
| **4** | Ets98B RNAi (I) | *w1118; P{GD4451}v10932* | 10932 |
| **4** | Ets98B RNAi (II) | *P{KK107560}VIE-260B* | 107292 |
| **4** | Ets98B RNAi (III) | *y1 v1; P{TRiP.JF03116}attP2* | 28700 |
| **4** | Fak RNAi (I) | *w1118; P{GD6840}v17957* | 17957 |
| **4** | Fak RNAi (II) | *P{KK101680}VIE-260B* | 108608 |
| **4** | Fak RNAi (III) | *y1 sc* v1 sev21; P{TRiP.GL00269}attP2* | 35357 |
| **4** | Fak RNAi (IV) | *P{KK101680}VIE-260B* | 108608 |
| **4** | Fak RNAi (V) | *y1 v1; P{TRiP.HMS02792}attP40* | 44075 |
| **4** | Fit1 RNAi (I) | *P{KK109279}VIE-260B* | 105767 |
| **4** | Fit1 RNAi (II) | *y1 sc* v1 sev21; P{TRiP.HMC02930}attP40* | 44536 |
| **4** | Fit1 RNAi (IIII) | *y1 v1; P{TRiP.JF01986}attP2* | 25966 |
| **4** | fw RNAi (I) | *w1118; P{GD3327}v39575/TM3* | 39575 |
| **4** | fw RNAi (II) | *P{KK109200}VIE-260B* | 106656 |
| **4** | Hasp RNAi (I) | *w1118; P{GD5411}v30767* | 30767 |
| **4** | Hasp RNAi (II) | *y1 sc* v1 sev21; P{TRiP.HMC05997}attP40* | 65101 |
| **4** | Hs3st-A RNAi (I) | *w1118; P{GD2075}v4998* | 4998 |
| **4** | Hs3st-A RNAi (II) | *w1118; P{GD10001}v25571* | 25571 |
| **4** | Hs3st-A RNAi (III) | *w1118; P{GD10001}v25572* | 25572 |

| | | | |
|---|---|---|---|
| **4** | Hs3st-A RNAi (IV) | *y1 v1; P{TRiP.JF03033}attP2* | 28618 |
| **4** | Lap RNAi (I) | *w1118; P{GD4725}v12731* | 12731 |
| **4** | Lap RNAi (II) | *w1118; P{GD4725}v12732* | 12732 |
| **4** | Lap RNAi (III) | *y1 v1; P{TRiP.HMC02373}attP2* | 55241 |
| **4** | Lpr2 RNAi (II) | *y1 sc* v1 sev21; P{TRiP.HMS03722}attP2* | 54461 |
| **4** | Mef2 RNAi (I) | *$w^{1118}$; P{GD17050}v46494* | 46494 |
| **4** | Mef2 RNAi (II) | *$w^{1118}$; P{GD17050}v46495/CyO* | 46495 |
| **4** | Mef2 RNAi (III) | *y[1] sc[*] v[1]; P{y[+t7.7] v[+t1.8]=TRiP.HMS01691}attP40* | 38247 |
| **4** | Mef2 RNAi (IV) | *y[1] v[1]; P{y[+t7.7] v[+t1.8]=TRiP.JF03115}attP2* | 28699 |
| **4** | Mef2 RNAi (V) | *w1118; P{GD5039}v15550* | 15550 |
| **4** | Nrx-IV RNAi (I) | *$w^{1118}$; P{GD2436}v8353* | 8353 |
| **4** | Nrx-IV RNAi (II) | *$w^{1118}$; P{GD2436}v9039* | 9039 |
| **4** | Nrx-IV RNAi (III) | *P{KK102207}VIE-260B* | 108128 |
| **4** | Nrx-IV RNAi (IV) | *$y^{1}$ $v^{1}$; P{TRiP.JF03142}attP2* | 28715 |
| **4** | Nrx-IV RNAi (V) | *$y^{1}$ $sc^{*}$ $v^{1}$; P{TRiP.HMS00419}attP2/TM3, $Sb^{1}$* | 32424 |
| **4** | Nrx-IV RNAi (VI) | *$y^{1}$ $sc^{*}$ $v^{1}$; P{TRiP.HMS01991}attP40* | 39071 |
| **4** | ocrl RNAi (I) | *w1118; P{GD11016}v34649* | 34649 |
| **4** | ocrl RNAi (II) | *P{KK101922}VIE-260B* | 110796 |
| **4** | ocrl RNAi (III) | *y1 sc* v1 sev21; P{TRiP.HMS01201}attP2/TM3, Sb1* | 34722 |
| **4** | p130Cas RNAi (I) | *w1118; P{GD7492}v41479* | 41479 |
| **4** | p130Cas RNAi (II) | *P{VSH330191}attP40* | 330191 |
| **4** | Pld3 RNAi (I) | *w1118; P{GD5427}v41225* | 41225 |
| **4, 5** | **Pld3 RNAi (II)** | *P{KK107515}VIE-260B* | 109798 |
| **4** | Pld3 RNAi (III) | *y1 v1; P{TRiP.JF01595}attP2* | 31122 |
| **4** | sl RNAi (I) | *w1118; P{GD1535}v7173* | 7173 |

| | | | |
|---|---|---|---|
| **4** | sl RNAi (II) | *w1118; P{GD1535}v7174* | 7174 |
| **4, 5, 6** | **sl RNAi (III)** | *y1 sc* v1 sev21; P{TRiP.HMS00695}attP2* | 32906 |
| **4** | sl RNAi (IV) | *P{KK101565}VIE-260B* | 108593 |
| **4** | Wwox RNAi (I) | *P{KK108459}VIE-260B* | 108350 |
| **4** | Wwox RNAi (II) | *y1 v1; P{TRiP.HMC03298}attP2* | 51747 |
| **4** | zyd RNAi (I) | *w1118; P{GD3723}v40987* | 40987 |
| **4** | zyd RNAi (II) | *w1118; P{GD3723}v40988* | 40988 |
| **4** | zyd RNAi (III) | *y1 v1; P{TRiP.JF01872}attP2* | 25851 |
| **6** | LacZ + sl | *w-;UAS-LacZ/CyO;UAS-sl RNAi/TM3* | 32906 |
| **6** | arf51f + sl | *w-;UAS-arf51fRNAi/CyO;UAS-slRNAi/TM3* | 24224, 32906 |
| **6** | pten + sl | *w-;UAS-ptenRNAi/CyO;UAS-slRNAi/TM3* | 101475, 32906 |
| **6** | Pld3 + sl | *w-;UAS-Pld3RNAi/CyO;UAS-slRNAi/TM3* | 109798, 32906 |
| **6** | hspc300 + sl | *w-;UAS-hspc300RNAi/CyO;UAS-slRNAi/TM3* | 35794, 32906 |
| **6** | shark + sl | *w-;UAS-sharkRNAi/CyO;UAS-slRNAi/TM3* | 33059, 32906 |

***Table 3.*** *Combines all stocks information including fly gene, genotype, stock number, source, vector, insertion site and the type of line.*

## 2.3 Neuronal Axotomy

Prior to injury, progeny were separated into two equal groups which would later reflect injured and uninjured conditions. Running uninjured controls alongside experimental flies ensured that any changes observed were implicitly due to underlying genetic manipulations. Non-lethal surgical ablation methods were performed on various olfactory organs, targeting different neuronal networks (**Fig. 9a**). The ends of maxillary palps (**Fig. 9b**) were cut using micro scissors (Stainless Scissors, 54K, FST Germany), before putting the flies back in the incubator for the required amount of time.

For other experiments more neurons were targeted for neurodegeneration by injuring the antennae (**Fig. 9c**). Here third segments of both antennae were removed using dissection forceps (Carbon Forceps, Dumont), before returning sample flies to the relevant incubator for the desired period. Sample brains were later dissected and stained using an optimised immunohistochemistry assay.

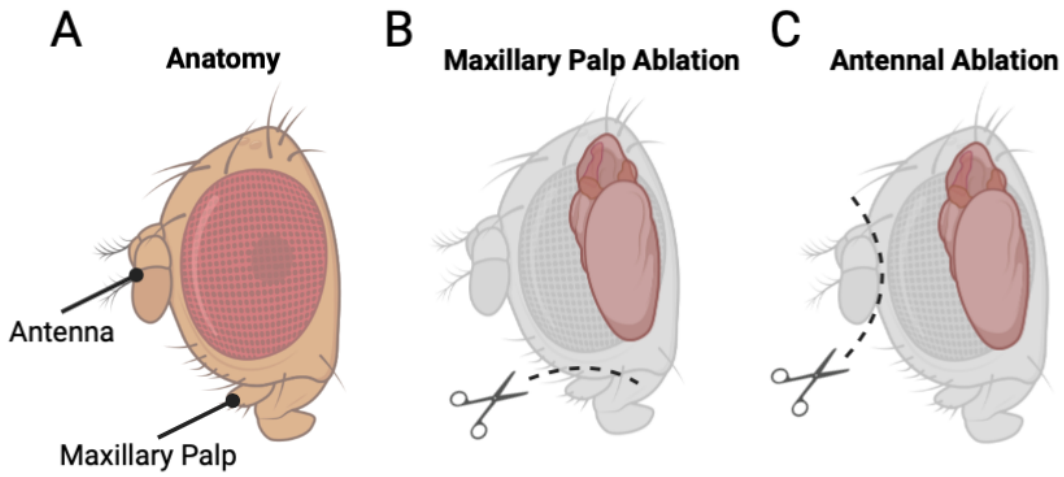


***Fig. 9. Injuring Different Olfactory Organs Triggers the Degeneration of Various Neuronal Networks.*** *This diagram illustrates various methods of injury used to assess glial function.* ***a)*** *represents the profile view of the fly head, outlining the tusk-like projections known as maxillary palps and the antenna situated between the eyes.* ***b)*** *shows antennal ablation methods and* ***c)*** *shows maxillary palp ablation methods respectively. Image made in ©BioRender - biorender.com.*

## 2.4 Brain Dissections

*Drosophila* brain dissections are some of the more notorious and technically challenging dissections, requiring attention to detail. Part of the project required the optimisation of dissection techniques to acquire efficient results. Previous literature has described various methods for achieving the best outcome and a combination of these led to the final method (Wu and Luo 2006; Tito et al. 2016). Prior to dissections, the heads of the flies were removed and fixed. Each brain was dissected in a black tinted dissection dish, using 0.1mm diameter pins (Insect Pins, Austerlitz) and forceps (Carbon Forceps, Dumont). To stabilise the head, a single pin (Minutien Pin 0.2mm, BMR Supplies) was pierced through the clypeus region, a gap between the proboscis and antennae. The head capsule was then gently removed using forceps, keeping the central brain and optic lobes intact before proceeding to staining methods.

## 2.5 Immunohistochemistry

Endogenous neuronal GFP signal was insufficient to determine phenotypes under the microscope, therefore samples were stained to facilitate signal detection. The protocol largely followed the previously established staining techniques (Vosshall et al. 2000), however, some adjustments were made to accommodate fly strains. Adult heads were removed and transferred to 0.5mL tubes of 4% paraformaldehyde (PFA) for 16 mins and washed in 0.1% PBS-Triton Xion 10x (PTx) 5 times over 30 mins. Brains were dissected in 0.1% PTx and fixed in 4% PFA for a further 16 mins in a multi-welled dish (Pyrex Plate – 9 well, EMS). Here, heads were kept on ice in between dissections. After dissecting, brains were washed in 0.1% PTx 5 times over 30 mins and blocked in 10% normal goat serum (in PTx 0.1%) for 1 hour. Finally, samples were incubated in primary antibody and diluted in blocking solution overnight at 4$^{o}$C. The following day, samples were washed in 0.1% PTx 5 times over 30 mins – 1 hour and then incubated in secondary antibodies under foil, diluted in in Ptx or blocking solution for 2 hours at RT. After incubation, the samples were washed a further 5 times in 0.1% PTx solution before mounting (**Table 4**). Antibodies used, included Anti-GFP IgG (A11122, Thermo), Anti-GFP IgG (ab290, Abcam), Anti-Draper (8A1, DSHB) and Anti-rabbit (rb) secondary IgG (A21206, Thermo), Anti-mouse (ms) secondary IgG (A11004, Thermo) (**Table 5**).

| Name | Stock Number | Host | Dilution |
|---|---|---|---|
| *a-GFP* | A11222 | rb | 1:1000 |
| *a-GFP* | Ab290 | rb | 1:1000 |
| *a-Draper* | 8A1 | ms | 1:50 |
| *a-repo* | 8D12 | ms | 1:100 |
| *anti-rb 488* | A21206 | dk | 1:500 |
| *anti-ms 568* | A11004 | gt | 1:500 |

***Table 4:*** *Outlines primary and secondary antibodies used in subsequent chapters for immunohistochemistry assays.*

## 2.6 Slide Mounting

Mounting involved making a bridge using 2 strips of double-sided sticky tape with a 3mm gap in the centre of the slide (76x26mm Slides, Thermo). Brains were positioned in the gap before placing a large (22x40mm) coverslip (Cover Glass, Thermo) on top and immersing in vectashield with/without DAPI (Mounting Medium with/without DAPI, Vector).

## 2.7 Confocal Microscopy

Z-stack images of adult brains were captured using a spinning disk confocal microscope (LSM 900, Zeiss) using 20X-40X objectives. In Zen 2.6 (Blue Edition) programme, settings were made according to the strength of the GFP signal. Fluorescence was measured in i) 488nm channel (GFP) and/or ii) 561nm channel (mcherry). For most experiments, laser intensity was set to 50% in all channels, with an exposure time of 150 ms and binning settings 2 x 2. Only when investigating phosphoinositide dynamics were settings altered slightly, such that laser intensity was set to 15% in all channels, and binning settings to 3 x 3. All images were recorded with the specific contrast settings outlined in **Table 5**.

| Chapter | Experiment | Channel | Black | Gamma | N1 | N2 | White |
|---|---|---|---|---|---|---|---|
| **3** | Optimisation | 488 nm | 100 | 1 | 0.45 | 1 | 7500 |
| | | 561 nm | 0 | 1 | 0.45 | 1 | 15000 |
| **4** | Screen | 488 nm | 0 | 1 | 0.45 | 1 | 5000 |
| | | 561 nm | 0 | 1 | 0.45 | 1 | 15000 |
| **4** | Verification | 488 nm | 100 | 1 | 0.45 | 1 | 7500 |
| **5** | Characterisation | 488 nm | 100 | 1 | 0.45 | 1 | 7500 |
| **6** | Epistasis | 488 nm | 100 | 1 | 0.45 | 1 | 7500 |
| **6** | Draper | 488 nm | 0 | 1 | 0.45 | 1 | 1000 |
| **6** | PIP2 | 488 nm | 0 | 1 | 0.45 | 1 | 16384 |
| **6** | PIP3 | 488 nm | 0 | 1 | 0.45 | 1 | 16384 |
| **6** | GCAMP | 488 nm | 0 | 1 | 0.45 | 1 | 500 |

***Table 5:*** *Summarises the imaging setting details of each experiment in order of appearance.*

## 2.8 Fluorescence Measurements

Fluorescence was measured consistently across experiments; however some adjustments were made to accommodate the assay in question.

### 2.8.1 Olfactory Neuron GFP Analysis

In a qualitative analysis of engulfment phenotypes in all **Chapters**, hyper-stacks from each brain were examined slice per slice, using Fiji (http://imagej.net/Contributors), and the presence of an axon/glomeruli was recorded in a binary format. Binary measurements were converted into percentages for each experimental group by taking an average of the presence/absence of structures at each time point. In quantitative analysis of engulfment phenotypes, slices were inspected and z-projected if glomeruli or axons were present - if there was no obvious staining, all slices were projected. Using the freehand selection tool, the right glomerulus was accurately traced, and mean pixel fluorescence was measured (**Fig.10a**). Next, this selection was translated to a local representative section of background, without altering the area, and mean GFP intensity was measured (**Fig.10b**). This process was repeated for the

left glomerulus. In addition, a small segment of axon (**Fig.10c**) and background (**Fig.10d**) were traced on both sides of the brain using the same protocol. Mean structure fluorescence was then normalised to background fluorescence and averaged per brain producing a single n value.

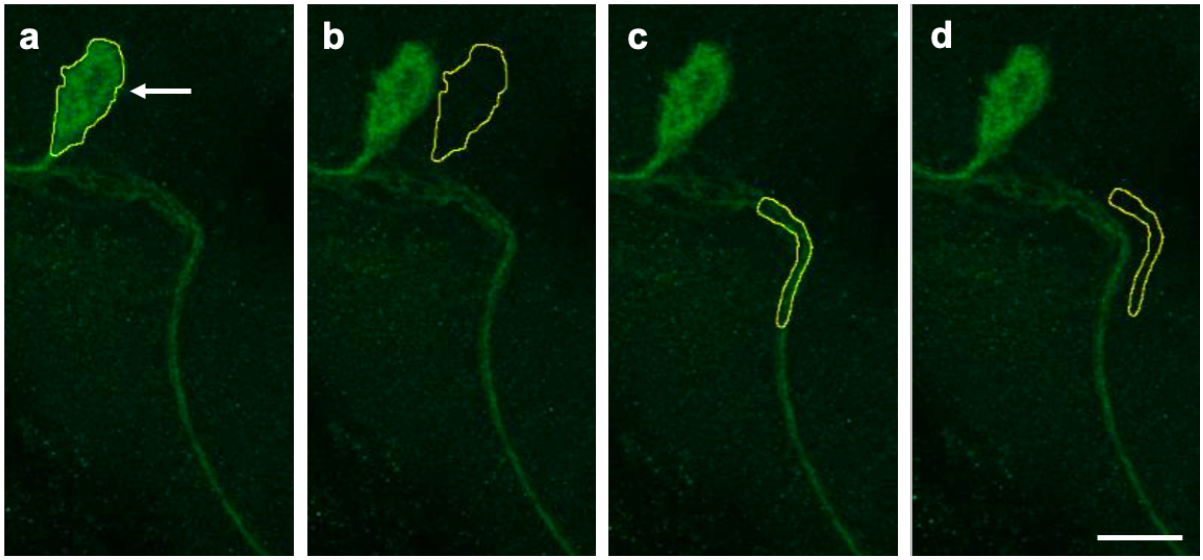


***Fig. 10. Example Tracing of Neuronal Structures.*** *Measurements were taken summarising the mean fluorescence of a determined area using the freehand tool.* ***a)*** *Glomeruli (white arrow) were traced after projecting slices with the same trace taking a measurement adjacent to the original area* ***b)*** *representing background fluorescence.* ***c)*** *a representative section of traced axon which was then moved across to take a background measurement* ***d)****. Scale bar 50µm. Genotypes: a – d: w-;OR85e-mCD8::GFP/+;repo-GAL4/+.*

### 2.8.2 Antennal Lobe Analysis

In a quantitative analysis of glial changes after antennal injury in **Chapter 6**, slices were inspected and z-projected. Using macros designed for each experiment, a reading was taken from individual antennal lobes and averaged to produce a single n value for each brain sample. Based on previously published analysis methods (MacDonald et al. 2006), Draper upregulation was measured by drawing a consistently shaped rectangle **(Table 6)** on the border of the antennal lobe, where Draper signal is most prominent. Mean gray value measurements were taken on both sides of the

brain, with the average producing a single data point. In PIP2 and PIP3 experiments, GFP signal was quantified by drawing an equal-sized oval and taking mean gray value measurements of the individual antennal lobes. The data was combined per brain producing a single data point. The same methods were used when investigating $Ca^{2+}$ changes except using another specialised macro.

| Chapter | Experiment | Macro |
|---|---|---|
| **6** | Draper | *makeRectangle (303, 257, 91, 26)* |
| **6** | PIP2 | *makeOval (327, 218, 142, 149)* |
| **6** | PIP3 | *makeOval (327, 218, 142, 149)* |
| **6** | GCAMP | *makeOval (433, 323, 244, 230)* |

***Table 6:*** *Summarises the macros used to analyse images in Chapter 6.*

### 2.8.3 Imaging Statistical Analysis

Statistical analysis was performed on GraphPad Prism Software (version 9.3.1), with data checked for normality by Shapiro-Wilk tests and QQ plots assessed for normal distribution. For large datasets and qualitative comparisons, analysis was achieved through a Kruskal Wallis test or a 1-way ANOVA, accompanied by Dunn's, Sidak's or Dunnett's multiple comaprisons (MC) tests to investigate individual differences. When comparing two or more variables, a 2-way ANOVA was used with Tukey's MC tests.

## 2.9 Molecular Biology

### 2.9.1 DNA Extraction

Wildtype gDNA samples were used to test and optimise genetic primers for qPCR (**Table 9**). Unaged whole-body samples were freshly prepared using a squishing buffer DNA extraction method adapted from (Gloor et al. 1991). Fly tissue was homogenised in 50uL of squishing buffer (SB): 10 mM Tris-Cl pH 8.2, 1 mM EDTA, 25 mM NaCl. A further 100uL of squish buffer was added along with 1uL Proteinase K (200 ug/mL), before incubating at 37$^{o}$C for 60 mins. Finally, to degrade the enzyme, samples were incubated for a further 10 mins at 85$^{o}$C before storing at -20$^{o}$C.

### 2.9.2 Polymerase Chain Reaction

Freshly extracted DNA was prepared and expanded using 5X GoTaq® DNA Polymerase and a protocol adapted from Promega corporation (Part #9PIM300). Reagents were added to DNA samples according to **Table 7** and incubated in a thermal cycler (SimpliAmp™ Thermal Cycler, Applied Biosystems), preheated to 95$^{o}$C. The thermal cycling protocol included an initial denaturation step, followed by an annealing step set to the temperature recommended for each primer set (61$^{o}$C). DNA was then expanded over a further 35 cycles before a final extension at 73$^{o}$C (**Table 8**). Primers used in this experiment are listed in **Table 9**.

| **Reagent** | **25uL RxN** | **Final Concentration** |
|---|---|---|
| GoTaq Green Master Mix, 2X | 12.5uL | 1X |
| 10uM Forward Primer | 0.25-2.5uL (1.25uL) | 0.5uM |
| 10uM Backward Primer | 0.25-2.5uL (1.25uL) | 0.5uM |
| Template DNA (30ng/uL) | 1-5uL (4uL) | <1000ng |
| | | |
| Nuclease Free $H_2O$ | Up to 25uL (6uL) | - |
| | | |
| ***Total reaction volume:*** | 25uL | - |

***Table 7:*** *List of reagents and quantities used in PCR reaction.*

| Step | Temp (°C) | Time |
|---|---|---|
| Initial Denaturation | 95 | 2 minutes |
| | 95 | 30 seconds |
| 35 Cycles | *50-72 | 45 seconds |
| | 73 | 1 minute |
| Final Extension | 73 | 5 minutes |
| Hold | 4-10 | |

***Table 8:*** *Summary of incubation temperatures and times used at each step.*

| Gene/Name | Direction | Sequence |
|---|---|---|
| ACTIN-1 | FWD | TCG ATC ATG AAG TGC GAC GT |
| ACTIN-1 | REV | ACC GAT CCA GAC GGA GTA CT |
| PLD3-1 | FWD | ATG CCG GAA TAC AAG AAG CTA GA |
| PLD3-1 | REV | CGC GGT TGG AAG TAG GAG C |
| SL-1 | FWD | CCG GTC GAT AAG TCC TGG AA |
| SL-1 | REV | CTG CCA CCT TCA AGT TTC CC |

***Table 9:*** *List of primers used in PCR experiments.*

### 2.9.3 Gel Electrophoresis

PCR samples were run on a 1.5% agarose gel using a protocol adapted from addgene.org (Addgene: Protocol - How to Run an Agarose Gel). A 1.5% agarose gel was prepared according to the size of DNA fragments (100bp-3kb). Agarose was mixed in Tris-acetate-EDTA (TAE) buffer 1X: 242g Tris-Base, 57.1mL Acetate (100% acetic acid) and 100mL of 0.5M Sodium EDTA in 1L ddH2O. After bringing the mixture to a boil, 2.5uL of Nucleic Acid Stain (SafeView, NBS Biologicals) was added and left to set for approx. 1 hr. 10uL of DNA sample mixed with Gel loading buffer (BlueJuice™, ThermoFisher) was loaded into wells and run at 80-100V for 1-2hours in TAE 1X buffer. Gels were then imaged using image analysis software GENESys (version 1.6.7.0) in a G:Box (Chemi-XX9, Syngene).

### 2.9.4 Snap Freezing

In RNA quantification experiments, *Drosophila* heads were frozen using a characterised “snap freezing” method adapted from (Jensen et al. 2013). This method ensures minimal RNA degradation and freezes transcripts in time to promote qPCR accuracy. After selection, whole flies were transferred to vials and immersed in liquid nitrogen. Then, whilst keeping everything chilled on dry ice, samples were pushed through a sieve leaving the heads which were immediately transferred to a fresh tube and stored at -80$^{o}$C.

### 2.9.5 RNA Extraction

RNA was extracted from frozen heads using TRIzol reagent (TRIzol™, ThermoFisher) and a method adapted from TRIzol® Max™ Bacterial RNA Isolation Kit (#16096020, ThermoFisher). >10 heads were homogenised in 250µL of TRIzol, with a further 250µL added after tissue breakdown. Samples were incubated for 5 mins at RT, then spun for 5 mins at 10,000xg (4$^{o}$C) to pellet undissolved tissue. After transferring the supernatant to a fresh tube, 100µL chloroform (200µL per 1mL TRIzol) was added, shaken and incubated for a further 5 mins at RT. Samples were thereafter centrifuged for 15 mins at full speed (4$^{o}$C), with the upper aqueous phase removed and loaded into a fresh tube. An equal volume of isopropanol was added, incubated for 10 mins at RT and spun for a further 10 mins at full speed (4$^{o}$C). The supernatant was discarded and washed with 70% ethanol (EtOH) to disrupt the pellet before being spun at full speed for 3 mins (4$^{o}$C). After repeating this step 1-2 times, the RNA pellet was left to dry for 30 mins before being resuspended in ~20µl RNase-free water and stored at -80$^{o}$C for further use.

### 2.9.6 cDNA Synthesis

RNA was converted into cDNA using QuantiTect® Reverse Transcription Kit (No. 205311, QIAGEN). RNA samples were quantified using a nanodrop (DeNovix DS-11, ThermoFisher), then diluted in RNAse free water to make up consistent concentrations (1ug/14µL). Precipitates were dissolved in Wipeout buffer before vortexing to minimise

genomic DNA (gDNA) expansion, by adding 1ug of RNA template to optimised quantities of reagents as listed in **Table 10**. A reverse-transcription master mix (MM) was prepared on ice according to **Table 11**. Template RNA was added as a final step and incubated for 15 mins at 42°C, then for 3 mins at 95°C to inactivate the reverse transcriptase. Note that half the samples were incubated with reverse transcriptase whilst the other half were incubated in a second master mix with RNAse-free water to use as controls in later experiments. Reverse-transcription reactions were then stored at -20°C.

| **Reagent** | **Volume/reaction** |
|---|---|
| gDNA Wipeout Buffer, 7X | 2µL |
| Template RNA, up to 1ug* | Variable (5µL) |
| RNAse-free water | Variable (7µL) |
| ***Total reaction volume:*** | 14µL |

***Table 10:*** *List of reagents added to eliminate genomic DNA.*
**This corresponds to the entire amount of RNA present, including any rRNA, mRNA, viral RNA and carrier RNA present, and regardless of primers or cDNA analysed.*

| **Reagent** | **Volume/reaction** |
|---|---|
| Quantiscript Reverse Transcriptase*# | 1µL |
| Quantiscript RT Buffer, 5X+ | 4µL |
| RT Primer Mix | 1µL |
| Template RNA (entire product of gDNA elimination) | 14µL |
| ***Total reaction volume:*** | 20µL |

***Table 11:*** *List of reagents added for reverse transcription.*
**Also contains RNAse inhibitor.*
*+Include $Mg^{2+}$ and dNTPs.*
*#Substituted for RNAse-free water in control reactions.*

### 2.9.7 Real-time qPCR

Real-time PCR (qPCR) was carried out to quantify expanded transcripts using Maxima SYBR™ Green/ROX qPCR Master Mix (2X) (#K0251, ThermoFisher) following a method adapted from ThermoFisher (#K0525, ThermoFisher). DNA was diluted 1/5 in nuclease-free (NF) water and master mixes were prepared with different primers according to **Table 12**. Primers used included PLD3-1FWD/REV (**Table 8**) and primers specific to housekeeping genes *GAPDH* and *RP49*. 7µL of MM was plated along with 3µL of cDNA on a MicroAmp™ 384-Well Reaction Plate with barcode (#4309849, ThermoFisher), according to **Fig. 11**. We plated three biological replicates per genotype with four technical replicates and two controls per group. The plate was run in a QuantStudio™ 7 Flex Real-Time PCR System (#4485701, ThermoFisher) using Quantstudio software (QuantStudio™ 5, ThermoFisher). Temperature and cycles were set according to **Table 13** and left to run for 1-2 hrs before analysis.

| **Reagent** | **Volume/reaction** |
|---|---|
| SYBR™ Green | 570µL |
| FWD Primer (10uM) | 34µL |
| REV Primer (10uM) | 34µL |
| ROX (5uM) | 2.3µL |
| NF Water | 159.7µL |
| ***Total reaction volume:*** | 800µL* |

***Table 12:*** *List of reagents added to make SYBR master mix for qPCR.*
**Amounts used to prepare the master mix for 12 biological repeats per primer set.*

| Step | Temp (°C) | Time |
|---|---|---|
| Hold Stage | 58 | 2 minutes |
| | 95 | 30 seconds |
| PCR Stage, 40X | 95 | 15 seconds |
| | 61 | 30 seconds |
| | 72 | 30 seconds |
| Melt Curve Stage | 95 | 15 seconds |
| | 60 | 1 minute |
| | 95 | 15 seconds |

***Table 13:*** *Summary of incubation temperatures and times used at each qPCR stage.*

### 2.9.8 qPCR Analysis

qPCR analysis was performed following methods adapted from (Pfaffl 2001; Ruijter et al. 2009). Firstly, data was cleaned in QuantStudio (QuantStudio™ 5, ThermoFisher), where wells were analysed, and data excluded where obvious errors (such as melt curve irregularities) were identified. Data were then exported as an Excel sheet (Excel, Microsoft). Using RStudio (R 4.1.2), data were uploaded and analysed for significance using a preloaded package (library(qpcR)), following a script optimised by Dr Daniel Maddison. Results were uploaded to GraphPad Prism Software (version 9.3.1) and plotted as bar charts with significance annotated according to the results of R analysis.

### 2.9.9 Protein Extraction & Quantification

In protein quantification experiments, *Drosophila* heads were removed using forceps (Carbon Forceps, Dumont) and placed in 1.5mL Eppendorf tubes on dry ice. Samples were prepared for western blot (WB) analysis via a Bicinchoninic Acid (BCA) protein assay using BCA Pierce™ BCA Protein Assay Kit (#23227, ThermoFisher). >10 heads were homogenised in 50µL of proteinase inhibitor in RIPA lysis buffer 1X, then placed on ice for 20 mins. Samples were then centrifuged at full speed for 20 mins (4°C), with the supernatant collected and placed in a fresh tube on ice. Total protein concentration was investigated by preparing Bovine serum albumin (BSA) standards as in **Table 14**.

100µL of reagents A and B were mixed 50:1 and added to 12.5µL of protein sample and incubated at 37°C for 30 mins before measuring the absorbance at or near 565nm on a plate reader (FLUOstar OMEGA). Absorbance was analysed using OMEGA software and Mars Data Analyser. Standards were plotted using Wizard tool and data was exported to Excel (Excel, Microsoft) to view the raw and processed/corrected data. The average 562nm absorbance measurement of Blank standard replicates was subtracted from 562nm measurements of all other individual standard and unknown sample replicates, preparing a standard curve plotting the average Blank-corrected measurement for each BSA standard vs its concentration ug/mL. These calculations gave the protein concentration of each unknown sample. Samples were then diluted to 40ug/20µL and stored at -80°C.

| **Vial** | **Volume of Dilunt dd$H_2O$ (µL)** | **Volume of Source of BSA (µL)** | **Final BSA Concentration (ug/mL)** |
|---|---|---|---|
| **A** | 0 | 300 of stock | 2000 |
| **B** | 125 | 375 of stock | 1500 |
| **C** | 325 | 325 of stock | 1000 |
| **D** | 175 | 175 of vial B | 750 |
| **E** | 325 | 325 of vial C | 500 |
| **F** | 325 | 325 of vial E | 250 |
| **G** | 325 | 325 of vial F | 125 |
| **H** | 400 | 100 of vial G | 25 |
| **I** | 400 | 0 | 0 = Blank |

***Table 14:*** *Dilution Scheme for Standard Test Tube Protocol and Microplate Procedure – working range 20-2000µg/mL.*

### 2.9.10 Western Blotting

Western blots were prepared using a lab-optimised protocol by Uroosa Chughtai. Protein lysate was diluted in LaemmLi loading buffer (#1610737) to make a consistent concentration and boiled at 95$^{o}$C for 5 mins before being loaded. 5µL of protein ladder Page ruler plus (#26619, ThermoFisher) was added to well 1 and 40µL of sample were added to subsequent wells of NuPAGE Bis-Tris 20-well gel. The gel was placed in a Mini gel tank (#A25977, ThermoFisher), filled with Bolt MES SDS buffer 1X in dd$H_2O$. The gel was then run at 150V for approx. 40 mins, removed from the tank and the protein transferred to a membrane. Using a nitrocellulose (NC) mini stack (IB23002, ThermoFisher), protein was blotted in a dry transfer reaction using an iBlot$^{TM}$ 2 Gel Transfer Device (IB21001, ThermoFisher). Membrane total protein was assessed using Ponceau S before being submerged in blocking solution (5% Milk in TBS-T) for 1hr. Samples were then incubated in primary antibodies (**Table 4**) overnight at 4$^{o}$C. The following day, blots were washed in TBS-T before incubating in secondary antibodies (**Table 15**) for 1hr in 5% milk, with final washed in TBS-T before imaging.

| Name | Stock Number | Host | Dilution |
|---|---|---|---|
| IR anti-ms 800CW | ab216772 | gt | 1:10000 |
| IR anti-rb 800CW | ab216773 | gt | 1:10000 |
| IR anti-rb 680CW | ab216777 | gt | 1:10000 |

***Table 15:*** *Outlines secondary antibodies used for western blot assays.*

### 2.9.11 SCope Analysis

As RNAi expression was restriced to glial populations, we selected for *repo*$^{+}$ cells using the laso tool in the SCope (http://scope.aertslab.org/#/) filtered adult brain dataset. This isolated cells, where *repo* expression was dense, taking them forward for analysis. Normalised (counts per million) *Draper, sl* and *Pld3* expression were mapped within the same selection and exported by cluster of age, genotype and cell. Mean expression of *Draper, sl* and *Pld3* was recorded per cluster (Excel) and summarised in a heat map (MATLAB, v.R2020a). Since the dataset included mean values across different ages (0/1/3/6/9/15/30/50 days), we repeated the analysis for each time point. We repeated analysis on 5 clusters (10/14/60/66/70) for which data existed at each time point. Additionally, we split this analysis by genotype: W1118 vs. DGRP-55.

# 3 Biological and Environmental Variability on the Rate of Glial Engulfment

## 3.1 Introduction

Research already exists to ascertain the essential roles of *Drosophila* glia in neural circuit formation, function, and plasticity to propose hypotheses for human glial function and pathologies (Awasaki et al. 2006; MacDonald et al. 2006; Ziegenfuss et al. 2008; Logan et al. 2012; MacDonald et al. 2013; Musashe et al. 2016; Ray et al. 2017). Increasing evidence highlights the heterogeneous nature of neurodegenerative disorders, attributing pathology to both environmental and genetic origins (Jones et al. 2015; Cuyvers and Sleegers 2016; Leonenko et al. 2019; Uddin et al. 2021). To untangle the complex array of risk factors in microglial function in AD, we have used a frequently published system which measures the rate of glial engulfment in response to neuronal injury (MacDonald et al. 2006). Highly sensitive glia are swiftly recruited to the site of injury, responding to damage and stress by extending membrane projections, upregulating pro-inflammatory genes, and initiating a phagocytic pathway to clear damaged neurons (Ziegenfuss et al. 2008). Activated glia round-up and sequester dying material, efficiently removing debris over a period of 5 days. This rapid clearance of dying cells helps to repress potentially damaging secondary inflammatory responses which can exacerbate tissue damage and cell stress (Purice et al. 2016). This balance of inflammatory activation and neuronal health preservation suggests biological adaptation, especially as the brain becomes more vulnerable with age (Takahashi et al. 2005). To understand how certain contexts may impact glial engulfment in our model, the chapter explores biological and environmental variability such as sex, rearing temperature, and age on the process of engulfment.

### 3.1.1 Sexual Dimorphism in Glial Biology

Sex-specific variation is becoming increasingly important in biomedical research, especially with the underrepresentation of females in clinical trials and model studies (Geller et al. 2011; Parekh et al. 2011; Poon et al. 2013; Liu and Dipietro Mager 2016). Sex differences are continuously being documented in the field of neuroscience sometimes becoming the focus of study. Such variations have been observed in the increased incidence of Alzheimer's disease in women compared to men (Anstey et al. 2021), sexual dimorphism of the brain in mouse models (Spring et al. 2007) and *Drosophila* innate immune responses to infection (Belmonte et al. 2020).

Select studies have found that women are almost twice as likely to develop Alzheimer's disease compared to men (Beam et al. 2018; Anstey et al. 2021). The most plausible explanation is prolonged life expectancy in women however this is also a caveat in many studies wanting to address any underlying biological and pathological differences. Emerging evidence also proposes sex-specific reasons, which suggest unique biological differences beyond longevity, such as sleep patterns, stress, depression, hormonal differences, immunity, and genetic variation (Goveas et al. 2011; Vest and Pike 2013; Johansson 2014; Choleris et al. 2018; Paranjpe et al. 2021). In a study that identified sex differences in human olfactory function, researchers also identified that female bulbs contained 49.3% more neurons and 38.9% more non-neuronal cells (including glia) than men (Oliveira-Pinto et al. 2014).

A comprehensive study, using 3D magnetic resonance imaging (MRI) investigated the morphological asymmetry in male and female mouse brains and found that certain brain regions varied significantly in size between sexes (Spring et al. 2007). Structures such as the thalamus were larger in males and the anterior hippocampus larger in females (Spring et al. 2007). Equally, another study identified genetic variation in Estrogen Receptor 1 (Esr1)+ neuronal populations of male and female mice in oestrous states, leading to sex-specific behaviours. Together, the biological, and functional specialisation of dimorphic cell types enabled sex hormone-responsive populations to regulate diverse behaviours (Li and Dulac 2018). Finally, sex-specific phenotypes have been observed in *Drosophila* immunity, whereby studies found profound sex dimorphisms in immune system response at baseline, after infection and with age (Shen et al. 2009; Leech et al. 2019). Dimorphic survival was observed after infection by specific pathogens, such that females were more likely to survive a *Kalithea* (virus) infection and males were more likely to survive a *Pseudomonas aeruginasa* (bacterium) infection (Belmonte et al. 2020). Equally, during development female white prepupae have been reported to contain higher numbers of specialised immune cells known as hemocytes, but this difference wasn't visible as they reached adulthood (Kleinhesselink et al. 2011). Although not always the case, the consistent discovery of sex-specific phenotypes calls for studies to take new approaches to research, whereby sexes are investigated separately, and both are prioritised where possible. Understanding the evolutionary causes of sex-specific variation will expand

our understanding of sexual dimorphism in disease and will help to inform sex-targeted and sex-appropriate medical interventions.

### 3.1.2 Temperature Control of Glial Phenotypes

Among other variables, environmental conditions such as rearing temperature can alter *Drosophila* phenotypes during experimentation, sometimes resulting in entire publications dedicated to the cause. However, the role of temperature extends to neuron-glial interactions and behaviour in other models (Bracho and Orkand 1972). Therapeutic hypothermia is used to treat brain injury in experimental models and patients and has been shown to modulate glial hyperactivation under different injury conditions (Kim et al. 2013).

Hypothermia treatment can provide neuroprotection by regulating signalling pathways, including glutamate signalling, cell death, and stress response (Kim et al. 2013). In other studies, microglial cultures were subjected to both mild (33$^{o}$C) and moderate (29°C) hypothermic conditions at different stages before, during or after stimulation, which led to changes in microglial phenotypes (Seo et al. 2012). Treating microglia at early-, co-, and delayed-hypothermic treatments inhibited the production of inflammatory mediators to varying degrees. When modelling stab wounds, delayed local hypothermia reduced migration towards the site of injury in rat brains (Seo et al. 2012). In murine models, hypothermia has been shown to affect the volume of glial cells, such that moderate hypothermia (27$^{o}$C) led to a rapid cell swelling which partially recovered, shedding light on the physical impacts of temperature on glia (Plesnila et al. 2000). Across *Drosophila* studies, scientists tailor the temperature at which flies are raised (18$^{o}$C, 25$^{o}$C or 29$^{o}$C) to suit the experiment; for instance, if using GAL4 to mediate gene expression, a higher temperature is preferable to maximise expression levels and improve the possibility of identifying a phenotype. However, adjusting temperature to suit the study may result in unknown downstream effects. For instance, *Drosophila* typically grow faster when raised at warmer temperatures but can eclose smaller in size, with the reverse being true at lower temperatures (Miquel et al. 1976; Vermeulen and Bijlsma 2003). Furthermore, adult *Drosophila* acclimated to warm (21.5$^{o}$C) or cold conditions (6$^{o}$C) can have starkly different transcriptomes. A study

found that cold acclimation led to an extensive reorganisation of the transcriptome with downstream effects on the metabolome resulting in better cold tolerance (MacMillan et al. 2016). Results implicated dopamine signalling and $Na^+$-driven transport as well as previously identified genes and pathways such as heat shock proteins, $Ca^{2+}$ signalling and reactive oxygen species (ROS) detoxification (MacMillan et al. 2016). Developmental temperature has also been associated with changes in the connectome, such that brain connectivity inversely scales with rearing temperature. Developmental temperature affected the number of synapses and synaptic partner availability during development (Gallio et al. 2011; Kiral et al. 2021). These studies highlight how sensitive *Drosophila* are to their environment during development but also in adulthood and demonstrate the importance of testing models at various temperatures to avoid additive phenotypes. There are few studies available on the impact of temperature on glial function and *Drosophila* present an excellent model to study it. Despite the emerging temperature-specific differences in many aspects of *Drosophila* neurobiology, it remains unclear if glial phenotypes such as engulfment can vary with rearing temperature.

### 3.1.3 Age and Glial Dysfunction

Advanced age is the greatest risk factor in dementia, highlighting the heterogeneous nature of neurodegenerative disease, and yet the mechanisms that cause the senescent brain to be more vulnerable are unclear (Stephan et al. 2018; Gabandé-Rodríguez et al. 2020; Delage et al. 2021). Glial responses provide neuroprotection but are also known to exacerbate aspects of disease when unregulated (Abbott 2018; Bachiller et al. 2018; Moore et al. 2019). Given the correlation between glial activity and neuronal health, glial function may decline with age rendering the aged brain more susceptible to infection, neurodegeneration, and trauma (Spittau 2017).

Age-related research has largely focused on neuronal cell populations; however, emerging evidence from genetic and transcriptomic studies showed that glial cells are the first to change with age, responding differently to “stress” in the ageing CNS (Soreq et al. 2017; Palmer and Ousman 2018). Glial cells are likely to upregulate pathways that negatively impact neuronal and synaptic function in ageing brains (Boisvert et al.

2018; Clarke et al. 2018). Signs of cellular senescence have also been observed in glial populations of ageing cultures, such as telomere shortening (Flanary and Streit 2004). Mouse studies have unveiled morphological and functional differences in microglia and astrocytes in aged animals compared to young counterparts. The cells often displayed enlarged soma and shorter projections in older animals and appeared functionally restricted (Hefendehl et al. 2014). These age-related changes with growing evidence of transcriptional changes suggest glia may become compromised in their ability to respond to neuronal degeneration or stress (Niraula et al. 2016). This is supported by certain cell culture studies where microglia harvested from older animals displayed defective phagocytic activity (Damani et al. 2011). Recent studies in *Drosophila* have explored glial function in ageing animals and found their ability to phagocytose neuronal debris in response to injury is significantly delayed in aged flies. This steep delay is attributed to reduced PI3K signalling and by consequence lower upregulation of conserved phagocytic receptor Draper/MEGF10 (Purice et al. 2016). The study also discovered that early hallmarks of Wallerian degeneration in injured neurons were delayed in aged animals (Purice et al. 2016). This research stresses the need to interrogate the molecular dynamics of glia and neurons in ageing subjects and to apply this knowledge to disease model systems.

## 3.2 Aims and Objectives

It has been proposed that glial function may vary as a result of sex, temperature or age. Previous studies using the glial engulfment model have not disclosed further testing of such variables on the model system and how manipulating sex or temperature could impact the rate of engulfment. Although existing research in *Drosophila* has highlighted a significant decline in phagocytic activity in aged flies, only two age ranges were investigated (young flies were between 7 and 14 days old, whereas aged flies were between 56 and 63 days old) (Purice et al. 2016), leaving a significant gap between age groups. This chapter seeks to understand the effect of biological variables on the efficiency of glial engulfment and aims to identify the ideal conditions for future use of the model system.

## 3.3 Experimental Design

Glial engulfment rate is measurable using the characterised ORN model system introduced above and in **Chapter 1**. This injury response system was harnessed to investigate the impact of multiple experimental variables on glial function. *w-;+/+,+/+*, and ;*UAS-Draper RNAi* (#27086*)* males were crossed to *w-;OR85e-mCD8::GFP/+;repo-GAL4/TM3, Sb, e-* virgins and raised under specific conditions depending on the variable in question **Fig. 11**. Crosses which addressed the effect of temperature were kept at RT for 24 hrs before being reared in separate incubators set to 25°C and 29°C respectively. Parents were flipped onto fresh food every 2 days and F1 progeny were aged for 7 days upon eclosion. Crosses used to address sex and age-specific variables were kept at RT for 24 hrs, before being transferred to a 29°C incubator, where parents were flipped onto fresh food every 2 days. For experiments addressing sex differences, F1 progeny were split into male and female groups and aged for 7 days before analysis. In age-specific experiments, mixed F1 progeny were split into 4 groups and aged for 1, 7, 14 and 30 days before analysis. Five brains per experimental group were injured, dissected, and stained consistently, as outlined in **Chapter 2.** The presence/absence of neuronal axons and overlapping synapses at glomeruli was recorded as a percentage and investigated for significance as described in **Chapter 2.** Normality and gaussian distribution were assessed using the Shapiro-Wilk test and QQ plots were checked for outliers. Data were then analysed using a 2-way ANOVA and Tukey's MC tests. A table of the *Drosophila* lines used in this Chapter can be found below (**Table 16**).

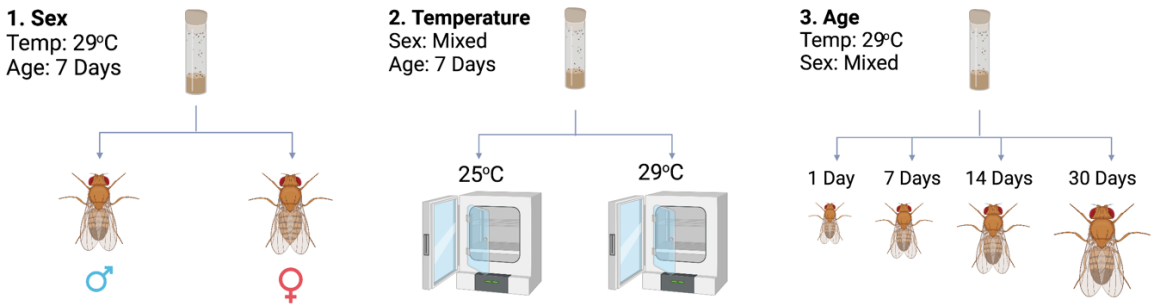

***Fig. 11. Outline of Experimental Design.*** *A graphical representation of the specifications of each experiment dependent on the variable being studied.* ***(1)*** *Investigates the impact of sex, where males and females were separated before dissection and analysis.* ***(2)*** *Investigates temperature, where flies were raised at 25°C and 29°C.* ***(3)*** *Studies the impact of age, where F1 progeny were aged for 1, 7, 14 and 30 days before injury and analysis.*

| **Stock** | ***Genotype*** | **Stock Number** | **Source** |
|---|---|---|---|
| Virgin Line | *w-;OR85e-mCD8::GFP/+;repo-Gal4/TM3, Sb, e-* | n/a | Lab Stock |
| w- | w-;+/+;+/+ | n/a | Lab Stock |
| Draper RNAi | *w1118; P{GD14423}v27086* | 27086 | VDRC |

***Table 16.*** *A table combining all stock information used in this Chapter, including name abbreviation, genotype, stock number and source.*

## 3.4 Results

### 3.4.1 The Rate of Glial Engulfment of Injured Neurons is not Differentially Affected by Sex

Existing data suggest that glia take approximately 5 days to successfully engulf injured neurons, starting with axons after 24hrs and eventually glomeruli by 5DPA (MacDonald et al. 2006). When comparing *w-* males (**Fig. 12a**) and females (**Fig. 12b**), GFP+ structures declined at similar rates post-injury. GFP+ axons were recorded in 40% of males and females equally after 1DPA, reducing to 20% by day 3 and 0% by day 5 (**Fig. 12c**). A 2-way ANOVA revealed that there was no significant difference between experimental groups or time points. Similarly, GFP+ glomeruli were recorded in 100% of samples in both male and female groups up to 3DPA, reducing to 20% in males and 0% in females by day 5 (**Fig. 12d**). Statistical comparisons suggested data were significantly different across timepoints ($p<0.0001$), however not between groups, implying that the sex of flies had no significant bearing on the rate of engulfment. When knocking down *Draper,* neuronal structures were equally visible in males (**Fig. 12e**) and females (**Fig. 12f**), despite injury. GFP+ axons were observed in 100% of male and female samples respectively up to 5DPA (**Fig. 12g**). This did not vary significantly between groups, nor time points, according to statistical analysis. Results were mirrored when recording GFP+ glomeruli, which were recorded in 100% of male and female brains up to 5DPA (**Fig. 12h**). A 2-way ANOVA revealed no significant difference between groups or timepoints, suggesting that the sex of the fly did not impact glial engulfment deficits as a result of *Draper* KD.

When comparing the engulfment rate between biological groups*,* there was a clear deficit in *Draper* KD flies across males and females. According to a 2-way ANOVA, there was a significant difference between GFP+ axons ($p<0.0001$) and glomeruli ($p<0.001$) across genotypes in both groups, with no significant difference between time points. Tukey's MC tests revealed a significant pairwise difference between *wild-type* and *Draper* KD GFP+ axon count in male ($p<0.0001$) and female ($p<0.0001$) samples (**Fig. 12i**). Similarly, there was a significant pairwise difference between GFP+ glomeruli incidence in male ($p<0.05$) and female ($p<0.01$) groups (**Fig. 12j**).

Overall, neuronal debris was only visible in *wild-type* flies at early time points after injury, which was consistent across males and females. In *Draper* KD flies, significantly more GFP+ debris was recorded in male and female groups up to 5DPA. This suggests that the rate of engulfment is not dependent on the sex of the fly under both biological conditions.

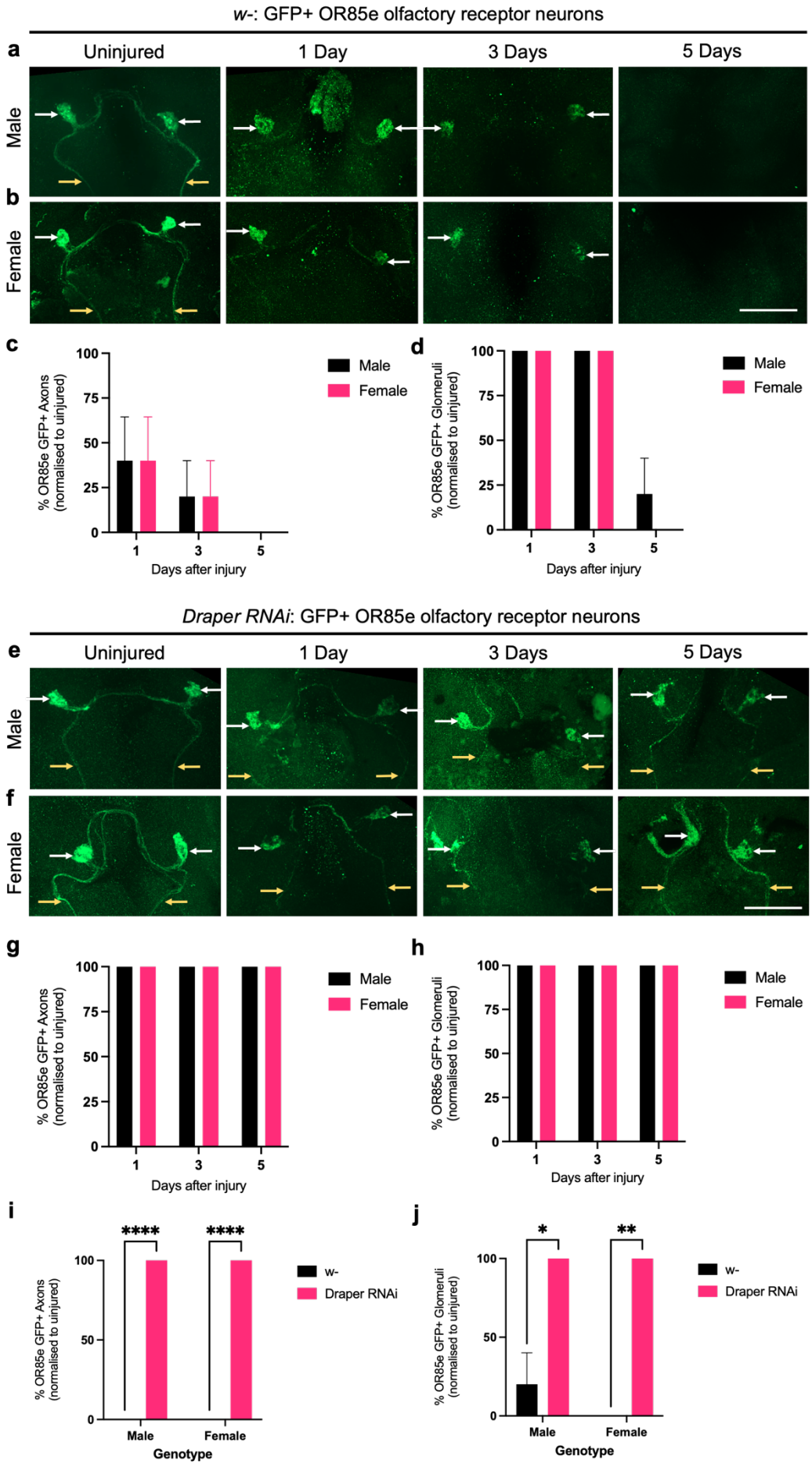
w-: GFP+ OR85e olfactory receptor neurons
a
Uninjured
1 Day
3 Days
5 Days
Male
b
Female
c
% OR85e GFP+ Axons (normalised to uinjured)
100
75
50
25
0
1
3
5
Days after injury
Male
Female
d
% OR85e GFP+ Glomeruli (normalised to uinjured)
Draper RNAi: GFP+ OR85e olfactory receptor neurons
e
f
g
h
i
****
****
w-
Draper RNAi
Male
Female
Genotype
j
*
**

***Fig. 12. Engulfment Rate Is Unaffected By The Sex. a)-b)*** *GFP-labelled maxillary ORN neurons before and after maxillary nerve axotomy in w- male* ***a)*** *and female* ***b)*** *flies respectively. Panels from left to right, show GFP+ axons (yellow arrows) and glomeruli (white arrows) fade by 5DPA.* ***c)*** *Percentage quantification of GFP+ debris in OR85e axons.* ***d)*** *Percentage quantification of GFP+ debris visible in OR85e glomeruli.* ***e)-f)*** *GFP labelled neurons before and after maxillary nerve injury in Draper KD male* ***e)*** *and female* ***f)*** *flies respectively. GFP+ axons and glomeruli were still visible 5DPA.* ***g)*** *Percentage quantification of GFP+ debris in OR85e axons.* ***h)*** *Percentage quantification of GFP+ debris visible in OR85e glomeruli.* ***i)-j)*** *Percentage incidence of OR85e axons* ***i)*** *and glomeruli* ***j)*** *in w- versus Draper KDs across male and female samples. Statistical analysis was achieved through a 2-way ANOVA and Tukey's MC tests. Graphs plotted with mean±S.E.M., with significance annotated; *p<0.05, **p<0.01, ****p<0.0001, n=5 brains per group. Scale bar = 50 µm.*

### 3.4.2 The Rate of Glial Engulfment of Injured Neurons is not Affected by Temperature

Next, the impact of temperature on the rate of glial engulfment was interpreted. As such progeny were raised at 25ºC and 29ºC respectively, with differences investigated after injury using confocal microscopy. When comparing *w-* flies raised at 25ºC (**Fig. 13a**) and 29ºC (**Fig. 13b**), GFP+ structures declined at similar rates post-injury. GFP+ axons were recorded in 40% of brains raised at 25ºC and 20% of brains raised at 29ºC after 1 day, reducing to 0% after 3- and 5DPA (**Fig. 13c**). Although axon incidence was significantly different between time points ($p<0.05$) statistical analysis revealed that the difference was not significant between experimental groups. When scoring GFP+ glomeruli, structures remained intact in 100% of brains raised at both temperatures after 1DPA, reducing to 40% in flies raised at 25ºC and 80% in flies raised at 29ºC after 3DPA (**Fig. 13d**). A 2-way ANOVA revealed that the difference between time points was significant ($p<0.01$). Although engulfment appeared slightly delayed in flies raised at 29ºC, the difference was not significant compared to those raised at 25ºC (**Fig. 13d**). This was further affirmed when GFP+ glomeruli were no longer visible in samples raised at 25ºC and only recorded in 20% of cases raised at 29ºC (**Fig. 13d**), suggesting engulfment may not be affected by rearing temperature.

When knocking down *Draper,* an obvious engulfment deficit was visible in flies raised at 25$^{o}$C (**Fig. 13e)** and 29$^{o}$C (**Fig. 13f**). Axons were recorded in 100% of animals raised at both temperatures, with no significant differences observed between experimental groups or time points (**Fig. 13g**). GFP+ glomeruli were also observed in 100% of brains raised at 25$^{o}$C and 29$^{o}$C, with no significant differences across time points and experimental groups (**Fig. 13h**). Overall, data suggested that *Draper* expression not-temperature dependent.

When comparing the engulfment rate between biological groups*,* there was a clear engulfment deficit in *Draper* KD flies regardless of rearing temperature. According to a 2-way ANOVA, there was a significant difference between the incidence of axons ($p<0.0001$) and glomeruli ($p<0.001$) after injury between biological groups, with no significant difference across time points. Tukey's MC tests revealed a significant pairwise difference between *w-* and *Draper* KD GFP+ axon count in 25$^{o}$C ($p<0.0001$) and 29$^{o}$C ($p<0.0001$) conditions (**Fig. 13i**). Similarly, there was a significant pairwise difference between GFP+ glomeruli count between groups raised at 25$^{o}$C ($p<0.01$) and 29$^{o}$C ($p<0.05$) (**Fig. 13j**).

Overall, rearing temperature did not appear to significantly alter the incidence of GFP+ structures in *w-* flies after injury. Knocking down *Draper* at either temperature led to a delay in the phagocytosis, visible up to 5 days after injury. These data suggest that rearing temperature does not have a significant bearing on the engulfment of neuronal debris in *w-* or inhibited conditions.

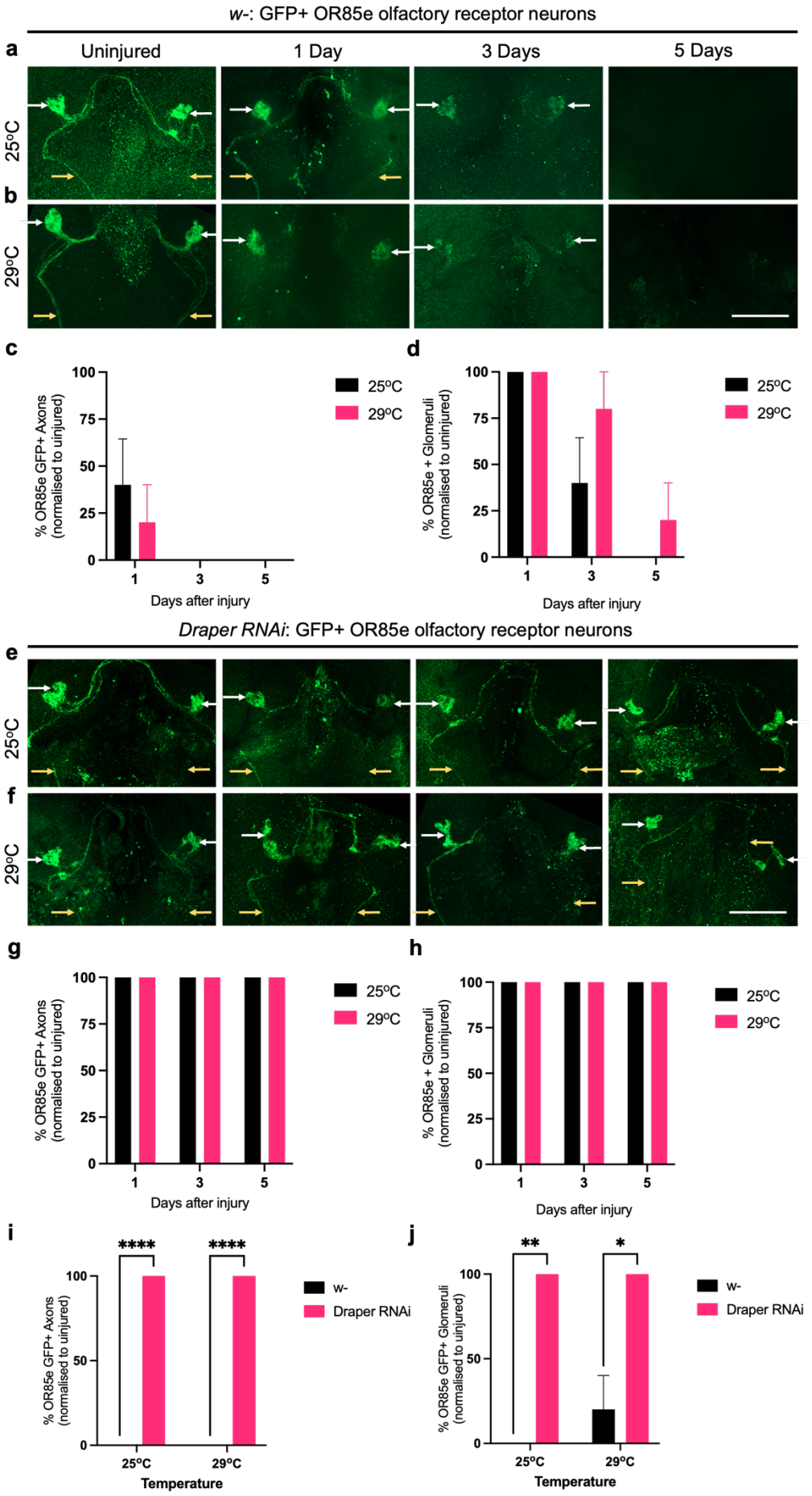
w-: GFP+ OR85e olfactory receptor neurons
a
Uninjured
1 Day
3 Days
5 Days
25°C
b
29°C
c
% OR85e GFP+ Axons (normalised to uinjured)
100
75
50
25
0
1
3
5
Days after injury
25°C
29°C
d
% OR85e + Glomeruli (normalised to uninjured)
Draper RNAi: GFP+ OR85e olfactory receptor neurons
e
f
g
h
i
****
****
w-
Draper RNAi
25°C
29°C
Temperature
% OR85e GFP+ Glomeruli (normalised to uninjured)
j
**
*

***Fig. 13. Engulfment Rate Is Unaffected By Rearing Temperature. a)-b)*** *GFP-labelled maxillary ORN neurons before and after maxillary nerve axotomy in w- flies raised at 25$^{o}$C* ***a)*** *and 29$^{o}$C* ***b)*** *respectively. Panels from left to right, show GFP+ axons (yellow arrows) and glomeruli (white arrows) fade by 5DPA.* ***c)*** *Percentage quantification of GFP+ debris in OR85e axons.* ***d)*** *Percentage quantification of GFP+ debris visible in OR85e glomeruli.* ***e)-f)*** *GFP labelled neurons before and after maxillary nerve injury in Draper KD flies raised at 25$^{o}$C and 29$^{o}$C respectively. GFP+ axons and glomeruli were still visible 5 days after injury.* ***g)*** *Percentage quantification of GFP+ debris in OR85e axons.* ***h)*** *Percentage quantification of GFP+ debris visible in OR85e glomeruli.* ***i)-j)*** *Percentage incidence of OR85e axons* ***i)*** *and glomeruli* ***j)*** *in w- versus Draper KDs across different rearing temperatures. Statistical analysis was achieved through a 2-way ANOVA and Tukey's MC tests. Graphs plotted with mean±S.E.M., with significance annotated; *p<0.05, **p<0.01, ***p<0.001, ****p<0.0001, n=5 brains per group. Scale bar = 50 µm.*

### 3.4.3 The Rate of Glial Engulfment of Injured Neurons Decreases with Age

The data in this section was collected with the help of Miss Rajini Chandrasegaram as part of a supervised undergraduate project in the lab. To examine the effect of age on glial engulfment, we aged experimental progeny for 1, 7, 14 and 30 days before injury and analysis using confocal microscopy. In flies with a wild-type background aged between 1 (**Fig. 14a**) and 7 days (**Fig. 14b**), we observed a gradual decline in GFP+ axons and glomeruli, suggesting effective engulfment. However, when examining flies aged for 14 days (**Fig. 14c**) and 30 days (**Fig. 14d**), neuronal structures were still visible during the typical engulfment period. In 1-day-old flies, we observed the immediate disappearance of GFP+ axons in 100% of brains, whereas we continued to record axons in 25% of 7-day-old brains, eventually reducing to 0% after 3DPA (**Fig. 14e**). Ageing for 14+ days led to visible axons in up to 100% of brains after 1-, 3- and 5DPA (**Fig. 14e**). A 2-way ANOVA revealed that differences in axon incidence were significant between age-groups ($p<0.0001$), but not across time points, suggesting age may indeed impact the rate of engulfment. Tukey's MC tests revealed a significant pairwise difference of axon incidence between 1- and 30-day after 1-, 3- and 5DPA (all $p<0.0001$) (**Fig. 14e**). Equally significant findings were discovered between 7- and

30-day old flies, as well as 1- and 14-day old flies. This was also the case in 30-day old flies where GFP+ axons were recorded in 100% of cases, significantly higher than 1- and 7-day old flies according to Tukey's multiple comparisons (**Fig. 14e**), suggesting a gradual decline in axon engulfment with age. Furthermore, when scoring for the presence of glomeruli, we saw the lack of GFP+ structures at 5 days in 100% of 1-day-old brains and 80% of 7-day-old brains (**Fig. 14f**). A 2-way ANOVA suggested that results varied significantly across experimental groups ($p<0.01$), and between time points ($p<0.001$). Tukey's MC tests showed that glomerulus recordings were lower in younger ($p<0.0001$) compared to older animals, where we recorded GFP+ glomeruli in 100% of both 14- and 30-day-old brains (**Fig. 14f**). Multiple comparisons showed a significant pairwise difference between GFP+ glomeruli count between 1- and 30-day old flies raised 5DPA ($p<0.0001$). This was also true when comparing 1- and 14-day-old flies, where GFP+ glomeruli were increasingly recorded in older animals 5DPA ($p<0.0001$) (**Fig. 14f**).

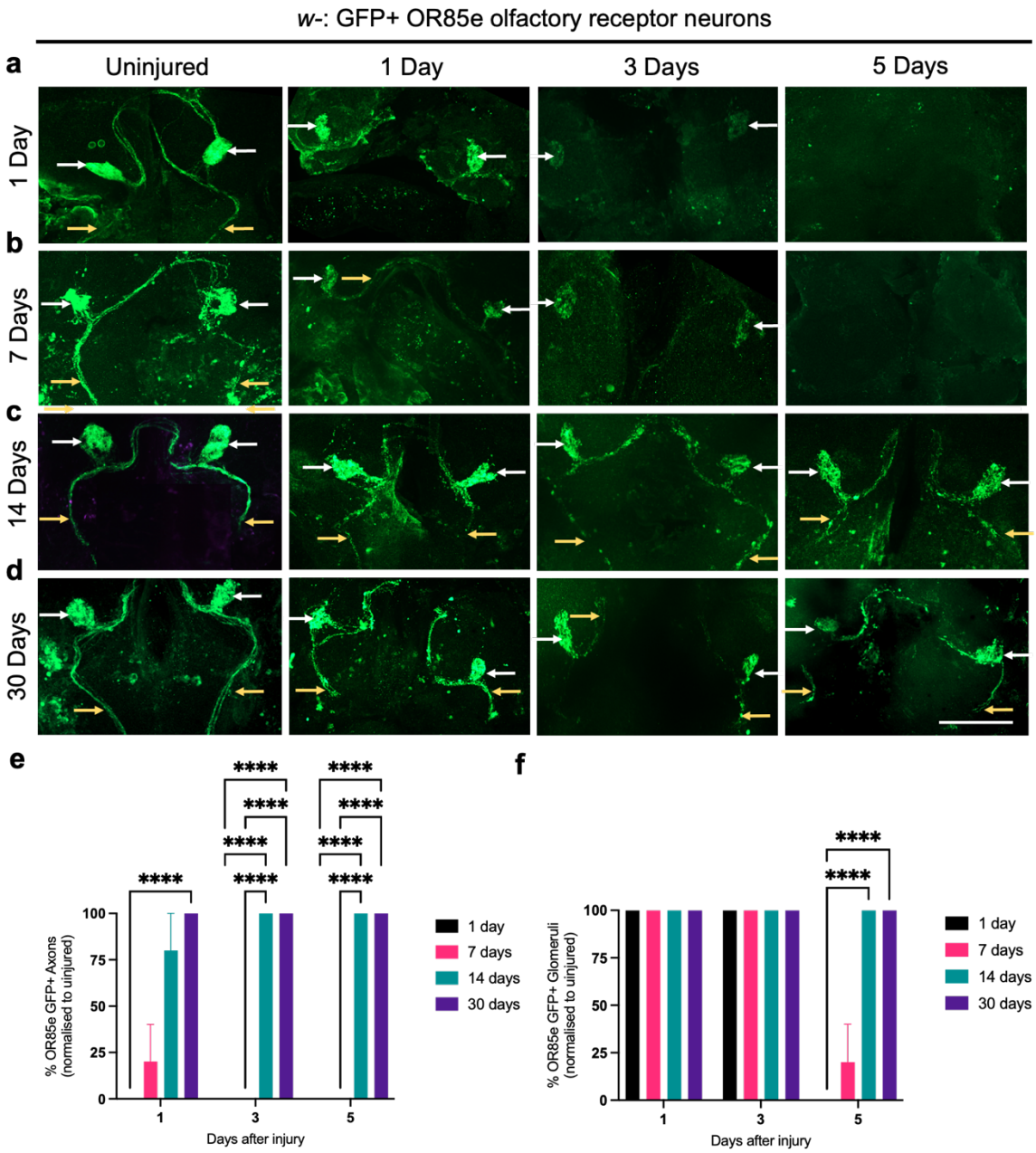


***Fig. 14. Less Neuronal Debris is Cleared with Age. a)-b)*** *GFP-labelled maxillary ORN neurons before and after maxillary nerve axotomy in w- flies aged to 1 day* ***a),*** *7 days* ***b)****, 14 days* ***c)*** *and 30 days* ***d)****. Panels from left to right, display GFP+ axons (yellow arrows) and glomeruli (white arrows) fading at different rates per experimental group.* ***e)*** *Percentage quantification of GFP+ debris in OR85e axons.* ***f)*** *Percentage quantification of GFP+ debris visible in OR85e glomeruli. Statistical analysis was achieved through a 2-way ANOVA and Tukey's MC tests. Graphs plotted with mean±S.E.M., with significance annotated; ****p<0.0001, n=5 brains per group. Scale bar = 50 µm.*

When knocking down *Draper* we saw GFP+ neuronal debris from the age of 7 days. In 1-day-old samples, we found that GFP+ structures gradually declined after injury (**Fig. 15a**). Ageing flies to 7- (**Fig. 15b**), 14- (**Fig. 15c**) and 30-day (**Fig. 15d**), led to visible axons in 100% of brains. Axons were not recorded in 1-day-old flies 1DPA, and in only 60% after 5 days (**Fig. 15e**). A 2-way ANOVA revealed that differences in axon incidence were significant across age groups ($p<0.0001$), but not across time points. Tukey's MC tests demonstrated that axon numbers were lower in 1-day-old flies compared to 7-, 14- and 30-day-old flies (all $p<0.0001$) (**Fig. 15e**). GFP+ glomeruli were recorded up to 5DPA in 100% of all age groups except 1-day-old flies where we observed them in 80%. Statistical analysis suggested that differences did not vary between age groups or across time points, demonstrating that glomerulus engulfment was not age dependent (**Fig. 15f**).

When comparing *w-* and *Draper* KD flies after 5DPA, we generally recorded more GFP+ axons in flies with compromised Draper levels. A 2-way ANOVA revealed that differences were significant between biological groups ($p<0.01$) and across ages ($p<0.01$). Tukey's MC tests revealed significantly more GFP+ axons ($p<0.0001$) were recorded in 7-day-old *Draper* KDs compared to *w-* flies of the same age (**Fig. 15g**). Statistical analysis suggested that the difference between glomerulus incidence was not significant between biological groups at any age (**Fig. 15h**).

Comparing younger *w-* flies (1 & 7 days) to older flies (14 & 30 days), it is clear that engulfment of neuronal debris declines with increasing age. Knocking down *Draper* led to an expected engulfment deficit in flies aged 7 days and above, however, younger flies (1 day) still exhibited engulfment potential when assessing axons. Taken together, data suggest that ageing glia may not engulf injured neurons more readily and that *Draper* could be required in older animals for engulfment.

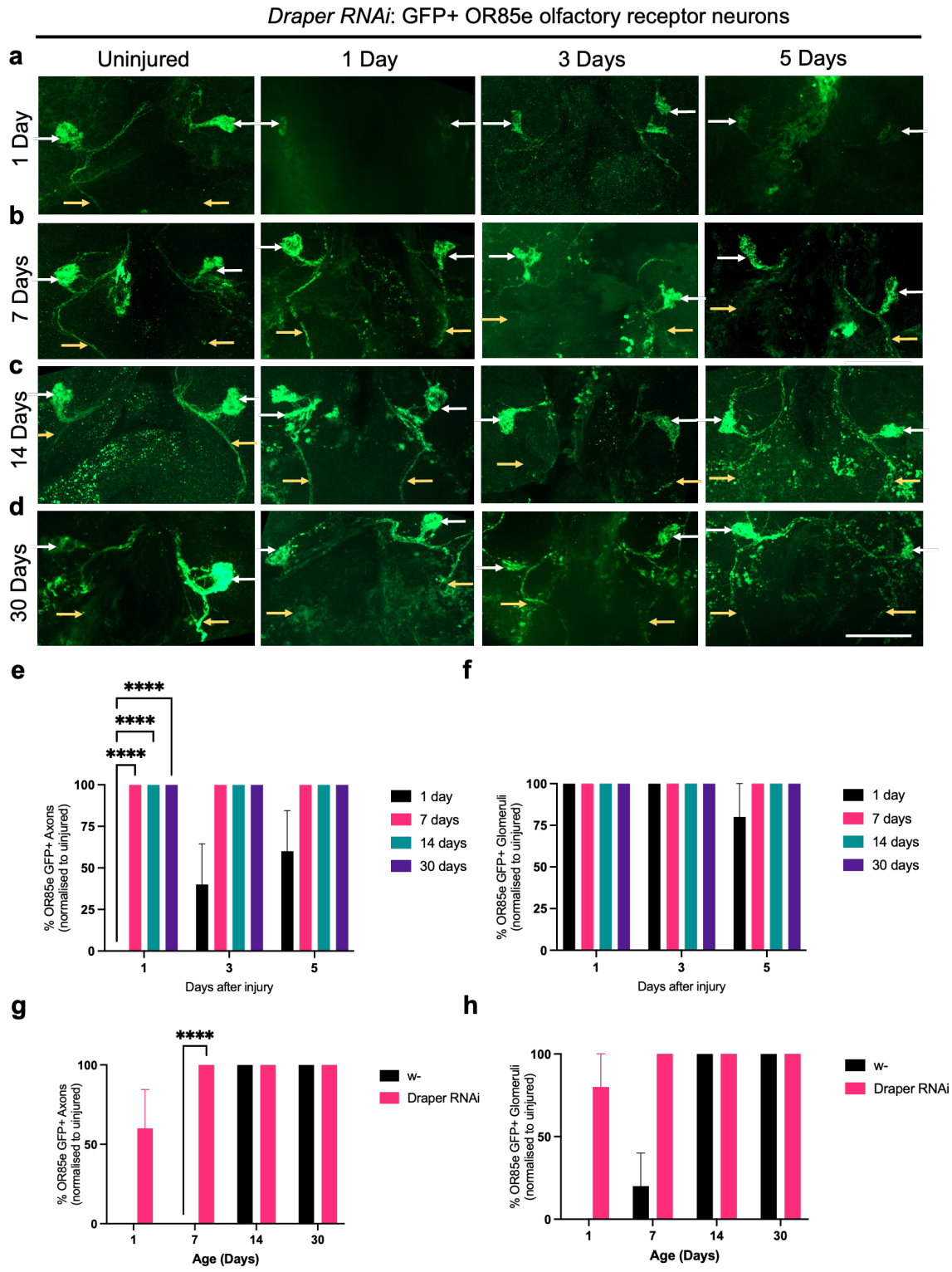
*Draper RNAi*: GFP+ OR85e olfactory receptor neurons
a
Uninjured
1 Day
3 Days
5 Days
1 Day
b
7 Days
c
14 Days
d
30 Days
e
****
****
****
% OR85e GFP+ Axons (normalised to uninjured)
100
75
50
25
0
1
3
5
Days after injury
1 day
7 days
14 days
30 days
f
% OR85e GFP+ Glomeruli (normalised to uninjured)
100
75
50
25
0
1
3
5
Days after injury
1 day
7 days
14 days
30 days
g
****
% OR85e GFP+ Axons (normalised to uninjured)
100
50
0
1
7
14
30
Age (Days)
w-
Draper RNAi
h
% OR85e GFP+ Glomeruli (normalised to uninjured)
100
50
0
1
7
14
30
Age (Days)
w-
Draper RNAi

***Fig. 15. Knocking down Draper led to A Delay After 7 Days of Age. a)-d)*** *GFP-labelled maxillary ORN neurons before and after maxillary nerve axotomy in Draper KD flies aged to 1 day* ***(a),*** *7 days* ***(b)****, 14 days* ***(c)*** *and 30 days* ***(d)****. Panels from left to right, display GFP+ axons (yellow arrows) and glomeruli (white arrows) fading at different rates per experimental group.* ***e)*** *Percentage quantification of GFP+ debris in OR85e axons.* ***f)*** *Percentage quantification of GFP+ debris visible in OR85e glomeruli.* ***g)-h)*** *Percentage incidence of OR85e axons* ***g)*** *and glomeruli* ***h)*** *in w- versus Draper KDs, in male and female flies of different ages. Statistical analysis was achieved through a 2-way ANOVA and Tukey's MC tests. Graphs plotted with mean±S.E.M., with significance annotated; ****p<0.0001, n=5 brains per group. Scale bar = 50 µm.*

## 3.5 Discussion

Evidence collected in this chapter outlines the optimal conditions for working with the ORN engulfment model system. Crucially, glial phagocytosis of neuronal debris after injury did not appear significantly dependent on sex or rearing temperature; however, the engulfment rate was significantly reduced in older flies compared with younger flies.

### 3.5.1 Sex Does Not Impact The Rate Of Engulfment

When addressing sex variation on the process of neuronal debris clearance, no significant difference was recorded in either axon or glomerulus presence after injury. This indicated that the rate of glial engulfment was not sex-dependent and therefore males and female flies could be used equally in future experiments. Although there is very little research on sex-specific glial function, there is data that supports transcriptomic modulation in neurons in response to injury. In a study investigating sex as a variable influencing patient recovery after traumatic brain injury (TBI), researchers caused injury to *Drosophila* using a high-impact trauma device and measured transcriptional changes at various time points post-injury (Shah et al. 2020). Overall, female flies exhibited more transcriptional changes than males, upregulating immune response and mitochondrial genes. Females also performed better in locomotor assays compared to males, suggesting that sex differences may influence genetic responses to injury and lead to varied outcomes (Shah et al. 2020). We found that in 20% of cases 5 days after injury, there was a slight delay in the glial response of male flies. The delay was not significant implying that glial response is broadly the same in both sexes. It would be recommended to investigate a larger sample size under multiple conditions to understand the extent of the phenotype, however, it is likely that genes implicated in glial engulfment are not sex-dependently regulated. Indeed, knocking down *Draper* led to an expected inhibition of engulfment, such that neuronal structures were still present 5 days after injury. These data confirm that *Draper* is required for effective engulfment (MacDonald et al. 2006; Ziegenfuss et al. 2008), but also that it is required equally across males and females. In conclusion, although sex

does not play a significant role in glial engulfment of neuronal debris, the investigation of sex on other glial processes warrants investigation.

### 3.5.2 Rearing Temperature has a Negligible Impact on Glial Function

When assessing glial engulfment rate at different rearing temperatures (25ºC and 29ºC), there was no obvious change in the response between groups. The results suggested that effective phagocytosis of neuronal debris took 5 days regardless of the environmental temperature. This was intriguing as *Drosophila* research often highlights how sensitive cells are to temperature changes, leading to diversity in cell physiology and function (Miquel et al. 1976; Vermeulen and Bijlsma 2003). For instance, larval neuromuscular junction (NMJ) can be induced to increase in size, bouton number and neuronal branching frequency by increasing rearing temperature to 29ºC/30ºC (Sigrist et al. 2003; Brink et al. 2012). A recent study found that elevated temperature (30ºC) could also increase the extent of glial processes at NMJs during embryogenesis (Brink et al. 2012). Comparing flies raised at 18ºC, 25ºC and 30ºC, researchers found that GFP labelled glia formed larger processes and expanded into synaptic regions more frequently at 30ºC. Temperature appeared to affect how glia physically interacted with synaptic structures (Brink et al. 2012). In neuronal studies, axonal arborization of mushroom body cells are increased in flies raised at higher 30ºC rather than 22ºC (Peng et al. 2007). The study also concluded that temperature could act in a cell-autonomous manner to regulate neuronal excitability and spontaneous activity through $Ca^{2+}$ accumulation (Peng et al. 2007). Here, if anything, glial engulfment of injured neurons may have been slightly delayed in 20% of wildtype flies raised at 29ºC, however, it was not significant. To study this effect further, it would be valuable to examine a larger sample and include lower rearing temperatures such as 18ºC for comparison. For the purposes of GAL4-driven expression, optimal temperatures range from 25ºC to 29ºC, thus 18ºC was not included in this study (Mondal et al. 2007). Optimal expression temperature was confirmed when knocking down *Draper* since engulfment was significantly inhibited in samples raised at both temperatures. Overall, data suggest that *Drosophila* engulfment experiments could be set up at either temperature, however, it may be preferable to raise animals at 29ºC to ensure maximum GAL4 expression.

### 3.5.3 Glial Engulfment Rate is Highly Dependent on Age

When exploring the impact of age on glial engulfment we found that neuronal structures were still visible after 5 days in animals over the age of 14 days. Our findings clearly demonstrate a correlation between age and neuronal debris clearance, in that clearance rate, reduces with increasing age. This confirms existing research in the field, whereby the glial engulfment rate using the same model decreased in old compared to young animals (Purice et al. 2016). However, in the cited publication, young flies range from 7-14 days old. We found that by 14 days glia were engulfing neuronal debris at a slower rate suggesting that the glial ageing process in *Drosophila* occurs earlier than previously thought. Alternatively, differences between studies mean that this finding could be due to varying conditions between labs, such as food or difference in genetic background. The age-dependent effect of engulfment poses some intriguing questions such as whether Draper itself is more active at younger ages or whether older flies are unable to eliminate debris due to decreased autophagosome/ lysosome function. Autophagy deficits and lysosomal impairments are considered strong hallmarks of ageing cells (Nixon 2020) and are thought to contribute to protein accumulations associated with age-dependent neurodegenerative disorders (Nixon 2020). Decreased lysosomal dysfunction in microglia may be a significant driver of amyloid pathology in AD (Solé-Domènech et al. 2016), where the lack of lysosome acidification may play a prominent role. Although we did not observe a significant change in glial engulfment, higher rearing temperatures (in this case 29$^{o}$C) could still impact the results of our study. Research suggests that higher rearing temperatures significantly increase the ageing process in flies (Miquel et al. 1976). In a study, identifying the fundamental changes that occur in response to changing environments, data implied that many age parameters are temperature sensitive. Researchers found that maintaining Oregon R flies at higher temperatures led to significantly shorter lifespans, increased $O_2$ utilisation and accelerated loss of vitality, such as negative geotaxis performance and mating behaviour, as well as fine structural changes including ribosomal loss (Miquel et al. 1976). This could suggest that 14-day-old flies in our study are physically “older” than 14-day-old flies in the publication and would explain the discrepancies between data (Purice et al. 2016). To further investigate the change, we would propose investigating later ages and a time-point beyond 5DPA to

understand the extent of the phenotype. Equally, mechanisms could be verified through single-cell sequencing techniques comparing data from injured and uninjured flies of various age groups. Finally, it would be worth investigating other hallmarks of glial endocytosis, including lysosomes or lysosomal pH changes using tools such as Lysosomal-associated membrane protein 1 (LAMP1) (Cheng et al. 2018).

Purice et al. attribute age-dependent engulfment changes to Draper and PI3K activity, which they confirmed reduced with age (Purice et al. 2016). When *Draper* is knocked down in our studies, we observe a significant delay in flies aged 7+, however, flies aged 1-day post-eclosion displayed phagocytic ability, despite knockdown. This is likely due to inefficient knockdown at early ages. Although RNAi expression can occur during development, it is dependent on the activity patterns of the promoter driving GAL4 expression (Mondal et al. 2007). Reversed polarise (repo) is required in some events of stem cell differentiation in development and is continually expressed in adult glia to mediate glial function and neurotransmitter recycling, however, it is increasingly expressed at later stages (Xiong et al. 1994). Therefore, in this case, the targeted and additive expression of RNAi is likely to take effect beyond the age of 1 day. It would be recommended to investigate true levels of *Draper* expression persisting after knockdown, through qPCR or Western blot analysis, throughout the life course of the fly. Perdurance of the Draper protein may also explain why KD was not sufficient at early stages. Overall, data suggest using 7 days as a minimum age for sufficient *Draper* KD in future experiments.

## 3.6 Summary of Key Findings

- The rate of neuronal debris engulfment by glia is not significantly impacted by the sex of the fly.
- The rate of neuronal debris engulfment by glia is not significantly affected by the temperature at which the flies are raised.
- An increase in age causes a gradual but significant delay in the rate of neuronal debris engulfment by glia.

# 4 Screening for AD Risk Genes for Roles in Engulfment

## 4.1 Introduction

Current research into the role of novel AD risk genes is largely limited to their individual role in neuronal networks of the brain. Primary research comprises of genetic manipulations in mono-cell cultures and mouse models, however more recent approaches aim to address the cumulative effects of multiple risk genes in a wider range of CNS cells. Microglia perform multiple core functions in the human brain, including phagocytosis, which when dysregulated has been hypothesised to promote the onset of AD (Mandrekar-Colucci and Landreth 2010). Dysregulated microglia can lead to the excessive elimination of synapses or equally a lack of amyloid-beta engulfment, both impacting neuronal health (Mandrekar-Colucci and Landreth 2010). GWAS and Meta-analysis have identified multiple AD risk genes, some of which may be related to microglial function (Lambert et al. 2013; Escott-Price et al. 2014; Jones et al. 2015; Bellenguez et al. 2020; Bellenguez et al. 2022). However, little is known of the function of risk gene variants in microglia and how they may promote disease. *Drosophila* provide a versatile model for functional genetic studies, with a wide range of genetic tools enabling researchers to investigate genetic pathways in disease and cell-specific backgrounds (Shklyar et al. 2015; Heigwer et al. 2018; Melcarne et al. 2019). This chapter summarises the reasoning and process behind a reverse-candidate screen aimed to investigate the role of AD risk gene orthologs in glial engulfment using a well-characterised ablation model.

### 4.1.1 Alzheimer's Risk Genes

Prior to the 21$^{st}$ century, AD research centred around two main theories: namely the amyloid and tau hypotheses. More recently, researchers identified a correlation between the age of onset and specific risk factors, both environmental and genetic (Gatz et al. 2006; Waring and Rosenberg 2008; Reitz and Mayeux 2014). Intrigue into hereditary risk factors began with the *APOE* gene locus, encoding apolipoprotein E and playing a major role in amyloid processing. Inheriting a single copy of the *APOE-ε4* variant could significantly increase the chance of developing AD symptoms (from 20% to 90%) and reduce the age of onset (from 84 to 68 years), depending on the inheritance of the *APOE-ε4* variant (Corder et al. 1993; Genin et al. 2011).

Between 2009 and 2011, GWA studies investigated a European cohort of Alzheimer's patients and compared their data to a control cohort to discover nine new loci that could additionally increase the carrier's chance of developing AD, including *CLU, CR1, PICALM, BIN1, ABCA7, MS4A6A/MS4A4E, EPHA1, CD33* and *CD2AP* (in order of publication) (Harold et al. 2009; Seshadri et al. 2010; Hollingworth et al. 2011; Naj et al. 2011). The discovery of these genes led to the evolution of the once proteo-centric hypothesis to a genetic disease; implying risk genes could be a major contributing factor in the pathology of AD. In addition, the functions of risk genes were often attributed to an immune response, suggesting that AD may involve more cell types than previously thought. In 2013, a rare susceptibility variant in *TREM2* was identified using similar cohorts (Jonsson et al. 2013). *TREM2* is highly enriched in macrophage lineages and associated with an increasing body of evidence suggesting specific roles in microglia, putting the cell on the map (Clayton et al. 2017; Efthymiou and Goate 2017; McQuade and Blurton-Jones 2019; Takatori et al. 2019).

The search for further genetic factors and increasing interest in CNS immune cells led to a mass collaboration between genetics experts to perform a large- scale meta-analysis of four GWAS collections from European cohorts. Combining cohorts brought totals to 17,008 cases and 37,154 controls, leading to the unveiling of 11,632 SNPs showing moderate evidence of association ($p<1 \times 10^{-3}$). After careful analysis, researchers singled out a further 11 loci with genome-wide significance ($p<5 \times 10^{-8}$), in addition to the already existing variants (Lambert et al. 2013). The associated genes included *INPP5D, MEF2C, HLA-DRB5, NME8, ZCWPW1, PTK2B, CELF1, SORL1, FERMT2, SLC42A4* and *CASS4* (Lambert et al. 2013). These were confirmed in 2014, with the addition of a new locus in *TP53INp1* (Escott-Price et al. 2014). The collaboration has gone on to discover further risk loci, including *PLCγ2* and *ABI3* in 2017 and another nine significant loci in 2019, including *ADAMTS4, HESX1, CLNK, CNTNAP2, ADAM10, APH1B, KAT8, ALPK2* and *AC074212.3,* reaching genome-wide significance ($p<5 \times 10^{-8}$) (Sims et al. 2017; Jansen et al. 2019). Some of these were confirmed in a further GWA study published later that year, where a further three genetic loci including *IQCK, ACE* and *WWOX* were unveiled (Kunkle et al. 2019). Additional risk genes such as *TRIP4* and *PLD3* were found in separate studies (Cruchaga et al. 2014; Ruiz et al. 2014; Blanco-Luquin et al. 2018).

Genetic risk factors may differ between global populations and so in 2021, a GWA study was conducted on a new cohort of 3962 AD patients and 4074 controls to discover novel susceptibility loci in the Japanese population. Interestingly, several familiar loci reached significance including *APOE* and *SORL1*, however, two novel loci were also uncovered, namely *FAM47E* and *OR2B2* (Shigemizu et al. 2021). The list of AD risk genes is ever-growing as more institutions come together to investigate the genetics of AD and has evolved our understanding of the disease in the hope of leading us to more specific therapies. Most recently, Bellenguez and colleagues identified 31 new genes, which further implicate microglial involvement as well as amyloid and tau pathways (Bellenguez et al. 2022). Many of the uncovered SNPs are found in non-coding regions of the genome, but there has been significant progress to determine the causative gene in the loci through eQTL analysis (Zhao et al. 2019). The functional contributions of genetics in pathology remain largely unknown, therefore future studies are essential to understanding the molecular mechanisms of disease.

### 4.1.2 Microglia in Alzheimer's Disease

Microglia are prominent macrophages that form part of the innate immune response of the brain. They play many crucial roles in CNS maintenance, injury response and defence against infection (Benarroch 2013). Their homeostatic functions extend to the sculpting of neural circuits by engulfment and removal of unwanted neurons or synapses (Li and Barres 2017). In AD, research has identified the proliferation and activation of microglia to be concentrated around amyloid plaques (von Bernhardi 2007; Joshi et al. 2014). The reactive gliosis in AD histopathology reflects the potential role microglia play in the disease, with increasing evidence suggesting they are important contributors of disease.

A key argument is that many AD-associated risk genes are selectively expressed and enriched in microglia relative to other brain cells (Srinivasan et al. 2016; Hansen et al. 2018). Pathway analysis also implicates immunity alongside lipid metabolism and tau/amyloid processing (Kunkle et al. 2019). *TREM2* is a more studied example and is almost exclusively expressed in myeloid cells (Sims et al. 2017). Studies in TREM2 have highlighted functions such as phagocytosis, which could lead to impaired Aβ clearance in AD (Wang et al. 2015c; Yeh et al. 2016). Other microglial functions that

could be affected include chemotaxis, survival, and proliferation (Hsieh et al. 2009; Kleinberger et al. 2014; Sims et al. 2017). Most microglial functions are presumed protective and inhibited in AD, however certain research suggests they may have a harmful role to play, accelerating neurodegeneration (Block et al. 2007; Neumann et al. 2008; Whitelaw 2018). Microglia are likely to induce complement-mediated synapse loss in AD through initiated phagocytic mechanisms (Hong et al. 2016). A new theory suggests either dysregulation of microglia by complement, or cell dysfunction may be at the centre of this process, leading to early synapse loss (Hong et al. 2016). In addition, transcriptional profiling of microglial gene expression implies different states of microglial activation may occur during AD, pertaining to the discussion that microglial pro-inflammatory state may correlate with increased neurodegeneration (Block et al. 2007; von Bernhardi 2007; Mandrekar-Colucci and Landreth 2010; Joshi et al. 2014; Lopategui Cabezas et al. 2014; Li and Barres 2017; Hansen et al. 2018; Vilalta and Brown 2018; Whitelaw 2018). Central to an emerging field of dementia research, microglia are evolving our understanding of disease and may provide solutions for treatment. However, their role in pathology is yet to be defined and how their functions are mediated by AD risk genes is currently being studied.

### 4.1.3 Conserved AD Risk Gene Orthologs

*Drosophila* have many orthologs for AD identified risk genes with varying degrees of conservation. We identified individual orthologs using DIOPT (version 8.5), an online tool, that integrates the results of multiple ortholog-mapping tools based and tests conserved regions of human and *Drosophila* DNA. Conserved risk gene fly knockouts (KOs) (**Fig. 16**) and mutant gene transgenics could be generated and analysed for pathological traits associated with AD. If AD-like pathology and dysfunction were to be observed, we would then consider these as new disease models. Since emerging evidence implicates AD risk genes in microglial function, orthologs will be assessed for their capacity to mediate glial engulfment in flies. Genetic tools such as the GAL4 system have been employed in my reverse candidate screen to regulate the expression of i) risk gene RNAis and ii) fluorescent reporter proteins (*mcherry*), all in a cell-specific manner using the pan glial driver reverse polarised (*repo*). Combining these tools with our characterised model system from **Chapter 3**, this chapter investigates novel engulfment phenotypes when knocking down fly versions of AD risk

genes. In this, *Drosophila* can help us to interpret GWAS data to ascertain important roles in glial function, enabling us to triage gene 'hits' before characterising them in more specific models of disease.

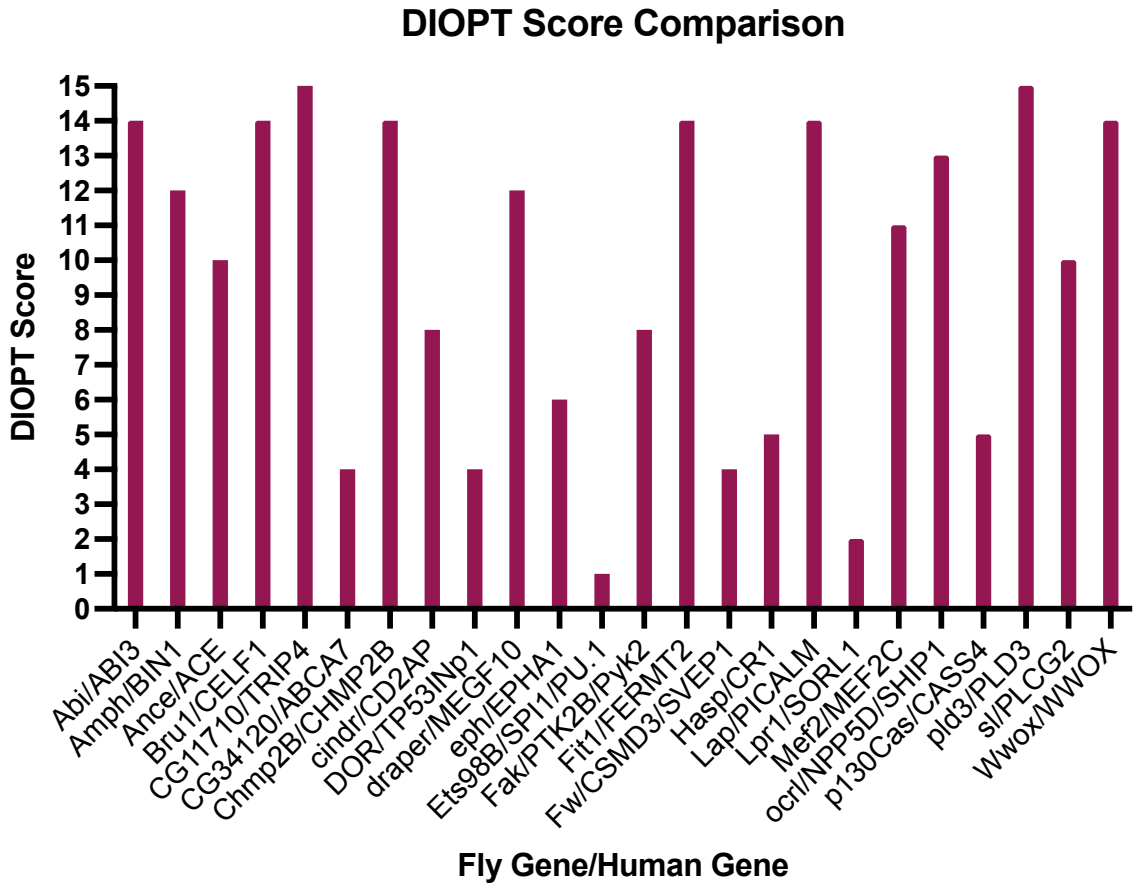


***Fig. 16. AD Risk Gene Orthologs.*** *This figure lists the Drosophila genes closest to human AD risk genes, based on their DIOPT Scores. Higher scores support a given orthologous gene-pair relationship, with a maximum score of 15.*

## 4.2 Aims and Objectives

The present chapter aims to determine the role of conserved AD risk gene orthologs in the engulfment process of glial cells, using a characterised engulfment model. *Drosophila* orthologs of current (2018) human AD risk genes will be individually knocked down in glia cells, and any effect on the characterised engulfment pattern analysed and compared to controls. RNAi expression will be driven by GAL4 under the control of the glial-specific promoter *repo* (reversed polarity), which will also drive *mcherry* expression (both under UAS control), labelling glia. Neurons will be independently labelled with GFP. Developmental phenotypes will be recorded in a lethality assay and changes to engulfment recorded using binary assessment criteria. If the screen yields any candidates, these will be verified for repeatable outcomes in a secondary assay. Such investigations will help to determine the functional roles of AD risk genes.

## 4.3 Experimental Design

Using DIOPT, fly orthologs for AD risk genes were identified, along with other interesting dementia-related genes, such as *CHMP2B (CHMP2B), Ets98B* (*SPI1* ortholog) and *fw* (*CSMD3/SVEP1* ortholog). Multiple RNAis for each gene were sourced from different stock centres, including BDSC and Vienna *Drosophila* Resource Centre (VDRC) to test the penetrance of any given phenotype, subject to availability. Each source generates RNAi lines differently – since 2008, BDSC has used a method created through the Transgenic RNAi Project (TRiP), which developes transgenic RNAi lines through an optimised approach (Ni et al. 2008). All constructs are designed to knockdown gene expression under the control of a UAS, however, they vary in terms of i) vector insertion site (attP1-20) and ii) the vector itself. Most sourced RNAis from BDSC, use vectors VALIUM10/20 and insertion sites attP2 and attP40, for which appropriate control lines were sourced, namely #36303 (attP2 site control), #36304 (attP40 site control) and #35786 (VALIUM10/20 control). I sourced #60101, an empty KK vector line with both landing sites, which served as a control for VDRC lines.

RNAi lines and appropriate controls were crossed with flies whose olfactory neurons were labelled with GFP and where GAL4 expression was driven by *repo* (*w-;OR85e,mCD8::GFP/CyO;repo-GAL4,UAS-cherry/TM3, Sb, e-*). Crosses were kept at RT for the first 24 hrs, then transferred to a 29$^{o}$C incubator, with parents passed on to fresh food every 2 days. At 29$^{o}$C *GAL4* expression is maximised, promoting effective knockdown by RNAis (as outlined in **Chapter 3**). Developmental phenotypes were recorded in a lethality assay, where values were awarded to crosses with no yield (0), low yield (0.5) or high yield (1). Live F1 progeny were selected and aged for 7-8 days before being injured via maxillary palp ablation techniques as outlined in **Chapter 2**. Flies were kept for an additional 24hrs before being dissected and stained alongside uninjured controls. Their brains were mounted as described in **Chapter 2** and imaged using confocal microscopy. GFP signal was used as a readout for glial engulfment function. Engulfment function was determined by recording visible neurons through the incidence of axons and glomerulus structures, presented as a percentage across experimental groups. *mcherry* signal was assessed to determine the presence of glia in all genotypes, to ensure glia were dysfunctional and not ablated.

“Hits” were verified by crossing RNAis and appropriate controls to *w-;OR85e,mCD8::GFP/CyO;repo-GAL4/TM3, Sb, e-* virgins and raised in identical conditions. Data generated when analysing the amount of remaining neuronal debris (as a hallmark of engulfment deficits) was first tested for normality. Normality of residuals was investigated using the Shapiro-Wilk test and QQ plots were checked for outliers. Screen data were then separated according to the structure recorded (axon/glomerulus) and then into uninjured and injured groups. A 1-way ANOVA with Dunnett’s multiple comparisons test was used to assess the significance of phenotypes caused by different genetic backgrounds, e.g. comparing axon incidence percentages of *RNAi (X)* to *w-,repo-mcherry* controls. The same statistical method was used to verify phenotypes in later experiments. A table of the *Drosophila* lines used in this Chapter can be found below (**Table 17)**.

| **Stock** | ***Genotype*** | **Stock Number** | **Source** |
|---|---|---|---|
| Virgin Line 1 | *w-;OR85e-mCD8::GFP/+;repo-GAL4/TM3, Sb, e-* | n/a | Freeman Stock |
| Virgin Line 2 | *w-;OR85e-mCD8::GFP/+;repo-GAL4, UAS-mcherry/TM3, Sb, e-* | n/a | Freeman Stock |
| w- | *w-;+/+;+/+* | n/a | Lab Stock |
| UAS-GFPvallium | *y,v; P{y[+t7.7] v[+t1.8]=UAS-GFP.VALIUM10}attP2* | 35786 | BDSC |
| attP40 | *y,v;p(caryP)attP40* | 36304 | BDSC |
| attP2 | *y,v;;p(caryP)attP2* | 36303 | BDSC |
| KK | *P{attP,y+,w3'}VIE-260B* | 60101 | VDRC |
| Draper RNAi (I) | *w1118; P{GD2628}v4833* | 4833 | VDRC |
| **Draper RNAi (II)** | *w1118; P{GD14423}v27086* | 27086 | VDRC |
| Abi RNAi (I) | *y1 v1; P{TRiP.HMC03190}attP40* | 51455 | BDSC |
| Abi RNAi (II) | *y1 sc* v1 sev21; P{TRiP.HMS01597}attP2* | 36707 | BDSC |
| Abi RNAi (III) | *P{KK108071}VIE-260B* | 100714 | VDRC |
| Ance RNAi (I) | *y1 sc* v1 sev21; P{TRiP.HMS03009}attP2* | 36749 | BDSC |
| Ance RNAi (I) | *y1 sc* v1 sev21; P{TRiP.GLC01369}attP2* | 51394 | BDSC |
| Amph RNAi (I) | *w1118; P{GD1311}v7190* | 7190 | VDRC |
| Amph RNAi (II) | *w1118; P{GD1311}v9264* | 9264 | VDRC |
| ApolPP RNAi | *y1 v1; P{TRiP.HM05157}attP2* | 28946 | BDSC |
| bru1 RNAi (I) | *y1 v1; P{TRiP.HMS01899}attP40* | 38983 | BDSC |
| bru1 RNAI (II) | *y1 sc* v1 sev21; P{TRiP.GL00314}attP2* | 35394 | BDSC |
| bru1 RNAi (III) | *y1 v1; P{TRiP.HMJ21531}attP40* | 54812 | BDSC |
| bru1 RNAi (IV) | *w1118; P{GD8699}v41567* | 41567 | VDRC |
| bru1 RNAi (V) | *w1118; P{GD8699}v41568* | 41568 | VDRC |
| bru1 RNAi (VI) | *w1118; P{GD17093}v48237/TM3* | 48237 | VDRC |
| bru1 RNAi (VII) | *P{KK110026}VIE-260B* | 107459 | VDRC |

| | | | |
|---|---|---|---|
| cindr RNAi (I) | *w1118; P{GD8679}v38854* | 38854 | VDRC |
| cindr RNAi (II) | *P{VSH330422}attP40* | 330422 | BDSC |
| CG11710 RNAi (I) | *P{KK102304}VIE-260B* | 109760 | VDRC |
| CG11710 RNAi (II) | *y1 sc* v1 sev21; P{TRiP.HMC05087}attP40* | 60093 | BDSC |
| CG17600 RNAi (I) | *w1118; P{GD3716}v51085* | 51085 | VDRC |
| CG17600 RNAi (II) | *y1 sc* v1; P{TRiP.HMS01812}attP2* | 38345 | BDSC |
| CG17600 RNAi (III) | *P{KK105222}VIE-260B* | 102833 | VDRC |
| CG34120 RNAi (I) | *P{KK104441}VIE-260B* | 100472 | VDRC |
| CG34120 RNAi (II) | *$w^{1118}$; P{GD3704}v11673/TM3* | 11673 | VDRC |
| CG34120 RNAi (III) | *$w^{1118}$; P{GD15895}v48377* | 48377 | VDRC |
| CG34120 RNAi (IV) | *P{KK106128}VIE-260B* | 100384 | VDRC |
| CG34120 RNAi (V) | *P{KK105495}VIE-260B* | 101700 | VDRC |
| CHMP2B RNAi (I) | *y1 v1; P{TRiP.HMJ21039}attP40* | 50942 | BDSC |
| CHMP2B RNAi (II) | *y1 v1; P{TRiP.HMS01844}attP40* | 38375 | BDSC |
| DOR RNAi (I) | *w1118; P{GD5124}v41186* | 41186 | VDRC |
| DOR RNAi (II) | *y1 v1; P{TRiP.HMJ22607}attP40* | 60389 | BDSC |
| DOR RNAi (III) | *P{KK111208}VIE-260B* | 105330 | VDRC |
| Eph RNAi (I) | *w1118; P{GD14481}v27236* | 27236 | VDRC |
| Eph RNAi (II) | *P{KK101831}VIE-260B* | 110448 | VDRC |
| Eph RNAi (III) | *w1118; P{GD2535}v4771* | 4771 | VDRC |
| Ets98B RNAi (I) | *w1118; P{GD4451}v10932* | 10932 | VDRC |

| | | | |
|---|---|---|---|
| Ets98B RNAi (II) | *P{KK107560}VIE-260B* | 107292 | VDRC |
| Ets98B RNAi (III) | *y1 v1; P{TRiP.JF03116}attP2* | 28700 | BDSC |
| Fak RNAi (I) | *w1118; P{GD6840}v17957* | 17957 | VDRC |
| Fak RNAi (II) | P{KK101680}VIE-260B | 108608 | VDRC |
| Fak RNAi (III) | *y1 sc* v1 sev21; P{TRiP.GL00269}attP2* | 35357 | BDSC |
| Fak RNAi (IV) | *P{KK101680}VIE-260B* | 108608 | VDRC |
| Fak RNAi (V) | *y1 v1; P{TRiP.HMS02792}attP40* | 44075 | BDSC |
| Fit1 RNAi (I) | *P{KK109279}VIE-260B* | 105767 | VDRC |
| Fit1 RNAi (II) | *y1 sc* v1 sev21; P{TRiP.HMC02930}attP 40* | 44536 | BDSC |
| Fit1 RNAi (IIII) | *y1 v1; P{TRiP.JF01986}attP2* | 25966 | BDSC |
| fw RNAi (I) | *w1118; P{GD3327}v39575/TM3* | 39575 | VDRC |
| fw RNAi (II) | *P{KK109200}VIE-260B* | 106656 | VDRC |
| Hasp RNAi (I) | *w1118; P{GD5411}v30767* | 30767 | VDRC |
| Hasp RNAi (II) | *y1 sc* v1 sev21; P{TRiP.HMC05997}attP 40* | 65101 | BDSC |
| Hs3st-A RNAi (I) | *w1118; P{GD2075}v4998* | 4998 | VDRC |
| Hs3st-A RNAi (II) | *w1118; P{GD10001}v25571* | 25571 | VDRC |
| Hs3st-A RNAi (III) | *w1118; P{GD10001}v25572* | 25572 | VDRC |
| Hs3st-A RNAi (IV) | *y1 v1; P{TRiP.JF03033}attP2* | 28618 | BDSC |
| Lap RNAi (I) | *w1118; P{GD4725}v12731* | 12731 | VDRC |
| Lap RNAi (II) | *w1118; P{GD4725}v12732* | 12732 | VDRC |
| Lap RNAi (III) | *y1 v1; P{TRiP.HMC02373}attP2* | 55241 | BDSC |
| Lpr2 RNAi (II) | *y1 sc* v1 sev21; P{TRiP.HMS03722}attP 2* | 54461 | BDSC |
| Mef2 RNAi (I) | *$w^{1118}$; P{GD17050}v46494* | 46494 | VDRC |
| Mef2 RNAi (II) | *$w^{1118}$; P{GD17050}v46495/CyO* | 46495 | VDRC |
| Mef2 RNAi (III) | *y[1] sc[*] v[1]; P{y[+t7.7] v[+t1.8]=TRiP.HMS01691}attP40* | 38247 | BDSC |
| Mef2 RNAi (IV) | *y[1] v[1]; P{y[+t7.7] v[+t1.8]=TRiP.JF03115}attP2* | 28699 | BDSC |

| | | | |
|---|---|---|---|
| Mef2 RNAi (V) | *w1118; P{GD5039}v15550* | 15550 | VDRC |
| Nrx-IV RNAi (I) | *$w^{1118}$; P{GD2436}v8353* | 8353 | VDRC |
| Nrx-IV RNAi (II) | *$w^{1118}$; P{GD2436}v9039* | 9039 | VDRC |
| Nrx-IV RNAi (III) | *P{KK102207}VIE-260B* | 108128 | VDRC |
| Nrx-IV RNAi (IV) | *$y^1$ $v^1$; P{TRiP.JF03142}attP2* | 28715 | BDSC |
| Nrx-IV RNAi (V) | *$y^1$ $sc^*$ $v^1$; P{TRiP.HMS00419}attP2/TM3, $Sb^1$* | 32424 | BDSC |
| Nrx-IV RNAi (VI) | *$y^1$ $sc^*$ $v^1$; P{TRiP.HMS01991}attP40* | 39071 | BDSC |
| ocrl RNAi (I) | *w1118; P{GD11016}v34649* | 34649 | VDRC |
| ocrl RNAi (II) | *P{KK101922}VIE-260B* | 110796 | VDRC |
| ocrl RNAi (III) | *y1 sc* v1 sev21; P{TRiP.HMS01201}attP2/TM3, Sb1* | 34722 | BDSC |
| p130Cas RNAi (I) | *w1118; P{GD7492}v41479* | 41479 | VDRC |
| p130Cas RNAi (II) | *P{VSH330191}attP40* | 330191 | BDSC |
| Pld3 RNAi (I) | *w1118; P{GD5427}v41225* | 41225 | VDRC |
| **Pld3 RNAi (II)** | *P{KK107515}VIE-260B* | 109798 | VDRC |
| Pld3 RNAi (III) | *y1 v1; P{TRiP.JF01595}attP2* | 31122 | BDSC |
| sl RNAi (I) | *w1118; P{GD1535}v7173* | 7173 | VDRC |
| sl RNAi (II) | *w1118; P{GD1535}v7174* | 7174 | VDRC |
| **sl RNAi (III)** | *y1 sc* v1 sev21; P{TRiP.HMS00695}attP2* | 32906 | BDSC |
| sl RNAi (IV) | *P{KK101565}VIE-260B* | 108593 | VDRC |
| Wwox RNAi (I) | *P{KK108459}VIE-260B* | 108350 | VDRC |
| Wwox RNAi (II) | *y1 v1; P{TRiP.HMC03298}attP2* | 51747 | BDSC |
| zyd RNAi (I) | *w1118; P{GD3723}v40987* | 40987 | VDRC |
| zyd RNAi (II) | *w1118; P{GD3723}v40988* | 40988 | VDRC |
| zyd RNAi (III) | *y1 v1; P{TRiP.JF01872}attP2* | 25851 | BDSC |

***Table 17**: This table combines all stock information including fly RNAis, human orthologs, DIOPT (conservation) score, stock number, source, vector, insertion site and the type of line.*

## 4.4 Results

### 4.4.1 Expressing Some AD Risk Gene Orthologues Led to Developmental Phenotypes

RNAis targeting 30+ AD risk gene orthologs were crossed, with values awarded in cases of no yield (0), low yield (0.5) or high yield (1), revealing any lethal phenotypes. Occasionally crosses produced 1 or 2 offspring of the correct genotype, hence a third category was introduced – 'low yield'. Most genes that led to a viable phenotype also had RNAis that caused a 'low yield' or 'lethal' outcome, summarised in **Fig. 17**. 'Low yield' crosses arose from expressing *CG34120* RNAi (IV) #100384, *bru1* RNAi (II) #35394, *CHMP2B* RNAi (I) #50942, *DOR* RNAi (II) #60389, *Fit1* RNAi (II) #44536, *Pld3* RNAi (I) #41225 and *sl* RNAi (IV) #108593. 'Lethal' crosses arose from expressing *bru1* RNAi (I) #54812, *Eph* RNAi (II) #110448 and *Mef2* RNAis (I) #46494 and (II) #46495. These results imply that glial-specific knockdown of target genes had a severe impact on the health of flies, particularly during development. RNAis targeting the same genes later yielded viable phenotypes, which could support important roles in glial function. Other RNAis that produced a 'low yield' phenotype included *CG17600* RNAi (I) #51085, *Ets98B* RNAi (I) #10932, *Fak* RNAi (I) #17957, and *Nrx-IV* RNAi (V) #32424. Lethal phenotypes were observed when crossing *CG11710* RNAi (I) #109760, *Hst3st-A* RNAis (II) #25571 and (III) #25572, all remaining *Nrx-IV* RNAis and *ocrl* RNAi (II) #110796 and all *zyd* RNAis. This suggests that many AD risk genes perform essential roles in glial function and warrant further investigation.

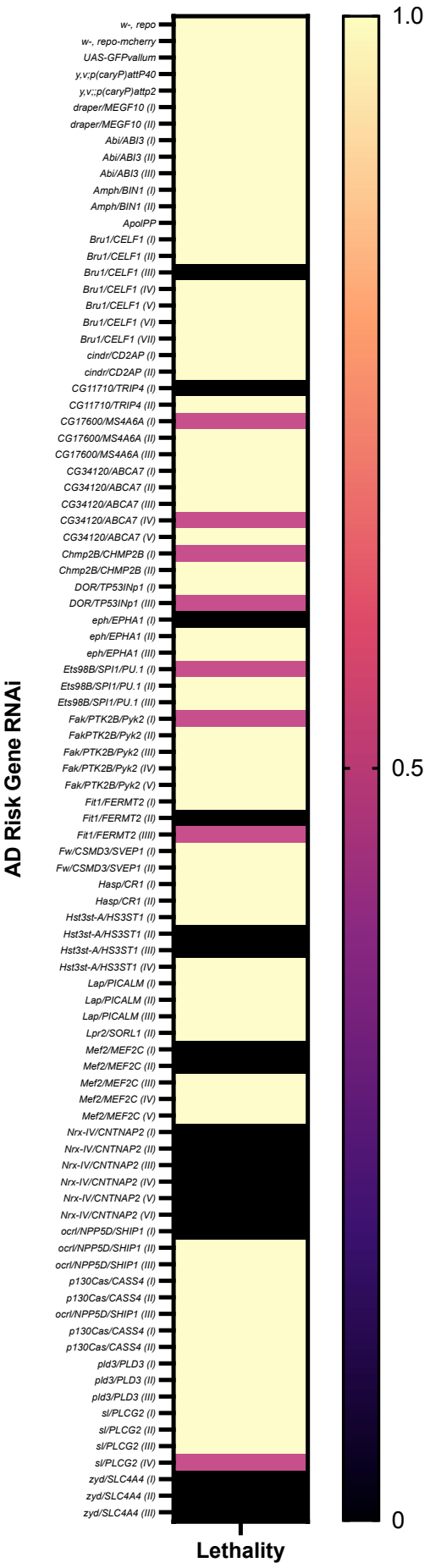
w-, repo
w-, repo-mcherry
UAS-GFPvallum
y,v;p(caryP)attP40
y,v;;p(caryP)attp2
draper/MEGF10 (I)
draper/MEGF10 (II)
Abi/ABI3 (I)
Abi/ABI3 (II)
Abi/ABI3 (III)
Amph/BIN1 (I)
Amph/BIN1 (II)
ApoIPP
Bru1/CELF1 (I)
Bru1/CELF1 (II)
Bru1/CELF1 (III)
Bru1/CELF1 (IV)
Bru1/CELF1 (V)
Bru1/CELF1 (VI)
Bru1/CELF1 (VII)
cindr/CD2AP (I)
cindr/CD2AP (II)
CG11710/TRIP4 (I)
CG11710/TRIP4 (II)
CG17600/MS4A6A (I)
CG17600/MS4A6A (II)
CG17600/MS4A6A (III)
CG34120/ABCA7 (I)
CG34120/ABCA7 (II)
CG34120/ABCA7 (III)
CG34120/ABCA7 (IV)
CG34120/ABCA7 (V)
Chmp2B/CHMP2B (I)
Chmp2B/CHMP2B (II)
DOR/TP53INp1 (I)
DOR/TP53INp1 (III)
eph/EPHA1 (I)
eph/EPHA1 (II)
eph/EPHA1 (III)
Ets98B/SPI1/PU.1 (I)
Ets98B/SPI1/PU.1 (II)
Ets98B/SPI1/PU.1 (III)
Fak/PTK2B/Pyk2 (I)
FakPTK2B/Pyk2 (II)
Fak/PTK2B/Pyk2 (III)
Fak/PTK2B/Pyk2 (IV)
Fak/PTK2B/Pyk2 (V)
Fit1/FERMT2 (I)
Fit1/FERMT2 (II)
Fit1/FERMT2 (IIII)
Fw/CSMD3/SVEP1 (I)
Fw/CSMD3/SVEP1 (II)
Hasp/CR1 (I)
Hasp/CR1 (II)
Hst3st-A/HS3ST1 (I)
Hst3st-A/HS3ST1 (II)
Hst3st-A/HS3ST1 (III)
Hst3st-A/HS3ST1 (IV)
Lap/PICALM (I)
Lap/PICALM (II)
Lap/PICALM (III)
Lpr2/SORL1 (II)
Mef2/MEF2C (I)
Mef2/MEF2C (II)
Mef2/MEF2C (III)
Mef2/MEF2C (IV)
Mef2/MEF2C (V)
Nrx-IV/CNTNAP2 (I)
Nrx-IV/CNTNAP2 (II)
Nrx-IV/CNTNAP2 (III)
Nrx-IV/CNTNAP2 (IV)
Nrx-IV/CNTNAP2 (V)
Nrx-IV/CNTNAP2 (VI)
ocrl/NPP5D/SHIP1 (I)
ocrl/NPP5D/SHIP1 (II)
ocrl/NPP5D/SHIP1 (III)
p130Cas/CASS4 (I)
p130Cas/CASS4 (II)
ocrl/NPP5D/SHIP1 (III)
p130Cas/CASS4 (I)
p130Cas/CASS4 (II)
pld3/PLD3 (I)
pld3/PLD3 (II)
pld3/PLD3 (III)
sl/PLCG2 (I)
sl/PLCG2 (II)
sl/PLCG2 (III)
sl/PLCG2 (IV)
zyd/SLC4A4 (I)
zyd/SLC4A4 (II)
zyd/SLC4A4 (III)
AD Risk Gene RNAi
Lethality
1.0
0.5
0

***Fig. 17. Knocking down AD Risk Genes Sometimes Yielded Lethal Phenotypes****. A heat-map representation of the incidence of lethal, 'low yield' and viable crosses. Lethality is represented by an awarded value – no yield (0), low yield (0.5) and highyield (1) (black-yellow). RNAis are listed on the y-axis and phenotypes on the x-axis.*

### 4.4.2 Knocking Down AD Risk Gene Orthologs Led to Multiple Engulfment Phenotypes

Viable F1 progeny were selected and aged for 7/8 days before maxillary palp ablation. Experimental samples were aged a further day after injury and compared to uninjured groups, with differences recorded using confocal microscopy, where neuron-GFP signal was used as a readout for glial engulfment. A 'hit' was determined where the phenotype appeared different compared to respective control lines and scored based on criteria outlined above (**Section 4.3**). Phenotypes included i) gain-of-function (GOF)/acceleration in engulfment, such that neurons were no longer visible 1-day post-ablation (1DPA) or ii) loss-of-function (LOF)/inhibition of engulfment, such that neuronal GFP remained visible in axons and glomeruli 1DPA. Finally, *mcherry* signal was used to determine the presence of glia in all genotypes. Knocking down gene orthologs led to the findings described below (**Fig. 18**).

Across controls, similar results were observed, such that axons and glomeruli were visible in 100% of uninjured flies (**Fig. 19a**). 1DPA, GFP+ axons were recorded in 21% of *w- ,repo-mcherry* brains (**Fig. 19a'**), 0% of *UAS-GFPvallium* controls and *attP40* control brains, 28% of *attP2 control* brains and 25% of control *KK* brains. Glomeruli were still visible in 100% of injured cases at this timepoint, conforming to data from **Chapter 3**. Statistical analysis via 1-way ANOVA and Dunnett's multiple comparisons tests demonstrated that data did not vary significantly between control groups, suggesting RNAi-specific genotypes were genuine and not a result of the construct background. Glial signal was also consistent throughout images (**Fig. 19a-a'**). Knocking down *Draper*, a known regulator of engulfment, led to expected results (**Fig. 19b-b'**). Despite injury, GFP+ axons were recorded in 100% of *Draper* RNAi (I) #4833 and (II) #27086 brains. A 1-way ANOVA found a significant difference between axon incidence between genotypes ($p<0.0001$), and Dunnett's multiple comparisons tests

revealed that axons were recorded in more *Draper* RNAi (I) and (II) brains (both p<0.0001). This is a typical LOF phenotype that has been characterised and discussed in previous studies (MacDonald et al. 2006) and used a benchmark for other potential modulators of engulfment.

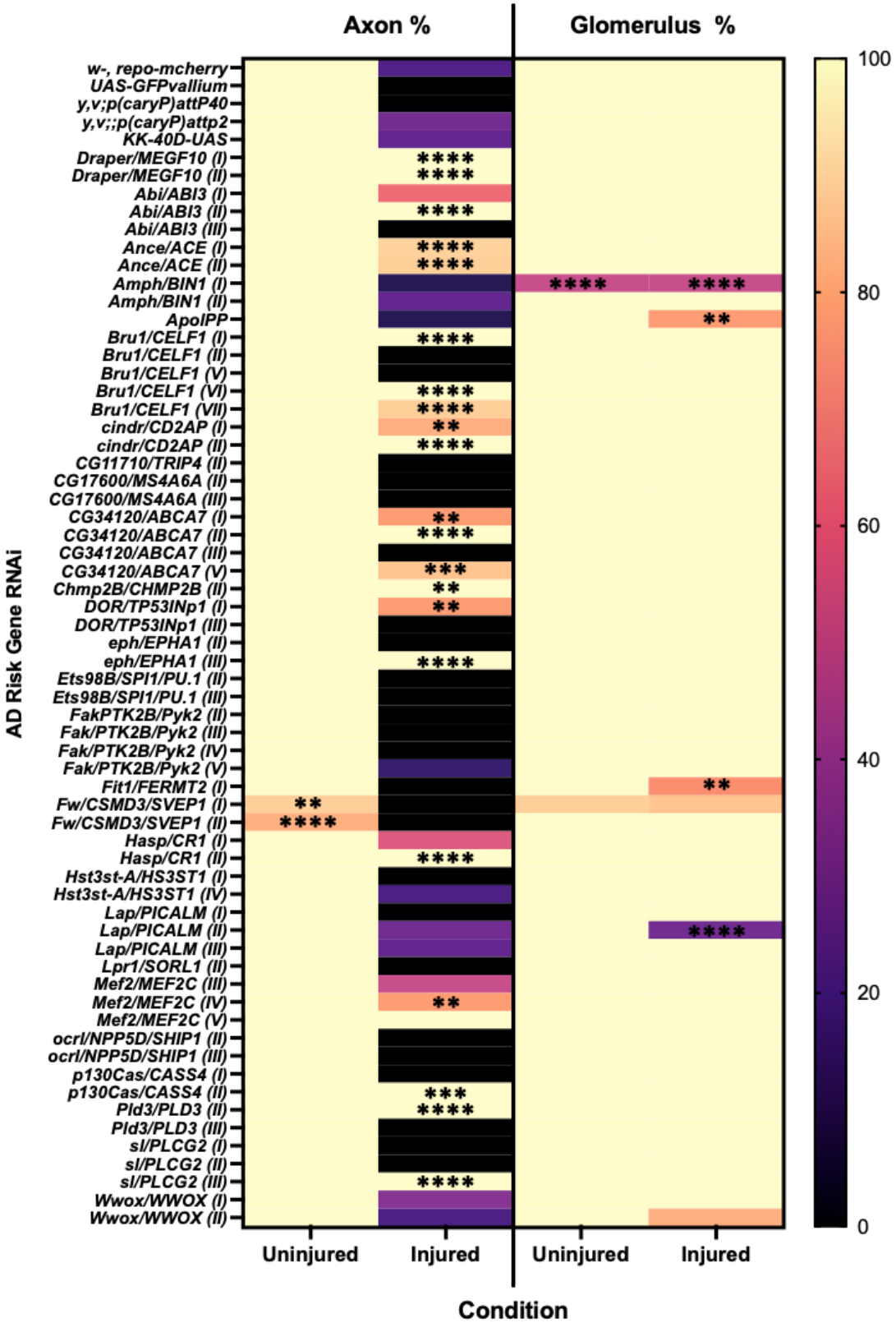

***Fig. 18. Knocking down AD Risk Genes Led to LOF/GOF Phenotypes.*** *A heat-map representation of the incidence of uninjured and injured (1 DPA) axon and glomerulus phenotypes (from left to right). Incidence is represented in percentage form from 0-100% (black-yellow). RNAis are listed on the y-axis and phenotypes on the x-axis. Statistical comparisons were achieved for separate groups (ex: Uninjured: Axon %) by 1-way ANOVA and Dunnett's multiple comparisons test, with significant differences annotated as * p<0.05, **p<0.01, ***p<0.001 and ****p<0.0001, n=3-15 brains per group.*

Knocking down extracellular and synaptic proteins such as *Ance, Amph* and *Hasp* and *Lap* led to different engulfment phenotypes. *Angiotensin-converting enzyme (Ance)* encodes a member of the peptidyl-dipeptidase A family of zinc metalloproteases. Its product is an extracellular glycosylated enzyme with broad specificity, cleaving dipeptides from the carboxy terminus of oligopeptides. Its closest human ortholog is Angiotensin-converting *enzyme 1 (ACE1). In Ance* KD conditions, axon structures were recorded in up to 89% of brains expressing either RNAi (I) #36749 (**Fig. 19c-c'**) and (II) #51394, despite injury. Statistical analysis revealed that axon GFP was recorded significantly more frequently in *Ance* RNAi (I) ($p<0.0001$) and RNAi (II) ($p<0.0001$) compared to *w-;repo-mcherry* control brains – suggesting an engulfment deficit. *Amphiphysin (Amph)* encodes a protein involved in regulating muscles transverse tubule formation and exhibits post-synaptic localisation at the neuromuscular junction. Its closest ortholog is *Bridging Integrator 1 (BIN1)*. When knocking down *Amph* (**Fig. 19d-d'**), axons appeared intact in only 12% of RNAi (I) #7190 brains after injury, in addition to a loss of glomeruli in 50% of cases. The loss of glomerulus signal was significant compared to *w-;repo-mcherry* control ($p<0.0001$), according to multiple comparisons tests – suggesting an unusual GOF phenotype. *Hig-anchoring scaffold protein (hasp*) is predicted to have peptidase inhibitor activity and localise at the synaptic cleft in fly neurons. It is the closest ortholog to *Complement C3b/C4b receptor 1 (CR1)* in humans. Knocking down *Hasp* led to a LOF phenotype (**Fig. 19e-e'**). GFP was recorded in axons, despite injury, in 100% of RNAi (II) #65101 brains, a significantly higher recording compared to *w-;repo-mcherry* controls ($p<0.0001$). Glomeruli were intact in 100% of brains, altogether suggesting a LOF phenotype. KD results suggest that *Amph* may have a conflicting role to play in engulfment and that *Ance* and *Hasp* may promote it (**Fig. 18, Fig. 19c-e'**).

Genes that could modulate membrane dynamics, mediating processes such as adhesion, migration, and endosome/vesicle formation also displayed potential roles in glial engulfment. Knocking down *Abelson interacting protein* (*Abi*), a regulator of actin cytoskeleton organisation like human ortholog *ABI3*, led to a phenotype in 2/3 RNAis. GFP+ axons were recorded in 53% of RNAi (III) #100714 brains and in 100% of RNAi (II) #51455 brains after injury (**Fig. 19f-f'**). Dunnett's MC tests revealed that axon incidence was higher in RNAi (II) compared to *w- ;repo-mcherry* control ($p<0.0001$). Glomerulus structures were also recorded in all brains, suggesting a LOF phenotype. A similar engulfment deficit was observed when knocking down *CIN85 and CD2AP related* (*cindr)* (**Fig. 19g-g'**), the fly equivalent of *CD2- association protein* (*CD2AP)*. *cindr* also regulates the actin cytoskeleton and links cell surface junctions. Here, GFP was observed in axons after 1DPA in 80% of RNAi (I) #38854 brains and 100% of (II) #330422 brains. Dunnett's multiple comparisons tests revealed axon incidence was significantly higher in RNAi (I) ($p<0.01$) and RNAi (II) ($p<0.0001$). Glomeruli remained intact in all brains after injury, suggesting an engulfment phenotype. *p130Cas* (*Cas Scaffold Protein Family Member 4* (*CASS4)* ortholog), encodes a protein predicted to colocalise with the plasma membrane and perform functions in cell-cell adhesion. Knocking down *p130Cas* (**Fig. 19h-h'**), led to an engulfment phenotype, where both axon and glomerulus structures were recorded in 100% of RNAi (II) #330191 brains. Dunnett's MC tests showed that axon numbers were higher ($p<0.0001$) compared to controls after ablation. Knocking down *Fermitin 1 (Fit1)* predicted to have a role in cell adhesion and orthologous to *Fermitin Family Member 2 (FERMT2),* led to an interesting phenotype*.* After injury, GFP+ glomeruli were observed in 72% of RNAi (I) #105767 brains (**Fig. 19i-i'**). Dunnett's MC tests showed that the reduction was significant compared to controls ($p<0.01$), in addition to no axon GFP. A similar phenotype was observed when knocking down *furrowed* (*fw)* (*CSMD3/SVEP1* ortholog), a selectin also involved in homophilic cell adhesion. In the *fw* RNAi (I) #39575 (**Fig. 19j-j'**), axons and glomeruli were only visible in 88% of uninjured brains, a significant decrease compared to the control ($p<0.01$). Furthermore, glomeruli were only observed in 85% of brains after injury. Equally, when expressing RNAi (II) #106656 axons were visibly fewer, even in uninjured conditions. This phenotype suggested an acceleration of engulfment due to knocking down *fw.* Overall, data suggest membrane modulators may play a variety of roles in glial engulfment (**Fig. 18, Fig. 10e-j'**).

Knocking down genes encoding transmembrane proteins, including *CG34120, CHMP2B* and *Eph* led to glial engulfment deficits. *CG34120* is orthologous to ATP Binding Cassette Subfamily A Member 7 (ABCA7). It expresses an ATPase-coupled transmembrane transporter protein predicted to function in lipid transport. Knocking down *CG34120* led to a loss of function phenotype in 3/5 of RNAi crosses, namely RNAi (I) #100472, (II) #11673 (**Fig. 19k-k'**) and (V) #101700. Multiple comprisons revealed that GFP+ were observed in more brains expression RNAis (I) #100472 ($p<0.01$), (II) #11673 ($p<0.0001$) and (V) #101700 ($p<0.001$), compared to *w-;repo-mcherry*. Glomeruli also appeared intact in all RNAis after ablation, suggesting that *CG34120* may play a role in glial engulfment, enhanced by the fact that the same phenotype was observed using three separate RNAi lines. Similarly, when knocking down Charged multivesicular body protein 2b (CHMP2B) orthologous to *CHMP2B* in humans, engulfment was impaired (**Fig. 19l-l'**). Residual GFP was recorded in both axon bundles and glomeruli after injury in 100% of RNAi (II) #38375 RNAi brains. Dunnett's MC tests revealed that results were significantly higher compared to controls ($p<0.01$). Knocking down *Eph* receptor tyrosine kinase (Eph), orthologous to Eph receptor A1 (EPHA1), led to a similar result (**Fig. 19m-m'**). Axons were visible after ablation in 100% of RNAi (III) #4771 brains, a significant result compared to *w-,repo-cherry* ($p<0.0001$). Overall, data suggest that transmembrane proteins CG34120, CHMP2B and Eph may a role in promoting glial engulfment (**Fig. 18, Fig. 19k-m'**).

Investigations continued with phosphoinositide pathway member Phospholipase D family member 3 (Pld3) the fly ortholog of human PLD3 (**Fig. 19n-n'**). Dunnett's MCs revealed that brains expressing RNAi (II) #109798, more axons were observed after injury compared to control backgrounds ($p<0.0001$), suggesting a LOF phenotype. Small wing (*sl*), orthologous to *Phospholipase C Gamma* 2 (*PLCγ2*) presented with a similar outcome. It is required as a general modulator downstream of the insulin pathway and interacts with a number of factors, some of which are common to the *Draper* pathway. Knocking down *sl* led to a strong LOF phenotype in 1/4 RNAis (**Fig. 19o-o'**). After injury, axons and glomeruli were visible in 100% of RNAi (III) #32906 brains, a significant increase compared to *w-;repo- mcherry* ($p<0.0001$), according to Dunnett's multiple comparisons test. Both genes presented a potential role in glial engulfment, with knockdown leading to LOF phenotypes (**Fig. 18, Fig. 19n-o'**).

Finally, transcription factors such as *bru1, DOR* and *Mef2* may also be involved in glial engulfment. *Bruno 1 (bru1*), a CUGBP Elav-Like Family Member 1 *(CELF1)* ortholog, encodes an RNA binding protein acting in multiple forms of post-transcriptional gene regulation. Seven distinct *bru1* RNAis were investigated, of which three led to phenotypes. After injury, axon GFP was still detectable in 100% of RNAi (I) #38983 and (VI) #48237 brains (**Fig. 19p-p'),** and 88% of RNAi (VII) #107459 brains. Dunnett's MC tests suggested that axon incidence was higher in experimental lines compared to controls (all $p<0.0001$). GFP+ glomeruli were recorded in 100% of brains, suggesting a delay in engulfment as a result. This is further supported by the repeatable phenotype across multiple RNAis. When knocking down *Diabetes and obesity regulated (DOR*), orthologous to *TP53INp1*, an engulfment delay was observed (**Fig. 19q-q'**). Axon bundles were recorded in 75% ablated RNAi (I) #60389 brains, significantly higher than control lines ($p<0.01$). Similarly, knocking down *Mef2* led to a LOF phenotype in 3/5 RNAis (**Fig. 19r-r'**). *Myocyte enhancer factor 2 (Mef2*) belongs to the MADS-box family of transcription factors and is orthologous to *MEF2C* in humans. After injury, GFP was observed in the axons of 50% of RNAi (III) #38247 brains, 75% of (IV) #28699 brains and 100% of (V) #15550 brains. Multiple comparisons revealed that RNAi #28699 was significantly different to the control ($p<0.01$). Overall, knocking down these transcription factors caused a LOF phenotype, suggesting a potential role in engulfment (**Fig. 18, Fig. 19p-r'**).

Generally, based on *mcherry* signal alone, there were no significant phenotypes to report, however, the odd phenotype observed when knocking down *Amph* could be explained by glial ablation. Glial fluorescence appeared consistent across KDs, suggesting that engulfment phenotypes were a result of dysfunction glia as opposed to glial apoptosis. Equally, when *mcherry* data was missing due to technical faults (in the case of *cindr* and *CHMP2B* KDs), the presence of glia could not be verified. **Fig. 19g-g'** and **l-l'** are missing glial panels as a result of microscopy complications, therefore no explicit conclusions were made for these RNAi lines.

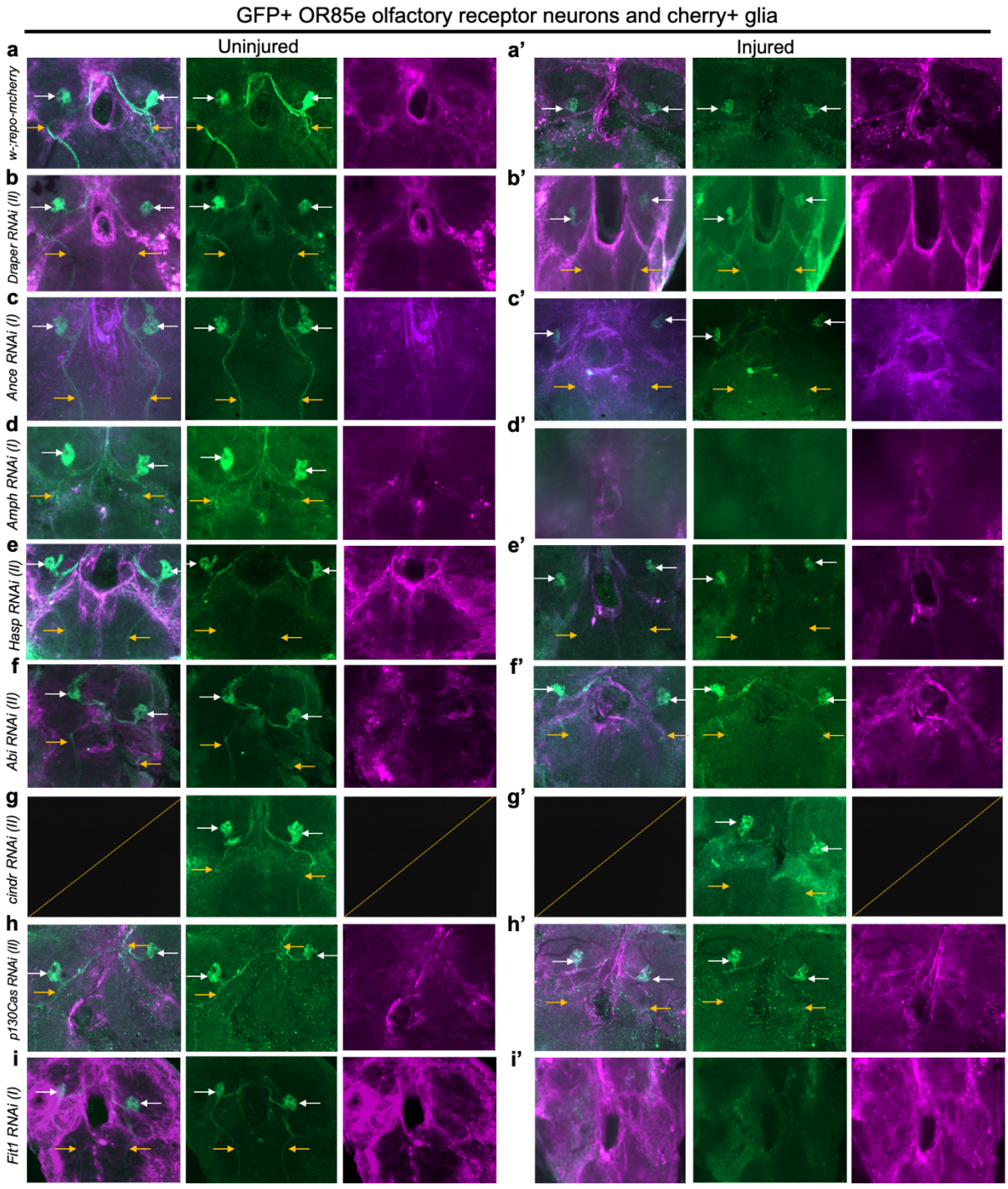
GFP+ OR85e olfactory receptor neurons and cherry+ glia
Uninjured
Injured
a
a'
w-;repo-mcherry
b
b'
Draper RNAi (II)
c
c'
Ance RNAi (I)
d
d'
Amph RNAi (I)
e
e'
Hasp RNAi (II)
f
f'
Abi RNAi (II)
g
g'
cindr RNAi (II)
h
h'
p130Cas RNAi (II)
i
i'
Fit1 RNAi (I)

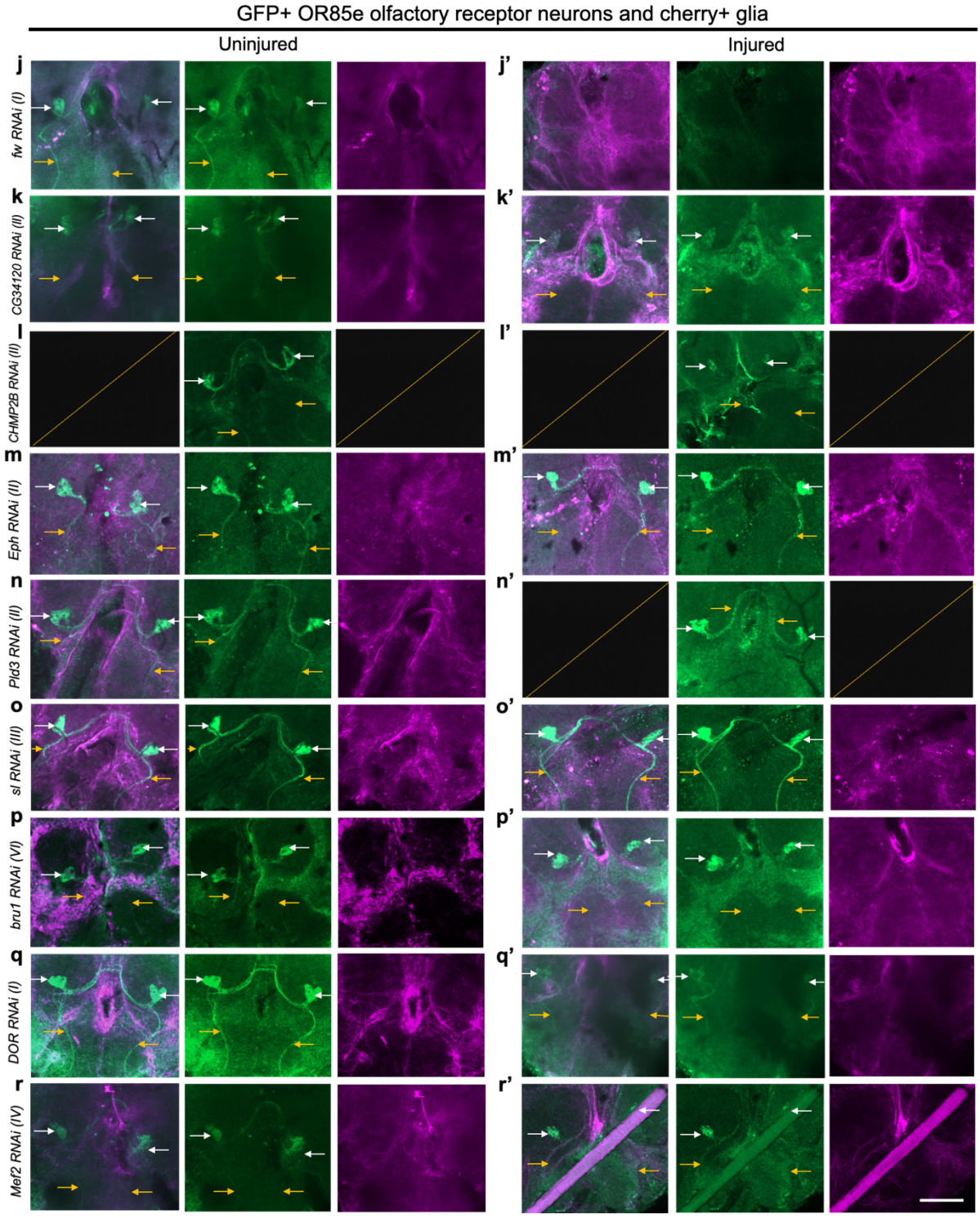
GFP+ OR85e olfactory receptor neurons and cherry+ glia
Uninjured
Injured
j
fw RNAi (I)
j'
k
CG34120 RNAi (II)
k'
l
CHMP2B RNAi (II)
l'
m
Eph RNAi (II)
m'
n
Pld3 RNAi (II)
n'
o
sl RNAi (III)
o'
p
bru1 RNAi (VI)
p'
q
DOR RNAi (I)
q'
r
Mef2 RNAi (IV)
r'

***Fig. 19. Knocking down AD Risk Genes Led to Various Engulfment Phenotypes.*** *__a-r'__) Z-stack projection of representative brains with GFP labelled neurons (green), mcherry labelled glia (magenta) before __x)__ and 1 day after maxillary nerve axotomy __x')__ respectively. Panels from top to bottom, show GFP+ axons (yellow arrows) and glomeruli (white arrows) across different RNAi lines. __a-a'__) w-,repo-cherry controls, with intact neurons before injury __a__) fading to just glomeruli after injury __a'__). __b-b'__) Draper RNAi (II), with intact neurons visible before __b__) and after injury __b'__). __c-c'__) Ance RNAi (I) with visible axons and glomeruli before __c__) and after injury __c'__). __d-d'__) shows Amph RNAi (I) brains which lose GFP signal before __d__) and after injury __d'__). __e-e'__) Hasp Rai (II) brains, with visible neurons before __e__) and after injury __e'__). __f-f'__) display Abi RNAi (II) brains whose neurons express GFP before __f__) and after injury __f'__). __g-g'__) represent cindr RNA (II) brains, intact neurons before __g__) and after injury __g'__)*. __h-h'__) p130Cas RNAi (II), displaying GFP+ axons before __h__) and after __h'__) ablation. __i-i'__) Fit1 (I), with neurons intact before injury __i__) but gone after injury __i'__). __j-j'__) fw RNAi (I), with neurons already fading before __j__) and after injury __j'__). __k-k'__) CG34120 RNAi (II) brains with neurons intact before __k__) and after injury __k'__). __l-l'__)* CHMP2B RNAi (II) with axons in tact before __l__) and after __l'__) injury. __m-m'__) Eph RNAi (II) expressing brain, with both GFP-expressing axons and glomeruli before __m__) and __m'__). __n-n'__) Pld3 RNAi (II) expressing brain had intact neurons before __n__) and after injury __n'__)*. __o-o'__) sl RNAi (III) brains with GFP-expressing axons before __o__) and after __o'__) injury. __p-p'__) bru1 RNAi (VI) expressing brains showing intact neurons before __p__) and after injury __p'__). __q-q'__) DOR RNAi (I), with intact brains before __q__) and after injury __q'__). __r-r'__) Mef2 RNAi (IV) expressing brains with visible neurons before __r__) and after injury __r'__). Glia were present in all repo panels (__a-r'__). Scale bar = 50μm. *Cases where mcherry signal was not recorded due to technical issues.*

### 4.4.3 Verifying Screen Candidates Yielded Similar Phenotypes

Having identified a number of genes which could be involved in engulfment, the strongest 'hit' RNAis were crossed, injured and prepared for analysis. Results were analysed in the same manner as the screen, recording axons and glomeruli as percentages after ablation (**Fig. 20**), to determine a phenotype. *w-, repo* and *Draper* RNAi (II) #27086 were used as negative and positive controls respectively. As expected, in *w-;repo* controls, neurons were intact in injured samples, with axons visible in only 23% of injured samples (**Fig. 21a**). Axons were still visible in 100% of *Draper* RNAi (II) #27086 brains, despite injury (**Fig. 21b**). A 1-way ANOVA revealed that axon incidence was significantly different between experimental groups after injury ($p<0.0001$) (**Fig. 20**). Dunnett's MC tests revealed that the number of axons was significantly higher in *Draper* KD flies compared to controls ($p<0.0001$), suggesting a LOF phenotype. Axons were also recorded in the brains of injured *Abi* (RNAi (II) #51455) (**Fig. 21c**), *bru1* (RNAi (I) (#38983) (**Fig. 21d**), *CHMP2B* (RNAi (II) #38375) (**Fig. 21f**), *Mef2* (RNAi (IV) #28699) (**Fig. 21i**), *Pld3* (RNAi (II) #109798) (**Fig. 21k**) and *sl* (RNAi (III) #32906) (**Fig. 21l**) expressing flies. Dunnett's multiple comparisons tests revealed that the incidence of GFP+ axons was significantly higher in these KDs compared to *w-,repo* controls (**Fig. 20**) – suggesting repeatable engulfment deficits. Knocking down *CG34120* (RNAi #11673) (**Fig. 21f**), *cindr* (RNAi #330191) (**Fig. 21e**), *Hasp* (RNAi #65101) (**Fig. 21h**) and *p130Cas* (#330191) (**Fig. 21j**) led to phenotypes mimicking the control, whereby reduced axon bundles were visible after injury (**Fig. 21**). Data suggest that most genes identified as 'hits' in section **4.4.2** were verifiable and likely to contribute to glial engulfment of dying neurons.

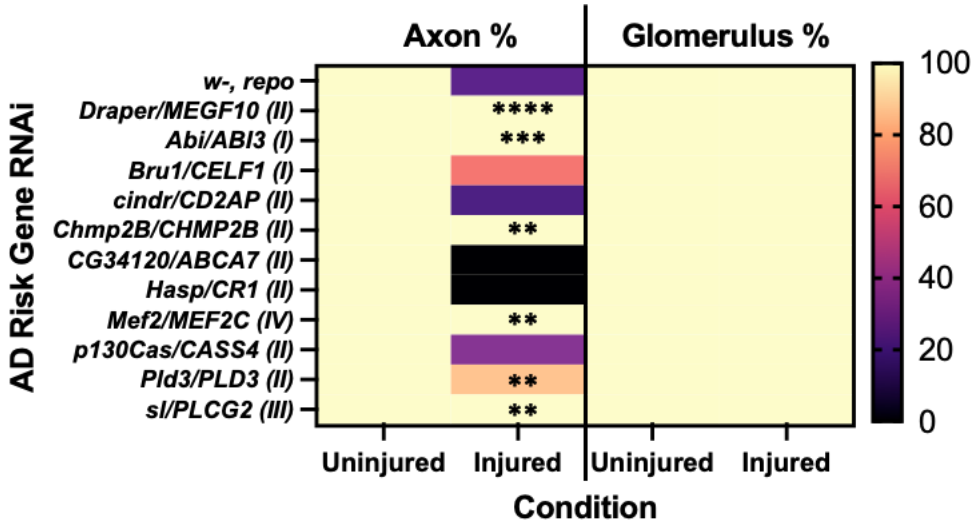

***Fig. 20. Verifying Screen Hits Led to Some Repeatable Phenotypes.*** *A heat-map representation of the incidence of injured and control axon and glomerulus phenotypes (from left to right). Incidence is represented in percentage form from 0-100% (black-yellow). RNAis are listed on the x-axis and phenotypes on the y-axis. Statistical comparisons were achieved for separate groups (ex: Control: Axon %) by 1-way ANOVA and Dunnett's multiple comparisons test, with significant differences annotated as *p<0.05, **p<0.01, ***p<0.001 and ****p<0.0001, n=2-17 brains per group.*

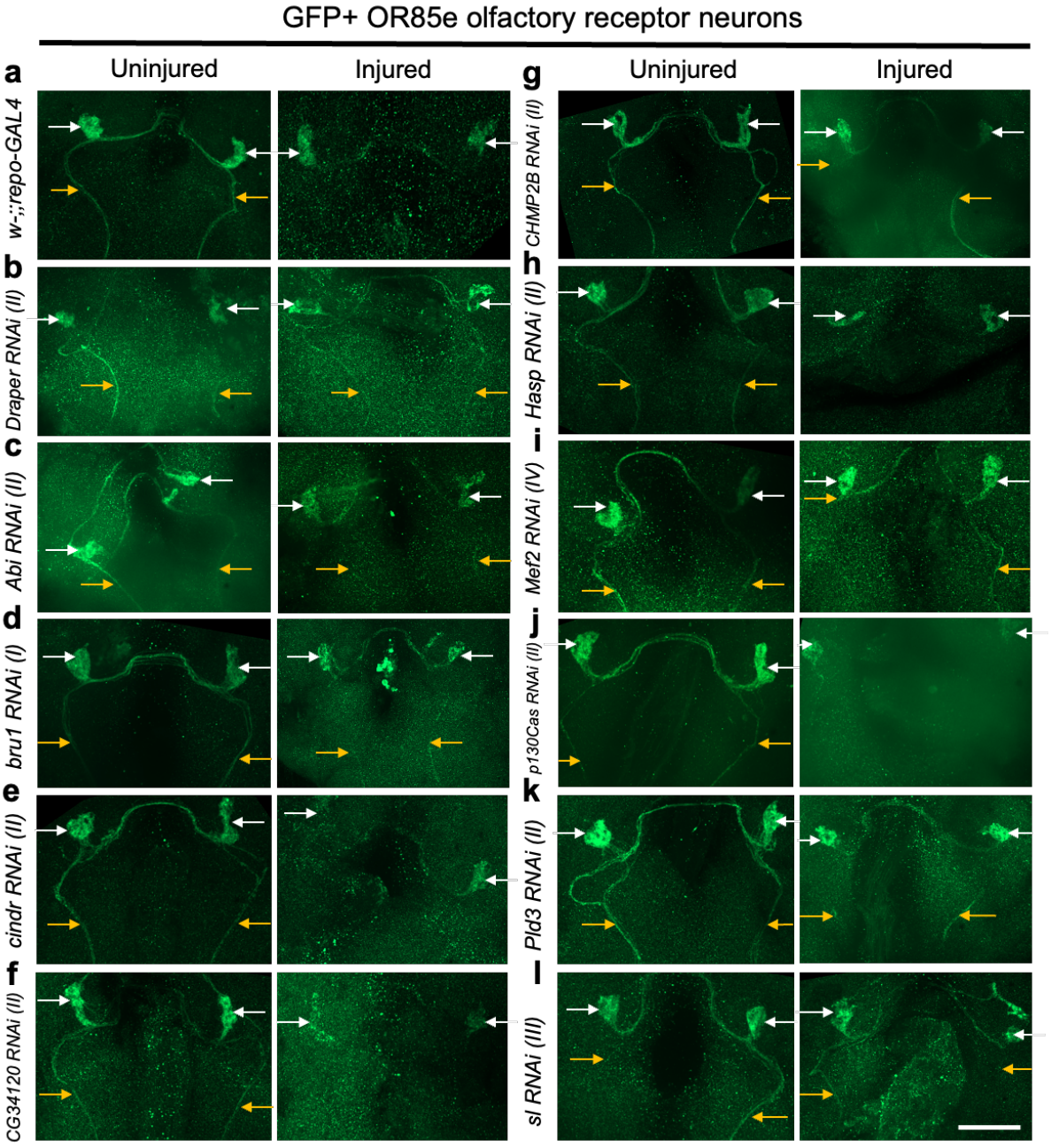

***Fig. 21. Knocking down AD Risk Genes Led to Various Engulfment Phenotypes.*** ***a-r'****) Z-stack projections of representative brains with GFP labelled neurons (green), in uninjured conditions (left panel) and 1 day after injury (right panel). Panels from top to bottom, show GFP+ axons (yellow arrows) and glomeruli (white arrows) across different RNAi lines.* ***a****) w-,repo-cherry controls, with intact neurons before injury fading to just glomeruli after injury.* ***b****) Draper RNAi (II), with intact neurons visible before and after injury.* ***c****) Abi RNAi (II) brains where axons are visible before and after injury.* ***d****) bru1 RNAi (I) expressing brains where neurons express GFP before and after injury.* ***e****) cindr RNA (II) with only glomerulus visible after injury.* ***f****) CG34120 RNAI (II) brains, where GFP is no longer visible in axons after ablation.* ***g****) CHMP2B RNAi (II) brains, with intact neurons before and after injury.* ***h****) Hasp RNAi (II) brains show GFP only in glomeruli after injury.* ***i****) Mef2 RNAi (IV) brains, with intact axons and glomeruli despite ablation.* ***j****) p130Case RNAi (II) brains, showing only GFP+ glomeruli after injury.* ***k****) Pld3 RNAi (II), with GFP+ axons after injury.* ***l****) sl RNAi (III), where axons and glomeruli are visible before and after injury. Scale bar = 50μm.*

## 4.5 Discussion

The reverse candidate screen yielded several 'hit' genes, which displayed a potential role in glial engulfment. Most KDs led to a loss-of-function phenotype; whereby GFP-expressing axons were still recorded after ablation. Knocking down *Fit1* and *fw* led to an acceleration in engulfment, such that reduced numbers of both axons and/or glomeruli were recorded compared to controls. Upon validating LOF screen 'hits', *Abi* (RNAi #51455), *bru1* (RNAi #38983), *CHMP2B* (RNAi #38375), *Mef2* (RNAi #28699), *Pld3* (RNAi #109798), and *sl* (RNAi #32906) produced verifiable phenotypes, whereby axons and glomeruli were visible in most brains despite injury. Overall, data support further research into *Abi*, *bru1*, *CHMP2B, Fit1, Fw, Mef2, Pld3 and sl*, genes, and demonstrate an important role to play in glial engulfment.

### 4.5.1 Several AD Risk Genes are Involved in Glial Engulfment

*Abelson interacting protein (Abi)* is presumed to regulate actin dynamics in the formation of phagocytic cups, as an interactor protein to the WAVE regulatory complex. The WAVE regulatory complex is a multi-subunit complex which mediates actin dynamics, through activation of Arp2/3-mediated actin nucleation (Juang and Hoffmann 1999; Kunda et al. 2003; Lin et al. 2009). This gene may behave downstream of *Draper* due to its role in actin organisation, which is core to phagocytosis. *Abi* is the closest ortholog to *ABI3* in humans, which is also an interactor of the WAVE complex and is involved in actin polymerisation (Sekino et al. 2015). Although little has been tested in microglia, ABI3 is enriched and probably involved in microglial motility and/or phagocytosis, supporting further investigation into this gene. Recent stem cell research suggests a role of for ABI3 in microglial function such as motility and uptake of zymosan-conjugated pHrodo beads, which in *ABI3* KO microglia was significantly lower (Rolova et al. 2020). Overall, although research is in its infancy, there is a lot of excitement about this gene in microglial function.

*Angiotensin converting enzyme (Ance)* encodes a member of peptidyl-dipeptidase family, the product of which has broad specificity and function. Known functions include hormone processing, response to symbiotic bacteria and spermatid development, however little is known of its role in the *Drosophila* nervous system

(Houard et al. 1998; Hurst et al. 2003; Xi et al. 2008). Its potential role in engulfment could be due to Ance being orthologous to both human *ACE (angiotensin I converting enzyme)* and *ACE-2 (angiotensin I converting enzyme 2),* both of which have been implicated in Alzheimer's pathology. Studies in post-mortem brains have investigated the expression and distribution of ACE-2 in relation to AD hallmarks, such as Aβ and tau pathologies and found that ACE-2 levels were significantly lower with increased Aβ aggregation and higher in cases of phosphorylated tau pathology (Kehoe et al. 2016). The same study identified that ACE-2 converts $A\beta_{43}$ to $A\beta_{42}$, which in turn is cleaved by ACE-1 to less toxic $A\beta_{40}$ and $A\beta_{41}$ species (Kehoe et al. 2016). More recently, research unveiled a risk variant in ACE which was also associated with Aβ-accelerated neurodegeneration overall adding to a growing body of evidence to support its importance in Alzheimer's (Cuddy et al. 2020). The role of these enzymes in glia is less understood and warrants further investigation.

*Bruno-1 (bru1)* encodes an RNA binding protein, which plays various regulatory roles in post-translation gene regulation, including repression and activation of translation and alternative splicing of pre-mRNAs (Spletter et al. 2015). bru1 activity is mainly required in gametogenesis, developmental patterning and muscle organisation (Sugimura and Lilly 2006; Xin et al. 2013; Spletter et al. 2015). Known for it's role as a splicing factor, previous research has not uncovered a role in glial phagocytosis. Its ubiquitous role in RNA processing could, however, regulate glial health with downstream impacts on function.

*Charged multivesicular body protein 2b* (*CHMP2B*) encodes an endosomal sorting complex required for transport (ESCRT)-III component and plays an important role in generating multivesicular bodies in the endosome-lysosomal pathway and is attributed to autophagosome maturation (Cheruiyot et al. 2014; Krasniak and Ahmad 2016). It does not belong to the AD risk gene list, however, studies have identified a role for this gene in frontotemporal dementia, linking it to the NOTCH-signalling pathway in fly models (Cheruiyot et al. 2014). Early research in the human version *CHMP2B* also discusses its role in dementia, whereby rare mutations in the gene can cause autosomal dominant frontotemporal dementia (FTD), where mutations can lead to C-terminal truncations which can have a severe impact on endosome-lysosomal pathways (Skibinski et al. 2005; Lindquist et al. 2008; M. Isaacs et al. 2011; Cheruiyot

et al. 2014). Additionally, it has been found to localise in glial cytoplasmic inclusions in Multiple system atrophy (MSA), with further suggestions that it the gene may play a role in regulating a-synuclein aggregation (Tanikawa et al. 2012). The results combined with some supporting literature provide a good case to study the gene further, potentially in the wider context of dementia and glial function.

*Myocyte enhancer factor 2 (Mef2)* encodes a transcription factor belonging to a family required for muscle development. It is responsible for the expression of muscle protein genes, however, it also regulates expression in other tissues such as neural tissue (Ruiz et al. 2014; Tansey et al. 2018). A genetic interaction screen published in 2020, revealed a role for *Mef2* in neurodevelopment (Straub et al. 2020). They assessed several parameters including bang sensitivity and climbing behaviour (often used to assay cognitive function), resulting in a range of phenotypes when knocking down *Mef2*. *Mef2* is orthologous to *MEF2C* in humans which carries out similar functions. A more recent AD risk gene GWA study, deems the gene no longer reaching genome-wide significance, however it may still tell an interesting story in microglia (Kunkle et al. 2019). A 2017 article claims that *MEF2C* regulates an inflammatory microglial response which diminishes with age (Deczkowska et al. 2017). They show that *MEF2C* KO mice have exaggerated microglial responses and that MEF2C expression is regulated by long-term exposure to interferon type 1 (IFN-1). Current results pair well with the literature to warrant further study, with an emphasis on glial function.

*Pld3* (*PLD3* ortholog) is predicted to have catalytic activity as a membrane-associated protein, interacting in the phosphoinositide cycle (Gaudet et al. 2011). *PLD3* is a fairly new gene in the field of Alzheimer's research, however, a recent paper investigates the role of PLD3 in an Aβ-model fly, suggesting that a specific V232M substitution impairs the neuroprotective function of PLD3 through impaired O- glycosylation (Demirev et al. 2019). An *in vitro* study from the same year sees an increase in Aβ levels in response to *PLD3* mutations identified in GWA studies. They attribute the reduction to changes in autophagy through the mTOR pathway (Tan et al. 2019). An influential study from 2017, studied the effect of knocking out *PLD3*, concluding this had no effect on APP processing, but that levels of Aβ increased due to endosomal-lysosomal systems (Fazzari et al. 2017). Previous research has also identified an accumulation of PLD3 in neuritic plaques of AD brains (Satoh et al. 2014). There is

very little research into the role of *PLD3* in glia, however my results provide intrigue to further investigate its role in engulfment, which I hypothesise may regulate Aβ accumulation.

*Small wing (sl)* encodes a phosphatidylinositol-specific phospholipase type C (PLC), required for growth downstream of the insulin pathway. It also interacts with the Ras-MAPK pathways, known to interact with the *Draper* pathway (Murillo-Maldonado et al. 2011; Fullard and Baker 2015). *sl* is widely studied in flies, particularly its role in wing and eye development (Mankidy et al. 2003). Similar to mouse-related studies, it is associated with $Ca^{2+}$ regulation in cells (Sullivan and Rubin 2002). It is orthologous to *PLCγ2* in humans, a controversial gene in the history of Alzheimer's research as its variant has been described as protective against the disease. *PLCγ2* (Phospholipase C-gamma 2) encodes PLCγ2, an enzyme that cleaves membrane phospholipid $PIP_2$ into secondary messengers $IP_3$ and diacyl-glycerol (DAG), propagating a range of downstream signals (Koss et al. 2014). A recent study investigated the distribution of *PLCγ2* in human and mouse brain tissue and assessed enzymatic function in transfected cell lines with the P522R variant (Magno et al. 2019). They found that *PLCγ2* was almost exclusively expressed in microglia and granule cells, in particular, plaque-associated microglia of mouse models and that the mutation only had a small effect on enzyme function. PLCγ2 is also theorised to be involved in the same signalling pathway as TREM2, an inflammatory gene (Sims et al. 2017). *PLCγ2* is clearly an interesting, microglia-specific gene which requires further study to unravel it's complex functions.

*Fermitin 1* (*Fit1*) is largely understudied in *Drosophila*, however, it is presumed to have cell adhesion functions and aid in the defence response to Gram-negative bacteria (Gaudet et al. 2011). A recent functional screen found *Fit1* and *Fit2* to modify Tau toxicity, along with *cindr* (*CD2AP* ortholog) (Ojelade et al. 2019). Its human counterpart is *FERMT2* (known as kindlin-2), is an integrin activation-interacting protein. It has been shown to participate in angiogenesis in mice and promote breast cancer through the promotion of genome instability (Pluskota et al. 2011; Zhao et al. 2013). A 2016 GWA analysis in from a Chinese cohort of patients, suggested that in fact *FERMT2* does not reach genome-wide significance in their sample population (Zhang et al. 2016a). However, another study from that year implies FERMT2 as a major modulator

of APP metabolism in a high-content siRNA screen (Chapuis et al. 2017). It appears that *FERMT2* is a mystery in the world of dementia and its role in glia has not yet been investigated.

*Furrowed* (*fw)* encodes a selectin that mediates the interaction of planar cell polarity and is involved in homophilic cell adhesion (Chin and Mlodzik 2013). *fw* is orthologous to both *CSMD3* (CUB and Sushi multiple domains 3) and *SVEP1* (sushi, von Willebrand factor type A, EGF and pentraxin domain containing 1). *CSMD3* is a transmembrane protein required for neuronal maturation, which has been implicated in a range of cognitive disorders, including schizophrenia (Sakamoto et al. 2016). CSMD is strongly expressed in the brain however little is known of its function in disease (Gutierrez et al. 2019). Equally, the selectin gene *SVEP1* is largely understudied in the field of dementia. It has been attributed to lymphatic vessel formation and potentially astrocyte-to-astrocyte contact (Karpanen et al. 2017; Li et al. 2019b). The GOF phenotype observed in the screen implies that fw acts as a negative regulator of engulfment and there may be more to discover about its context of glial function.

### 4.5.2 Reverse Candidate Screening

A reverse candidate screen is a ‘quick and dirty’ method to identify novel roles for specific genes. RNAis are often used as they are readily available, easy to breed into fly lines and generally reliable for initial investigation. A disadvantage to using RNAis is the possibility of off-target effects, which produce varying degrees of knockdown, or in some cases do not function (Qiu et al. 2005). Repo-GAL4 is considered a strong driver and has previously been used for engulfment screening (MacDonald et al. 2006), however, *GAL4* expression may have been further diluted due to the introduction of an additional *UAS* construct (*mcherry*). It is recommended that ‘hits’ are validated by repeating experiments and confirming knockdown using an antibody or qPCR (Holmes et al. 2010). Most ‘hits’ were verified in a second smaller screen and sometimes multiple RNAis targeting the same gene led to a similar result, such as *bru1.* It is also important to note that ‘negative data’ (here, a control phenotype) does not exclude the possibility of non-hit genes play a role in glial engulfment. It is also recommended to study candidate genes further by sourcing and studying knockout/knockin mutant lines (Heigwer et al. 2018).

## 4.6 Summary of Key Findings

- A reverse candidate knockdown screen revealed genes *Abi, bru1, cindr, CG34120, DOR, Fit1, fw, Hasp, Lap, Mef2, p130Cas, Pld3* and *sl* to play a potential role in glial engulfment.
- A lethality assay exposed several RNAis to cause a lethal phenotype when expressed in glia, including RNAis specific to the afore-mentioned candidates.
- Repeating the engulfment assay in the strongest 'hit' RNAis confirmed *Abi* RNAi (II) #51455, *bru1* RNAi (I) #38983, *CHMP2B* RNAi (II) #38375, *Mef2* RNAi (IV) #28699, *Pld3* RNAi (II) #109798, and *sl* RNAi (III) #32906 as modulators of engulfment. *Fit1* RNAi (I) #10567 and *fw* RNAi (I) #39575 and engulfment mechanisms relating to these genes has yet to be explored.

# 5 sl and Pld3 Help Regulate Engulfment of Neuronal Debris

## 5.1 Introduction

Results from the engulfment screen in addition to existing data from the lab indicate that *sl* and *Pld3* could be important modulators of glial function. Both genes are considered significant genetic risk factors in AD and are typically enriched in microglia (Efthymiou and Goate 2017; Sims et al. 2017). Their sequences encode for members of the phosphoinositide pathway, which regulates phospholipid turnover at the membrane and initiates important downstream events such as Target of Rapamycin (TOR) signalling and autophagy (Foster 2013; Xie et al. 2020; Lenoir et al. 2021). *sl* and *Pld3* are highly conserved with DIOPT scores of 10 and 15 respectively, which promotes *Drosophila* as a model to investigate their specific functions.

### 5.1.1 PLCγ2 Variants Confer Reduced Risk of AD

Recent advances in sequencing technology have identified rare mutations in AD-patient cohorts revealing coding variants in the Phospholipase C-gamma 2 (*PLCγ2)* locus (Sims et al. 2017). One variant of *PLCγ2*, P522R was recently associated with decreased risk of pathology whereas M28L confers increased AD risk (Efthymiou and Goate 2017; Bonham et al. 2019; Bellenguez et al. 2022). Interestingly, the variant P522R was identified to confer reduced risk in other neurodegenerative disorders and is likely to increase longevity (Magno et al. 2019; Maguire et al. 2020). *PLCγ2* encodes an enzyme involved in relaying extracellular information to the cell. Such signals direct many cellular processes, from proliferation to cell motility (Magno et al. 2021). Upon activation of certain transmembrane immune receptors including TREM2, the enzyme cleaves membrane-associated phosphatidylinositol 4,5-bisphosphate (PIP2), catalysing its conversion to inositol 1,4,5-trisphosphate (IP3) and diacylglycerol (DAG) (Hernandez et al. 1994; Koss et al. 2014). IP3 then releases $Ca^{2+}$ from internal stores whereas DAG activates protein kinase C (PKC). PIP2 conversion is equally catalysed by PI3K in a parallel reaction to produce Phosphatidylinositol-3,4,5-triphosphate (PIP3) (Osaki et al. 2004). Downstream of PI3K, PIP3 species can instigate other survival pathways such as TOR signalling and upregulation of Signal transducer and transcription activator 92E (*STAT92E*) (**Fig. 22).** *PLCγ2* has been classically studied in immune cells such as B cells, natural killer (NK) cells and mast cells, where PLCγ2 appears to perform essential roles in responses to infection, by recognising invading

pathogens and initiating inflammatory pathways (Kim et al. 2004). However, neuroscience research is now uncovering further roles for the gene in microglia. Like TREM2, PLCγ2 is selectively expressed in microglia over other cells in the CNS. A recent study investigated the distribution of *PLCγ2* in human and mouse brain tissue and assessed enzymatic function in transfected cell lines with the P522R variant (Magno et al. 2019). They found that *PLCγ2* was almost exclusively expressed in microglia and granule cells, especially plaque-associated microglia of mouse models and that mutations only had a small effect on enzyme function.

A single *PLCγ* gene has been identified in *Drosophila*, known as *small wing (sl)*. Due to low redundancy in the *Drosophila* genome, this sequence encodes the only *PLCγ* ortholog, which encodes a protein equally similar to PLCγ1 and PLCγ2 (Manning et al. 2003). *sl* encodes for a phosphatidylinositol-specific phospholipase type C that is required as a general modulator for growth downstream of the insulin pathway (Murillo-Maldonado et al. 2011). It is known to interact with Ras/mitogen-activated protein kinase (Ras-MAPK) pathway, the latter known to interact with the *Draper* engulfment pathway (Murillo-Maldonado et al. 2011; Fullard and Baker 2015). Therefore, it is feasible that *sl* is an upstream regulator of engulfment. In *Drosophila, sl* is often studied in the context of development due to its requirement in the formation of the eyes and wings (Mankidy et al. 2003). sl promotes growth and suppresses ectopic differentiation in these developing tissues, meaning cells can become their normal size, differentiate as expected and produce the intended tissue (Murillo-Maldonado et al. 2011). Mutants of the gene have led to various phenotypes, such as small wings, ectopic wing veins, and extra R7 photoreceptor cells. In cell differentiation, sl is seen to be activated upstream by the insulin receptor, which negatively modulates Epidermal Growth Factor (EGF) signalling to promote fate-determination, however in some circumstances growth is promoted through EGF activity (Wang et al. 2000). The insulin receptor, therefore, modulates differentiation as well as growth through sl (Murillo-Maldonado et al. 2011). During photoreceptor R7 development, *sl* inhibits receptor tyrosine kinase (RTK) signalling. Examination of the eye morphology of *sl* mutant reveals a defect in the increased presence of R7 photoreceptors. Such phenotypes are likely due to the overactivation of the Ras/Raf/MEK/MAPK cassette, suggesting that *sl* could negatively regulate Ras-mediated signalling during development *in vivo* (Thackeray et al. 1998). Like mouse-related studies, it is associated with $Ca^{2+}$

regulation in cells (Sullivan and Rubin 2002). Interestingly, $Ca^{2+}$ has been implicated in the Draper pathway, whereby deficits in phagocytosis are associated with the knockdown of another calcium modulator, junctophilin Undertaker (Cuttell et al. 2008). Although cell and mouse models exist to study the function of *PLCγ2,* progress can be slow and limited. *Drosophila* enable us to study a gene in detail without sacrificing time and include all the benefits of a live model. Importantly, *sl* is largely understudied in fly neurodegenerative models, especially glia, therefore it would be of great interest to contribute to existing knowledge of *PLCγ2* using the elegant fruit fly.

### 5.1.2 PLD3 may Play a Role in Amyloid Processing and Endosomal Trafficking

GWA studies have shown that rare variants in the type-II transmembrane *Phospholipase D3 (PLD3),* another member of the phosphoinositide pathway, are associated with an increased risk of developing AD in some European and Han Chinese cohorts (Cruchaga et al. 2014; Schulte et al. 2015). Three variants have been identified, including p.V232M, p.I163M and p.R356H. Each has been studied in various contexts, with some pertaining to amyloid pathology and cognitive decline, however, this relationship is controversial, with many failed replications (Wang et al. 2015a; Fazzari et al. 2017; Engelman et al. 2018). In particular, p.I163M and p.R356H cause reduced PLD3 activity and have led to increased amyloid-beta levels in some cellular models of AD (Tan et al. 2019). In AD brains, PLD3 protein levels are moderately lower, with downregulated transcriptional levels (Blanco-Luquin et al. 2018). Some studies show PLD3 co-localisation with APP in endosomes and that loss of PLD3 function can result in increased Aβ production (Mukadam et al. 2018). Mouse studies revealed multiple pathological phenotypes, such as amyloid accumulation and poor memory performance in animals with lower PLD3 levels (Nackenoff et al. 2021). How PLD3 mediates AD phenotypes at a molecular level is heavily debated, with evidence supporting altered APP processing, endo-lysosomal functioning, and endoplasmic reticulum (ER) homeostasis (Fazzari et al. 2017; Nackenoff et al. 2021). PLD3 is expressed in most cells of the CNS, although appears highly expressed in specific regions of the brain, including the hippocampus and cortex (Cruchaga et al. 2014). Interestingly, it does not co-localise with activated microglia and astrocytes in the human brain (Satoh et al. 2014). Belonging to a family of phospholipases, including

PLD1 and PLD2, known functions include endocytic trafficking and APP processing in cellular models (Iyer et al. 2004; Oliveira et al. 2010). PLDs perform an important role in converting phosphatidylcholine (PC) to phosphatidic acid (PA) and choline, which can impact membrane dynamics and cell signalling, among other important cellular processes (**Fig. 22**) (Bruntz et al. 2014). Occasionally, PLDs have also displayed nuclease activity and cardiolipase activity, however how the protein family functions in glia are not understood.

In *Drosophila,* there exists a highly conserved ortholog also known as *phospholipase D3 (Pld3),* which encodes for a protein with many predicted functions, including the regulation of inflammatory cytokine production and modulating single-stranded DNA 3'-5' exodeoxynuclease activity. Pld3 is often located in the endoplasmic reticulum membrane or lysosomal lumen. To investigate the obscure nature of PLD3 variant p.V232M, a major *Drosophila* study sought to understand the specific role of Pld3 in amyloid models (Demirev et al. 2019). The substitution in flies, impaired O-glycosylation, attenuating Pld3's trafficking to the lysosome, leading to enlarged lysosomes, and plausible aberrant protein recycling. Models with the mutation were less neuroprotective and less able to perform in cognitive assays (Demirev et al. 2019). This study remains the only one to investigate *Pld3* in the *Drosophila* CNS and to model the functions of individual variants. Equally, the role of PLD3 in AD pathogenesis is largely understudied and unclear, especially with its controversial nature and little data in microglia, making it an exciting gene to pursue.

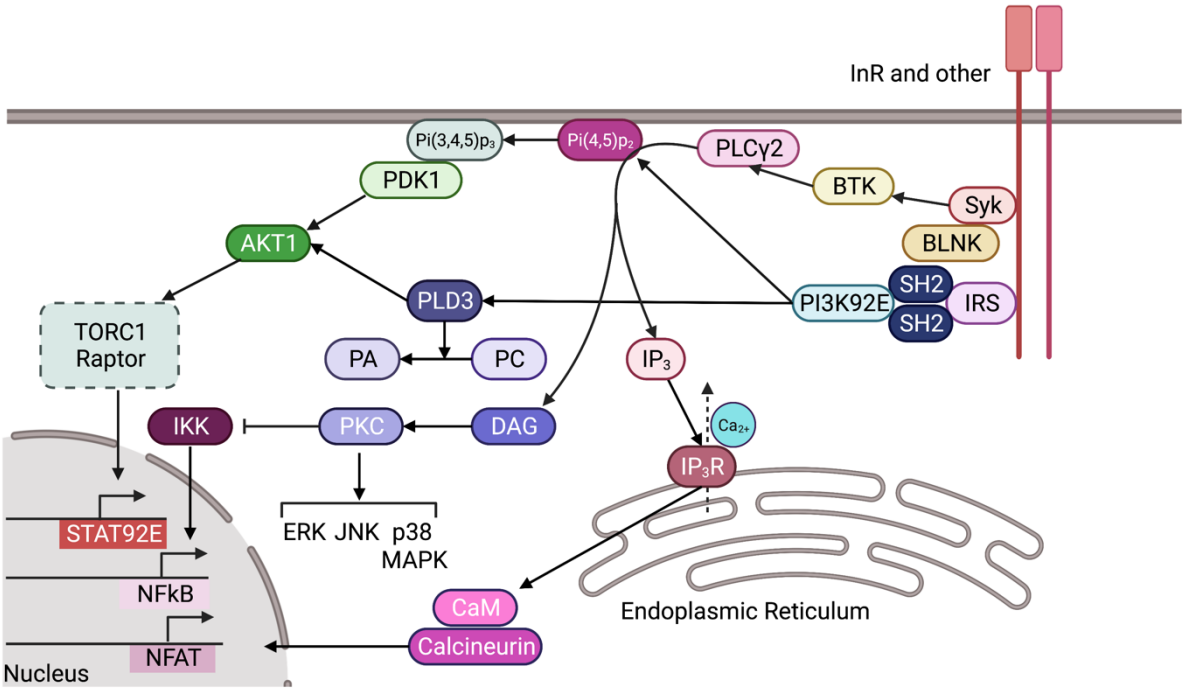


***Fig. 22. Schematic of sl and Pld3 Roles in Phospholipid Pathway.*** *To the right, a representation of InR and other receptors initiating the phosphoinositide pathway. Activation of PLCγ2 converts PIP2 into IP3 and DAG. IP3 releases Ca2+ from the endoplasmic reticulum and DAG activates PKC. Activation of PI3K92E converts PIP2 in PIP3 species, later initiating survival pathways such as mTor and upregulating STAT92E. PLD3 activation promotes PC to PA conversion and has been known to activate AKT1/PKB upstream of TORC1.*

## 5.2 Aims and Objectives

Previous results alongside existing evidence forge a possible role for *sl (PLCγ2)* and *Pld3 (PLD3)* in glial engulfment function. Neither gene has been studied in the context of adult glial engulfment in the *Drosophila* model, leaving space to contribute to existing theories. This chapter will employ multiple assays to characterise these genetic hits and unravel their role(s) in glial function. Here, I utilise online resources and qPCR to ascertain expression levels of *sl* and *Pld3* respectively in *Drosophila* brain tissue. Equally, I will continue to use the highly published ORN injury model system, where I will explore the extent of *sl* and *Pld3's* role in glial engulfment function.

## 5.3 Experimental Design

Gene expression data was investigated using the online resource SCope (http://scope.aertslab.org/#/). We selected repo$^{+}$ cells in the filtered adult brain dataset, followed by analysis methods highlighted in **Chapter 2.** Gene knockdown was confirmed using qPCR with results presented the supplementary data section of the thesis (**Fig. S1-3**). Using the injury model system, described in **Chapters 3 & 4**, further time points at 3, 5, 7 and 14DPA were investigated to ascertain the strength of the delayed phenotype observed in **Chapter 4**. Analysis was performed using qualitative and quantitative methods described in **Chapter 2**, firstly recording axon/glomeruli as percentages and then taking fluorescence measurements from each neuronal structure. Normality was investigated using the Shapiro-Wilk test and QQ plots were checked for normal distribution. A 2-way ANOVA and Sidak's multiple comparisons tests were used to assess qualitative and quantitative recordings of phenotypes. A table of *Drosophila* lines used in this Chapter can be found below (**Table 18**).

| **Stock** | ***Genotype*** | **Stock Number** | **Source** |
|---|---|---|---|
| Virgin Line 1 | *w-;OR85e-mCD8::GFP/+;repo-GAL4/TM3, Sb, e-* | 7415 | Lab Stock |
| Virgin Line 3 | *w-;+/+;P{w[+mC]=tubP-GAL4}LL7/TM6b, Hu, Tb* | 90974 | Lab Stock |
| Wildtype | *w-;+/+;+/+* | Lab | Lab Stock |
| attP2 | *y,v;;p(caryP)attp2* | 36303 | BDSC |
| KK | *P{attP,y+,w3'}VIE-260B* | 60101 | VDRC |
| sl RNAi (III) | *y,sc,v,sev; P{TRiP.HMS00695}attP2* | 32906 | BDSC |
| sl RNAi (IV) | *P{KK101565}VIE-260B* | 108593 | VDRC |
| Pld3 RNAi (II) | *P{KK107515}VIE-260B* | 109798 | VDRC |
| Pld3 RNAi (III) | *y,v; P{TRiP.JF01595}attP2* | 31122 | BDSC |
| Draper RNAi (II) | *w1118; P{GD14423}v27086* | 27086 | VDRC |

***Table 18.*** *A table combining all stock information used in this Chapter, including name abbreviation, genotype, stock number and source.*

## 5.4 Results

### 5.4.1 *sl* and *Pld3* are Enriched in *Drosophila* Primary Phagocytes

Computational data in this section were collected with the help of Miss Hannah Clarke, as part of a supervised rotation project in the lab. Since RNAi constructs were previously expressed under the pan-glial driver *repo*, we refined the search to exclusively *repo*$^{+}$ cell types (**Fig. 23a**) to explore changes in *sl, Pld3* and *Draper* expression across cell types in the *Drosophila* brain. Mean normalised *Draper* expression appeared highest in glia of the adult brain; in particular, astrocytes, chiasm, cortex and ensheathing glia (**Fig. 23b**). Notably, values represent enrichment as opposed to absolute expression. Mean normalised *sl* and *Pld3* expression overlapped in most cells, crucially in ensheathing glia (Clusters 14), the primary phagocytes of the central brain (**Fig. 23b**) (Freeman 2015). Astrocytes, chiasm glia, cortex glia, Cluster 54 cells, perineural and subperineural glia also appeared to co-express *sl, Pld3* and *Draper.* Equally, none of the genes showed enrichment in hemocytes (Cluster 43 cells), which are important in *Drosophila* embryonic development (Wood and Jacinto 2007). In addition, genes appeared enriched in other cell types with 'no direct annotation', such as *Draper* levels in Cluster 50 cells, *sl* levels in Cluster 15 cells, as well as *Pld3* in Cluster 69 cells (**Fig. 23b**). Since the dataset included samples from different age groups, we compared gene expression levels throughout the lifespan of the fly. In ensheathing glia, *Draper* expression gradually increased over time, peaking at a 2-fold increase at 3 and 15 days before returning to baseline by 50 days (**Fig. 23c**). In the same cell type, *sl* expression fluctuated, increasing at 1 day, then later between 9 and 15 days and finally at 50 days. Similarly, *Pld3* expression rose and fell at young and middle-aged time points before peaking at 30 days (**Fig. 23c**). Overall, the data suggest that *sl, Pld3* and *Draper* are co-expressed in ensheathing glia and that gene expression varies with age.

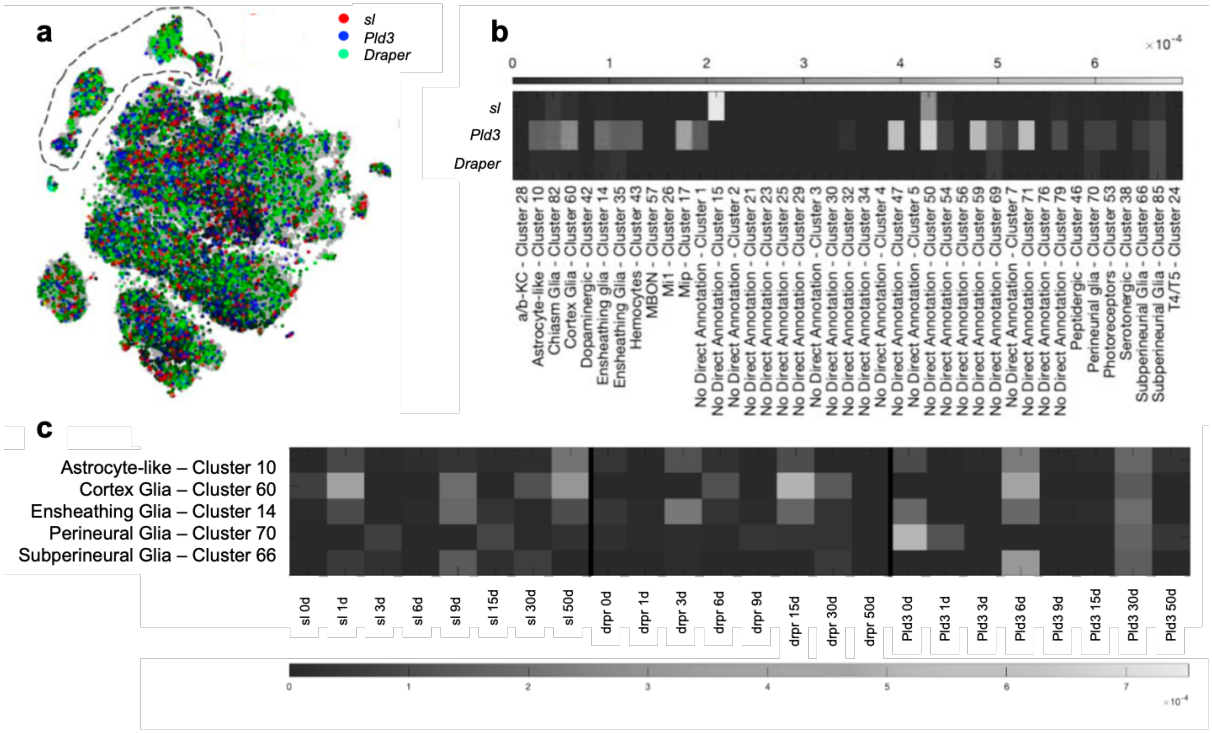


***Fig. 23. SCope Analysis of Gene Expression in Glia. a)*** *Representation of SCope dataset expression levels of sl (red), Pld3 (blue) and Draper (green). Dotted line selection represents cells with dense repo expression, which were selected for analysis.* ***b)*** *Heat-map representation of counts per million normalised AUC values of sl, Pld3 and Draper enriched expression by cell type.* ***c)*** *Heat-map representation of counts per million normalised AUC values of sl, Pld3 and Draper enriched expression by age (0, 1, 3, 6, 9, 15, 30 and 50 days) across select glial subtypes. Focus: Ensheathing glia – Cluster 14. n=1-550 per group.*

### 5.4.2 Knocking Down *Draper* Causes A Glial Engulfment Deficit

To optimise analysis methods and investigate a known phenotype with a significant engulfment deficit, *Draper RNAi* (#27086) flies were investigated alongside a *w-* control. Progeny were raised at 29$^{o}$C and aged for 7-8 days with injured and uninjured groups assessed using confocal microscopy. Engulfment rate was measured by counting neuronal structures and measuring mean fluorescence using ImageJ. As expected, *w-* injured neurons were fully engulfed by 5DPA (**Fig. 24a**), whereas neurons were still visible in *Draper* KD flies (**Fig. 24b**) despite injury. In *w-* samples, GFP+ axons were recorded in 20% of brains after 1DPA, dropping to 0% after 5DPA (**Fig. 24c**). GFP+ glomeruli were only recorded in 80% of cases after 3DPA and were only visible in 10% of cases at later time points (**24d**). Knocking down *Draper* in glia, led to complete inhibition of neuronal engulfment, whereby axon bundles and glomeruli were observed in all animals over the course of 14 days, despite injury. There was a significant effect observed in qualitative axon analysis for timepoint ($p<0.0001$) and genotype ($p<0.0001$) by 2-way ANOVA. Sidak's MC tests showed that axon incidence was higher in *Draper* KD flies at all DPA compared to age-matched controls (all $p<0.0001$), (**Fig. 24c**). A 2-way ANOVA revealed that results varied significantly for glomerulus incidence between time points ($p<0.0001$) and genotypes ($p<0.0001$). Multiple comparisons showed that glomerulus incidence was higher in *Draper* KD flies at 5 ($p<0.0001$), 7 ($p<0.0001$) and 14 ($p<0.0001$) DPA (**Fig. 24d**). This was reflected when measuring mean fluorescence. A 2-way ANOVA revealed that axon fluorescence was significantly different between genotypes ($p<0.0001$) and across time points ($p<0.001$). Post hoc tests showed that axon fluorescence was significantly higher in *Draper* KD flies at 3 ($p<0.01$), 5 ($p<0.05$), 7 ($p<0.05$) and 14 ($p<0.05$) DPA compared to age-matched controls (**Fig. 24e**). A 2-way ANOVA also showed that glomerulus fluorescence was significantly different between genotypes ($p<0.05$) and across time points ($p<0.0001$), with MC tests showing that GFP readings were higher than controls at 5 ($p<0.05$) and 14 ($p<0.05$) DPA (**Fig. 24f**).

Data, therefore, suggest that knocking down *Draper* is sufficient to block engulfment up to 14DPA, an expected outcome which confirmed the use of analysis methods for further experiments.

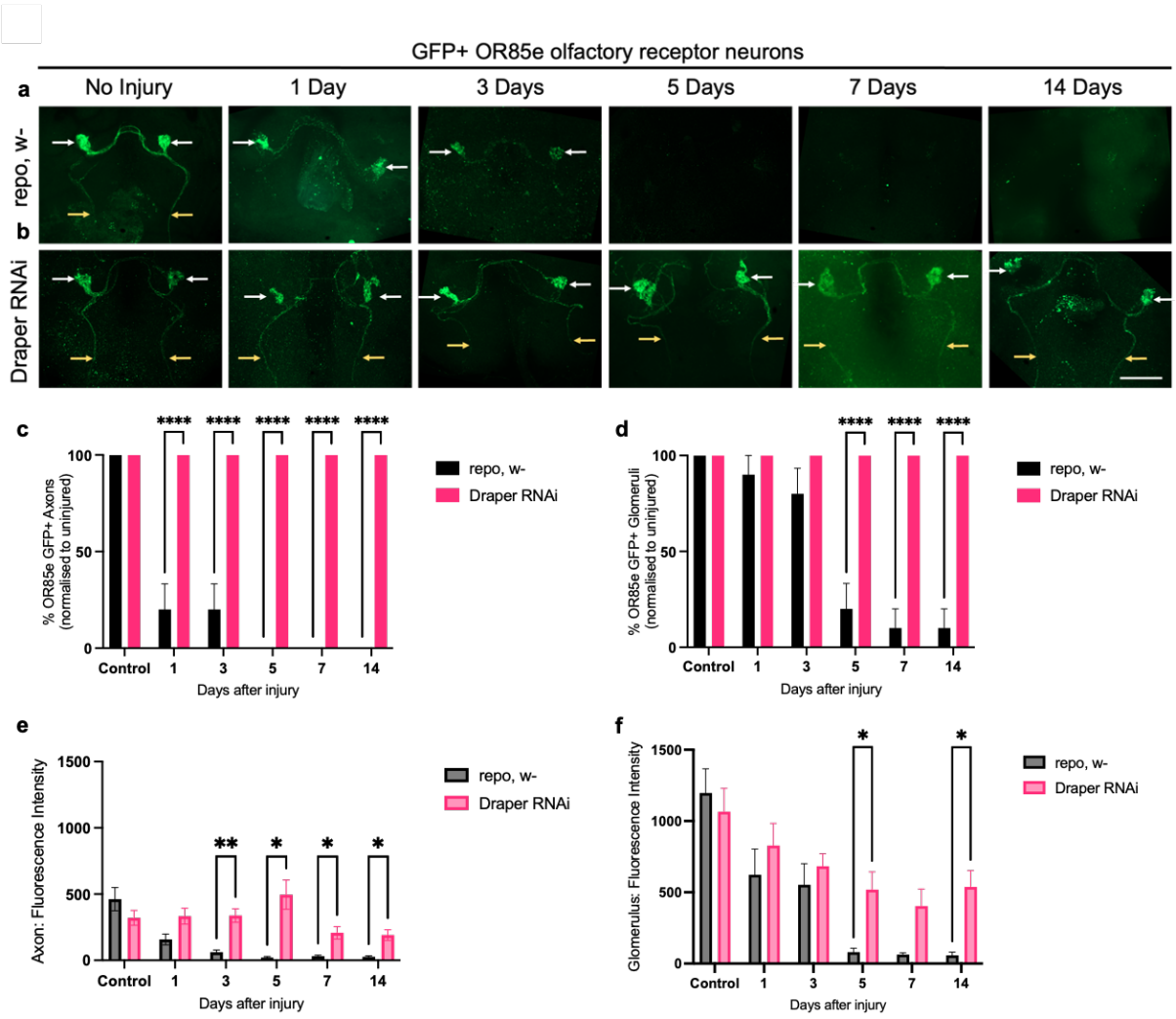


***Fig. 24. Knocking Down Draper Causes A Significant Delay In Engulfment. a)*** *GFP-labelled maxillary ORN neurons before and after injury in w- background flies. Timepoints include 1, 3, 5, 7 and 14DPA.* ***(b)*** *Labelled neurons of Draper RNAi-expressing flies, under uninjured conditions and later time points after injury.* ***c)*** *Qualitative analysis of GFP+ debris in OR85e axons in wildtype and Draper KD flies.* ***d)*** *Percentage of antennal lobes containing visible GFP+ OR85e glomeruli before and after injury.* ***e)*** *Quantitative analysis of GFP fluorescence in OR85e axons.* ***f)*** *Mean GFP fluorescence in OR85e glomeruli. Mean±S.E.M were plotted on graphs. Statistical analysis was achieved by 2-way ANOVA and Sidak's MC tests. Graphs plotted with mean±S.E.M., with significance annotated; *p<0.05, **p<0.01 and ****p<0.0001, n=8-10 brains per group. Scale bar = 50μm.*

### 5.4.3 Knocking Down *sl* Leads To A Partial Engulfment Deficit

To assess the penetrance of engulfment phenotypes observed in **Chapter 4**, *sl RNAi* (#32906) flies were compared to appropriate landing site control flies (attP2). In *attP2* controls, injured neurons were fully engulfed by 5DPA (**Fig 25a**), however, repo-driven knockdown of *sl* led to the recording of certain GFP+ structures after injury (**Fig. 25b**). In control samples, axon numbers dropped to 20% after 1DPA (**Fig. 25c**) and glomeruli were only recorded in 70% of cases after 3DPA, reducing to only 1 case by 5DPA (**Fig. 25d**). Knocking down *sl* in glia, led to the partial delay of neuronal engulfment, such that axons were recorded at later time points and glomeruli were recorded up to 14DPA (**Fig. 25d**). There was a significant effect observed in qualitative axon analysis for timepoint ($p<0.0001$) and genotype ($p<0.01$) by 2-way ANOVA. Sidak's MC tests revealed that axon incidence was higher in *sl* KD flies at 1 ($p<0.0001$) and 3 ($p<0.01$) DPA (**Fig. 25c**). When counting glomeruli, a higher percentage was recorded in *sl* KD flies. A 2-way ANOVA revealed that results varied significantly between time points ($p<0.0001$) and genotypes ($p<0.0001$). Multiple comparisons showed that glomerulus incidence was higher in *sl* KDs at 3 ($p<0.05$), 5 ($p<0.0001$) and 7 ($p<0.0001$) and 14 ($p<0.0001$) DPA (**Fig. 25d**). Similar results were observed when measuring fluorescence. As fluorescence in *attP2* controls descends after 1DPA, mean fluorescence in *sl* KD flies gradually decreases in OR85e+ structures. There was a significant effect observed in quantitative analysis for timepoint ($p<0.0001$) and genotype ($p<0.001$) by 2-way ANOVA. Sidak's MC tests showed that axon fluorescence was significantly higher in *sl* KD flies at 1DPA ($p<0.001$) (**Fig. 25e**). A 2-way ANOVA also revealed significant differences between time points ($p<0.0001$) and genotypes ($p<0.05$) for glomerulus GFP with multiple comparisons showing higher recording in *sl* KDs than controls at 5 ($p<0.05$) and 7 ($p<0.01$) DPA (**Fig. 25f**).

This demonstrates that knocking down *sl* modifies glial function, leading to the partial engulfment of neurons, leaving visible glomeruli up to 14DPA.

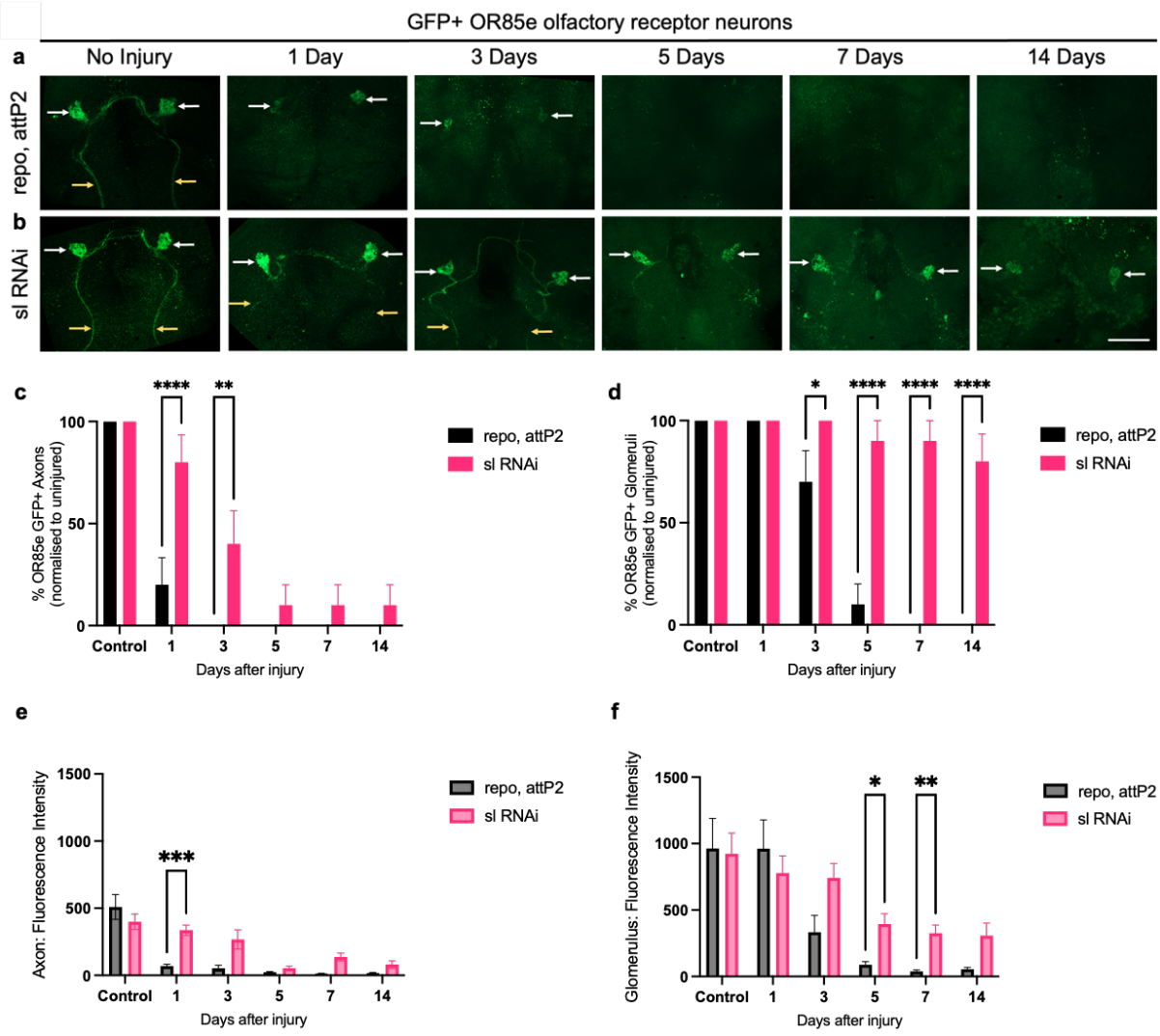


***Fig. 25. Knocking Down sl Causes A Delay In Engulfment. a)*** *GFP-labelled maxillary ORN neurons before and after injury in attP2 background flies. Timepoints include 1, 3, 5, 7 and 14DPA.* ***b)*** *Labelled neurons of sl RNAi-expressing flies, under uninjured conditions and later time points after injury.* ***c)*** *Qualitative analysis of GFP+ debris in OR85e axons in attP2 and sl KD flies.* ***d)*** *Percentage of antennal lobes containing visible GFP+ OR85e glomeruli before and after injury.* ***e)*** *Quantitative analysis of GFP fluorescence in OR85e axons.* ***f)*** *Mean GFP fluorescence in OR85e glomeruli. Statistical analysis was achieved by 2-way ANOVA and Sidak's MC tests. Graphs plotted with mean±S.E.M., with significance annotated; *p<0.05, **p<0.01, ***p<0.001 and ****p<0.0001, n=10 brains per group. Scale bar = 50μm.*

### 5.4.4 Knocking Down *Pld3* Leads to a Partial Glial Engulfment Deficit

To assess the penetrance of other engulfment phenotypes observed in **Chapter 4**, *Pld3* RNAi (#109798) flies were compared to appropriate landing site control flies (KK). In *KK* controls, injured neurons were fully engulfed by 3DPA (**Fig 26a**), however, repo-driven knockdown of *Pld3* led to the recording of certain GFP+ structures after injury (**Fig. 26b**). In control samples, axon numbers dropped to 0% after 1DPA (**Fig. 26c**) and glomeruli were recorded in as little as 50% of cases after 3DPA (**Fig. 26d**). Knocking down *Pld3* in glia, led to the partial delay of neuronal engulfment, such that axons were recorded at later time points and glomeruli were visible up to 14DPA. There was a significant effect observed in qualitative axon analysis for timepoint ($p<0.0001$) and genotype ($p<0.01$), by 2-way ANOVA. Sidak's MC tests revealed that axon incidence was higher in *Pld3* KD flies at 1 ($p<0.0001$) and 3 ($p<0.001$) DPA (**Fig. 26c**). When counting glomeruli, A 2-way ANOVA revealed that results varied significantly for glomerulus incidence between time points ($p<0.0001$) and genotypes ($p<0.0001$). Multiple comparisons showed that glomerulus incidence was higher in *Pld3* KD flies at 3 ($p<0.001$), 5 ($p<0.0001$) and 7 ($p<0.0001$) and 14 ($p<0.0001$) DPA (**Fig. 26d**). This was reflected when measuring mean fluorescence, which abruptly decreases after 1DPA in KK controls and gradually descends in OR85e+ structures of *Pld3* KD flies. There was a significant effect observed in quantitative analysis across time points ($p<0.0001$) and genotypes ($p<0.01$). Sidak's MC tests showed that axon fluorescence was higher in *Pld3* KD flies as late as 3DPA ($p<0.05$) (**Fig. 26e**). A 2-way ANOVA also revealed significant differences between time points ($p<0.0001$) and genotypes ($p<0.0001$) for glomerulus GFP with multiple comparisons showing higher recording than controls at 3, ($p<0.01$), 5 ($p<0.05$) and 7 ($p<0.01$) DPA (**Fig. 26f**).

This demonstrates that knocking down *Pld3* modifies glial function in a similar fashion to *sl*, leading to the partial engulfment of neurons, leaving visible glomeruli up to 14DPA.

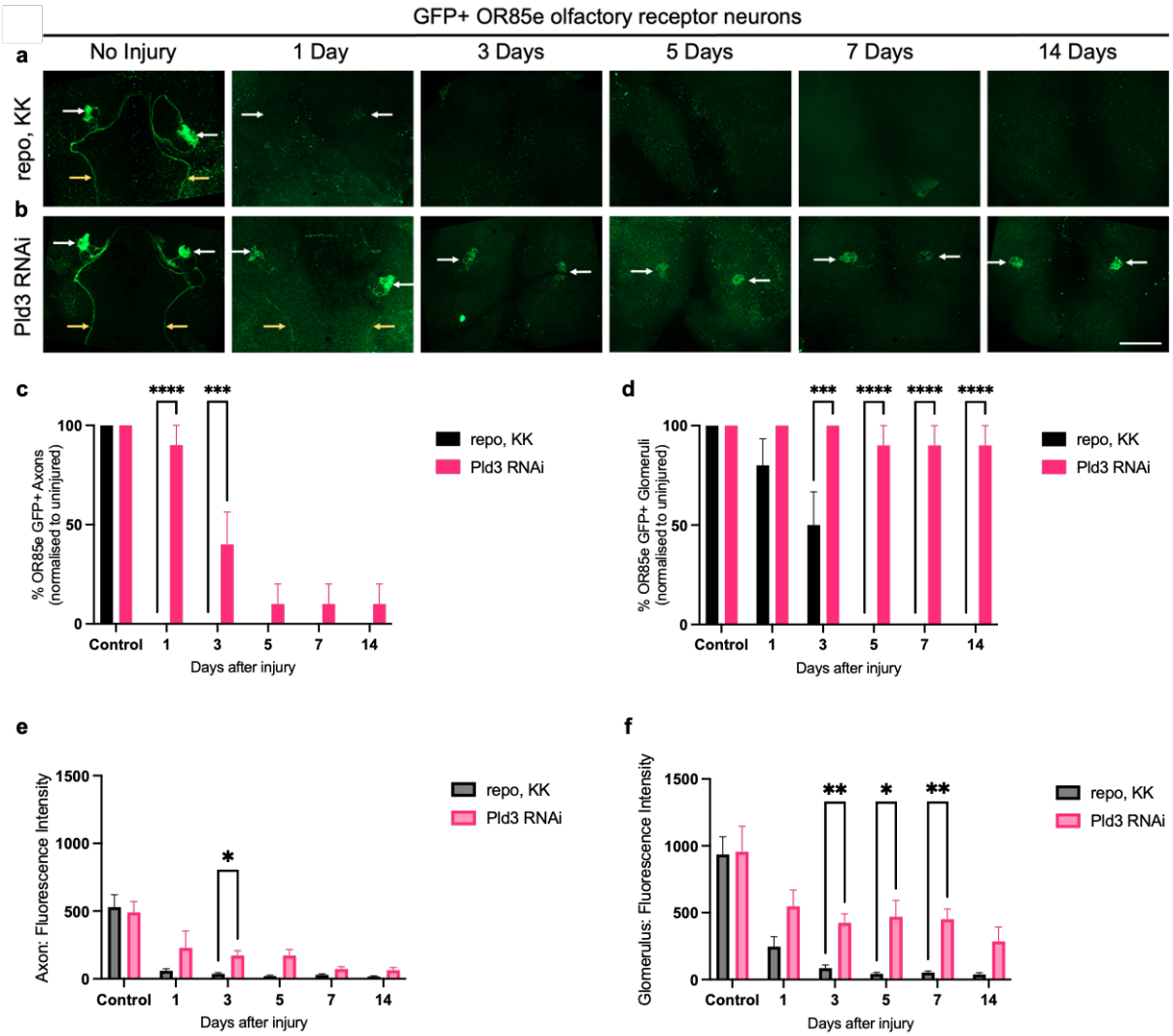


***Fig. 26. Knocking Down Pld3 Causes A Delay In Engulfment. a)*** *GFP-labelled maxillary ORN neurons before and after injury in KK background flies. Timepoints include 1, 3, 5, 7 and 14DPA.* ***b)*** *Labelled neurons of Pld3 RNAi-expressing flies, under uninjured conditions and later time points after injury.* ***c)*** *Qualitative analysis of GFP+ debris in OR85e axons in KK and Pld3 KD flies.* ***d)*** *Percentage of antennal lobes containing visible GFP+ OR85e glomeruli before and after injury.* ***e)*** *Quantitative analysis of GFP fluorescence in OR85e axons.* ***f)*** *Mean GFP fluorescence in OR85e glomeruli. Statistical analysis was achieved by 2-way ANOVA and Sidak's MC tests. Graphs plotted with mean±S.E.M., with significance annotated; *p<0.05, **p<0.01, ***p<0.001 and ****p<0.0001, n=10 brains per group. Scale bar = 50μm.*

## 5.5 Discussion

This chapter expands on the role of *sl* and *Pld3* in *Drosophila* CNS glia. Previous work had uncovered an engulfment phenotype due to glial-specific knockdown of *sl* and *Pld3*. A SCope analysis revealed enriched expression of *sl, Pld3* and *Draper* in the dominant phagocytes of the brain – ensheathing glia. Quantitative analysis techniques were optimised in an experiment where *Draper* (the major engulfment regulator) was knocked down, which significantly delayed engulfment up to 14DPA. Knocking down *sl* or *Pld3* both led to a partial engulfment deficit, due to the presence of GFP+ glomeruli up to 14 days after ablation.

### 5.5.1 Co-Expression Of AD Risk Gene Orthologs In Glia

We investigated potential changes in mRNA expression of *sl* and *Pld3* alongside the major glial phagocytosis regulator *Draper*, revealing selective expression of all 3 genes in glial cells. Interestingly gene expression was enriched in ensheathing glia, the phagocyte responsible for published ORN engulfment phenotypes (Freeman 2015). To suggest *sl* and *Pld3* as modulators of glial engulfment, one would predict gene expression to overlap with *Draper* in active phagocytes. One would also expect that human PLCγ2 and PLD3 may act via a shared pathway and be co-expressed in microglia and/or astrocytes alike. Indeed, *PLCγ2* is highly expressed in cells of the myeloid lineage, in particular microglia and granule cells (Magno et al. 2019). *PLCγ1* however, is ubiquitously expressed (Vaqué et al. 2014). The expression of *PLD3* is more ambiguous, with different databases suggesting alternative expression patterns. RNA-sequencing data from the Barres Lab suggests *PLD3* is expressed in microglia, however, this is inconsistent with data from the Allen Brain Atlas where *PLD3* is in fact not (Lein et al. 2006; Hawrylycz et al. 2012). Our explorations do confirm expression in *Drosophila* glia, which could support existing evidence that both genes are active in these phagocytic cells. Our results also unveiled expression variability with age and genotype, an important detail to consider in neurodegenerative disease analyses due to age being a major risk factor. Our data also suggests that *sl* and *Pld3* were highly enriched within “No direct annotation clusters”. Non-annotated clusters may represent “generic neurons” so repo positivity should be assessed cautiously. In addition, N values could be low and highly variable across different cell populations. Overall, our

data confirm existing results in the field and support the role of the genes in glial function.

### 5.5.2 PLD3 and PLCγ2 as Modulators of Phagocytosis

Having confirmed expression in ensheathing glia, *sl* and *Pld3's* involvement in glial phagocytosis was further interpreted. Via qualitative and quantitative methods, the delay in engulfment is visually obvious in both backgrounds, due to the incidence of GFP+ glomeruli days after their full engulfment in controls. Point mutations in human orthologs of *sl* (*PLCγ2*) and *Pld3* (*PLD3*) have been associated with AD pathology and immune function. *PLCγ2* research reveals two major variants, P522R which decreases an individual's risk of AD development and M28L which increases disease risk (Sims et al. 2017; Tsai et al. 2020).

Existing research into the role of PLCγ2 implies that PLCγ2-P522R-expressing cells, with increased PLCγy2 functionality, displayed impaired phagocytosis but enhanced endocytosis (Maguire et al. 2020). Equally, recent studies observed that PLCγ2-KO macrophages displayed reduced phagocytic activity and survival in addition to compromised cellular adhesion and migration (Obst et al. 2021). Signalling receptors, such as B cell receptor (BCR), upstream of PLCγ2 have been shown to recruit SYK, BTK, and BLNK to phosphorylate and activate PLCγ2 (Jackson et al. 2021). Incidentally, SYK is orthologous to shark, which is recruited to Draper upon injury (Ziegenfuss et al. 2008). Together, these studies highlight an important role for PLCγ2 in glial engulfment, but the cell biological mechanism is still unclear (Andreone et al. 2020; Magno et al. 2021). In **Chapter 6**, experiments address whether $Ca^{2+}$ signalling or known components of the Draper pathway are involved in sl-dependent glial engulfment of neuronal debris.

Furthermore, PLD3 missense mutations are predicted to increase disease risk and reduce cognition, however, research is conflicting with many failed replications (Jiao et al. 2014; Hooli et al. 2015; Zhang et al. 2016a). Although PLD3 is largely understudied, members of the PLD family may be involved in the maturation of phagosomes and progression into the endosomal-lysosomal system, as inhibition of PLD1/PLD2 impedes phagocytosis (Iyer et al. 2004; Gavin et al. 2018). A 2011 study showed that PLD4 expression was upregulated in response to lipopolysaccharide

(LPS) stimulation and that it co-localised with phagosomes. PLD4 KD also led to a significantly reduced ratio of phagocytotic cell numbers and correlated with the activation state of microglia (Otani et al. 2011). PLD3 exhibits 5' exonuclease activity on single-stranded DNA, hydrolysing it at an acidic pH associated with lysosomes, therefore PLD3 may be involved in the maturation stages in engulfment (Cappel et al. 2021). Interestingly, a study found that PLD3 activity also increased when $Ca^{2+}$ was added to the reaction mixture in Polyacrylamide gel electrophoresis (PAGE) and End-labelled Fluorescence-Quenched Oligonucleotide (EFQO) assays (Cappel et al. 2021). Therefore, is possible that the PLD3 is activated by $Ca^{2+}$ in glial cells which may enhance engulfment through the endosomal-lysosomal pathway. Whether PLD3 follows the functions of other family members in phagocytosis is unknown. An informative further experiment would be to explore glial phenotypes in humanised wildtype and variant mutant backgrounds for both PLCγ2 and PLD3.

Indeed, how PLD3 mediates AD phenotypes at a molecular level is generally disputed with evidence supporting altered APP processing, reduced cognition, and endo-lysosomal function. PLCγ2 and PLD3 impact AD susceptibility in opposing directions yet when *Drosophila* counterparts are knocked down, they appear to reserve the same role in glial phagocytosis. This could be explained by the binary role of microglia in disease, whereby hyperactive microglia have been known to over-eliminate important synapses and underactive microglia appear unable to remove senile plaques or neuronal debris (Solito and Sastre 2012). Therefore, PLD3 and PLCγ2 may converge in engulfment function relevant to specific ligands, in this case dying neurons. In **Chapter 6**, experiments on a potential epistatic relationship between Pld3 and sl in glial engulfment of neuronal debris.

### 5.5.3 Phagocytosis and the Phosphoinositide Pathway

Crucially, both *sl* and *Pld3* are members of the phosphoinositide cycle and phosphoinositides (PIs) have previously been associated with phagocytosis of microorganisms and pathogens (Bohdanowicz and Grinstein 2013; Desale and Chinnathambi 2021). Therefore, PI pathway-dependent mechanisms may also play a role in the engulfment of cellular debris. Other elements of the pathway have been implicated in phagocytosis, whereby PIP2 dynamics change at different stages of phagosome formation, with higher levels in young phagosomes compared to lower

levels prior to sealing. Since PIP2 is hydrolysed by PLCγ2, this could support *sl* playing a role in Draper-mediated engulfment, by blocking phagosome maturation. Downstream elements of the PI signalling have been characterised, such as TOR signalling and autophagy – another cell mechanism of "eating" where cytoplasmic debris is sequestered and degraded for recycling purposes or due to damage (Sanjuan and Green 2008, Etchegaray et al. 2016). Autophagy and phagocytosis have been linked historically, both being cellular catabolic pathways that utilise lysosomes to digest material. The main distinctions are that autophagy marks intracellular material, while phagocytosis consumes extracellular particles (Sanjuan and Green 2008). Equally, links between autophagy and phagocytosis in *Drosophila* have been raised previously: It has been suggested that *Draper* may activate TORC1 to subsequently inhibit autophagy and facilitate phagocytosis via a redistribution of proteins common to both processes and priming them for phagocytosis (Etchegaray et al. 2016). Other research has linked Draper-mediated phagocytosis to TOR signalling, such that knocking down raptor, a member of the TORC1 complex, leads to deficits in phagocytosis in axonal injury models (Doherty et al. 2014). Such deficiencies can be rescued through TORC1 activation or inhibition of Atg1 (Etchegaray et al. 2016). It is, therefore, possible that sl-dependent regulation of PIs may have two effects, firstly impairing engulfment inhibiting phagophore formation and secondly inhibiting autophagy-mediated clearance of debris. The latter may have significant effects on glial cell function overall, even when they are not required to engulf dying neurons. It would be of interest to study a pathway relationship between raptor and sl and whether other processes such as mitophagy are perturbed upon *sl* KD.

Interestingly, some variants of PLD3, that reduce catalytic activity, have been shown to hyperactivate mTOR (Tan et al. 2019), which may propose a potential interaction between Draper and Pld3 in flies. In addition, upstream of TOR signalling, PI3K is suggested to mediate levels of Draper through STAT92E activation. PI3K is required for the effective clearance of glomeruli after injury due to its role in Draper upregulation (Doherty et al. 2014; Purice et al. 2016). Equally, expression after injury appears to be controlled by Rac1, the dJNK cascade and activation of Akt1 via the insulin receptor (InR) (MacDonald et al. 2013; Musashe et al. 2016). Interestingly, activated InR is considered to recruit and activate sl for phospholipid turnover (Murillo-Maldonado et al. 2011). Plus, overexpression of Pld3 has been shown to decrease InR signalling via

Akt – suggesting further interactions between sl, Draper and Pld3 (Zhang et al. 2009). Informative experiments would include knocking down combinations of sl, Pld3 and InR within the same organism to see how phagocytosis is affected, if no additive effect on phagocytosis is observed with co-expression of RNAi this would suggest that they may act in the same genetic pathway. We explore possible interactions between sl, Pld3 and other factors in **Chapter 6**. It would also be recommended to knock down known members of the PI and Draper pathways, such as shark (SYK homolog) or PI3K, thereby gaining a broader understanding of the network.

## 5.6 Summary of Key Findings

- *sl* and *Pld3* are enriched in *Drosophila* primary phagocytes.
- Knocking down *Draper* led to the complete engulfment deficit of neuronal debris by glia, verified through qualitative and quantitative methods.
- Knocking down AD risk gene orthologs *sl* and *Pld3* led to a partial engulfment deficit of neuronal debris by glia.

# 6 Draper and Phosphoinositide Signalling Converge to Mediate Engulfment

## 6.1 Introduction

**Chapter 5** indicated that sl and Pld3 are important modulators of neuronal debris engulfment, leading to a partial engulfment deficit when knocked down. Although existing evidence suggests a role for PLCγ2 in phagocytosis, little is known of the mechanism of function (Maguire et al. 2020; Maguire et al. 2021). Equally, PLD3 is heavily understudied, especially in the field of microglial biology (Fazzari et al. 2017). Being highly conserved in *Drosophila*, this chapter employs diverse tools to investigate molecular mechanisms.

### 6.1.1 Phosphoinositide Signalling

The phosphoinositide pathway mediates many cellular behaviours and has previously been associated with processes of endocytosis, phagocytosis and micropinocytosis (Gillooly et al. 2001; Balla 2013; Bohdanowicz and Grinstein 2013; Lystad and Simonsen 2016; Lin et al. 2020). Phosphatidylinositols (PIs) are essential components of the lipid bilayer in cell membranes, and thus their regulation is vital to the cell's ability to mediate the influx and efflux of materials (Bohdanowicz and Grinstein 2013). Membranes are generally composed of two fatty acids linked through ester bonds to a glycerol backbone containing a polar head group. The amphiphilic/-phobic properties of the membrane provide a selective barrier for the cell and lipid turnover plays an essential part (Casares et al. 2019). PIs are small lipid molecules composed of an inositol ring and two fatty acid chains connected through a glycerol backbone, a structure which enables them to anchor themselves in the membrane, facing the cytoplasm (Dickson and Hille 2019). PIs can be phosphorylated by lipid kinases which typically target 3, 4, and/or 5 hydroxyl groups in the inositol ring. Phosphorylation produces a variety of products such as phosphatidylinositol monophosphates (PI3P, PI4P, and PI5P), diphosphates ($PI(3,4)P_2$, $PI(3,5)P_2$, $PI(4,5)P_2$) in addition to triphosphate ($PI(3,4,5)P_3$), collectively known as phosphoinositides (Gericke et al. 2013). PIs are universal signalling entities that regulate cell activities through direct interaction with membrane proteins such as ion channels and G-protein-coupled receptors (GPCRs) (Balla 2013). They can recruit certain cytosolic proteins containing domains that directly bind phosphoinositides, such as pleckstrin homology (PH), PTB or PDZ domains, among others (Arcaro and Guerreiro 2007; Balla 2013; Reversi et al.

2014; Cauvin and Echard 2015; Hammond and Balla 2015; Lystad and Simonsen 2016; Marat and Haucke 2016).

The primary event, initiating the pathway is agonist-induced PLC activation where $PI(4,5)P_2$ (hereafter referred to as PIP2 ) is hydrolysed and its products recycled (**see Fig. 22**). Diacylglycerol (DAG) is produced which activates protein kinase C (PKC) but can also be converted to phosphatidic acid (PA) by various DG-kinase enzymes (DGK). PIP2 hydrolysis also produces IP3, an important secondary messenger which mobilises to storage organelles, binding IP3 receptors (IP3Rs). IP3 binds all four monomers of the IP3R tetramer, causing a conformational change, releasing calcium ($Ca^{2+}$) into the cytosol (Steelman et al. 2015). Much of the inositol used for PI synthesis is derived from the sequential dephosphorylation of $PI(3,4,5)P_3$ (hereafter referred to as PIP3) another product of PIP2 hydrolysis. PIP2 in this case is hydrolysed by PI3K and dephosphorylated by PTEN, central mediators of receptor tyrosine kinases (Balla 2013). PIP3 is the effect of multiple downstream targets of PI3K. Downstream of PIP2 hydrolysis, PIP3 recruits phosphoinositol-dependent kinase 1 (PDK1) which phosphorylates AKT and subsequently mediates downstream processes such as survival and growth. AKT phosphorylation can sometimes be achieved in a PI3K-independent manner such as through Src or Tank-binding kinase 1 (TBK1) (Joung et al. 2011; Mahajan and Mahajan 2012). Some studies have shown that AKT can be activated by increases in cellular $Ca^{2+}$ concentration (Soderling 1999). Loss of PTEN function leads to over-activation of AKT and is common in cancer cells (Georgescu 2010). PLD's principal substrate is phosphatidylcholine (PC), which it hydrolyses to produce phosphatidic acid (PA), and soluble choline in a cholesterol-dependent process (Petersen et al. 2016). Mammalian PLD interacts directly with kinases such as PKC, ERK and TYK. PA is extremely short-lived and is rapidly hydrolysed by the enzyme to form DAG by phosphatidate phosphatase (PAP), which can have many downstream implications (Dey et al. 2020). PI4P5 kinase, which promotes PIP2 synthesis is also activated by PLD's product and small GTPase ADP ribosylation factor 6 (ARF6). Most PLDs require PIP2 as a cofactor for activity, which promotes PLD trafficking to its substrate PC (Kolesnikov et al. 2012). In *Drosophila* these principles are broadly conserved.

Prior research has linked phosphoinositide signalling to phagocytosis as it is believed to play a role in cytoskeleton organisation (Botelho et al. 2000). Historically, the oldest known function of PIs in cellular signalling is the role of PIP2 as a substrate for PLC, generating second messengers such as DAG. However, more recently it has become clear that many PIs, including PIP2, can bind proteins in cells, regulate their activity and hence influence ongoing cellular events (Mandal 2020). Proteins whose activity is influenced by PIs include those that regulate cell membrane functions (e.g., channels and transporters), vesicular transport and cytoskeletal function (Balla 2013). PIP2 exhibits biphasic expression during engulfment, with high concentrations in young phagosomes decreasing prior to sealing, correlating with actin disassembly (Botelho et al. 2000). Subsequently, increasing PIP2 concentrations inhibits closure (Botelho et al. 2000). Crucially, PIP2 and active PLCγ2 are present at the phagosome and was shown to be essential for effective particle ingestion. PI3Ks are known regulators of phagocytosis which act consecutively in phagosome formation and maturation accompanied by transient PIP3 accumulation (Gillooly et al. 2001). The ever-broadening impacts of the phosphoinositide pathway are becoming more apparent, with increasing evidence to suggest that various members of the pathway, PLCγ2 and PLD3 included, may play a role in immune phagocytic function.

### 6.1.2 Draper and the Phosphoinositide Pathway

As previously outlined, Draper is the main receptor known to initiate phagocytosis by glia, macrophages, and epithelia in *Drosophila* (Freeman et al. 2003; MacDonald et al. 2006; Logan and Freeman 2007; Doherty et al. 2009; Zheng et al. 2017). Injury stimuli activate the transmembrane receptor via adaptor protein ced-6 (Awasaki et al. 2006). Non-receptor tyrosine kinase Shark binds Draper, recruiting Src42A leading to phosphorylation. Removal of Src42A inhibits Shark binding and prevents phagocytosis (Ziegenfuss et al. 2008). Phosphorylation promotes Rac1 function, such that loss of Rac1 displays a similar phenotype to *Draper* KD (Ziegenfuss et al. 2012). Downstream, transcriptional changes occur in Jra and STAT92E, leading to Draper upregulation (Doherty et al. 2014). STAT92E has many downstream impacts including the upregulation of various members of the PI cycle, such as Pld3 (Jenkins and Frohman 2005). Recent research suggests that the son of sevenless (Sos) may activate Rac1 as loss of downstream receptor kinase (drk), daughter of sevenless

(Dos) and Sos reduces axonal phagocytosis (Lu et al. 2014). It is important to note that sl is equally activated by receptor tyrosine kinases (Manning et al. 2003), simultaneously with the drk/Dos/Sos cassette (Li 2005). Research in the *Drosophila* eye suggests that the normal function of sl is to inhibit MAPK signalling (Thackeray et al. 1998; Powe et al. 1999; Schlesinger et al. 2004; Murillo-Maldonado et al. 2011) at the level of Ras85D, downstream of Sos (Sullivan and Rubin 2002). Existing evidence of tyrosine kinase PI3K suggests that levels decrease with the age of the fly, correlating with decreased engulfment (Purice et al. 2016). PI3K has also been associated with the regulation of Draper expression (Doherty et al. 2014). Draper levels can be mediated by PI3K activity, such that PI3K KD leads to a partial delay in neuronal debris engulfment, similar to what is observed in sl KD investigated here (Doherty et al. 2014; Purice et al. 2016). Some Draper expression is controlled by Rac1, the dJNK cascade (MacDonald et al. 2013) and activation of AKT1 via the insulin receptor (InR) (Musashe et al. 2016). Activation of InR has also been known to initiate downstream members of the PI pathway such as PLCγ2 (Murillo-Maldonado et al. 2011). These are some of the existing associations between Draper and elements of phosphoinositide signalling, however, the two pathways are not explicitly linked in *Drosophila* or mammalian literature and there are still many unknowns.

### 6.1.3 Models of the Phosphoinositide Pathway

In *Drosophila* research, there exist many tools to model the phosphoinositide pathway, including some that track PI activity *in vivo* (Corbin et al. 2004; Reversi et al. 2014; Hardie et al. 2015; Li et al. 2020b). In 2002, Bruce Edgar and colleagues devised a tool which could act as an indicator for PI3K activity through its product PIP3. To study the pathway in development, they used a pleckstrin homology domain-green fluorescent protein (PH-GFP) fusion to gauge activity (Britton et al. 2002). As previously mentioned, PH domains are essential to bind phosphoinositides, in this case, the construct expresses GFP fused to the PH domain of the general receptor for phosphoinositides, isoform 1 (Grp1) under the control of alphaTub84B, such that it is expressed ubiquitously. Grp1 localises at the membrane in the presence of PIP3 and therefore can be used to ascertain PI signalling through PI3K. Interestingly, Grp1 regulates the actin cytoskeleton in response to PIP3 signals at the surface of the cell (Corbin et al. 2004). Hugo Bellen's lab also recently designed an important tool to

follow changes in PIP2 dynamics. The study identified a positive feedback loop between transmembrane protein flower (fwe) and PIP2 at periactive zones, controlling bulk endocytosis during development (Li et al. 2020b). To observe any changes, they expressed a GFP fusion protein of a PH domain in human $PLC_{\delta1}$ ($PLC_{\delta1}$-PH-EGFP), which localises at sites of high PIP2 concentration. The construct was inserted downstream of a UAS site, regulated by GAL4. They were therefore able to record changes in PIP2 levels via GFP in specific tissues, in this case, synaptic boutons of larval NMJs using *nSyb-GAL4.* $Ca^{2+}$ changes are often observed downstream of PI signalling (Putney and Tomita 2012), therefore GCAMPs are often used in PI pathway research (Reversi et al. 2014; Liu et al. 2020). GCAMP6f is a genetically encoded fluorescent cytoplasmic $Ca^{2+}$ indicator which is both highly sensitive and decays quickly. The line used, has a construct downstream of a UAS, therefore can be regulated using a GAL4 driver and allows one to be specific about where $Ca^{2+}$ occur (Asteriti et al. 2017). These tools are highly optimised and essential to understanding changes at various stages of the phosphoinositide pathway *in vivo*.

## 6.2 Aims and Objectives

Both AD risk genes, *PLCγ2* and *PLD3* encode members of the phosphoinositide pathway, which has crucially been associated with phagocytosis. Supporting this, current results suggest that *Drosophila* orthologs may play a role in glial engulfment, where downregulation causes a partial delay in debris clearance (see **Chapter 5**). To understand how these proteins interact with known elements of the phagocytosis pathway, this chapter seeks to employ various methods. Firstly, I used immunohistochemistry to investigate how *sl* KD impacts Draper upregulation and generated double KDs with available RNAis from both pathways. In addition, tools that report PIP3, PIP3 and $Ca^{2+}$ levels were used to investigate factors upstream and downstream of sl and Pld3.

## 6.3 Experimental Design

When investigating the downstream effects of *sl* KD, *yw;Sp/CyO;repo-GAL4/TM6b, Hu, tb* virgins were crossed to *w-;+/+,+/+*, ;*UAS-Draper RNAi* (#27086*) and ;;UAS-sl RNAi* (#32906), raised at 25$^{o}$C for 6 days, then shifted to 29$^{o}$C to boost expression, before being aged for 7 days after eclosion. Draper levels were assessed in brains after third segment antennal injury using IHC protocols outlined in **Chapter 2** and confirmed via Western Blot using protocols described in **Chapter 2**. Primary antibody a-Draper (8A1) was used for both experiments. Epistatic relationships were investigated using the injury model system, described in previous **Chapters** after 5DPA. Phosphoinositide dynamics in response to injury were recorded in various models. Here, *w-;repo]/CyO; UAS-PLCdelta-PH-EGFP}3/TM6B, Hu, Tb* and *w-; P{w[+mC]=tGPH}2; repo-GAL4/ TM3, Sb, e-* were crossed to *;;UAS-LacZ/TM6b*, *;;UAS-sl RNAi* (#32906) *;UAS-Draper RNAi* (#27086*),* raised at 25$^{o}$C for 6 days, then shifted to 29$^{o}$C and aged for 7 days after eclosion. After third segment antennal ablations were performed, brains were fixed and mounted, and GFP levels were assessed using macros outlined in **Chapter 2.** Thereafter, the same driver lines and approach were used in detailed mechanism studies. Equally, to assess $Ca^{2+}$ dynamics after injury, *w-;20XUAS-IVS-GCaMP6f}attP40;repo-GAL4/TM6b, Hu, Tb* virgins were crossed to w-;+/+;+/+, *;;UAS-LacZ/TM6b*, *;;UAS-sl RNAi* (#32906) and *;UAS-Draper RNAi* (#27086*)* before being treated and prepared identically to phosphoinositide experiments. A table of the *Drosophila* lines used in this **Chapter** can be found below (**Table 20**). Normality was investigated using the Shapiro-Wilk test and QQ plots were checked for normal distribution. Qualitative data were analysed using a Kruskal Wallis test with specific comparisons achieved through Dunn's MC tests. Fluorescence data were analysed using a 1-way ANOVA and Dunnett's MC tests when comparing genotypes. When comparing multiple variables, data were assessed using a 2-way ANOVA and Tukey's MC tests. A table of *Drosophila* lines used in this Chapter can be found below (**Table 19**).

| **Stock** | ***Genotype*** | **Stock Number** | **Source** |
|---|---|---|---|
| Virgin Line 1 | *w-;OR85e-mCD8::GFP/+;repo-Gal4/TM3, Sb, e-* | 7415 | Freeman Lab Stock |
| Virgin Line 4 | *w-;+/+;repo-GAL4/TM6b, Hu, Tb* | 7415 | Freeman Lab Stock |
| Virgin Line PIP2 | *w-;repo]/CyO; UAS-PLCdelta-PH-EGFP}3/TM6B, Hu, Tb* | 39693 | Gift |
| Virgin Line PIP3 | *w-; P{w[+mC]=tGPH}2; repo-GAL4/ TM3, Sb, e-* | 8163 | Gift |
| Virgin Line GCAMP | *w-;20XUAS-IVS-GCaMP6f}attP40;repo-GAL4/TM6b, Hu, Tb* | 42747 | Lab Stock |
| Wildtype | *w-;+/+;+/+* | Lab | Lab Stock |
| *Lacz* | *w-;;P{w[+mC]=UAS-lacZ.ExeI}/TM6b* | 8530 | Lab Stock |
| sl RNAi (III) | *y,sc,v,sev; P{TRiP.HMS00695}attP2* | 32906 | BDSC |
| Draper RNAi (II) | *w1118; P{GD14423}v27086* | 27086 | VDRC |
| *Lacz + sl* | *w-;UAS-Lacz/CyO;UAS-sl RNAi/TM3* | 32906 | Made |
| *arf51f + sl* | *w-;UAS-arf51fRNAi/CyO;UAS-slRNAi/TM3* | 24224, 32906 | Made |
| *pten + sl* | *w-;UAS-ptenRNAi/CyO;UAS-slRNAi/TM3* | 101475, 32906 | Made |
| *pld3 + sl* | *w-;UAS-pld3RNAi/CyO;UAS-slRNAi/TM3* | 109798, 32906 | Made |
| *hspc300 + sl* | *w-;UAS-hspc300RNAi/CyO;UAS-slRNAi/TM3* | 35794, 32906 | Made |
| *shark + sl* | *w-;UAS-sharkRNAi/CyO;UAS-slRNAi/TM3* | 33059, 32906 | Made |

***Table 19.*** *Combines all stock information used in this Chapter, including name abbreviation, genotype, stock number and source.*

## 6.4 Results

### 6.4.1 Knocking Down *sl* May Impact *Draper* Upregulation In Response To Injury

Modifying *sl* expression can change the rate at which glia sequester degenerating material after injury, and published data shows Draper to be the key mediator of that response (MacDonald et al. 2006). Logan et al., show that Draper is upregulated in response to injury through STAT92E (Purice et al. 2016), therefore, to identify whether this process was targeted, I investigated the impact of *sl* KD on Draper upregulation, typically observed between 24-48hrs after injury (MacDonald et al. 2006). In *wild-type,* uninjured animals, glial membranes were found to delineate the borders of antennal lobes, but 1 day after injury Draper-positive membranes appeared to increase their membrane surface area around the region (**Fig. 27a**). As expected, in *Draper* KD animals, glial membranes were less visible with a trending reduction in Draper-specific signal, and after injury, the reduction was consistent with signal lightly increasing (**Fig. 27a**). Knocking down *sl* did not affect Draper staining of glial membranes in uninjured conditions, however, appeared to inhibit the characteristic upregulation of Draper after injury (**Fig. 27a**). A 2-way ANOVA revealed significant differences between Draper-specific fluorescence in antennal lobes at injured conditions ($p<0.01$) but no significance between genotypes (**Fig. 27b**). Tukey's MC tests confirmed a localised increase in Draper-fluorescence in *wild-type* flies after injury ($p<0.01$), which was not observed in *Draper* or *sl* KD flies (**Fig. 27b**). Qualitative analysis of western blot, comparing injured and uninjured samples from controls, *Draper* KD and *sl* KD animals suggested similar results (**Fig. 27c**); between control samples, a higher level of Draper protein was detected 24 hours after injury, which was lost following either *Draper* or *sl* KD.

Overall, data implied that knocking down *sl* did not impact baseline Draper expression, however, prevented its upregulation after injury. This suggests that sl could be required for Draper-mediated engulfment (**Fig. 27**).

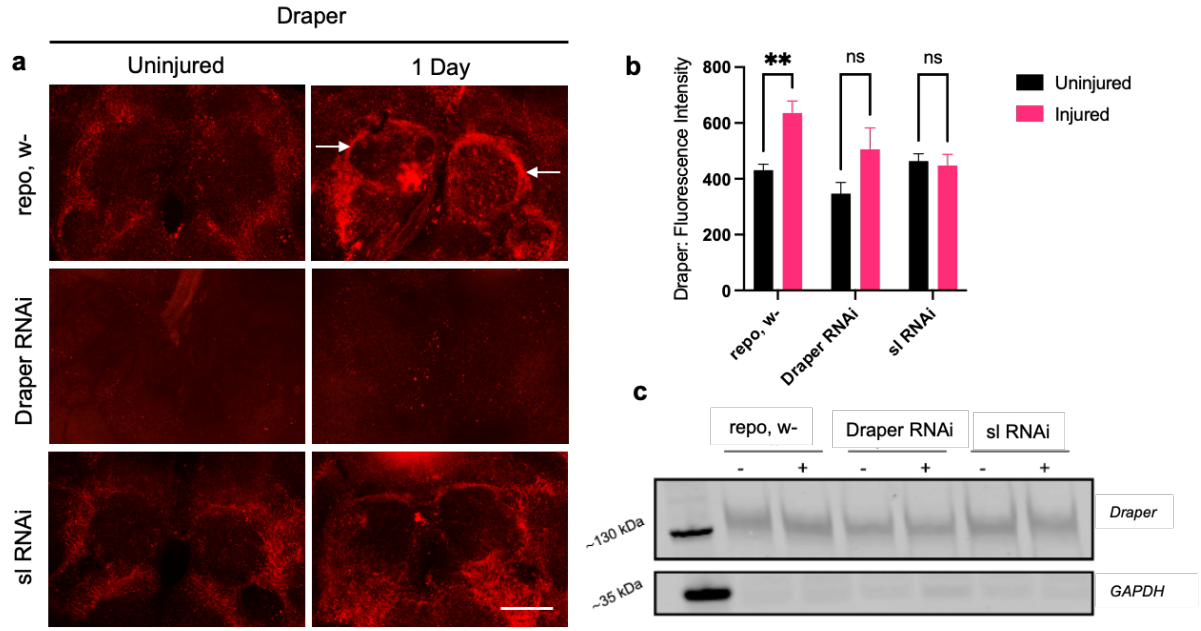


***Fig. 27. Knocking Down sl Prevents The Upregulation Of Draper After Injury.***

***a)*** *Representative confocal z-stacks of Draper immunostained brains before and after injury in w- background flies, Draper and sl KD flies. White arrows highlight regions of antennal lobes, where Draper classically accumulates, showing regions used for the quantification of Draper.* ***b)*** *Quantification of Draper fluorescence in antennal lobe ensheathing glia before and after antennal nerve injury.* ***c)*** *Western blotting with α-Draper (top panel) and α-GAPDH general protein stain (bottom panel) of head lysates from controls, Draper and sl KD flies. Statistical analysis was achieved through a 2-way ANOVA and Tukey's MC tests. Graphs plotted with mean±S.E.M., with significance annotated; **p<0.01, n=7-10 brains per group. Scale bar = 50μm.*

### 6.4.2 Knocking Down PTEN Rescues *sl* KD Engulfment Phenotype

To ascertain the mechanism contributing to the engulfment phenotype observed, *sl* was knocked down alongside candidates of the engulfment and PI pathways. A later time point of 5DPA was chosen to observe either "rescue" or "exacerbation" phenotypes. Knocking down *arf51f* and *sl* yielded a lethal phenotype, an interesting result, however, was not taken further. As a control, *sl* was knocked down alongside a *UAS-LacZ* construct to account for any diluted GAL4 expression. Knocking down *sl* with different factors led to various phenotypes, determined by the presence/absence of neuronal structures after injury (**Fig. 28a**). Indeed, knocking down *sl* whilst expressing *LacZ* yielded an engulfment deficit, although not as strong as that previously recorded at 1DPA (see **Chapter 5**). GFP-positive axons were no longer observed, however, glomeruli were visible in 70% of cases 5DPA. When knocking down *shark* and *sl* together, GFP-positive axons and glomeruli were visible in 100% of animals despite injury. A Kruskal Wallis test revealed that there was a significant difference in the percentage of axon percentages between genotypes ($p<0.0001$) (**Fig. 28b**). Dunn's MC tests demonstrated that the incidence of axons was higher in *shark* + *sl* KD flies ($p<0.0001$). When knocking *PTEN* and *sl*, GFP-positive structures were no longer visible, such that axons were never recorded, and glomeruli were only recorded in 10% of cases after injury. There was a significant effect observed in qualitative glomerulus analysis by Kruskal Wallis ($p<0.05$) (**Fig. 28c**). Dunn's MC tests revealed that glomerulus incidence was lower in *PTEN* + *sl* KD compared to controls ($p<0.05$). Other epistatic combinations did not yield significant results, including knocking down *Pld3* + *sl* together**.** When measuring fluorescence in axon structures, a 1-way ANOVA revealed a significant change between genotypes ($p<0.001$). Dunnett's MC tests suggested that mean GFP fluorescence was higher in axons of *shark* + *sl* KDs compared to control conditions ($p<0.01$) (**Fig. 28d**). In quantitative measurements of glomerulus GFP, a 1-way ANOVA revealed a significant difference across genotypes ($p<0.05$). Dunnett's MC tests showed that glomerulus fluorescence was not significant in *PTEN* + *sl* KDs, although trending downwards and that mean fluorescence was higher in *shark* + *sl* KDs ($p<0.05$), (**Fig. 28e**).

Overall, knocking down *PTEN* alongside *sl* appeared to rescue the engulfment deficit, which suggests that PTEN may inhibit the impact of sl in engulfment. *Pld3* and *sl* knocked down together led to a phenotype identical to *sl* alone, suggesting they may share an upstream element but most likely operate in parallel pathways to mediate engulfment. Knocking down *shark* and *sl* together led to a stronger engulfment deficit than *sl* KD alone, suggesting that shark may operate upstream of sl to regulate engulfment (**Fig. 28**).

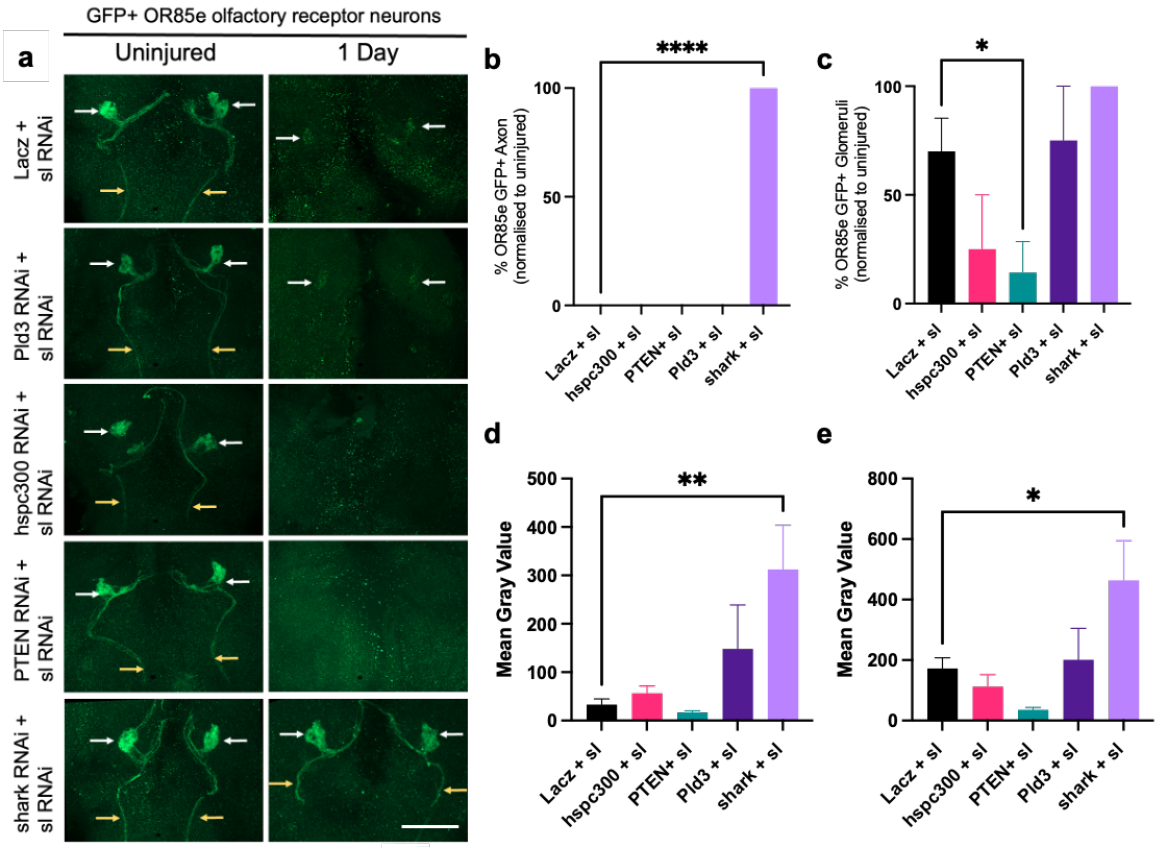


***Fig. 28. Knocking Down Various Factors Alongside sl Led to Multiple Phenotypes.*** ***a)*** *GFP-labelled maxillary ORN neurons before and 5 days after injury, showing axons (yellow arrows) and glomeruli (white arrows).* ***b)*** *Qualitative analysis of GFP+ debris in OR85e axons across experimental lines.* ***d)*** *Percentage of antennal lobes containing visible GFP+ OR85e glomeruli before and after injury.* ***e)*** *Quantitative analysis of GFP fluorescence in OR85e axons.* ***f)*** *Mean GFP fluorescence in OR85e glomeruli. Statistical analysis was achieved through a Kruskal Wallis test with Dunn's MC tests or a 1-way ANOVA and Dunnett's MC tests. Graphs plotted with mean±S.E.M., with significance annotated; *p<0.05, **p<0.01 and ****p<0.0001. n=7-10 brains per group. Scale bar = 50μm.*

### 6.4.3 Phosphoinositide Dynamics Change In Response To Injury

With existing evidence implicating phosphoinositides in engulfment (Swanson 2014), I investigated changes in PIP2 and PIP3 dynamics after injury using fluorescent reporter lines. When assessing PIP2 levels, glial-specific GFP appeared to decline over time, seeing a slight increase between 1min and 6hrs after injury, reducing suddenly around 24hrs and dipping by 48hrs after injury**.** After 5 days, PIP2-related GFP levels returned closer to uninjured levels, appearing to increase slightly in the process (**Fig. 29a**). A 1-way ANOVA suggested a significant change in PIP2-specific fluorescence over time ($p<0.001$) (**Fig. 29b**). Dunnett's multiple comparisons revealed that PIP2 fluorescence reduced significantly 48hrs after injury ($p<0.001$) and that levels were higher than in uninjured conditions after 5DPA ($p<0.01$) (**Fig. 29b**). Conversely, when observing changes in PIP3, nothing changed immediately after injury, however after 6hrs fluorescence levels seemed to increase in the antennal lobes. The same was true at 24hrs post-ablation, with fluorescence appearing to peak after 48hrs. By 5 days, GFP fluorescence had begun to reduce (**Fig. 29c**). A 1-way ANOVA suggested that PIP3-fluorescence changed over time compared to uninjured conditions, with multiple comparisons tests revealing that fluorescence was higher 6hrs ($p<0.001$), 24hrs ($p<0.001$), 48hrs ($p<0.0001$) and 5 days after injury ($p<0.0001$) (**Fig. 29d**).

The sudden decrease in PIP2-related GFP culminating at 48hrs post-ablation and PIP3 concentration likely to increase in cells local to the site of ablation could imply a requirement for PI dynamics in the effective engulfment of neuronal debris (**Fig. 29**).

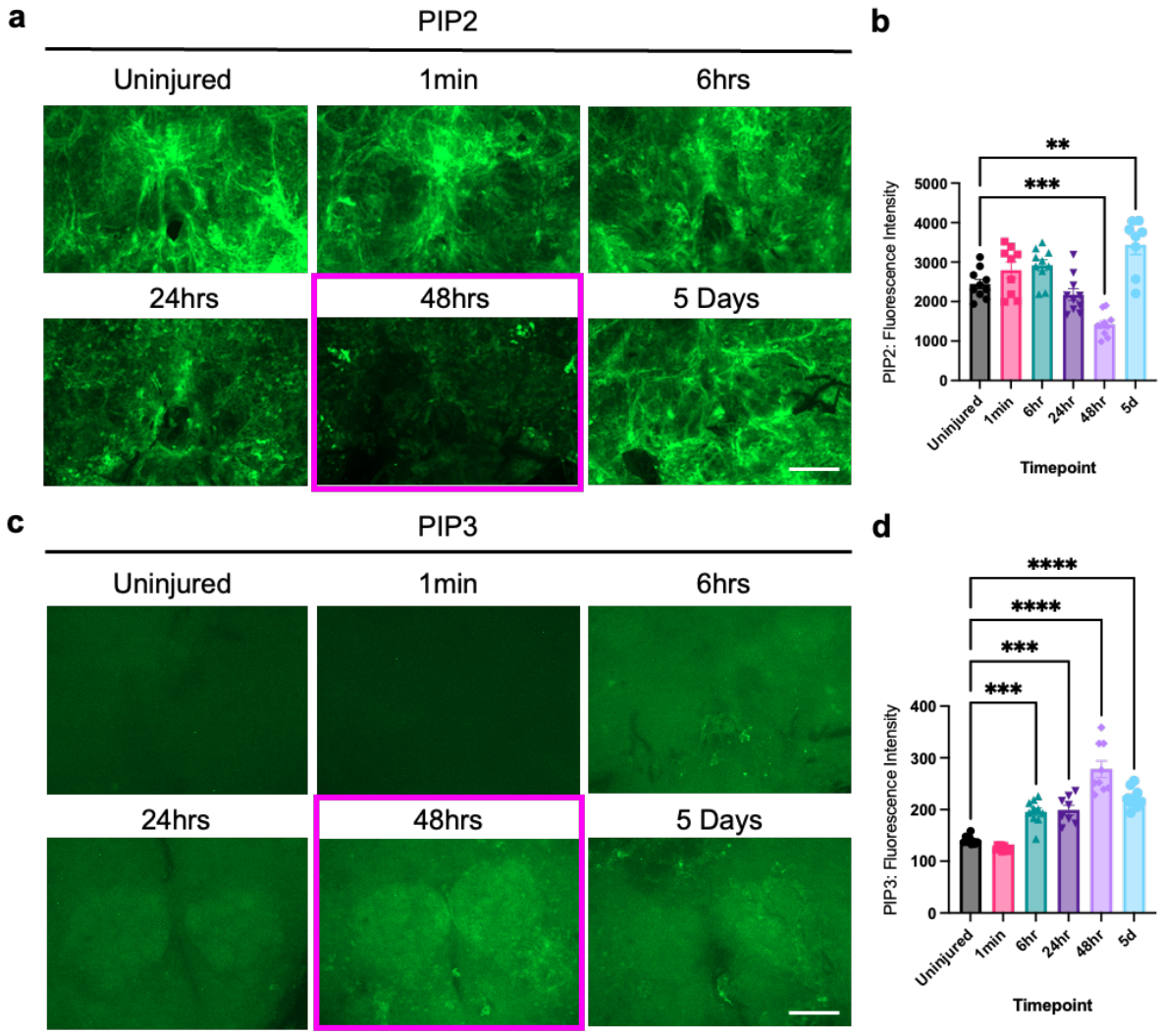


***Fig. 29. Phosphoinositide Dynamics Alter In Response to Injury. a)*** *Representative confocal z-stacks of PIP2 reporter brains before and 1min, 6hrs, 24hrs, 48hrs and 5 days after injury in LacZ-expressing flies.* ***b)*** *Quantification of PIP2-related fluorescence in antennal lobe ensheathing glia before and after antennal nerve injury.* ***c)*** *Representative confocal z-stacks of PIP3 reporter brains before and 1min, 6hrs, 24hrs, 48hrs and 5 days after injury in LacZ-expressing flies.* ***d)*** *Quantification of PIP3-related fluorescence in antennal lobe ensheathing glia before and after antennal nerve injury. Statistical analysis was achieved through a 1-way ANOVA and Dunnett's MC tests. Graphs plotted with mean±S.E.M., with significance annotated; **p<0.01, ***p<0.001, ****p<0.0001, n=8-10 brains per group. Scale bar = 50μm.*

### 6.4.4 Phosphoinositide Changes In Response To Injury Are Modified By *Draper* And *sl*

Having established a link between PI dynamics and injury, I investigated the effect of *sl* and *Draper* KD on the PI response at 48hrs post antennal ablation. A clear reduction in PIP2-related GFP was observed in *wild-type* and *LacZ*-expressing flies before and 48hrs after injury (**Fig. 30a**). Knocking down *Draper* led to a slight decrease in PIP2 levels in uninjured animals and a slight increase 48hrs after injury, reversing the effect seen in control lines. Knocking down *sl* led to an obvious change in baseline PIP2-related fluorescence and a slight decrease in PIP2-related fluorescence after injury (**Fig. 30a**). A 2-way ANOVA confirmed that changes observed between genotypes were significant ($p<0.01$) as were results amongst injured and uninjured samples **(Fig. 30b)**. Post hoc tests showed that baseline PIP2-related GFP was higher in *sl* KD flies than *LacZ* flies ($p<0.01$). Equally, multiple comparisons revealed that the characterised decrease in PIP2-related signal of *LacZ* flies ($p<0.01$), was not observed in *Draper* KD flies and less significant in *sl* KD flies ($p<0.05$) after injury (**Fig. 30b**). When investigating PIP3 dynamics, uninjured *wild-type and LacZ*-expressing flies exhibited low levels of PIP3-related GFP, which markedly increased 48hrs after injury. In *Draper* KD flies, there was no obvious change between fluorescence levels in uninjured/injured groups, however, knocking down *sl* saw an increase in GFP signal after injury (**Fig. 30c**). A 2-way ANOVA confirmed significant differences amongst experimental lines ($p<0.001$) but no changes between genotypes. MC tests revealed that baseline PIP3-related signal was consistent and that the characterised increase in PIP3-related signal of *LacZ* flies ($p<0.001$), was not observed in *Draper* KD flies (**Fig. 30d**).

The fact that knocking down *Draper* suppressed a characterised response in PIP2 and PIP3 species, suggests that Draper may operate upstream of PI signalling. Knocking down *sl* caused a significant increase in baseline PIP2 levels, implying sl is important in PIP2 metabolism. Equally, knocking down *sl* led to a less significant decrease in PIP2/PIP3 after injury (compared to *LacZ* controls), suggesting that sl may partially regulate this process in the context of engulfment (**Fig. 30**).

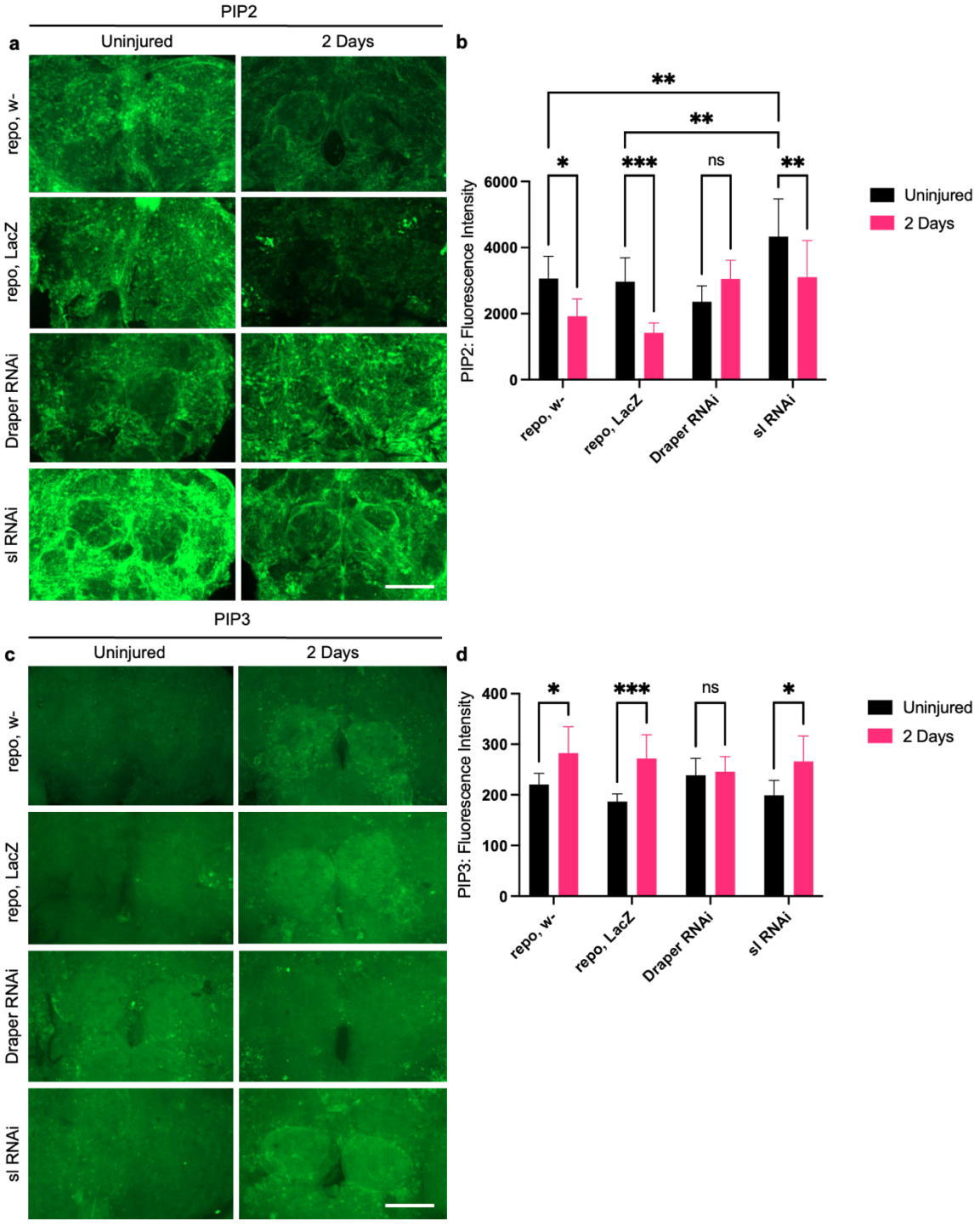
PIP2
a
Uninjured
2 Days
repo, w-
repo, LacZ
Draper RNAi
sl RNAi
b
PIP2: Fluorescence Intensity
6000
4000
2000
0
*
**
***
ns
**
repo, w-
repo, LacZ
Draper RNAi
sl RNAi
Uninjured
2 Days
PIP3
c
Uninjured
2 Days
repo, w-
repo, LacZ
Draper RNAi
sl RNAi
d
PIP3: Fluorescence Intensity
400
300
200
100
0
*
***
ns
*
repo, w-
repo, LacZ
Draper RNAi
sl RNAi
Uninjured
2 Days

***Fig. 30. Draper And sl May Mediate PI Dynamics After Injury. a)*** *Representative confocal z-stacks of PIP2 reporter brains before and 48hrs after injury in experimental lines.* ***b)*** *Quantification of PIP2-related fluorescence in antennal lobe ensheathing glia before and after antennal nerve injury.* ***c)*** *Representative confocal z-stacks of PIP3 reporter brains before and 48hrs after injury in experimental lines.* ***d)*** *Quantification of PIP3-related fluorescence in antennal lobe ensheathing glia before and after antennal nerve injury. Statistical analysis was achieved through a 2-way ANOVA with Tukey's MC tests. Graphs were plotted with mean±S.E.M., with significance annotated; *p<0.05, **p<0.01, ***p<0.001, n=8-10 brains per group. Scale bar = 50μm.*

### 6.4.5 Calcium Dynamics Change In Response To Injury

A downstream event of *sl* signalling is the release of $Ca^{2+}$ from internal stores. Flies were raised in the same conditions at PI experiments, before performing antennal injury and mounting alongside uninjured groups. GFP fluorescence was used as a readout for glial cytoplasmic $Ca^{2+}$ with comparisons drawn between uninjured groups and 1 min, 6hrs, 24hrs, 48hrs and 5-days after injury. Following the changes in GFP fluorescence associated with cytosolic $Ca^{2+}$, very low levels were observed before injury, with a sudden spike only 1 min after ablation (**Fig. 31a**). This increase very quickly subsided by 6hrs and remained low at 24hrs, 48hrs and 5 days after injury. In some cases, 48hrs after injury, higher levels of $Ca^{2+}$-related signal were observed (**Fig. 31a**). A 1-way ANOVA demonstrated that differences were significant over time ($p<0.0001$), and Dunnett's MC tests confirmed that fluorescence was higher 1 min after injury ($p<0.0001$) compared to the uninjured groups (**Fig. 31b**). The increase observed was exclusively in glia suggesting the response could be important in the initiation of neuronal debris engulfment.

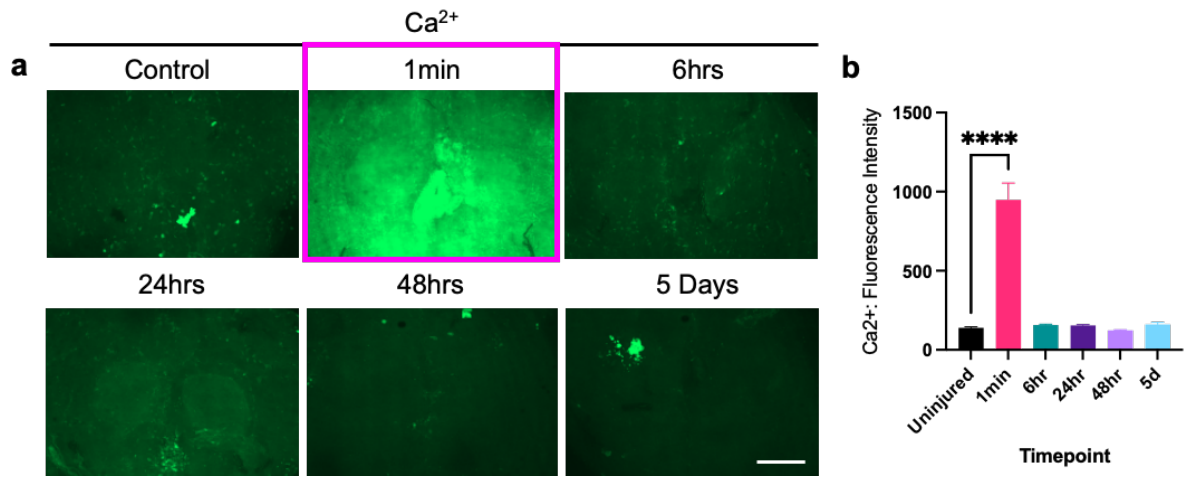


***Fig. 31. Cytosolic Calcium increases Immediately After Injury. a)*** *Representative confocal z-stacks of GCAMP reporter brains before and 1min, 6hrs, 24hrs, 48hrs and 5 days after injury in wild-type flies.* ***b)*** *Quantification of $Ca^{2+}$-related fluorescence in antennal lobe ensheathing glia before and after antennal nerve injury. Statistical analysis was achieved through a 1-way ANOVA with Dunnett's MC tests. Graphs were plotted with mean±S.E.M., with significance annotated; ****p<0.0001, n=7-10 brains per group. Scale bar = 50μm.*

### *6.4.6* Cytosolic $Ca^{2+}$ Elevation In Response to Injury May be Regulated By *sl*

In the knowledge that cellular $Ca^{2+}$ levels see an instant increase in *wild-type* glia after injury, I investigated the effect of *sl* and *Draper* KD on the response at 1 min post antennal ablation. In *w-* control flies, the sudden spike in $Ca^{2+}$-related GFP was observed between uninjured controls and 1 min after injury (**Fig. 32a**). This was not replicated in *LacZ*-expressing flies, likely due to an experimental complication. Knocking down *Draper* led to a similar change in the $Ca^{2+}$ response, such that there was an obvious increase between GFP levels in uninjured animals compared to brains 1 min after injury (**Fig. 32a**). In *sl* KD flies, there was an obvious incline in GFP levels in uninjured brains and no clear increase after injury (**Fig. 32a**). A 2-way ANOVA confirmed a significant difference between injured/uninjured conditions ($p<0.0001$) and between genotypes ($p<0.0001$). Multiple comparisons revealed that mean GFP fluorescence was higher at baseline in *sl* KD compared to *w-* ($p<0.001$) and *LacZ* ($p<0.01$) controls (Fig. 32b). Tukey's MC tests also showed that $Ca^{2+}$-related

fluorescence was higher in injured *wild-type* control animals ($p<0.0001$), as expected, reduced in *Draper* KD flies ($p<0.05$) and not significant in *sl* KD flies after injury (**Fig. 32b**). This suggests that sl and Draper may mediate the $Ca^{2+}$ specific response. observed after injury.

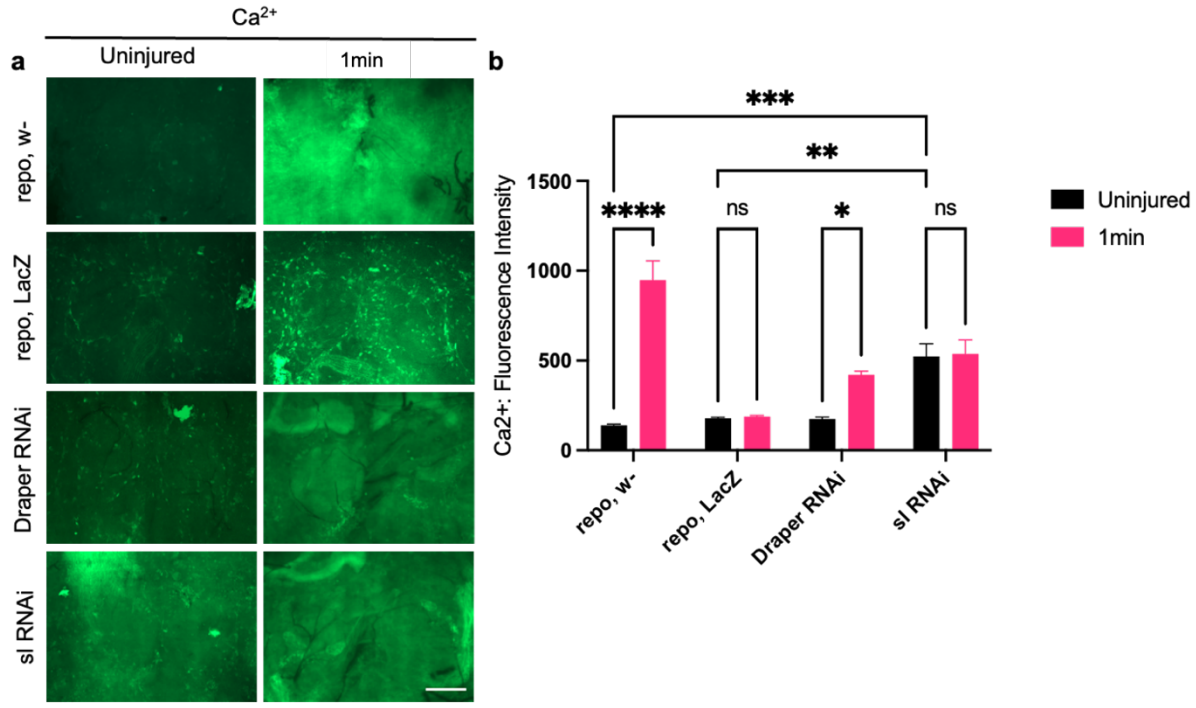


***Fig. 32. Knocking Down sl Prevents $Ca^{2+}$ in Response to Injury.*** ***a)*** *Representative confocal z-stacks of GCAMP reporter brains before and 1min after injury in experimental lines.* ***b)*** *Quantification of $Ca^{2+}$-related fluorescence in antennal lobe ensheathing glia before and after antennal nerve injury. Statistical analysis was achieved through a 2-way ANOVA with Tukey's MC tests. Graphs were plotted with mean±S.E.M., with significance annotated; *p<0.05, **p<0.01, ***p<0.001, ****p<0.0001, n=7-10 brains per group. Scale bar = 50μm.*

## 6.5 Discussion

This chapter elaborates on potential overlaps between molecular pathways that contribute to the observed phenotypes in *sl* and *Pld3* KDs. Assessing changes in Draper upregulation after injury, knocking down sl appeared to prevent upregulation suggesting a plausible overlap between the PI and Draper pathway. Further investigations of epistatic relationships also implied that PTEN may inhibit the role of sl in engulfment and that shark may promote it. Phosphoinositides are likely to change after injury since PIP2 species significantly declined 48hrs after axotomy, which coincided with a significant increase in local PIP3 species. Further evidence supports an overlap of pathways in that knocking down Draper inhibited both PIP responses and knocking down sl subdued them compared to *LacZ* controls. Knocking down *Draper* also reduced an observed $Ca^{2+}$ in *wild-type* glia 1 min after injury, which was completely inhibited when knocking down *sl*. Taken together, results suggest that *sl* is likely to modulate engulfment through the regulation of Draper expression after injury, and achieves this by signalling downstream of Draper pathway members.

### 6.5.1 Draper Upregulation Is Modified By Small Wing

When investigating the impact of *sl* KD on Draper upregulation, data revealed that although KD did not change baseline expression, it did prevent Draper upregulation after injury. This is supported by unpublished RNAseq data from our lab that confirms reduced *Draper* expression in *sl* KDs without injury (personal communication). Both datasets imply that the engulfment phenotype observed in previous chapters could be due to sl modulating levels of Draper and thus supporting a PI convergence model discussed in the literature (Doherty et al. 2014; Purice et al. 2016). This research implies that sl is required for sufficient Draper upregulation. sl may normally function to activate transcription factor STAT92E, previously identified as a regulator of engulfment that is downregulated during ageing (Purice et al. 2016). Partial engulfment phenotypes have been observed from knocking down other members of the phosphoinositide pathway including raptor and PI3K (Doherty et al. 2014). Depletion of PI3K signalling components and sl do not entirely block glial-specific Draper upregulation or clear neuronal debris, perhaps due to positive signalling through the residual Draper. Interestingly, research shows that loss of STAT92E in a

constitutively activated PI3K background does not suppress PI3K-dependent increase of Draper levels suggesting it could be upstream or operating in parallel (Doherty et al. 2014). A later paper suggested that changes in transcriptional reporters are dependent on *Drosophila* AP-1 and STAT92E together, suggesting multiple factors are required to upregulate Draper in response to injury (Lu et al. 2017). To determine whether sl functions upstream of these known engulfment modifiers, it would be interesting to overexpress STAT92E, AP-1 or Draper in a *sl* KD fly, to assess whether engulfment delay can be rescued.

### 6.5.2 Crossovers Between Draper And Phosphoinositide Signalling

PI3K and sl are likely to be linked since epistasis data revealed that PTEN KD rescued *sl*-mediated engulfment delay. PTEN promotes the conversion of PIP3 to PIP2, the reverse achieved by PI3K activity (Bunney and Katan 2010; Georgescu 2010). PTEN gene is also implicated in cytoskeletal regulation and apical-basal polarity (Goberdhan and Wilson 2003; Li et al. 2005; von Stein et al. 2005). PTEN was identified in a screen as a suppressor of Draper overexpression in addition to other members of insulin signalling, such as *chico*, suggesting it could be counteracting the effect of sl on Draper upregulation (Goberdhan et al. 1999). *Drosophila* research also implicates insulin-like receptor (InR) and downstream effector AKT1 activity to be essential for injury-induced activation of STAT92E (Musashe et al. 2016). Insulin signalling in mammals sits upstream of multiple survival pathways and has been associated with PI3K and PLCγ2, further intertwining their activities (Kayali et al. 1998; Lorenzo et al. 2002; Hopkins et al. 2020). Another protein that has been shown to mediate Draper signalling is shark, a nonreceptor tyrosine kinase belonging to the SYK family (Ziegenfuss et al. 2008). Interestingly, knocking down *shark* and *sl* together led to a significant delay in axonal and glomerulus engulfment, a more severe phenotype than *sl* KD alone. This result could support *sl* and *shark* working in parallel pathways, that may converge to modulate Draper signalling. Existing data already exists that links SYK family members to PLCγ2 (Kurosaki et al. 2000). Phosphorylated SYK provides docking sites for BTK and PLCγ2 SH2 domains, thus bringing the two together and facilitating PLCγ2 activation (Kurosaki et al. 2000). This suggests that *Drosophila* shark could function upstream of sl. Although possible, knocking down *shark* alone

yielded a complete engulfment deficit (see **Fig. S4**), making results difficult to interpret. Differences between engulfment phenotypes may be caused by different KD efficiencies of the two RNAis and for future experiments, it will be important to repeat epistasis investigations using mutants. It would be interesting to overexpress *sl* in a shark knockout background to investigate a rescue as well as assess whether sl and shark have a physical interaction through an immunoprecipitation assay. Draper expression could be dependent on the convergent activities downstream of InR and other receptors and STAT92E signalling. Interestingly, in *Drosophila,* where insulin signalling components including PI3K are downregulated, researchers have observed small wing phenotypes which could link sl to PI3K and insulin signalling (Xu et al. 2015). It would be of interest to KD/out PI3K, STAT92E or AKT1 and sl together to understand whether they are activated in the same pathway to mediate engulfment.

### 6.5.3 Phosphoinositide Dynamics May be Required For Engulfment

PI3K and sl both function to catalyse PIP2 in their respective reactions, therefore it was interesting to observe changes in PI dynamics after injury. Data revealed that between 24 and 48 hours after injury, there was a significant decrease in PIP2-related GFP and a significant increase in PIP3-related GFP. Although this has never been shown in *Drosophila* research, other models have linked PIP dynamics to changes in the cytoskeleton and phagocytic ability. Downstream of Fcγ receptor signalling, recruited SYK has been shown to bind substrates including PI3K and PLCγ2 (Tridandapani et al. 2000; Bezman and Koretzky 2007). Active PI3K has been shown to generate PIP3 at the phagocytic cup, which may also regulate activation of GTPase Rac and contractile proteins such as myosin. Both are important in actin remodelling and activation of other signalling molecules such as JNK and the nuclear factor NF-kB (Cox et al. 1999). A study from 2000, showed that phagocytosis requires localised PIP changes (Botelho et al. 2000). Imaging fluorescence chimaeras of pleckstrin homology in live macrophages to monitor PIP2 and DAG, revealed rapid accumulation of PIP2 at the phagocytic cup, with the disappearance of PIP2 as the phagosome seals. As the cup begins to close concentrations of PIP3 conversely increase. Interestingly, reduction of PIP2 has correlated with mobilisation of PLCγ2 and the formation of DAG (Botelho et al. 2000; Hoppe and Swanson 2004; Scott et al. 2005).

Crucially, knocking down sl here, led to a baseline increase in PIP2 preventing the full decline at 48hrs post-ablation, implicating sl as a potential mediator of engulfment through PIP2 dynamics. Overall these results suggest that PIP2 should not only be considered as a molecule that gives rise to signalling substrates such as IP3 and DAG, but also as a functional lipid species that controls the engulfment rate of glial cells through phagocytic cup formation. PIP2 accumulation at the glial membrane may result in phagosomes that cannot be sealed thus preventing the internalisation of neuronal debris after injury.

Whilst the Draper signalling pathway has been well characterised the involvement of lipids is an emerging field. Knocking down Draper caused an increase in PIP2 as opposed to the observed decrease in control flies, suggesting Draper may be required in the lipid response and could lie upstream of PIP2 metabolism. Results also showed that Draper KD prevented PIP3 levels from increasing post-injury. This suggests that Draper signalling is involved in both phagocytic cup formation and closure. In a *Drosophila* study, Draper-mcherry microclusters on 10% Phosphatidylserine (PS) bilayers recruited activating subunit PI3K to the plasma membrane, which could explain why PIP3 levels increase after injury (Williamson and Vale 2018). Equally, in MEGF10 studies, membrane lipids were quantified using a dot blot assay, revealing binding affinities of MEGF10 to phosphatidic acid, PI4P, PIP3, PIP2 and DAG, confirming a link (Iram et al. 2016). Perturbations to the dynamics of PIP2 and PIP3 signalling have been associated with neurodevelopmental and neurodegenerative disorders before, such as autism spectrum disorders (ASD) and Alzheimer's disease, among others (Arancio 2008; Gross 2017), overall suggesting that excessive microglial synaptic pruning, may contribute to disease.

### 6.5.4 Calcium Dynamics In Response to Injury

Metabolism of phosphoinositides leads to the production of diacylglycerol and IP3, which causes a rapid increase in cytoplasmic $Ca^{2+}$ concentration, due to the release of stored intracellular $Ca^{2+}$ and stimulated $Ca^{2+}$ entry from the extracellular space (Balla and Catt 1994). When investigating $Ca^{2+}$ levels after injury, there was an immediate increase in GCaMP-related fluorescence 1 min after ablation, suggesting

$Ca^{2+}$ changes are associated with early engulfment. This was not observed in *LacZ*-expressing controls (**Fig. S5**), however, this should be repeated. $Ca^{2+}$ signalling has been observed in macrophages before, such that activated mouse macrophages can propagate $Ca^{2+}$ signals to resting bystander cells by releasing ATP, with ATP signalling required for efficient phagocytosis (Zumerle et al. 2019). Equally, the release of $Ca^{2+}$ from the ER activates store-operated $Ca^{2+}$ entry (SOCE) channels in the phagosomal membrane, leading to sustained elevations or oscillatory elevations in cytosolic $Ca^{2+}$. Calcium is required for the solubilisation of actin meshwork surrounding nascent phagosomes (Nunes and Demaurex 2010). We find that axotomy causes significant $Ca^{2+}$ transients in the surrounding glial cells, therefore it may be contributing to the engulfment of neuronal debris. Calcium signalling plays many roles in cytoskeletal changes by regulating the activity of contractile proteins (Tan and Boss 1992), activation of actin filament severing (Yamamoto et al. 1982), and inhibition of actin crosslinking (Demma et al. 1990), among many other roles. *Draper* KD reduces the peak of the $Ca^{2+}$ transient in glia after neuronal ablation, suggesting that the prevention of engulfment may be mediated by the stability of actin filaments. Phagocytic receptors such as Fcγ receptors have been shown to activate PLC and PLD, resulting in the intracellular production of $Ca^{2+}$ (Nunes and Demaurex 2010).

Knocking down *sl* prevented the cytosolic increase in $Ca^{2+}$ observed in controls, which could explain the role of sl in phagocytosis. Crucially, PLCγ2-R522R expressing cells, show consistent hyper functionality manifested as enhanced release of cellular $Ca^{2+}$ in response to Fc-receptor ligation or exposure to Aβ oligomers (Maguire et al. 2021). Macrophages from the study exhibited impaired phagocytic engulfment of pHrodo-labelled bioparticles, but enhanced endocytic clearance of Aβ1-42 oligomers, implicating PLC-mediated $Ca^{2+}$ further in some engulfment functions (Maguire et al. 2021). It would be worth investigating humanised flies in both $Ca^{2+}$ and PI models to understand how the AD variant could alter signalling. An increase in PLCγ2 induced $Ca^{2+}$ has also been shown to be required for translocation of toll-like receptor 4 (TLR4) from the plasma membrane to endosomes, where Interferon regulatory factor 3 (IRF3) activation takes place during phagocytosis (Chiang et al. 2012). Results also suggested that knocking down *sl* led to a baseline increase in $Ca^{2+}$ concentration, therefore $Ca^{2+}$ may have reached saturation point preventing the typical increase after injury. Intriguingly, Draper also appears to function upstream of the $Ca^{2+}$ response,

since knocking down Draper prevents $Ca^{2+}$ incline after injury. Interestingly, Draper has been linked to $Ca^{2+}$ signalling before, whereby results implicated Junctophilin in phagocytosis and associated Draper-mediated phagocytosis with $Ca^{2+}$ homeostasis (Cuttell et al. 2008). Both global and localised $Ca^{2+}$ signals have been shown to occur during phagocytosis, although their functional impact on the mechanism of phagocytosis has been debated (Nunes-Hasler et al. 2020), however the emerging evidence and this chapter propose $Ca^{2+}$ and phosphoinositide signalling to play an important role in neuronal debris phagocytosis. Further investigations could be centred around a potential epistatic relationship between sl and Draper, mediating $Ca^{2+}$ transients, and investigating whether a $Ca^{2+}$ response is sufficient or redundant for engulfment.

## 6.6 Summary of Key Findings

This chapter highlights multiple ways in which sl may be involved in Draper-mediated phagocytosis.

- Knocking down *sl* prevents Draper upregulation after injury.
- PI models revealed that PIP2 and PIP3 dynamics change in opposing directions between 24-48hrs after injury when Draper upregulation usually occurs (MacDonald et al. 2006). This switch is likely needed for the engulfment process.
- Knocking down *Draper* prevented typical changes in PIP2 and PIP3, suggesting PI responses after injury could be mediated by downstream of Draper signalling.
- Knocking down *sl* led to a baseline increase in PIP2, and diminished the response ordinarily seen in control conditions, suggesting sl could be involved in phagocytosis through changes to PIP2 metabolism.
- PI signalling component PTEN, when knocked down rescued the delay in engulfment caused by knocking down *sl*, further implicating PIP homeostasis in phagocytosis.
- A GCAMP model revealed that cytosolic $Ca^{2+}$ levels increased 1min after injury, suggesting this response could be important for engulfment initiation.
- Knocking down *sl* led to a baseline increase in cytosolic $Ca^{2+}$, and diminished the response ordinarily seen in control conditions, suggesting sl could be involved in phagocytosis through changes to $Ca^{2+}$ homeostasis.
- Knocking down *Draper* also reduced the characterised $Ca^{2+}$ increase after injury, suggesting Draper could operate upstream of $Ca^{2+}$ signalling.

Overall, the evidence suggests sl could play many roles in phagocytosis, linking PI and Draper signalling and raising the prospect of PLCγ2 as a therapeutic target in Alzheimer's Disease.

# 7 Discussion

Although age is the largest risk factor in dementia, the heritability of AD is estimated to be between 58-70% (Bellenguez et al. 2022). A strong genetic factor modulating disease has fuelled the discovery of novel mechanisms underlying risk, which have reshaped our understanding of the disease and will likely drive new therapeutic designs (Rafii and Aisen 2020; Uddin et al. 2021). GWA studies have identified over 40 SNPs associated with AD-onset, illustrating the polygenicity of the condition (Bellenguez et al. 2022). Polygenic risk scores (PRS) enable scientists to discern between AD cases and controls with an accuracy of 84% (Baker and Escott-Price 2020). PRS operates using variants of biologically relevant gene sets and is important for identifying disease mechanisms and informing experiments and clinical trials. Despite the importance of polygenicity understanding how each gene could contribute to disease mechanisms may be vital to finding therapeutic targets. The recent discovery of a rare protective coding variant in PLCγ2 has generated a lot of excitement in the field and draws more attention to the role of microglia (Sims et al. 2017). Equally, the discovery of rare coding variants in the PLD3 locus has renewed the importance of APP processing and amyloid plaque formation (Lambert et al. 2013c; Fazzari et al. 2017). Both enzymes are associated with the phosphoinositide pathway (Falkenburger et al. 2010) with several known, localised downstream impacts. They could be amenable to drug development approaches, encouraging new opportunities for disease intervention. To inform drug design and contribute to the growing body of research, it is important to study the role of these genes in an *in vivo* context, providing global and mechanistic insight.

This thesis has sought to understand how risk-associated genetic loci contribute to microglia-associated pathologies in Alzheimer's patients. Thanks to the elegant fruit fly and its extensive toolbox, we have been able to investigate the roles of gene orthologs at a cellular and molecular level with a focus on glial engulfment. To identify the limitations of our engulfment model system, I assessed the impact of rearing sex, rearing temperature and age on the rate of neuronal debris clearance *w-* and *Draper* knockdown flies. Here, data suggested that the rate of complete debris engulfment took approximately 5 days and was not affected by the rearing temperature or sex of the fly. Although temperature conditions are often overlooked in dementia, scientists are becoming increasingly interested in the impact of the environment on the brain (Lenroot and Giedd 2008; Tooley et al. 2021). A 2016 study demonstrated a

relationship between residential temperature and cognitive ability in elderly men (>70 years), such that short-term exposure to high or low air temperature increased the risk of cognitive impairment (Dai et al. 2016). Other research also suggests that skin and core body temperature could present as early biomarkers for preclinical MCI or AD (Eggenberger et al. 2021). With global temperatures rising as a result of climate change (Collins et al. 2020), it is crucial to ascertain how our modified environment may impact our health and propose that studies investigate the potential impact on the brain and immune function (Gong et al. 2022). Equally, there has been a historical lack of representation in disease clinical trials, which has excluded the possibility of sex-specific variation in disease (Martinkova et al. 2021). Although my reports do not demonstrate a sex-specific phenotype in glial engulfment rate, they highlight the importance of representation in pre-clinical studies. This does not preclude the possibility of variation in higher organisms and would advocate further investigation in animal and cell models.

Results did discover that glial engulfment diminished with the age, suggesting that *Drosophila* glia become less respondent with time. This is supported by existing research in the model system, which establishes an engulfment deficit in 'old' animals (Purice et al. 2016). With inflammation and debris accumulation already being hallmarks of AD, phagocytes likely become increasingly dysfunctional with time (Li 2013). Since the biological process of ageing is a significant risk factor, it is crucial to explore molecular changes that occur in all CNS cells, and how these contribute to disease. Our data demonstrate that wild-type glia exhibit reduced phagocytic ability with increasing age, suggesting glia are sensitive to age-related changes regardless of risk-associated genetics. Interestingly, loss of function was observed in middle-aged flies, supporting the notion that phagocytosis could be an early sign of disease and a potential biomarker in research (Fiala and Veerhuis 2010). Purice and colleagues attribute glial changes in flies to a reduced expression of major engulfment regulator *Draper* (Purice et al. 2016). However, RNA sequencing data in mouse models, reveals that normal ageing induces A1-like astrocyte reactivity, coupled with elevated expression of *MEGF10* (*Draper* ortholog) (Clarke et al. 2018). It could be that phagocytes are activated in the early stages of ageing due to increased demand, with higher chances of infection (Castle 2000), debris accumulation and cytotoxic protein levels (Haynes 2020), then diminish with time as genetic and environmental strains

take their toll. Equally age-dependent changes could depend on cell type. However, the causative nature of glial cell function remains in question and we would urge further investigation, with a focus on potential gene targets which may modify age-related phenotypes in microglia and other immune cells (Candlish and Hefendehl 2021).

Having established the optimum conditions for later experiments, RNAi lines targeting individual risk gene orthologs were sourced and included in a reverse candidate screen. Knockdown was restricted to glial populations using pan-glial *repo* to drive GAL4 expression, with individual knockdowns investigated for significant changes in glial engulfment rate. The initial screen revealed that *Abi, bru1, CHMP2B, cindr, CG34120, DOR, Fit1, fw, Hasp, Lap, Mef2, p130Cas, Pld3* and *sl* could play a role in glial engulfment. Initial repeat experiments verified that *Abi, bru1, CHMP2B, Mef2, Pld3,* and *sl* were potential modulators. Initial literature investigations provided some explanations as to how these genes could regulate engulfment, however, *Pld3* and *sl*, were the most interesting to follow up. Analogous to human PLD3 and PLCγ2, which encode members of the phosphoinositide pathway and have variants associated with AD risk (Hooli et al. 2015; Sims et al. 2017). Both genes when knocked down, showed strong phenotypes and highlighted a potential pathway of interest to the engulfment field. Knocking down both genes led to a significant yet partial delay in neuronal debris clearance, such that GFP-positive glomeruli were visible and quantifiable 14 days after injury.

In the thesis, I show that *PLD3* ortholog *Pld3* causes a significant delay in injury-mediated engulfment by glia when knocked down. Despite being debated, most studies promote the notion that PLD3 activity correlates with reduced extracellular amyloid (Fazzari et al. 2017). Some attribute this to PLD3 being involved at the processing stage, however, our evidence may suggest a new role for PLD3 in amyloid clearance. Since knocking down *Pld3* caused a partial delay in neuronal debris engulfment, we presume that Pld3 may promote engulfment in response to certain stimuli, such as amyloid beta plaque formation. Most human PLD3 variants associated with increased risk are hypomorphic and when studied, are observed to exacerbate amyloid pathology and associate with cognitive decline (Wang et al. 2015a; Zhang et al. 2016b; Engelman et al. 2018).

Equally, knocking down *sl* yielded a similar glial engulfment deficit, implying an important role for PLCγ2 in human phagocytosis mechanisms. This can be compared with existing research that reports reduced phagocytic activity in macrophages with reduced PLCγ2 or PI3K activity (Obst et al. 2021). We find that brain resident glia use these same molecules for engulfment processes indicating a unified mechanism shared between in CNS and periphery. However, it is worth mentioning that recent data presents different roles for PLCγ2 in alternative types of engulfment, phagocytosis, and endocytosis. Maguire et al. demonstrated that expressing the hypermorphic PLCγ2-P522R variant in microglial lines led to reduced phagocytosis of bioparticles and enhanced endocytosis of Aβ (Maguire et al. 2021). The simplest interpretation of disparate data in the PLCγ research field and a conflicting function in phagocytosis is that although some receptors might signal preferentially or even exclusively via calcium or PIP signalling when multiple receptors are engaged, the requirements of either could be circumvented. Based on this finding we suggest that the engulfment of neuronal debris may be mediated through endocytosis mechanisms and that sl/PLCγ2 and Pld3/PLD3 promote neuronal debris engulfment. One clear area for further research would be to test the changes to engulfment in a *Drosophila* Aβ model (**Fig. S6**) to assess the effect on phagocytosis, and to investigate the potential interaction between PI3K, sl and Pld3. This is especially intriguing since researchers observed the same PIP2 response to multiple stimuli (Maguire et al. 2021), suggesting that PIP2 metabolism could be a differentiating step.

Dementia research suggests a duality in the role of microglia, such that increased phagocytosis of synapses can aggravate the disease, but reduced endocytosis of amyloid may equally accelerate pathology (Nizami et al. 2019). Microglial activation and increased subsequent inflammation and phagocytosis can promote the engulfment of stressed but viable neurons which has been postulated to enhance AD pathology (Gabandé-Rodríguez et al. 2020). Furthermore, inhibiting phagocytosis can prevent inflammatory neuronal death (Neher et al. 2011) and APOE-Ɛ4 -expressing cells demonstrate increased phagocytosis of apoptotic neurons (Muth et al. 2019). On the other hand, enhanced clearance of Aβ1-42 is favourable in AD to prevent the build-up of plaques, which can perturb metabolic processes, reduce blood flow, release deleterious reactive compounds, and induce apoptotic activity (Watson et al. 2005; Hampel et al. 2021). Crucially, knockdown of PLCγ2 does not fully inhibit Aβ

endocytosis (Maguire et al. 2021), adding to the theory that PLCγ2/sl may play a supporting role in the process of engulfment. A partial phenotype is comforting, explaining why PLD3 and PLCγ are risk-associated rather than causal in the onset of pathology and pertaining to the notion of additive causality (Rocchi et al. 2003; Hu et al. 2020). Regulated engulfment encouraged by PLCγ2/sl or PLD3/Pld3 activity may therefore help to prevent or promote Alzheimer's pathology. Although *Drosophila* provide a conserved and robust model for dementia research, boasting a range of genetic tools, developing these molecules as drug targets should be taken cautiously.

Staining for Draper revealed that knocking down *sl* prevented upregulation after injury. This proposes a likely reason for the delay in engulfment observed since Draper is upregulated as part of a positive feedback loop to promote the full engulfment of neuronal debris after injury (Logan et al. 2012). *Drosophila* research already ties Draper upregulation to members of the phospholipid pathway through PI3K and STAT92E activity (Doherty et al. 2014; Purice et al. 2016). Results suggested that PI3K signalling was dispensable for injury-induced Draper upregulation and that STAT92E was necessary, acting downstream of Draper to promote transcription (Purice et al. 2016). Together, our data propose that phosphoinositide signalling could be an adjacent process to STAT92E signalling, engaged when large amounts of neuronal debris require clearance. Signalling through PI3K or sl may promote STAT92E-dependent regulation of glial gene expression, proportional to the strength of Draper activation. It is recommended that this data be supported by investigations of PI3K/STAT92e activity in *sl* knockdowns to understand whether their activity converges to regulate Draper transcription. Equally, upstream regulators of MEGF10 transcription are largely unknown highlighting a need to investigate this area further in microglia and astrocyte models.

Pursuing this narrative, I investigated glial phenotypes using phosphoinositide models. Measuring fluorescently associated with changes in PIs revealed that PIP2 and PIP3 dynamics fluctuated in glia over time in response to injury. Several studies have implicated phosphoinositides as regulators of phagocytic and endocytic uptake in various phagocytes (Botelho et al. 2000; Brown et al. 2001; Bohdanowicz and Grinstein 2013). Both clathrin-independent (CIE) and clathrin-dependent endocytosis (CDE) have been associated with PIP2 metabolism (Naslavsky et al. 2003; Mayor et

al. 2014), in addition to other internalising processes from macropinocytosis (Zhang et al. 2022) and autophagy (Donaldson 2003; Nunes and Demaurex 2010; Lundquist et al. 2018). Following ablation, I observed a gradual decrease in glial PIP2-responsive GFP levels which dipped at 48hrs post-ablation, correlating with a gradual increase in local PIP3-responsive GFP, which peaked at 48hrs. My findings could be explained by existing data in the field that demonstrate changes in phosphoinositide levels in response to pro-inflammatory stimuli (Botelho et al. 2000; Maguire et al. 2020; Maguire et al. 2021). Research implies that PIP2 metabolism is required in phagocytic cup formation due to a depletion in PIP2 species during engulfment (Maguire et al. 2021).

Equally, knocking down *sl* in glia that express phosphoinositide reporters, led to an attenuated decrease in PIP2 levels in response to injury, suggesting *sl* could mediate PIP turnover during glial activation. PIP2 levels are critical for the modulation of actin dynamics and are known to play a role in phagosome formation and engulfment (Botelho et al. 2000; Scott et al. 2005). This is supported by recent findings by Maguire and colleagues, showing that the protective PLCγ2-P522R variant promotes a greater drop in PIP2 following the addition of FcγRII/III antibody, LSP and Aβ (Maguire et al. 2021). Equally, they demonstrated an increase in DAG production in the P522R variant expressing microglia when stimulated by FcγRII/III antibody. Taken together, it is likely that the control of PIP2 levels during engulfment determines the success of the process. Therefore, the tight regulation of PLCγ2 or sl could be essential in engaging engulfment in response to different stimuli.

I discovered that knocking down *Draper* prevents PIP2-specific responses to injury which could support a role for mammalian ortholog MEGF10 in PIP2-mediated engulfment and PLCγ2 activation. MEGF10, which functions to mediate engulfment in astrocytes (Iram et al. 2016), has rarely been studied in the context of the phospholipid pathway and associations with PLCγ2 have not been made before. However, in a study investigating the role of MEGF10 in skeletal muscle myopathy, a protein-lipid overlay assay found interactions between phospholipids and EGF protein (typically found in MEGF10) (Hughes 2016). Crucially, EGF protein associated with PIP2, but also PA and PS which are downstream of PLD3. Equally, Western blot and immunoprecipitation assays in murine macrophages revealed an association between a receptor tyrosine kinase (RTK) MerTK with PLCγ2 in response to phagocytic stimuli,

followed by phosphorylation of PLCγ2 (Todt et al. 2004). This response was observed following exposure to apoptotic leukocytes and was shown to be, in part, required for the effective clearance of debris (Todt et al. 2004). Incidentally, this supports my hypothesis that PLCγ2 may be important in the engulfment of neuronal material, however, it would be imperative to study potential interactions between PLCγ2 and MEGF10 and study the role further in astrocytes as well as microglia.

Interestingly, Maguire's study found that co-treatment with SHIP1, PI3K or PTEN inhibitors did not stabilise PIP2, suggesting that PIP2 metabolism is an upstream event exclusively mediated by PLCγ2 in this instance (Maguire et al. 2021). My epistasis investigations suggest that PTEN knockdown rescues the observed engulfment delay, implying that *sl*-mediated PIP2 regulation can be compensated by PTEN and potentially PI3K activity. Since knocking down *Draper* blocked PIP2-related signal after injury, this suggested Draper may inhibit factors which promote PIP2 synthesis such as PTEN. This could be supported by a study which identified a genetic interaction between PTEN and inhibitory Draper-II (Fullard and Baker 2015). Crucially, other published data where components which inhibit PIP2 hydrolysis, such as PTEN and SHIP1 have been shown to increase phagocytosis, which could provide another explanation for my findings (Mondal et al. 2012). Equally, I found that knocking down *shark* alongside *sl* led to a more prominent delay, such that axon structures were still visible 5 days after injury. This data suggest that shark and sl may be acting together to promote engulfment. This is plausible since mammalian studies have shown a clear interaction between PLCγ2 and shark ortholog syk, when mediating an anti-fungal immune response (Gorjestani et al. 2011), however, this interaction remains to be confirmed in *Drosophila*.

It is clear from my data and other studies (Maguire et al. 2021) that PIP2 changes must be precise to mediate engulfment, suggesting that PIP2 concentration may be rate limiting. Conversely, local PIP3 levels increased in correspondence with the PIP2 trough at 48hrs post-ablation, suggesting PIP3 dynamics may also be important. PIP3 changes in response to stimuli have been recorded in macrophage cultures before, in the case of Botelho and colleagues, confirming biphasic changes in PIP2 and PIP3 levels during phagosome cup formation (Botelho et al. 2000). As the cup begins to close, concentrations of PIP2 at the cup membrane reduce significantly in line with

PIP3 and DAG concentration increases (Botelho et al. 2000). Studies also report that PIP3 and DAG levels decrease after cup closure into a phagosome (Vieira et al. 2001; Henry et al. 2004), a trend observed in my PIP3-GFP readings. Crucially, knocking down *sl* only lightly subdued changes in PIP3 post-injury, suggesting sl is not responsible for mediating engulfment by modifying PIP3 levels. This is consistent with published data where mass enzyme-linked immunosorbent assays (ELISA) showed that expressing the hypermorphic PLCγ2 variant led to no significant changes in PIP3 levels after stimulus (Maguire et al. 2021).

Interestingly, knocking down *Draper* blocked typical changes in PIP3 species in response to injury, suggesting phosphoinositide changes occur downstream of Draper activation. Although phosphoinositide changes have never been studied within the Draper pathway, some evidence supports an interaction in *C.elegans* research. The study found that myotubularin 1 (MTM-1) promoted phagosome maturation, potentially through Draper ortholog Ced-1 receptor recycling (Neukomm et al. 2011). MTM-1 is responsible for regulating Phosphatidylinositol 3-phosphate (PI3P), a phospholipid found in the cell membrane which is generated via the phosphorylation of the inositol (Marat and Haucke 2016). PI3P was also seen to increase during phagosome maturation in mammalian studies, alongside changes in PIP3 (Vieira et al. 2001). Together, these findings promote a possible connection between the Draper/MEGF10 pathway with phosphoinositide signalling which could operate in glial phagocytosis.

PI3K and PLCγ2 mediated PIP2 metabolism are likely to be linked, converging during PIP2 hydrolysis, since products of both mechanisms have been observed to change at similar rates in the case of PIP3 and DAG (Vieira et al. 2001; Henry et al. 2004; Swanson 2014). Prevalent studies already associate PI3K with upstream receptors of PLCγ2 such as TREM2. Importantly, Peng and colleagues demonstrate that ligation of TREM2-activated PI3K induced the mobilisation of intracellular $Ca^{2+}$ and the reorganisation of actin (Peng et al. 2010). Published *Drosophila* studies have also implicated PI3K as being important in promoting engulfment since knocking down *PI3K* and downstream factors caused a significant delay in engulfment comparable to my findings in Pld3 and sl knockdowns (Doherty et al. 2014; Purice et al. 2016). This would provide a plausible explanation for phosphoinositide dynamics observed in response to injury since PI3K is one of the major modulators for PIP2 metabolism

converting it to PIP3 (Falkenburger et al. 2010). It would be recommended to investigate converging roles between PLCγ2 and PI3K through epistasis studies.

Downstream events of PI3K activity, such as AKT activation have been attributed to $Ca^{2+}$ signalling, such that simulated Store-operated $Ca^{2+}$ entry (SOCE) rapidly correlated with increased Akt activity in the absence of growth factors in cell suspension, linking $Ca^{2+}$ homeostasis to the Akt pathway (Divolis et al. 2016). I present evidence that neuronal injury induces a spike in $Ca^{2+}$-related fluorescence in control conditions, suggesting $Ca^{2+}$ signalling could be important in the phagocytic process in *Drosophila*. $Ca^{2+}$, being a ubiquitous second messenger, is already known to participate in numerous inflammatory processes, from chemotaxis and adhesion in mammalian systems to apoptotic cell (AC) clearance in *Drosophila* (Kinchen 2010; Nunes and Demaurex 2010; Nunes-Hasler et al. 2020). Although it is generally accepted that an increase in cytosolic $Ca^{2+}$ is an early signal of phagocytosis, whether the signal is necessary for engulfment is largely debated. Early studies recognised that the tight regulation of $Ca^{2+}$ was important for optimal rates of phagocytosis as a reduction or excess of cytosolic $Ca^{2+}$ can negatively impact engulfment rates, which phenocopies data in my thesis (Stossel 1973; Elferink 1982; DingYoung et al. 1984; Buisman et al. 1988). It is now being discussed that a cytosolic rise in $Ca^{2+}$ may regulate later steps in the process and could be required for efficient phagosome maturation, consistent with our findings (Worth et al. 2003; Henry et al. 2004; Cuttell et al. 2008; Hinkovska-Galcheva et al. 2008; Maguire et al. 2020; Maguire et al. 2021). Studies also indicate that $Ca^{2+}$ homeostasis is important for lysosomal function (Feng and Yang 2016) and that the ER may serve as the primary source of $Ca^{2+}$ for lysosomes as opposed to pH gradients (Garrity et al. 2016). More specifically, blocking IP3 receptors on the ER prevented $Ca^{2+}$ refilling of lysosomes in fibroblasts and led to impaired lysosome function (Garrity et al. 2016). It would be valuable to ascertain the role of $Ca^{2+}$signalling and *sl* in later stages of engulfment by knocking down *sl* in flies carrying lysosomal markers such as LAMP1.

My data also demonstrates that knocking down *sl* causes an increase in baseline levels of cytosolic $Ca^{2+}$, which in turn prevents the $Ca^{2+}$ spike observed in response to neuronal injury in local glia. Cuttell et al. showed that a key $Ca^{2+}$ channel at the ER membrane known as ryanodine receptor, Rya-r44F interacted with *Uta* upstream of

Draper and promoted downstream signalling events facilitating AC clearance (Cuttell et al. 2008; Kinchen 2010). Importantly, they confirmed that the observed rise in $Ca^{2+}$ was due to its release from the ER as opposed to extracellular $Ca^{2+}$ entry and that Draper could maintain Uta-mediated processes, via other mediators Stim and Orai to regulate $Ca^{2+}$ release from the ER (H et al. 2000; Cuttell et al. 2008; Kinchen 2010). Their studies support that ER-related $Ca^{2+}$ release could be an important event for effective engulfment and could provide some explanation for the role of sl and $Ca^{2+}$ signalling in our model.

Interestingly, knocking down Draper also prevented the expected $Ca^{2+}$ change, suggesting that Draper could be mediating phagocytosis through sl-mediated $Ca^{2+}$ signalling. Analogous findings were made by Weavers and colleagues, in embryonic system macrophages, where $Ca^{2+}$ bursts were observed in correlation with increasing Draper expression (Weavers et al. 2016). Changes in $Ca^{2+}$ signalling support an association between $Ca^{2+}$ and phagocytic mechanisms and could explain my findings in *sl* KD flies where Draper upregulation was inhibited. Similar links between $Ca^{2+}$ homeostasis and AC clearance have been observed in mammalian systems and *C.elegans* (Gronski et al. 2009). Moreover, research in stretched osteoblasts demonstrated that raising cells in $Ca^{2+}$-free medium attenuated PI3K phosphorylation and downstream messenger activation (Danciu et al. 2003), suggesting cytosolic $Ca^{2+}$ was important in the early response of osteoblasts to mechanical stimuli. These data also argue that Draper is activated in the recognition cues presented to glia after neuronal injury, initiating engulfment. This could also explain the impact of *sl* function in Draper upregulation and link PI3K function to early *sl*-mediated events.

Taken together, my results add to existing research that PLCγ2 facilitates receptor-mediated responses to inflammatory stimuli by regulating changes in cytosolic $Ca^{2+}$ and PIP2 metabolism (Kurosaki et al. 2000; Maguire et al. 2021). Maguire and colleagues found that expression of the hypermorphic PLCγ2-P522R variant conferred with receptor-mediated $Ca^{2+}$ release in macrophages and microglia. Equally, they found that this was associated with enhanced endocytosis of amyloid oligomers (Maguire et al. 2020). Some of the best-studied phagocytic receptors in mammals are FcγRs, which activate PLC and PLD molecules, resulting in the intracellular production of IP3 and DAG, leading to $Ca^{2+}$ release at the ER membrane. Initial events following

FcR ligation have been well established (García-García and Rosales 2002; Joshi et al. 2006). Receptor activation recruits Src homology 2 domain-containing proteins, such as tyrosine kinases of the Syk family and PI3K and initiates downstream events. Included, is the activation of PLCγ, which generates IP3 from PIP2. IP3 then binds and activated $Ca^{2+}$ channels at the ER (Berridge 1993). Interestingly, in neutrophils and monocytes, FcR engagement is not always accompanied by IP3 regulation (Melendez et al. 1998), since $Ca^{2+}$ change was unaffected by classical inhibitors of the IP3 axis (v. DAVIES-COX et al. 2001; Slaby and Lebiedz 2009). Alternative pathways for $Ca^{2+}$ regulation have been identified and involve the activity of PLD family members (Choi et al. 1996). Choi et al. found that specific FcR (IgER: FcRI) ligation triggered IP3-independent $Ca^{2+}$ transients via PLD-mediated stimulation of sphingosine kinase (SK), which generates the second messenger S1P (Choi et al. 1996; Melendez et al. 1998). S1P is a membrane-bound lipid, which may generate local $Ca^{2+}$ signals near the PM or phagosomal membrane, whereas IP3 being a diffusible messenger causes global $Ca^{2+}$ throughout the cytoplasm (Chuang et al. 2000). Consistent with my findings, PLD activation in response to IgG ligation was observed (Gewirtz and Simons 1997) and shown to be important in phagocytosis by neutrophils and monocyte-derived macrophages (Kusner et al. 1999; Melendez and Allen 2002). Equally, $Ca^{2+}$ transients are observed through CR engagement which appears to be mediated largely, by the PLD pathway (Löfgren et al. 1999), since PLD is strongly activated by CR3 and CR1 crosslinking or by phagocytosis of serum-opsonised zymosan (Fallman et al. 1992). Importantly, MEGF10 is a receptor for C1q, mediating the clearance of ACs by astrocytes (Iram et al. 2016). Researchers propose that different receptors might determine whether PLC or PLD signalling is engaged preferentially and that this could extend to different stimuli (Chuang et al. 2000; Gillooly et al. 2001; Melendez and Tay 2008; Beech et al. 2009; Maguire et al. 2021). Crucially, our data imply that both PLC and PLD orthologs are activated in Draper-mediated engulfment and are likely to operate in parallel (**Fig. 33**).

## 7.1 Conclusions and Hypothesis

In summary, I have shown that PLCγ2 and PLD3 orthologs promote *Drosophila* glial engulfment of neuronal debris after injury. The role of sl can be explained by a compromised $Ca^{2+}$ response to injury and the elevated PIP2 levels at baseline seen in *sl* KD flies, attenuating the PIP2 dip observed in glia required for engulfment. These functions are likely to reduce the upregulation of Draper, needed to complete the engulfment process, leading to a partial delay in debris clearance. Together, I propose that $Ca^{2+}$ is released downstream of Draper through sl, during very early stages of glial cell activation, potentially triggering other events from cytoskeletal changes and migration to the site of injury. In cases of large amounts of debris leading to strong Draper signalling at the membrane, PI3K is activated and sl is phosphorylated by shark, leading to the metabolism of PIP2 into PIP3, IP3 and DAG. Draper is thereafter upregulated through STAT92E or other transcription factors promoting the completion of the engulfment process (**Fig. 33**). Pld3 is likely to behave downstream of PI3K activation, equally promoting similar processes. These alterations in cell activities could directly impact the clearance of damaged cells and Aβ accumulates. My findings agree largely with existing research in the area and unveil mechanistic insight into the role of PLCγ2 and PLD3 in glial function.

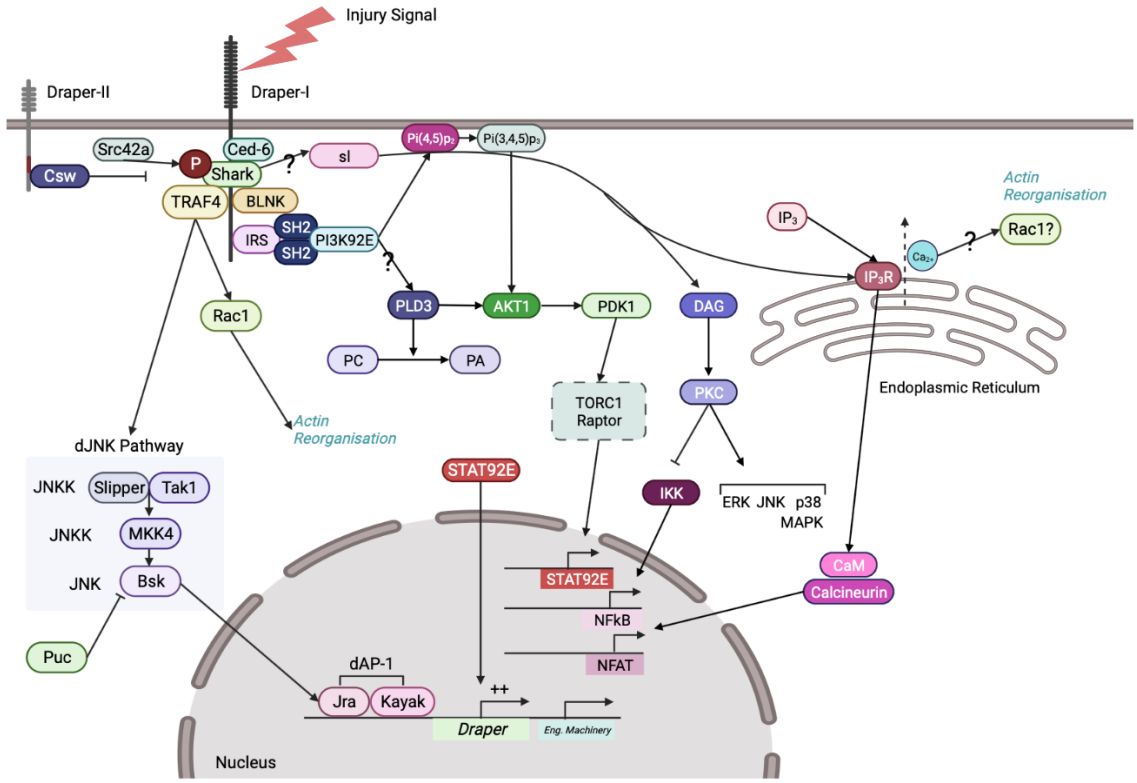


***Fig. 33. Proposed Mechanistic Diagram.*** *On the left is the outline of the activating Rac1 and JNK cascade, leading to the upregulation of engulfment machinery and Draper itself in response to injury. To the right the activation of sl and PI3K to initiate phosphoinositide signalling, $Ca^{2+}$ release from the ER and overlapping with Draper upregulation through STAT92E. Image made in ©BioRender - biorender.com.*

# 8 Supplementary Data

## 8.1 Confirmation of qPCR Primers

Traditional PCR and gel electrophoresis (**see Chapter 2**) confirmed the presence of single bands for each experimental primer set. *Pld3* was amplified using exon-spanning PLD3-1F/1R (**Lane 2**), and *sl* was amplified using exon-spanning SL-1F/R (**Lane 4**). demonstrating that these primers could be used in qPCR experiments (**Fig. S1**).

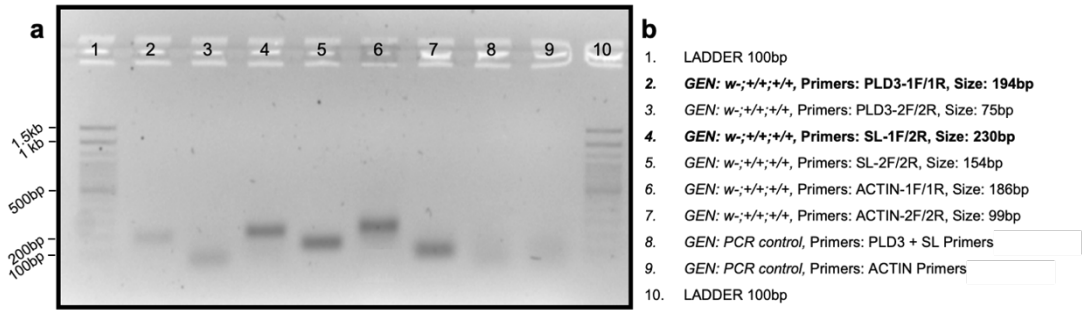


***Fig. S1. Exon-Spanning Primers Successfully Amplified Target Gene. a)*** *w- DNA was extracted and amplified via PCR and visualised through gel electrophoresis.* ***b)*** *To the right, a legend of the contents of each lane. Lane 2: Pld3 amplicon (size: 194bp) using exon-spanning primers PLD3-1F/1R. Lane 3: Pld3 amplicon (size: 75bp) using non-exon spanning primers PLD3-2F/2R. Lane 4: sl amplicon (size 230bp) using exon spanning primers SL-1F/R. Lane 5: sl amplicon (size: 154bp) using non-exon spanning primers SL-2F/R. Lanes 6-9: actin amplicon using actin-specific primers as controls.*

## 8.2 Tubulin-driven Pld3 RNAi Expression Led To Significant Gene Knockdown

To ensure *sl* and *Pld3* were effectively targeted and knocked down in my experimental flies, mRNA expression was quantified using qPCR. Lines were crossed to ;;*tub-GAL4* virgins to ensure maximum RNAi expression, facilitating detection during the assay. When comparing *sl* RNAis (III) (#32906) (**Fig. S2a**) and RNAi (IV) (#108593) (**Fig. S2b**) to their respective controls, no significant change was observed, in fact, expression levels seemed higher in KD lines. sl expression levels were significantly lower in RNAi (IV) compared to wildtype levels ($p < 0.0001$), suggesting this line led to gene knockdown (**Fig. S2c**). However, due to conflicting evidence in *sl* RNAi data, we investigated knockdown using a different assay (see **8.3**). *Pld3* expression, detected by qPCR, was significantly lower by 62% in *Pld3* RNAi (II) (#109798) heads ($p < 0.0001$) compared to the KK background (**Fig. S2d**). Equally, in *Pld3* RNAi (III) (#31122) heads, *Pld3* expression was significantly lower by 42% ($p < 0.0001$) compared to attP2 samples (**Fig. S2e**). Pld3 expression levels were significantly lower in both compared to wildtype expression levels ($p < 0.0001$), suggesting both lines led to gene knockdown (**Fig. S2f**).

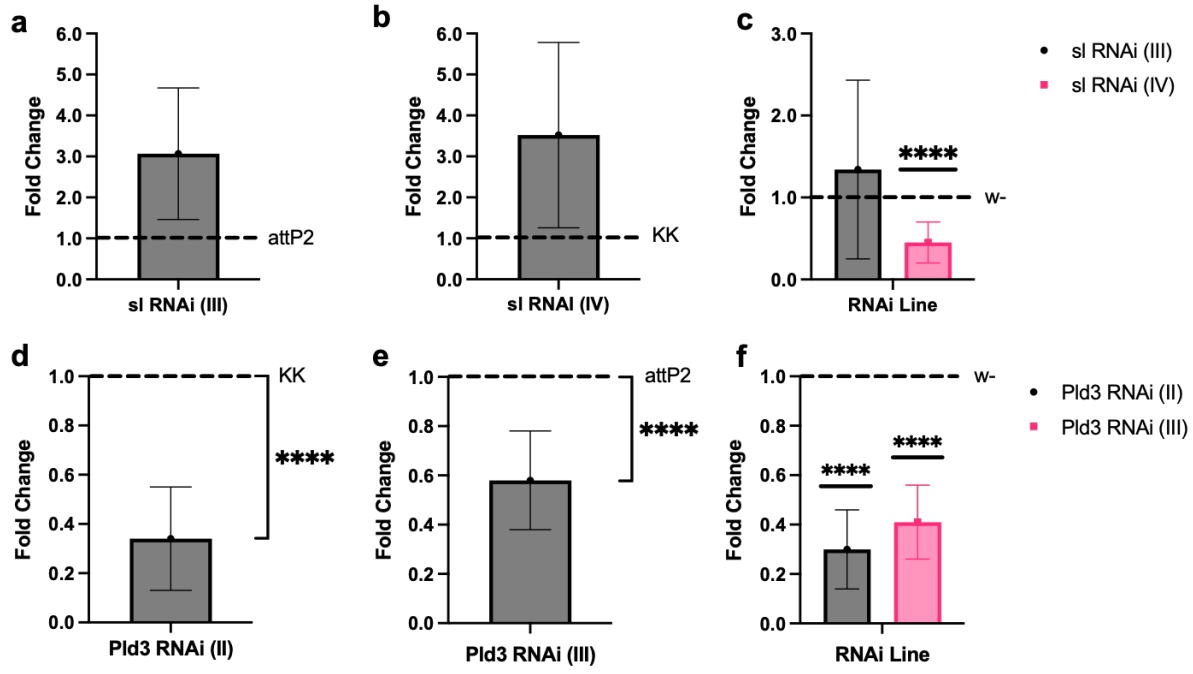

***Fig. S2. qPCR Revealed Significant Knockdown of Pld3****. **a)-c)** Expression was normalised to wildtype, KK and attP2 controls in sl RNAi (III) and (IV) respectively, and Pld3 RNAi (II) and (III). **a)** Shows the fold-change of sl expression in sl RNAi (III) samples compared to attP2 controls. **b)** Shows the fold-change of sl expression in sl RNAi (IV) samples compared to KK controls. **c)** Compares sl expression of both sl RNAi lines to wildtype control, sl RNAi (IV) yielded a stronger knockdown. **d)** Shows the fold-change decrease of Pld3 expression in Pld3 RNAi (II) samples compared to KK controls. **e)** Shows the fold-change decrease of Pld3 expression in Pld3 RNAi (III) samples compared to attP2 controls. **f)** Compares Pld3 expression of both Pld3 RNAi lines to wildtype control, Pld3 RNAi (II) yields a stronger knockdown.*

## 8.3 Tubulin-driven *sl* RNAi Expression Led To Significant Wing Size Reduction.

This data was acquired by collaborator Miss Eilish Mackinnon of the Peter's Group, DRI. With existing evidence suggesting *sl* regulates normal wing development (Mankidy et al. 2003), wing size was used as a readout for effective knockdown. *sl* RNAi lines were crossed to ;;*tub-GAL4* virgins and compared to *yw* controls. In parallel, crosses were compared to a *sl* CRIMIC mutant (#81213, BDSC), as a positive control. Comparing the mean area of wings across genotypes, demonstrated that expressing *sl* RNAi (I) (#108593) and *sl* RNAi (II) (#32906) led to smaller wings compared to *yw* controls (**Fig. S3a**). Statistical analysis revealed that the wings of flies expressing RNAi (I) were significantly smaller ($p<0.0001$) in both females (**Fig. S3b**) and males (**Fig. S3c**), which was also true for flies expressing RNAi (II) ($p<0.0001$). Wing area was comparable to sl CRIMIC data, suggesting knockdown was effective using both RNAis.

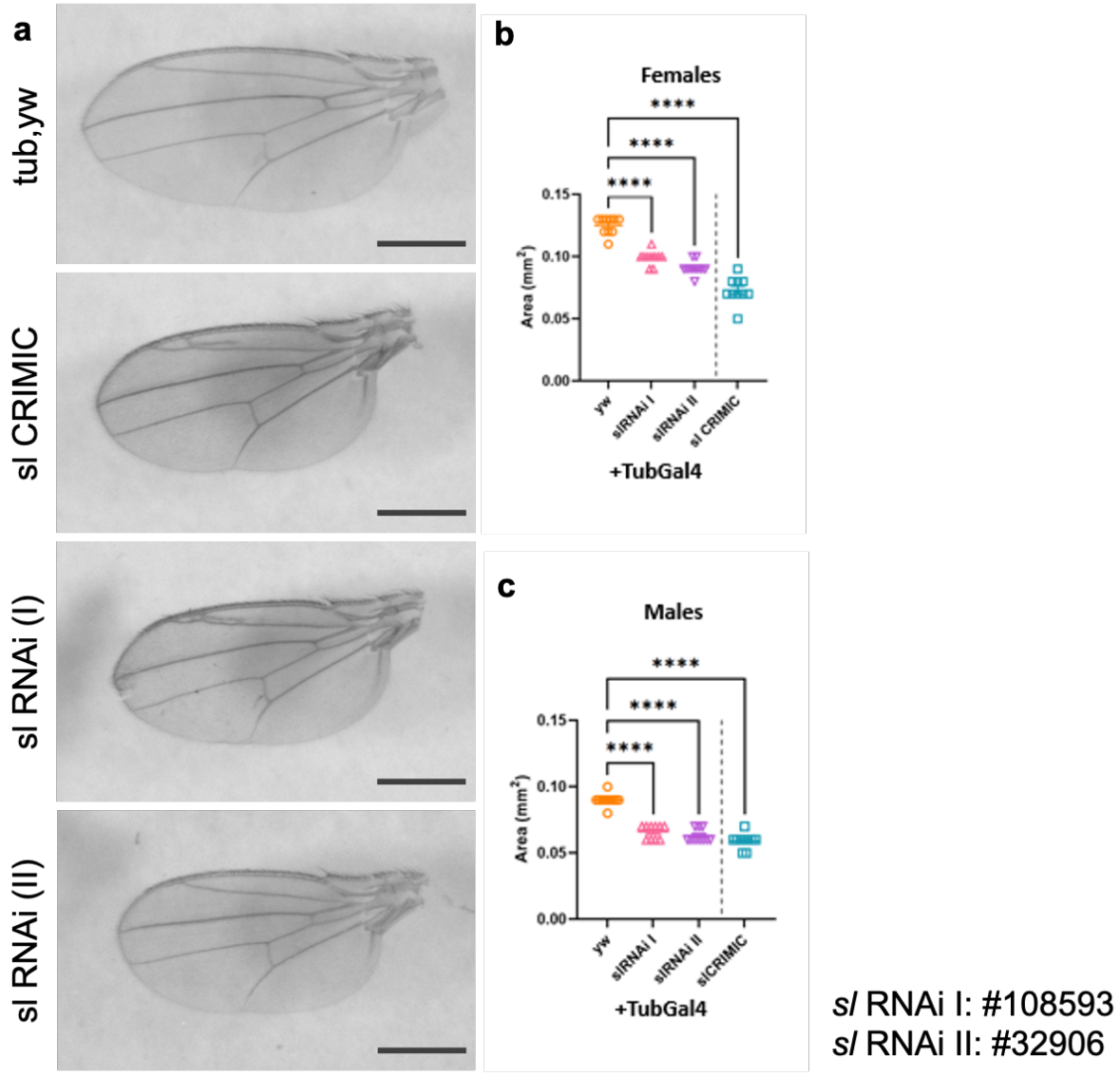


***Fig. S3. Knocking Down sl using RNAi Successfully Reduced Wing Size.*** *Figure adapted from E. Mackinnon.* ***a)*** *Representative images of wings across experimental lines.* ***b)*** *Quantification of wing area ($mm^2$) in female groups.* ***c)*** *Quantification of wing area ($mm^2$) in male groups. sl RNAi (II) (#32906) yielded a stronger knockdown. Statistical analysis was achieved through 1-Way ANOVA and MC tests. Graphs plotted with mean±S.E.M. and significance annotated; ****p<0.0001. n=20 wings per group. Scale bar = 0.5mm.*

## 8.4 Knocking Down *shark* Leads to an Engulfment Deficit

When knocking *shark* in a *LacZ* background, GFP-positive structures were visibly intact after injury, suggesting a stronger engulfment phenotype that *sl* KD alone (**Fig. S4a**). An unpaired t-test revealed that axon incidence did not go down after 5DPA (**Fig. S4b**), which was also the case for glomerulus recordings (**Fig. S4c**). Measuring fluorescence levels in neuronal structures suggested that mean GFP intensity did not reduce despite injury. An unpaired t-test comparing uninjured samples and after 5DPA found that data did not vary for axon GFP (**Fig. S4d**) or glomerulus GFP (**Fig. S4e**). Taken together, data would suggest that knocking down *shark* would be sufficient to drive an engulfment deficit, therefore data combining *shark* and *sl* KDs should be interpreted cautiously.

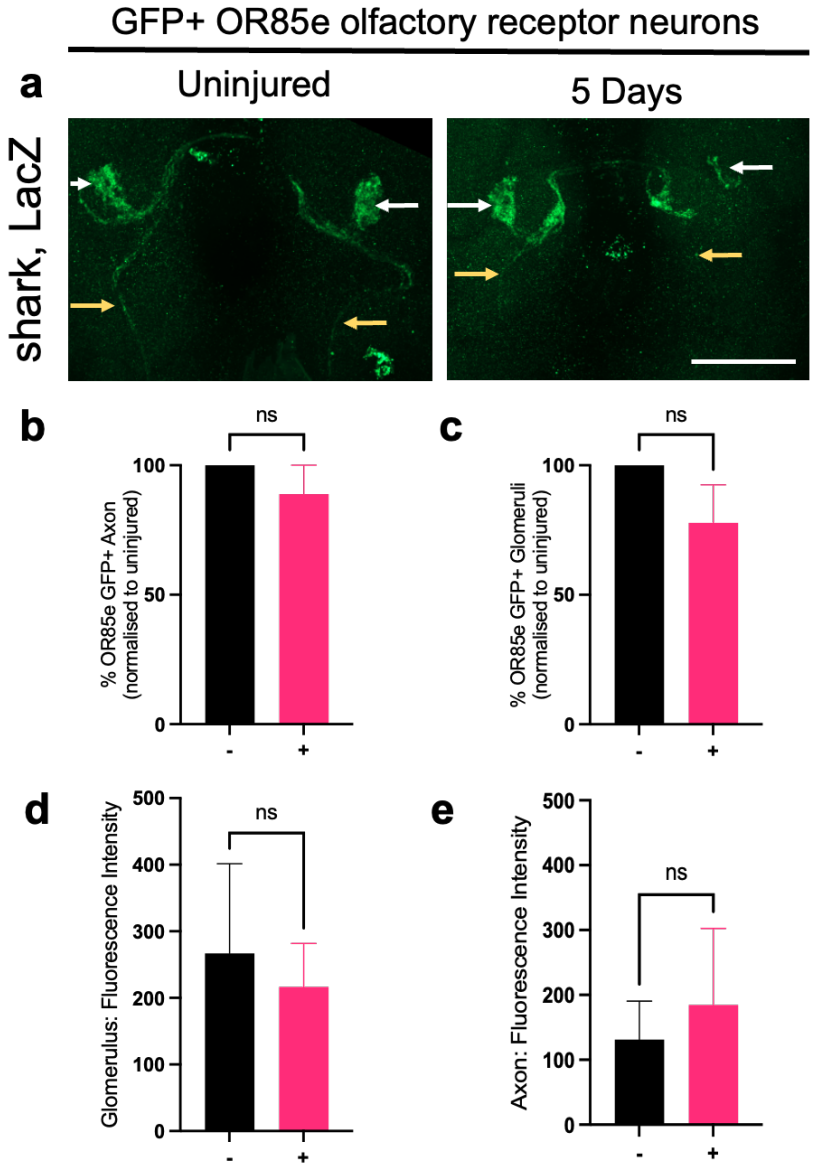


***Fig. S4. Knocking Down shark alongside LacZ Led to an Engulfment Deficit.*** ***a)*** *GFP-labelled maxillary ORN neurons before and 5 days after injury, showing axons (yellow arrows) and glomeruli (white arrows).* ***b)*** *Qualitative analysis of GFP+ debris in OR85e axons across experimental lines.* ***d)*** *Percentage of antennal lobes containing visible GFP+ OR85e glomeruli before and after injury.* ***e)*** *Quantitative analysis of GFP fluorescence in OR85e axons.* ***f)*** *Mean GFP fluorescence in OR85e glomeruli. Statistical analysis was achieved through an unpaired t-test. Graphs plotted with mean±S.E.M., with significance annotated; ns (not significant). n=7-10 brains per group. Scale bar = 50μm.*

## 8.5 Calcium Dynamics in *LacZ*-expressing Flies

GFP fluorescence was used as a readout for glial cytoplasmic $Ca^{2+}$ with comparisons drawn between uninjured groups at 1 min, 6hrs, 24hrs, 48hrs and 5-days after injury. Following the changes in GFP fluorescence associated with cytosolic $Ca^{2+}$, very low levels were observed before and after injury in LacZ-expressing flies (**Fig. 31a**). A 1-way ANOVA demonstrated that differences were not significant between time points (**Fig. 31b**). This data currently conflicts with *w-* data from **Chapter 6** and should be repeated for publication purposes.

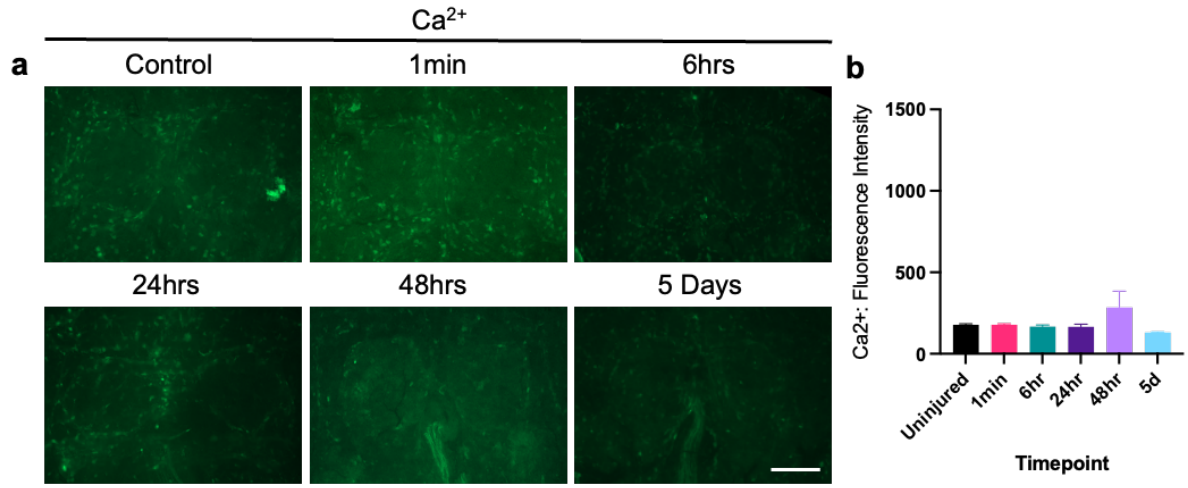


***Fig. S5. Cytosolic Calcium Changes in LacZ-expressing Flies. a)*** *Representative confocal z-stacks of GCAMP reporter brains before and 1min, 6hrs, 24hrs, 48hrs and 5 days after injury in LacZ flies.* ***b)*** *Quantification of $Ca^{2+}$-related fluorescence in antennal lobe ensheathing glia before and after antennal nerve injury. Statistical analysis was achieved through a 1-way ANOVA with Dunnett's MC tests. Graphs were plotted with mean±S.E.M., with significance annotated; ****p<0.0001, n=7-10 brains per group. Scale bar = 50μm.*

## 8.6 Novel Model System to Investigate Amyloid Engulfment in Drosophila

In order to investigate glial phenotypes in Aβ-expressing flies, I began to construct a dual binary system that combines GAL4 and QF2 genetic tools to target RNAi expression in glial poulations, whilst expressing Aβ in neurons. I optimised QF2 components by crossing *w-;;n-Syb-QF2/TM6b* (#51955, BDSC) to *;QUAS-Aβ* (#83347, BDSC) and aged flies for 1 week at 29°C. Brains were dissected and stained using α-Aβ(1-16) (803001, Biolegend). After only 1 week, Aβ accumulates were visible in the brain (**Fig. S6a**) and could be measured using two distinct analyses. An unpaired t-test revealed that mean fluorescence measurements of the central brain were higher in Aβ-expressing brains ($p<0.001$) compared to *w-* controls (**Fig. S6b**). Statistical analysis of a rough aggregate count also yielded significant results ($p<0.0001$) (**Fig. S6c**). This pilot data suggests that these tools would work in a binary model to measure amyloid-modifying phenotypes.

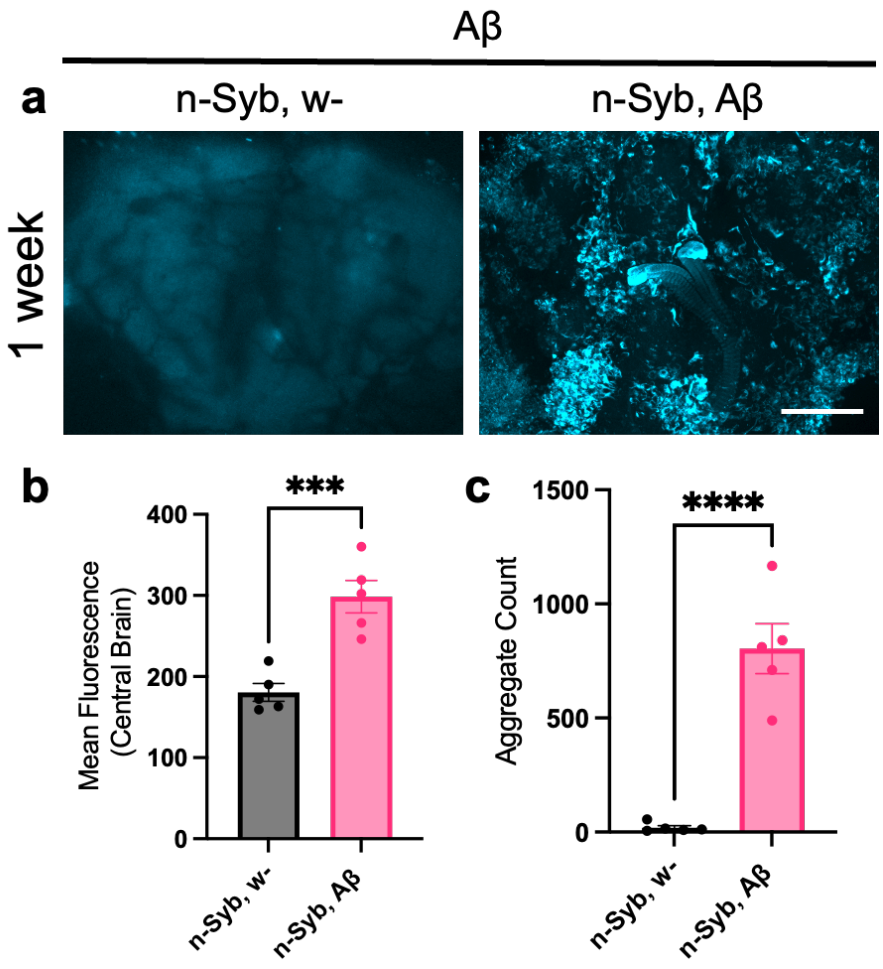

***Fig. S6. QF2-driven Aβ Expression Led to Quantifiable Pathology. a)*** *Representative confocal z-stacks of Aβ immunostained brains aged for 2 weeks in w- and Aβ-expressing flies.* ***b)*** *Quantification of Aβ-related fluorescence by mean fluorescence measurements of the central brain. c) Quantification of Aβ accumulates. Statistical analysis was achieved through an unpaired t-test. Graphs plotted with mean±S.E.M and significance annotated; ***p<0.001 and ****p<0.0001. n=5 brains per group. Scale bar = 50um.*

# Bibliography


- A, H., D, D., MW, K. and DW, M. 1989. Tau consists of a set of proteins with repeated C-terminal microtubule-binding domains and variable N-terminal domains. *Molecular and cellular biology* 9(4), pp. 1381–1388. Available at: https://pubmed.ncbi.nlm.nih.gov/2498649/ [Accessed: 13 July 2021].
- A, K. and JA, S. 2016. Vascular contributions to cognitive impairment, clinical Alzheimer's disease, and dementia in older persons. *Biochimica et biophysica acta* 1862(5), pp. 878–886. Available at: https://pubmed.ncbi.nlm.nih.gov/26769363/ [Accessed: 25 July 2021].
- A, M. et al. 2018. Pericyte degeneration causes white matter dysfunction in the mouse central nervous system. *Nature medicine* 24(3), pp. 326–337. Available at: https://pubmed.ncbi.nlm.nih.gov/29400711/ [Accessed: 25 July 2021].
- Abbott, A. 2018. Is "friendly fire" in the brain provoking Alzheimer's disease? news-feature. *Nature* 556(7702), pp. 426–428. doi: 10.1038/D41586-018-04930-7.
- *Addgene: Protocol - How to Run an Agarose Gel* [no date]. Available at: https://www.addgene.org/protocols/gel-electrophoresis/ [Accessed: 4 July 2022].
- *Aducanumab-avwa Injection: MedlinePlus Drug Information* [no date]. Available at: https://medlineplus.gov/druginfo/meds/a621033.html [Accessed: 22 June 2022].
- Afagh, A., Cummings, B.J., Cribbs, D.H., Cotman, C.W. and Tenner, A.J. 1996. Localization and cell association of C1q in Alzheimer's disease brain. *Experimental neurology* 138(1), pp. 22–32. Available at: https://pubmed.ncbi.nlm.nih.gov/8593893/ [Accessed: 20 June 2022].
- Aikawa, T., Holm, M.-L. and Kanekiyo, T. 2018. ABCA7 and Pathogenic Pathways of Alzheimer's Disease. *Brain sciences* 8(2). doi: 10.3390/brainsci8020027.
- AJ, H., TK, M., JA, J., AJ, C. and AR, G. 1989. The cholinergic pharmacology of tetrahydroaminoacridine in vivo and in vitro. *British journal of pharmacology* 98(1), pp. 79–86. Available at: https://pubmed.ncbi.nlm.nih.gov/2804555/ [Accessed: 25 July 2021].

- Alexander, A.G., Marfil, V. and Li, C. 2014. Use of Caenorhabditis elegans as a model to study Alzheimer's disease and other neurodegenerative diseases. *Frontiers in Genetics* 5(JUL). Available at: /pmc/articles/PMC4155875/ [Accessed: 22 June 2022].
- Allen, N.J. and Eroglu, C. 2017. Cell Biology of Astrocyte-Synapse Interactions. *Neuron* 96(3), pp. 697–708. Available at: https://pubmed.ncbi.nlm.nih.gov/29096081/ [Accessed: 20 June 2022].
- AM, P., GC, S., AW, P. and DM, B. 1988. Possible neurotransmitter basis of behavioral changes in Alzheimer's disease. *Annals of neurology* 23(6), pp. 616–620. Available at: https://pubmed.ncbi.nlm.nih.gov/2457353/ [Accessed: 25 July 2021].
- Andreone, B.J. et al. 2020. Alzheimer's-associated PLCγ2 is a signaling node required for both TREM2 function and the inflammatory response in human microglia. *Nature neuroscience* 23(8), pp. 927–938. Available at: https://pubmed.ncbi.nlm.nih.gov/32514138/ [Accessed: 25 April 2022].
- Anstey, K.J. et al. 2021. Association of sex differences in dementia risk factors with sex differences in memory decline in a population-based cohort spanning 20–76 years. *Scientific Reports 2021 11:1* 11(1), pp. 1–10. Available at: https://www.nature.com/articles/s41598-021-86397-7 [Accessed: 23 March 2022].
- Arancio, O. 2008. PIP2: a new key player in Alzheimer's disease. *Cellscience* 5(1), p. 44. Available at: /pmc/articles/PMC2890287/ [Accessed: 10 May 2022].
- Arcaro, A. and Guerreiro, A.S. 2007. The Phosphoinositide 3-Kinase Pathway in Human Cancer: Genetic Alterations and Therapeutic Implications. *Current Genomics* 8(5), p. 271. Available at: /pmc/articles/PMC2652403/ [Accessed: 29 April 2022].
- Arora, S. and Ligoxygakis, P. 2020. Beyond Host Defense: Deregulation of Drosophila Immunity and Age-Dependent Neurodegeneration. *Frontiers in immunology* 11. Available at: https://pubmed.ncbi.nlm.nih.gov/32774336/ [Accessed: 22 June 2022].
- Asteriti, S., Liu, C.H. and Hardie, R.C. 2017. Calcium signalling in Drosophila photoreceptors measured with GCaMP6f. *Cell Calcium* 65, p. 40. Available at: /pmc/articles/PMC5472182/ [Accessed: 9 May 2022].

- Atagi, Y. et al. 2015. Apolipoprotein E Is a Ligand for Triggering Receptor Expressed on Myeloid Cells 2 (TREM2). *The Journal of biological chemistry* 290(43), pp. 26043–26050. Available at: https://pubmed.ncbi.nlm.nih.gov/26374899/ [Accessed: 20 June 2022].
- Awasaki, T., Tatsumi, R., Takahashi, K., Arai, K., Nakanishi, Y., Ueda, R. and Ito, K. 2006. Essential role of the apoptotic cell engulfment genes draper and ced-6 in programmed axon pruning during Drosophila metamorphosis. *Neuron* 50(6), pp. 855–867. Available at: https://pubmed.ncbi.nlm.nih.gov/16772168/ [Accessed: 9 May 2022].
- Bachiller, S., Jiménez-Ferrer, I., Paulus, A., Yang, Y., Swanberg, M., Deierborg, T. and Boza-Serrano, A. 2018. Microglia in neurological diseases: A road map to brain-disease dependent-inflammatory response. *Frontiers in Cellular Neuroscience* 12, p. 488. doi: 10.3389/FNCEL.2018.00488/BIBTEX.
- Backman, L., Jones, S., Berger, A.-K., Laukka, E.J. and Small, B.J. 2004. Multiple cognitive deficits during the transition to Alzheimer's disease. *Journal of Internal Medicine* 256(3), pp. 195–204. doi: 10.1111/j.1365-2796.2004.01386.x.
- Baker, E. and Escott-Price, V. 2020. Polygenic Risk Scores in Alzheimer's Disease: Current Applications and Future Directions. *Frontiers in Digital Health* 2, p. 14. doi: 10.3389/FDGTH.2020.00014/BIBTEX.
- Bales, K.R. et al. 1999. Apolipoprotein E is essential for amyloid deposition in the APP(V717F) transgenic mouse model of Alzheimer's disease. *Proceedings of the National Academy of Sciences of the United States of America* 96(26), pp. 15233–15238. Available at: https://pubmed.ncbi.nlm.nih.gov/10611368/ [Accessed: 26 July 2022].
- Balla, T. 2013. Phosphoinositides: tiny lipids with giant impact on cell regulation. *Physiological reviews* 93(3), pp. 1019–1137. Available at: https://pubmed.ncbi.nlm.nih.gov/23899561/ [Accessed: 29 April 2022].
- Balla, T. and Catt, K.J. 1994. Phosphoinositides and calcium signaling New aspects and diverse functions in cell regulation. *Trends in endocrinology and metabolism: TEM* 5(6), pp. 250–255. Available at: https://pubmed.ncbi.nlm.nih.gov/18407216/ [Accessed: 10 May 2022].

- Ballard, C., Gauthier, S., Corbett, A., Brayne, C., Aarsland, D. and Jones, E. 2011. Alzheimer's disease. *The Lancet* 377(9770), pp. 1019–1031. doi: 10.1016/S0140-6736(10)61349-9.
- Barnett, K.C. and Kagan, J.C. 2020. Lipids that directly regulate innate immune signal transduction. *Innate Immunity* 26(1), p. 4. Available at: /pmc/articles/PMC6901815/ [Accessed: 21 June 2022].
- Beam, C.R., Kaneshiro, C., Jang, J.Y., Reynolds, C.A., Pedersen, N.L. and Gatz, M. 2018. Differences Between Women and Men in Incidence Rates of Dementia and Alzheimer's Disease. *Journal of Alzheimer's disease : JAD* 64(4), p. 1077. Available at: /pmc/articles/PMC6226313/ [Accessed: 23 March 2022].
- Beech, D.J., Bahnasi, Y.M., Dedman, A.M. and AL-Shawaf, E. 2009. TRPC channel lipid specificity and mechanisms of lipid regulation. *Cell Calcium* 45(6), p. 583. Available at: /pmc/articles/PMC3878645/ [Accessed: 26 May 2022].
- Beharry, C., Alaniz, M.E. and Alonso, A.D.C. 2013. Expression of Alzheimer-like pathological human tau induces a behavioral motor and olfactory learning deficit in Drosophila melanogaster. *Journal of Alzheimer's disease : JAD* 37(3), pp. 539–550. Available at: https://pubmed.ncbi.nlm.nih.gov/23948901/ [Accessed: 22 June 2022].
- Bekris, L.M., Yu, C.-E., Bird, T.D. and Tsuang, D.W. 2010. Genetics of Alzheimer Disease. *Journal of geriatric psychiatry and neurology* 23(4), p. 213. Available at: /pmc/articles/PMC3044597/ [Accessed: 12 July 2021].
- Bellenguez, C. et al. 2017. Contribution to Alzheimer's disease risk of rare variants in TREM2, SORL1, and ABCA7 in 1779 cases and 1273 controls. *Neurobiology of aging* 59, pp. 220.e1-220.e9. Available at: https://pubmed.ncbi.nlm.nih.gov/28789839/ [Accessed: 12 June 2022].
- Bellenguez, C. et al. 2022. New insights into the genetic etiology of Alzheimer's disease and related dementias. *Nature Genetics 2022* , pp. 1–25. Available at: https://www.nature.com/articles/s41588-022-01024-z [Accessed: 12 April 2022].
- Bellenguez, C., Grenier-Boley, B. and Lambert, J.C. 2020. Genetics of Alzheimer's disease: where we are, and where we are going. *Current opinion in neurobiology* 61, pp. 40–48. Available at: https://pubmed.ncbi.nlm.nih.gov/31863938/ [Accessed: 2 April 2022].

- Belmonte, R.L., Corbally, M.K., Duneau, D.F. and Regan, J.C. 2020. Sexual Dimorphisms in Innate Immunity and Responses to Infection in Drosophila melanogaster. *Frontiers in Immunology* 10, p. 3075. doi: 10.3389/FIMMU.2019.03075/BIBTEX.
- Benarroch, E.E. 2013. Microglia: Multiple roles in surveillance, circuit shaping, and response to injury. *Neurology* 81(12), pp. 1079–1088. Available at: https://pubmed.ncbi.nlm.nih.gov/23946308/ [Accessed: 14 June 2022].
- Berridge, M.J. 1993. Inositol trisphosphate and calcium signalling. *Nature 1993 361:6410* 361(6410), pp. 315–325. Available at: https://www.nature.com/articles/361315a0 [Accessed: 26 May 2022].
- Bertram, L. and Tanzi, R.E. 2019. Alzheimer disease risk genes: 29 and counting. *Nature Reviews Neurology* 15(4), pp. 191–192. Available at: http://www.nature.com/articles/s41582-019-0158-4 [Accessed: 28 June 2019].
- Bezman, N. and Koretzky, G.A. 2007. Compartmentalization of ITAM and integrin signaling by adapter molecules. *Immunological reviews* 218(1), pp. 9–28. Available at: https://pubmed.ncbi.nlm.nih.gov/17624941/ [Accessed: 10 May 2022].
- Bilen, J. and Bonini, N.M. 2005. *Drosophila* as a Model for Human Neurodegenerative Disease. *Annual Review of Genetics* 39(1), pp. 153–171. doi: 10.1146/annurev.genet.39.110304.095804.
- Billings, L.M., Oddo, S., Green, K.N., McGaugh, J.L. and LaFerla, F.M. 2005. Intraneuronal Abeta causes the onset of early Alzheimer's disease-related cognitive deficits in transgenic mice. *Neuron* 45(5), pp. 675–688. Available at: https://pubmed.ncbi.nlm.nih.gov/15748844/ [Accessed: 22 June 2022].
- Blanco-Luquin, I. et al. 2018. PLD3 epigenetic changes in the hippocampus of Alzheimer's disease. *Clinical Epigenetics* 10(1). Available at: /pmc/articles/PMC6134774/ [Accessed: 13 April 2022].
- Block, M.L., Zecca, L. and Hong, J.-S. 2007. Microglia-mediated neurotoxicity: uncovering the molecular mechanisms. *Nature Reviews Neuroscience* 8(1), pp. 57–69. Available at: http://www.ncbi.nlm.nih.gov/pubmed/17180163 [Accessed: 16 January 2019].

- Blurton-Jones, M. and LaFerla, F. 2006. Pathways by which Abeta facilitates tau pathology. *Current Alzheimer research* 3(5), pp. 437–448. Available at: https://pubmed.ncbi.nlm.nih.gov/17168643/ [Accessed: 22 June 2022].
- Bohdanowicz, M. and Grinstein, S. 2013. Role of phospholipids in endocytosis, phagocytosis, and macropinocytosis. *Physiological Reviews* 93(1), pp. 69–106. Available at: https://journals.physiology.org/doi/full/10.1152/physrev.00002.2012 [Accessed: 29 April 2022].
- Boisvert, M.M., Erikson, G.A., Shokhirev, M.N. and Allen, N.J. 2018. The Aging Astrocyte Transcriptome from Multiple Regions of the Mouse Brain. *Cell reports* 22(1), pp. 269–285. Available at: https://pubmed.ncbi.nlm.nih.gov/29298427/ [Accessed: 7 July 2022].
- Bolmont, T. et al. 2008. Dynamics of the microglial/amyloid interaction indicate a role in plaque maintenance. *The Journal of neuroscience : the official journal of the Society for Neuroscience* 28(16), pp. 4283–4292. Available at: https://pubmed.ncbi.nlm.nih.gov/18417708/ [Accessed: 20 June 2022].
- Bonham, L.W., Sirkis, D.W. and Yokoyama, J.S. 2019. The transcriptional landscape of microglial genes in aging and neurodegenerative disease. *Frontiers in Immunology* 10(JUN), p. 1170. doi: 10.3389/FIMMU.2019.01170/BIBTEX.
- Borchelt, D.R. et al. 1996. Familial Alzheimer's disease-linked presenilin 1 variants elevate Abeta1-42/1-40 ratio in vitro and in vivo. *Neuron* 17(5), pp. 1005–13.
- Bossers, K. et al. 2010. Concerted changes in transcripts in the prefrontal cortex precede neuropathology in Alzheimer's disease. *Brain : a journal of neurology* 133(Pt 12), pp. 3699–3723. Available at: https://pubmed.ncbi.nlm.nih.gov/20889584/ [Accessed: 26 July 2022].
- Botelho, R.J. et al. 2000. Localized Biphasic Changes in Phosphatidylinositol-4,5-Bisphosphate at Sites of Phagocytosis. *Journal of Cell Biology* 151(7), pp. 1353–1368. Available at: http://www.jcb.org/cgi/content/full/151/7/1353 [Accessed: 27 April 2022].
- Bracho, H. and Orkand, R.K. 1972. Neuron-glia interaction: dependence on temperature. *Brain Research* 36(2), pp. 416–419. doi: 10.1016/0006-8993(72)90747-0.

- Bramer, W.M., de Jonge, G.B., Rethlefsen, M.L., Mast, F. and Kleijnen, J. 2018. A systematic approach to searching: An efficient and complete method to develop literature searches. *Journal of the Medical Library Association* 106(4), pp. 531–541. Available at: /pmc/articles/PMC6148622/?report=abstract [Accessed: 22 June 2020].
- Brand, A.H. and Perrimon, N. 1993. Targeted gene expression as a means of altering cell fates and generating dominant phenotypes. *Development (Cambridge, England)* 118(2), pp. 401–15. Available at: http://www.ncbi.nlm.nih.gov/pubmed/8223268 [Accessed: 26 March 2018].
- Breijyeh, Z. and Karaman, R. 2020. Comprehensive Review on Alzheimer's Disease: Causes and Treatment. *Molecules (Basel, Switzerland)* 25(24). Available at: https://pubmed.ncbi.nlm.nih.gov/33302541/ [Accessed: 6 June 2022].
- Brink, D.L., Gilbert, M., Xie, X., Petley-Ragan, L. and Auld, V.J. 2012. Glial Processes at the Drosophila Larval Neuromuscular Junction Match Synaptic Growth. *PLOS ONE* 7(5), p. e37876. Available at: https://journals.plos.org/plosone/article?id=10.1371/journal.pone.0037876 [Accessed: 24 March 2022].
- Britton, J.S., Lockwood, W.K., Li, L., Cohen, S.M. and Edgar, B.A. 2002. Drosophila's Insulin/PI3-Kinase Pathway Coordinates Cellular Metabolism with Nutritional Conditions. *Developmental Cell* 2(2), pp. 239–249. doi: 10.1016/S1534-5807(02)00117-X.
- Brown, F.D., Rozelle, A.L., Yin, H.L., Balla, T. and Donaldson, J.G. 2001. Phosphatidylinositol 4,5-bisphosphate and Arf6-regulated membrane traffic. *The Journal of cell biology* 154(5), pp. 1007–1017. Available at: https://pubmed.ncbi.nlm.nih.gov/11535619/ [Accessed: 26 May 2022].
- Brown, G.C. and Neher, J.J. 2014. Microglial phagocytosis of live neurons. *Nature Reviews Neuroscience 2014 15:4* 15(4), pp. 209–216. Available at: https://www.nature.com/articles/nrn3710 [Accessed: 21 June 2022].
- Brunden, K.R., Trojanowski, J.Q. and Lee, V.M.Y. 2009. Advances in tau-focused drug discovery for Alzheimer's disease and related tauopathies. *Nature Reviews Drug Discovery 2009 8:10* 8(10), pp. 783–793. Available at: https://www.nature.com/articles/nrd2959 [Accessed: 10 June 2022].

- Bruntz, R.C., Lindsley, C.W. and Brown, H.A. 2014. Phospholipase D Signaling Pathways and Phosphatidic Acid as Therapeutic Targets in Cancer. *Pharmacological Reviews* 66(4), p. 1033. Available at: /pmc/articles/PMC4180337/ [Accessed: 13 April 2022].
- Buisman, H.P. et al. 1988. Extracellular ATP induces a large nonselective conductance in macrophage plasma membranes. *Proceedings of the National Academy of Sciences of the United States of America* 85(21), pp. 7988–7992. doi: 10.1073/pnas.85.21.7988.
- Bunney, T.D. and Katan, M. 2010. Phosphoinositide signalling in cancer: Beyond PI3K and PTEN. *Nature Reviews Cancer* 10(5), pp. 342–352. doi: 10.1038/nrc2842.
- Burns, A. and Iliffe, S. 2009. Alzheimer's disease. *BMJ (Clinical research ed.)* 338, p. b158. doi: 10.1136/BMJ.B158.
- Burr, A.A., Tsou, W.L., Ristic, G. and Todi, S. v. 2014. Using Membrane-Targeted Green Fluorescent Protein To Monitor Neurotoxic Protein-Dependent Degeneration of Drosophila Eyes. *Journal of neuroscience research* 92(9), p. 1100. Available at: /pmc/articles/PMC4144675/ [Accessed: 22 June 2022].
- Bushong, E.A., Martone, M.E., Jones, Y.Z. and Ellisman, M.H. 2002. Protoplasmic astrocytes in CA1 stratum radiatum occupy separate anatomical domains. *The Journal of neuroscience : the official journal of the Society for Neuroscience* 22(1), pp. 183–192. Available at: https://pubmed.ncbi.nlm.nih.gov/11756501/ [Accessed: 26 July 2022].
- Caccamo, A., Oddo, S., Billings, L.M., Green, K.N., Martinez-Coria, H., Fisher, A. and LaFerla, F.M. 2006. M1 receptors play a central role in modulating AD-like pathology in transgenic mice. *Neuron* 49(5), pp. 671–682. Available at: https://pubmed.ncbi.nlm.nih.gov/16504943/ [Accessed: 11 June 2022].
- Candlish, M. and Hefendehl, J.K. 2021. Microglia Phenotypes Converge in Aging and Neurodegenerative Disease. *Frontiers in Neurology* 12, p. 660720. Available at: /pmc/articles/PMC8133315/ [Accessed: 25 July 2022].
- Cappel, C., Gonzalez, A.C. and Damme, M. 2021. Quantification and characterization of the 5′ exonuclease activity of the lysosomal nuclease PLD3 by a novel cell-based assay. *The Journal of Biological Chemistry* 296, p. 100152. Available at: /pmc/articles/PMC7857491/ [Accessed: 25 April 2022].

- Casares, D., Escribá, P. v. and Rosselló, C.A. 2019. Membrane Lipid Composition: Effect on Membrane and Organelle Structure, Function and Compartmentalization and Therapeutic Avenues. *International Journal of Molecular Sciences* 20(9). Available at: /pmc/articles/PMC6540057/ [Accessed: 18 July 2022].
- Castle, S.C. 2000. Impact of age-related immune dysfunction on risk of infections. *Zeitschrift fur Gerontologie und Geriatrie* 33(5), pp. 341–349. Available at: https://pubmed.ncbi.nlm.nih.gov/11130187/ [Accessed: 25 July 2022].
- Castro, B.M. de et al. 2009. The Vesicular Acetylcholine Transporter Is Required for Neuromuscular Development and Function. *Molecular and Cellular Biology* 29(19), p. 5238. Available at: /pmc/articles/PMC2747982/ [Accessed: 11 June 2022].
- Cauvin, C. and Echard, A. 2015. Phosphoinositides: Lipids with informative heads and mastermind functions in cell division. *Biochimica et biophysica acta* 1851(6), pp. 832–843. Available at: https://pubmed.ncbi.nlm.nih.gov/25449648/ [Accessed: 29 April 2022].
- Chakrabarty, P. et al. 2015. IL-10 alters immunoproteostasis in APP mice, increasing plaque burden and worsening cognitive behavior. *Neuron* 85(3), pp. 519–533. Available at: https://pubmed.ncbi.nlm.nih.gov/25619653/ [Accessed: 15 June 2022].
- Chapuis, J. et al. 2017. Genome-wide, high-content siRNA screening identifies the Alzheimer's genetic risk factor FERMT2 as a major modulator of APP metabolism. *Acta Neuropathologica* 133(6), pp. 955–966. doi: 10.1007/s00401-016-1652-z.
- Chen, G.F., Xu, T.H., Yan, Y., Zhou, Y.R., Jiang, Y., Melcher, K. and Xu, H.E. 2017. Amyloid beta: structure, biology and structure-based therapeutic development. *Acta Pharmacologica Sinica 2017 38:9* 38(9), pp. 1205–1235. Available at: https://www.nature.com/articles/aps201728 [Accessed: 8 June 2022].
- Chen, X., Hu, Y., Cao, Z., Liu, Q. and Cheng, Y. 2018. Cerebrospinal fluid inflammatory cytokine aberrations in Alzheimer's disease, Parkinson's disease and amyotrophic lateral sclerosis: A systematic review and meta-analysis.

*Frontiers in Immunology* 9(SEP), p. 2122. Available at: /pmc/articles/PMC6156158/ [Accessed: 20 June 2022].

- Chen, X. and Yan, S. Du 2006. Mitochondrial Aβ A potential cause of metabolic dysfunction in Alzheimer's disease. *IUBMB Life* 58(12), pp. 686–694. doi: 10.1080/15216540601047767.
- Cheng, X.T., Xie, Y.X., Zhou, B., Huang, N., Farfel-Becker, T. and Sheng, Z.H. 2018. Characterization of LAMP1-labeled nondegradative lysosomal and endocytic compartments in neurons. *The Journal of Cell Biology* 217(9), p. 3127. Available at: /pmc/articles/PMC6123004/ [Accessed: 19 May 2022].
- Cheng-Hathaway, P.J. et al. 2018. The Trem2 R47H variant confers loss-of-function-like phenotypes in Alzheimer's disease. *Molecular Neurodegeneration* 13(1). Available at: /pmc/articles/PMC5984804/ [Accessed: 15 June 2022].
- Cheruiyot, A., Lee, J., Gao, F. and Ahmad, S.T. 2014. Expression of mutant CHMP2B, an ESCRT-III component involved in frontotemporal dementia, causes eye deformities due to Notch misregulation in *Drosophila*. *The FASEB Journal* 28(2), pp. 667–675. Available at: https://onlinelibrary.wiley.com/doi/abs/10.1096/fj.13-234138 [Accessed: 3 May 2020].
- Chew, H., Solomon, V.A. and Fonteh, A.N. 2020. Involvement of Lipids in Alzheimer's Disease Pathology and Potential Therapies. *Frontiers in Physiology* 11, p. 598. doi: 10.3389/FPHYS.2020.00598/BIBTEX.
- Chiang, C.Y., Veckman, V., Limmer, K. and David, M. 2012. Phospholipase Cγ-2 and intracellular calcium are required for lipopolysaccharide-induced toll-like receptor 4 (TLR4) endocytosis and interferon regulatory factor 3 (IRF3) activation. *Journal of Biological Chemistry* 287(6), pp. 3704–3709. Available at: http://www.jbc.org/article/S0021925820481803/fulltext [Accessed: 10 May 2022].
- Chin, M.L. and Mlodzik, M. 2013. The drosophila selectin furrowed mediates intercellular planar cell polarity interactions via frizzled stabilization. *Developmental Cell* 26(5), pp. 455–468. doi: 10.1016/j.devcel.2013.07.006.
- Choi, O.H., Kim, J.H. and Kinet, J.P. 1996. Calcium mobilization via sphingosine kinase in signalling by the Fc epsilon RI antigen receptor. *Nature* 380(6575), pp. 634–636. Available at: https://pubmed.ncbi.nlm.nih.gov/8602265/ [Accessed: 26 May 2022].

- Choleris, E., Galea, L.A.M., Sohrabji, F. and Frick, K.M. 2018. Sex differences in the brain: Implications for behavioral and biomedical research. *Neuroscience and biobehavioral reviews* 85, p. 126. Available at: /pmc/articles/PMC5751942/ [Accessed: 23 March 2022].
- Chuang, F.Y.S., Sassaroli, M. and Unkeless, J.C. 2000. Convergence of Fc gamma receptor IIA and Fc gamma receptor IIIB signaling pathways in human neutrophils. *Journal of immunology (Baltimore, Md. : 1950)* 164(1), pp. 350–360. Available at: https://pubmed.ncbi.nlm.nih.gov/10605030/ [Accessed: 26 May 2022].
- Chung, W.-S. et al. 2013. Astrocytes mediate synapse elimination through MEGF10 and MERTK pathways. *Nature* 504(7480), pp. 394–400. Available at: http://www.nature.com/articles/nature12776 [Accessed: 27 February 2019].
- Chung, W.S. et al. 2016. Novel allele-dependent role for APOE in controlling the rate of synapse pruning by astrocytes. *Proceedings of the National Academy of Sciences of the United States of America* 113(36), pp. 10186–10191. Available at: https://pubmed.ncbi.nlm.nih.gov/27559087/ [Accessed: 20 June 2022].
- Chung, W.S., Allen, N.J. and Eroglu, C. 2015. Astrocytes Control Synapse Formation, Function, and Elimination. *Cold Spring Harbor perspectives in biology* 7(9). Available at: https://pubmed.ncbi.nlm.nih.gov/25663667/ [Accessed: 20 June 2022].
- Claes, C. et al. 2022. The P522R protective variant of PLCG2 promotes the expression of antigen presentation genes by human microglia in an Alzheimer's disease mouse model. *Alzheimer's & dementia : the journal of the Alzheimer's Association*. Available at: https://pubmed.ncbi.nlm.nih.gov/35142046/ [Accessed: 26 July 2022].
- Clarke, L.E., Liddelow, S.A., Chakraborty, C., Münch, A.E., Heiman, M. and Barres, B.A. 2018. Normal aging induces A1-like astrocyte reactivity. *Proceedings of the National Academy of Sciences of the United States of America* 115(8), pp. E1896–E1905. Available at: www.pnas.org/cgi/doi/10.1073/pnas.1800165115 [Accessed: 7 July 2022].
- Clayton, K.A., van Enoo, A.A. and Ikezu, T. 2017. Alzheimer's Disease: The Role of Microglia in Brain Homeostasis and Proteopathy. *Frontiers in neuroscience* 11,

p. 680. Available at: http://www.ncbi.nlm.nih.gov/pubmed/29311768 [Accessed: 15 November 2018].

- Collins, M. et al. 2020. Frontiers in Climate Predictions and Projections. *Frontiers in Climate* 2, p. 8. doi: 10.3389/FCLIM.2020.571245/BIBTEX.
- Condello, C., Yuan, P., Schain, A. and Grutzendler, J. 2015. Microglia constitute a barrier that prevents neurotoxic protofibrillar Aβ42 hotspots around plaques. *Nature Communications 2015 6:1* 6(1), pp. 1–14. Available at: https://www.nature.com/articles/ncomms7176 [Accessed: 20 June 2022].
- Corbin, J.A., Dirkx, R.A. and Falke, J.J. 2004. GRP1 Pleckstrin Homology Domain: Activation Parameters and Novel Search Mechanism for Rare Target Lipid. *Biochemistry* 43(51), p. 16161. Available at: /pmc/articles/PMC3625374/ [Accessed: 29 April 2022].
- Corder, E. et al. 1993. Gene dose of apolipoprotein E type 4 allele and the risk of Alzheimer's disease in late onset families. *Science* 261(5123), pp. 921–923. Available at: http://www.sciencemag.org/cgi/doi/10.1126/science.8346443 [Accessed: 18 June 2019].
- Couto, A., Alenius, M. and Dickson, B.J. 2005. Molecular, anatomical, and functional organization of the Drosophila olfactory system. *Current biology : CB* 15(17), pp. 1535–47. doi: 10.1016/j.cub.2005.07.034.
- Cox, D., Tseng, C.C., Bjekic, G. and Greenberg, S. 1999. A requirement for phosphatidylinositol 3-kinase in pseudopod extension. *The Journal of biological chemistry* 274(3), pp. 1240–1247. Available at: https://pubmed.ncbi.nlm.nih.gov/9880492/ [Accessed: 10 May 2022].
- CP, C. et al. 1996. Presynaptic serotonergic markers in community-acquired cases of Alzheimer's disease: correlations with depression and neuroleptic medication. *Journal of neurochemistry* 66(4), pp. 1592–1598. Available at: https://pubmed.ncbi.nlm.nih.gov/8627315/ [Accessed: 25 July 2021].
- Craig, M.L., Waitumbi, J.N. and Taylor, R.P. 2005. Processing of C3b-opsonized immune complexes bound to non-complement receptor 1 (CR1) sites on red cells: phagocytosis, transfer, and associations with CR1. *Journal of immunology (Baltimore, Md. : 1950)* 174(5), pp. 3059–3066. Available at: https://pubmed.ncbi.nlm.nih.gov/15728520/ [Accessed: 20 June 2022].

- Crocker, P.R. and Redelinghuys, P. 2008. Siglecs as positive and negative regulators of the immune system. *Biochemical Society transactions* 36(Pt 6), pp. 1467–1471. Available at: https://pubmed.ncbi.nlm.nih.gov/19021577/ [Accessed: 14 June 2022].
- Crowther, D.C. et al. 2005. Intraneuronal Aβ, non-amyloid aggregates and neurodegeneration in a Drosophila model of Alzheimer's disease. *Neuroscience* 132(1), pp. 123–135. doi: 10.1016/j.neuroscience.2004.12.025.
- Cruchaga, C. et al. 2014. Rare coding variants in the phospholipase D3 gene confer risk for Alzheimer's disease. *Nature* 505(7484), pp. 550–554. Available at: https://pubmed.ncbi.nlm.nih.gov/24336208/ [Accessed: 2 April 2022].
- CT, W. et al. 2016. Genome-wide DNA methylation profiling in the superior temporal gyrus reveals epigenetic signatures associated with Alzheimer's disease. *Genome medicine* 8(1). Available at: https://pubmed.ncbi.nlm.nih.gov/26803900/ [Accessed: 12 July 2021].
- Cuddy, L.K. et al. 2020. Aβ-accelerated neurodegeneration caused by Alzheimer's-associated ACE variant R1279Q is rescued by angiotensin system inhibition in mice. *Science Translational Medicine* 12(563). Available at: https://stm.sciencemag.org/content/12/563/eaaz2541 [Accessed: 6 May 2021].
- Cuttell, L. et al. 2008. Undertaker, a Drosophila Junctophilin, links Draper-mediated phagocytosis and calcium homeostasis. *Cell* 135(3), pp. 524–534. Available at: https://pubmed.ncbi.nlm.nih.gov/18984163/ [Accessed: 2 April 2022].
- Cuyvers, E. and Sleegers, K. 2016. Genetic variations underlying Alzheimer's disease: evidence from genome-wide association studies and beyond. *The Lancet. Neurology* 15(8), pp. 857–868. Available at: https://pubmed.ncbi.nlm.nih.gov/27302364/ [Accessed: 12 June 2022].
- D, P., N, P., A, D., A, Q., R, S. and M, M. 2004. Impaired angiogenesis in a transgenic mouse model of cerebral amyloidosis. *Neuroscience letters* 366(1), pp. 80–85. Available at: https://pubmed.ncbi.nlm.nih.gov/15265595/ [Accessed: 25 July 2021].
- Dai, L., Kloog, I., Coull, B.A., Sparrow, D., Spiro, A., Vokonas, P.S. and Schwartz, J.D. 2016. Cognitive Function and Short-Term Exposure to Residential Air Temperature: A Repeated Measures Study Based on Spatiotemporal

Estimates of Temperature. *Environmental research* 150, p. 446. Available at: /pmc/articles/PMC5003630/ [Accessed: 25 July 2022].

- Damani, M.R., Zhao, L., Fontainhas, A.M., Amaral, J., Fariss, R.N. and Wong, W.T. 2011. Age-related alterations in the dynamic behavior of microglia. *Aging Cell* 10(2), pp. 263–276. Available at: https://onlinelibrary.wiley.com/doi/full/10.1111/j.1474-9726.2010.00660.x [Accessed: 9 April 2022].
- Danciu, T.E., Adam, R.M., Naruse, K., Freeman, M.R. and Hauschka, P. v. 2003. Calcium regulates the PI3K-Akt pathway in stretched osteoblasts. *FEBS Letters* 536(1–3), pp. 193–197. doi: 10.1016/S0014-5793(03)00055-3.
- D'Andrea, M.R., Cole, G.M. and Ard, M.D. 2004. The microglial phagocytic role with specific plaque types in the Alzheimer disease brain. *Neurobiology of aging* 25(5), pp. 675–683. Available at: https://pubmed.ncbi.nlm.nih.gov/15172747/ [Accessed: 2 April 2022].
- Darmanis, S. et al. 2015. A survey of human brain transcriptome diversity at the single cell level. *Proceedings of the National Academy of Sciences of the United States of America* 112(23), pp. 7285–7290. Available at: https://pubmed.ncbi.nlm.nih.gov/26060301/ [Accessed: 15 June 2022].
- Daws, M.R., Sullam, P.M., Niemi, E.C., Chen, T.T., Tchao, N.K. and Seaman, W.E. 2003. Pattern recognition by TREM-2: binding of anionic ligands. *Journal of immunology (Baltimore, Md. : 1950)* 171(2), pp. 594–599. Available at: https://pubmed.ncbi.nlm.nih.gov/12847223/ [Accessed: 15 June 2022].
- Dawson, G. 2015. Measuring Brain Lipids. *Biochimica et biophysica acta* 1851(8), p. 1026. Available at: /pmc/articles/PMC4457555/ [Accessed: 21 June 2022].
- de Jager, P.L. et al. 2014. Alzheimer's disease: Early alterations in brain DNA methylation at ANK1, BIN1, RHBDF2 and other loci. *Nature Neuroscience* 17(9), pp. 1156–1163. Available at: /pmc/articles/PMC4292795/?report=abstract [Accessed: 23 June 2020].
- de Roeck, A., van Broeckhoven, C. and Sleegers, K. 2019. The role of ABCA7 in Alzheimer's disease: evidence from genomics, transcriptomics and methylomics. *Acta neuropathologica* 138(2), pp. 201–220. Available at: https://pubmed.ncbi.nlm.nih.gov/30903345/ [Accessed: 12 June 2022].

- de Strooper, B. and Karran, E. 2016. The Cellular Phase of Alzheimer's Disease. *Cell* 164(4), pp. 603–615. Available at: https://pubmed.ncbi.nlm.nih.gov/26871627/ [Accessed: 25 July 2022].
- Deczkowska, A. et al. 2017. Mef2C restrains microglial inflammatory response and is lost in brain ageing in an IFN-I-dependent manner. *Nature Communications* 8(1), pp. 1–13. doi: 10.1038/s41467-017-00769-0.
- Delage, C.I., Šimončičová, E. and Tremblay, M.È. 2021. Microglial heterogeneity in aging and Alzheimer's disease: Is sex relevant? *Journal of Pharmacological Sciences* 146(3), pp. 169–181. doi: 10.1016/J.JPHS.2021.03.006.
- *Dementia | SLT | Expert providers of speech and language therapy throughout the UK.* [no date]. Available at: https://www.slt.co.uk/conditions/neurological-problems/dementia/ [Accessed: 22 June 2022].
- *Dementia UK report | Alzheimer's Society* [no date]. Available at: https://www.alzheimers.org.uk/about-us/policy-and-influencing/dementia-uk-report [Accessed: 6 June 2022].
- Demirev, A.V. et al. 2019. V232M substitution restricts a distinct O-glycosylation of PLD3 and its neuroprotective function. *Neurobiology of Disease* 129, pp. 182–194. doi: 10.1016/J.NBD.2019.05.015.
- Demma, M., Warren, V., Hock, R., Dharmawardhane, S. and Condeelis, J. 1990. Isolation of an abundant 50,000-dalton actin filament bundling protein from Dictyostelium amoebae. *Journal of Biological Chemistry* 265(4), pp. 2286–2291. doi: 10.1016/s0021-9258(19)39973-9.
- Deng, H., Dodson, M.W., Huang, H. and Guo, M. 2008. The Parkinson's disease genes pink1 and parkin promote mitochondrial fission and/or inhibit fusion in Drosophila. *Proceedings of the National Academy of Sciences of the United States of America* 105(38), p. 14503. Available at: /pmc/articles/PMC2567186/ [Accessed: 22 June 2022].
- Desale, S.E. and Chinnathambi, S. 2021. Phosphoinositides signaling modulates microglial actin remodeling and phagocytosis in Alzheimer's disease. *Cell Communication and Signaling* 19(1), pp. 1–12. Available at: https://biosignaling.biomedcentral.com/articles/10.1186/s12964-021-00715-0 [Accessed: 25 April 2022].

- Dey, P., Han, G.S. and Carman, G.M. 2020. A review of phosphatidate phosphatase assays. *Journal of Lipid Research* 61(12), p. 1556. Available at: /pmc/articles/PMC7707177/ [Accessed: 9 May 2022].
- Dhana, K., Evans, D.A., Rajan, K.B., Bennett, D.A. and Morris, M.C. 2020. Healthy lifestyle and the risk of Alzheimer dementia: Findings from 2 longitudinal studies. *Neurology* 95(4), pp. E374–E383. Available at: https://pubmed.ncbi.nlm.nih.gov/32554763/ [Accessed: 22 June 2022].
- Dickson, E.J. and Hille, B. 2019. Understanding phosphoinositides: rare, dynamic, and essential membrane phospholipids. *The Biochemical journal* 476(1), p. 1. Available at: /pmc/articles/PMC6342281/ [Accessed: 18 July 2022].
- DingYoung, E.J., Ko, S.S. and Cohn, Z.A. 1984. The increase in intracellular free calcium associated with IgG gamma 2b/gamma 1 Fc receptor-ligand interactions: role in phagocytosis. *Proceedings of the National Academy of Sciences of the United States of America* 81(17), pp. 5430–5434. Available at: https://pubmed.ncbi.nlm.nih.gov/6236462/ [Accessed: 26 May 2022].
- Divolis, G., Mavroeidi, P., Mavrofrydi, O. and Papazafiri, P. 2016. Differential effects of calcium on PI3K-Akt and HIF-1α survival pathways. *Cell biology and toxicology* 32(5), pp. 437–449. Available at: https://pubmed.ncbi.nlm.nih.gov/27344565/ [Accessed: 23 May 2022].
- Dodart, J.C., Mathis, C., Bales, K.R., Paul, S.M. and Ungerer, A. 2000. Behavioral deficits in APP(V717F) transgenic mice deficient for the apolipoprotein E gene. *Neuroreport* 11(3), pp. 603–607. Available at: https://pubmed.ncbi.nlm.nih.gov/10718322/ [Accessed: 26 July 2022].
- Doherty, J., Logan, M.A., Taşdemir, O.E. and Freeman, M.R. 2009. Ensheathing glia function as phagocytes in the adult Drosophila brain. *The Journal of neuroscience : the official journal of the Society for Neuroscience* 29(15), pp. 4768–81. Available at: http://www.ncbi.nlm.nih.gov/pubmed/19369546 [Accessed: 3 October 2018].
- Doherty, J., Sheehan, A.E., Bradshaw, R., Fox, A.N., Lu, T.-Y. and Freeman, M.R. 2014. PI3K Signaling and Stat92E Converge to Modulate Glial Responsiveness to Axonal Injury. Ravichandran, K. S. ed. *PLoS Biology* 12(11), p. e1001985. doi: 10.1371/journal.pbio.1001985.

- Donaldson, J.G. 2003. Multiple roles for Arf6: sorting, structuring, and signaling at the plasma membrane. *The Journal of biological chemistry* 278(43), pp. 41573–41576. Available at: https://pubmed.ncbi.nlm.nih.gov/12912991/ [Accessed: 26 May 2022].
- *Donepezil: MedlinePlus Drug Information* [no date]. Available at: https://medlineplus.gov/druginfo/meds/a697032.html [Accessed: 22 June 2022].
- Dotiwala, A.K., McCausland, C. and Samra, N.S. 2022. Anatomy, Head and Neck, Blood Brain Barrier. *StatPearls* . Available at: https://www.ncbi.nlm.nih.gov/books/NBK519556/ [Accessed: 21 June 2022].
- Drummond, E. and Wisniewski, T. 2017. Alzheimer's Disease: Experimental Models and Reality. *Acta neuropathologica* 133(2), p. 155. Available at: /pmc/articles/PMC5253109/ [Accessed: 21 June 2022].
- Efthymiou, A.G. and Goate, A.M. 2017. Late onset Alzheimer's disease genetics implicates microglial pathways in disease risk. *Molecular Neurodegeneration* 12(1), pp. 1–12. Available at: https://molecularneurodegeneration.biomedcentral.com/articles/10.1186/s13024-017-0184-x [Accessed: 12 April 2022].
- Eggenberger, P., Bürgisser, M., Rossi, R.M. and Annaheim, S. 2021. Body Temperature Is Associated With Cognitive Performance in Older Adults With and Without Mild Cognitive Impairment: A Cross-sectional Analysis. *Frontiers in Aging Neuroscience* 13, p. 29. doi: 10.3389/FNAGI.2021.585904/BIBTEX.
- Elferink, J.G.R. 1982. Interference of the calcium antagonists verapamil and nifedipine with lysosomal enzyme release from rabbit polymorphonuclear leukocytes. *Arzneimittel-forschung* 32(11), pp. 1417–1420. Available at: https://europepmc.org/article/med/6891245 [Accessed: 26 May 2022].
- Engelman, C.D., Darst, B.F., Bilgel, M., Vasiljevic, E., Koscik, R.L., Jedynak, B.M. and Johnson, S.C. 2018. The effect of rare variants in TREM2 and PLD3 on longitudinal cognitive function in the Wisconsin Registry for Alzheimer's Prevention. *Neurobiology of aging* 66, pp. 177.e1-177.e5. Available at: https://pubmed.ncbi.nlm.nih.gov/29395285/ [Accessed: 2 April 2022].
- Escott-Price, V. et al. 2014. Gene-wide analysis detects two new susceptibility genes for Alzheimer's disease. *PLoS ONE* 9(6). doi: 10.1371/journal.pone.0094661.

- Etchegaray, J.I., Elguero, E.J., Tran, J.A., Sinatra, V., Feany, M.B. and McCall, K. 2016. Defective Phagocytic Corpse Processing Results in Neurodegeneration and Can Be Rescued by TORC1 Activation. *The Journal of Neuroscience* 36(11), p. 3170. Available at: /pmc/articles/PMC4792933/ [Accessed: 2 April 2022].
- Evans, I.R., Rodrigues, F.S.L.M., Armitage, E.L. and Wood, W. 2015. Draper/CED-1 Mediates an Ancient Damage Response to Control Inflammatory Blood Cell Migration In Vivo. *Current Biology* 25(12), pp. 1606–1612. Available at: https://www.sciencedirect.com/science/article/pii/S0960982215004881?via%3Dihub#fig3 [Accessed: 7 May 2019].
- Falkenburger, B.H., Jensen, J.B., Dickson, E.J., Suh, B.C. and Hille, B. 2010. Phosphoinositides: lipid regulators of membrane proteins. *The Journal of Physiology* 588(Pt 17), p. 3179. Available at: /pmc/articles/PMC2976013/ [Accessed: 9 May 2022].
- Fallman, M., Gullberg, M., Hellberg, C. and Andersson, T. 1992. Complement receptor-mediated phagocytosis is associated with accumulation of phosphatidylcholine-derived diglyceride in human neutrophils. Involvement of phospholipase D and direct evidence for a positive feedback signal of protein kinase. *Journal of Biological Chemistry* 267(4), pp. 2656–2663. doi: 10.1016/S0021-9258(18)45931-5.
- Fazzari, P., Horre, K., Arranz, A.M., Frigerio, C.S., Saito, T., Saido, T.C. and de Strooper, B. 2017. PLD3 gene and processing of APP. *Nature* 541(7638), pp. E1–E2. Available at: https://pubmed.ncbi.nlm.nih.gov/28128235/ [Accessed: 25 April 2022].
- Feingold, K.R. and Grunfeld, C. 2021. Introduction to Lipids and Lipoproteins. *Endotext* . Available at: https://www.ncbi.nlm.nih.gov/books/NBK305896/ [Accessed: 21 June 2022].
- Feng, X. and Yang, J. 2016. Lysosomal Calcium in Neurodegeneration. *Messenger (Los Angeles, Calif. : Print)* 5(1–2), p. 56. Available at: /pmc/articles/PMC5659362/ [Accessed: 25 July 2022].
- Fernandez, C.G., Hamby, M.E., McReynolds, M.L. and Ray, W.J. 2019. The Role of APOE4 in Disrupting the Homeostatic Functions of Astrocytes and Microglia in

Aging and Alzheimer's Disease. *Frontiers in Aging Neuroscience* 11(FEB). Available at: /pmc/articles/PMC6378415/ [Accessed: 21 June 2022].

- Fernandez-Funez, P., de Mena, L. and Rincon-Limas, D.E. 2015. Modeling the complex pathology of Alzheimer's disease in Drosophila. *Experimental neurology* 274(0 0), p. 58. Available at: /pmc/articles/PMC4644457/ [Accessed: 22 June 2022].
- Fernández-Moreno, M.A., Farr, C.L., Kaguni, L.S. and Garesse, R. 2007. Drosophila melanogaster as a Model System to Study Mitochondrial Biology. *Methods in molecular biology (Clifton, N.J.)* 372, p. 33. Available at: /pmc/articles/PMC4876951/ [Accessed: 26 July 2022].
- Ferreira-Vieira, T.H., Guimaraes, I.M., Silva, F.R. and Ribeiro, F.M. 2016. Alzheimer's Disease: Targeting the Cholinergic System. *Current Neuropharmacology* 14(1), p. 101. Available at: /pmc/articles/PMC4787279/ [Accessed: 11 June 2022].
- Fiala, M. et al. 2005. Ineffective phagocytosis of amyloid-beta by macrophages of Alzheimer's disease patients. *Journal of Alzheimer's disease : JAD* 7(3), pp. 221–232. Available at: https://pubmed.ncbi.nlm.nih.gov/16006665/ [Accessed: 2 April 2022].
- Fiala, M. and Veerhuis, R. 2010. Biomarkers of inflammation and amyloid-β phagocytosis in patients at risk of Alzheimer disease. *Experimental gerontology* 45(1), p. 57. Available at: /pmc/articles/PMC2955441/ [Accessed: 25 July 2022].
- Filipello, F. et al. 2018. The Microglial Innate Immune Receptor TREM2 Is Required for Synapse Elimination and Normal Brain Connectivity. *Immunity* 48(5), pp. 979-991.e8. Available at: https://pubmed.ncbi.nlm.nih.gov/29752066/ [Accessed: 16 June 2022].
- Finelli, A., Kelkar, A., Song, H.-J., Yang, H. and Konsolaki, M. 2004. A model for studying Alzheimer's Aβ42-induced toxicity in Drosophila melanogaster. *Molecular and Cellular Neuroscience* 26(3), pp. 365–375. doi: 10.1016/J.MCN.2004.03.001.
- Finucane, H.K. et al. 2018. Heritability enrichment of specifically expressed genes identifies disease-relevant tissues and cell types. *Nature genetics* 50(4), pp. 621–629. Available at: https://pubmed.ncbi.nlm.nih.gov/29632380/ [Accessed: 13 June 2022].

- Fischer, D. et al. 2009. Conformational changes specific for pseudophosphorylation at serine 262 selectively impair binding of tau to microtubules. *Biochemistry* 48(42), pp. 10047–10055. Available at: https://pubs.acs.org/doi/abs/10.1021/bi901090m [Accessed: 10 June 2022].
- Flanary, B.E. and Streit, W.J. 2004. Progressive telomere shortening occurs in cultured rat microglia, but not astrocytes. *Glia* 45(1), pp. 75–88. Available at: https://pubmed.ncbi.nlm.nih.gov/14648548/ [Accessed: 7 July 2022].
- Fonseca, M.I., Zhou, J., Botto, M. and Tenner, A.J. 2004. Absence of C1q leads to less neuropathology in transgenic mouse models of Alzheimer's disease. *The Journal of neuroscience : the official journal of the Society for Neuroscience* 24(29), pp. 6457–6465. Available at: https://pubmed.ncbi.nlm.nih.gov/15269255/ [Accessed: 20 June 2022].
- Förstl, H. and Kurz, A. 1999. Clinical features of Alzheimer's disease. *European Archives of Psychiatry and Clinical Neuroscience 1999 249:6* 249(6), pp. 288–290. Available at: https://link.springer.com/article/10.1007/s004060050101 [Accessed: 7 June 2022].
- Foster, D.A. 2013. Phosphatidic Acid and Lipid Sensing by mTOR. *Trends in endocrinology and metabolism: TEM* 24(6), p. 272. Available at: /pmc/articles/PMC3669661/ [Accessed: 12 April 2022].
- Fourgeaud, L. et al. 2016. TAM receptors regulate multiple features of microglial physiology. *Nature* 532(7598), pp. 240–244. Available at: https://pubmed.ncbi.nlm.nih.gov/27049947/ [Accessed: 20 June 2022].
- Francis, P.T., Palmer, A.M., Snape, M. and Wilcock, G.K. 1999. The cholinergic hypothesis of Alzheimer's disease: A review of progress. *Journal of Neurology Neurosurgery and Psychiatry* 66(2), pp. 137–147. doi: 10.1136/jnnp.66.2.137.
- Freeman, M.R. 2015. Drosophila Central Nervous System Glia. *Cold Spring Harbor Perspectives in Biology* 7(11), p. a020552. Available at: http://cshperspectives.cshlp.org/content/7/11/a020552.full [Accessed: 18 January 2022].
- Freeman, M.R., Delrow, J., Kim, J., Johnson, E. and Doe, C.Q. 2003. Unwrapping Glial Biology: Gcm Target Genes Regulating Glial Development, Diversification, and Function. *Neuron* 38(4), pp. 567–580. Available at:

https://www.sciencedirect.com/science/article/pii/S0896627303002897 [Accessed: 11 February 2019].
- Freeman, M.R. and Doherty, J. [no date]. Glial cell biology in Drosophila and vertebrates. Available at: www.sciencedirect.com [Accessed: 5 March 2019].
- Fu, Q. et al. 2019. SHIP1 inhibits cell growth, migration, and invasion in non-small cell lung cancer through the PI3K/AKT pathway. *Oncology reports* 41(4), pp. 2337–2350. Available at: https://pubmed.ncbi.nlm.nih.gov/30720128/ [Accessed: 26 July 2022].
- Fu, R., Shen, Q., Xu, P., Luo, J.J. and Tang, Y. 2014. Phagocytosis of microglia in the central nervous system diseases. *Molecular neurobiology* 49(3), pp. 1422–1434. Available at: https://pubmed.ncbi.nlm.nih.gov/24395130/ [Accessed: 21 June 2022].
- Fullard, J.F. and Baker, N.E. 2015. Signaling by the Engulfment Receptor Draper: A Screen in Drosophila melanogaster Implicates Cytoskeletal Regulators, Jun N-Terminal Kinase, and Yorkie. *Genetics* 199(1), p. 117. Available at: /pmc/articles/PMC4286677/ [Accessed: 26 May 2022].
- Gabandé-Rodríguez, E., Keane, L. and Capasso, M. 2020. Microglial phagocytosis in aging and Alzheimer's disease. *Journal of neuroscience research* 98(2), pp. 284–298. Available at: https://pubmed.ncbi.nlm.nih.gov/30942936/ [Accessed: 2 April 2022].
- *Galantamine: MedlinePlus Drug Information* [no date]. Available at: https://medlineplus.gov/druginfo/meds/a699058.html [Accessed: 22 June 2022].
- Gallio, M., Ofstad, T.A., Macpherson, L.J., Wang, J.W. and Zuker, C.S. 2011. The Coding of Temperature in the Drosophila Brain. *Cell* 144(4), pp. 614–624. Available at: http://www.cell.com/article/S0092867411000675/fulltext [Accessed: 24 March 2022].
- Galloway, D.A., Phillips, A.E.M., Owen, D.R.J. and Moore, C.S. 2019. Phagocytosis in the brain: Homeostasis and disease. *Frontiers in Immunology* 10(MAR), p. 790. doi: 10.3389/FIMMU.2019.00790/BIBTEX.
- García-García, E. and Rosales, C. 2002. Signal transduction during Fc receptor-mediated phagocytosis. *Journal of Leukocyte Biology* 72(6), pp. 1092–1108. Available at: https://onlinelibrary.wiley.com/doi/full/10.1189/jlb.72.6.1092 [Accessed: 26 May 2022].

- Garrity, A.G., Wang, W., Collier, C.M.D., Levey, S.A., Gao, Q. and Xu, H. 2016. The endoplasmic reticulum, not the pH gradient, drives calcium refilling of lysosomes. *eLife* 5(MAY2016). Available at: /pmc/articles/PMC4909396/ [Accessed: 25 July 2022].
- Gasparoni, G. et al. 2018. DNA methylation analysis on purified neurons and glia dissects age and Alzheimer's disease-specific changes in the human cortex. *Epigenetics & chromatin* 11(1). Available at: https://pubmed.ncbi.nlm.nih.gov/30045751/ [Accessed: 12 June 2022].
- Gatz, M. et al. 2006. Role of genes and environments for explaining Alzheimer disease. *Archives of general psychiatry* 63(2), pp. 168–174. Available at: https://pubmed.ncbi.nlm.nih.gov/16461860/ [Accessed: 12 June 2022].
- Gaudet, P., Livstone, M.S., Lewis, S.E. and Thomas, P.D. 2011. Phylogenetic-based propagation of functional annotations within the Gene Ontology consortium. *Briefings in Bioinformatics* 12(5), pp. 449–462. Available at: https://academic.oup.com/bib/article-lookup/doi/10.1093/bib/bbr042 [Accessed: 6 May 2019].
- Gavin, A.L. et al. 2018. PLD3 and PLD4 are single stranded acid exonucleases that regulate endosomal nucleic acid sensing. *Nature immunology* 19(9), p. 942. Available at: /pmc/articles/PMC6105523/ [Accessed: 24 April 2022].
- Geller, S.E., Koch, A., Pellettieri, B. and Carnes, M. 2011. Inclusion, analysis, and reporting of sex and race/ethnicity in clinical trials: Have we made progress? *Journal of Women's Health* 20(3), pp. 315–320. doi: 10.1089/JWH.2010.2469.
- Genin, E. et al. 2011. APOE and Alzheimer disease: A major gene with semi-dominant inheritance. *Molecular Psychiatry* 16(9), pp. 903–907. doi: 10.1038/mp.2011.52.
- Georgescu, M.M. 2010. PTEN Tumor Suppressor Network in PI3K-Akt Pathway Control. *Genes & Cancer* 1(12), p. 1170. Available at: /pmc/articles/PMC3092286/ [Accessed: 27 April 2022].
- Gericke, A., Leslie, N.R., Lösche, M. and Ross, A.H. 2013. PI(4,5)P2-Mediated Cell Signaling: Emerging Principles and PTEN as a Paradigm for Regulatory Mechanism. *Advances in experimental medicine and biology* 991, p. 85. Available at: /pmc/articles/PMC3763917/ [Accessed: 18 July 2022].

- Gewirtz, A.T. and Simons, E.R. 1997. Phospholipase D mediates Fc gamma receptor activation of neutrophils and provides specificity between high-valency immune complexes and fMLP signaling pathways. *Journal of leukocyte biology* 61(4), pp. 522–528. Available at: https://pubmed.ncbi.nlm.nih.gov/9103240/ [Accessed: 26 May 2022].
- Gillooly, D.J., Simonsen, A. and Stenmark, H. 2001. Phosphoinositides and phagocytosis. *The Journal of Cell Biology* 155(1), p. 15. Available at: /pmc/articles/PMC2150801/ [Accessed: 29 April 2022].
- GK, W., MM, E., DM, B. and CC, S. 1982. Alzheimer's disease. Correlation of cortical choline acetyltransferase activity with the severity of dementia and histological abnormalities. *Journal of the neurological sciences* 57(2–3), pp. 407–417. Available at: https://pubmed.ncbi.nlm.nih.gov/7161627/ [Accessed: 25 July 2021].
- Gloor, G.B., Nassif, N.A., Johnson-Schlitz, D.M., Preston, C.R. and Engels, W.R. 1991. Targeted gene replacement in Drosophila via P element-induced gap repair. *Science (New York, N.Y.)* 253(5024), pp. 1110–1117. Available at: https://pubmed.ncbi.nlm.nih.gov/1653452/ [Accessed: 4 July 2022].
- Goberdhan, D.C.I., Paricio, N., Goodman, E.C., Mlodzik, M. and Wilson, C. 1999. Drosophila tumor suppressor PTEN controls cell size and number by antagonizing the Chico/PI3-kinase signaling pathway. *Genes & development* 13(24), pp. 3244–3258. Available at: https://pubmed.ncbi.nlm.nih.gov/10617573/ [Accessed: 9 May 2022].
- Goberdhan, D.C.I. and Wilson, C. 2003. PTEN: tumour suppressor, multifunctional growth regulator and more. *Human molecular genetics* 12 Spec No 2(REV. ISS. 2). Available at: https://pubmed.ncbi.nlm.nih.gov/12928488/ [Accessed: 9 May 2022].
- Goedert, M. and Jakes, R. 2005. Mutations causing neurodegenerative tauopathies. *Biochimica et Biophysica Acta (BBA) - Molecular Basis of Disease* 1739(2–3), pp. 240–250. doi: 10.1016/j.bbadis.2004.08.007.
- Goedert, M., Spillantini, M.G. and Crowther, R.A. 1991. Tau proteins and neurofibrillary degeneration. *Brain pathology (Zurich, Switzerland)* 1(4), pp. 279–86.

- Gong, J., Part, C. and Hajat, S. 2022. Current and future burdens of heat-related dementia hospital admissions in England. *Environment International* 159. Available at: /pmc/articles/PMC8739554/ [Accessed: 25 July 2022].
- Gordon, M.D., Manzo, A. and Scott, K. 2008. Fly neurobiology: development and function of the brain. Meeting on the Neurobiology of Drosophila. *EMBO reports* 9(3), pp. 239–42. doi: 10.1038/embor.2008.13.
- Gorjestani, S., Yu, M., Tang, B., Zhang, D., Wang, D. and Lin, X. 2011. Phospholipase Cγ2 (PLCγ2) is key component in Dectin-2 signaling pathway, mediating anti-fungal innate immune responses. *The Journal of biological chemistry* 286(51), pp. 43651–43659. Available at: https://pubmed.ncbi.nlm.nih.gov/22041900/ [Accessed: 26 May 2022].
- Götz, J. et al. 2007. A decade of tau transgenic animal models and beyond. *Brain pathology (Zurich, Switzerland)* 17(1), pp. 91–103. Available at: https://pubmed.ncbi.nlm.nih.gov/17493043/ [Accessed: 22 June 2022].
- Goveas, J.S., Espeland, M.A., Woods, N.F., Wassertheil-Smoller, S. and Kotchen, J.M. 2011. Depressive symptoms and incidence of mild cognitive impairment and probable dementia in elderly women: the Women's Health Initiative Memory Study. *Journal of the American Geriatrics Society* 59(1), pp. 57–66. Available at: https://pubmed.ncbi.nlm.nih.gov/21226676/ [Accessed: 23 March 2022].
- Gratuze, M., Leyns, C.E.G. and Holtzman, D.M. 2018. New insights into the role of TREM2 in Alzheimer's disease. *Molecular Neurodegeneration 2018 13:1* 13(1), pp. 1–16. Available at: https://molecularneurodegeneration.biomedcentral.com/articles/10.1186/s13024-018-0298-9 [Accessed: 20 June 2022].
- Greenspan, R., Jan, L., Jan, Y.-N. and O'farrell, P. 2010. *Drosophila Neurobiology Manual*.
- Greenwood, E.K. and Brown, D.R. 2021. Senescent Microglia: The Key to the Ageing Brain? *International Journal of Molecular Sciences* 22(9). Available at: /pmc/articles/PMC8122783/ [Accessed: 20 June 2022].
- Greeve, I. 2004. Age-Dependent Neurodegeneration and Alzheimer-Amyloid Plaque Formation in Transgenic Drosophila. *Journal of Neuroscience* 24(16), pp. 3899–3906. doi: 10.1523/JNEUROSCI.0283-04.2004.

- Gronski, M.A., Kinchen, J.M., Juncadella, I.J., Franc, N.C. and Ravichandran, K.S. 2009. An essential role for calcium flux in phagocytes for apoptotic cell engulfment and the anti-inflammatory response. *Cell death and differentiation* 16(10), pp. 1323–1331. Available at: https://pubmed.ncbi.nlm.nih.gov/19461656/ [Accessed: 26 May 2022].
- Gross, C. 2017. Defective phosphoinositide metabolism in autism. *Journal of neuroscience research* 95(5), pp. 1161–1173. Available at: https://pubmed.ncbi.nlm.nih.gov/27376697/ [Accessed: 10 May 2022].
- Gruss, H.J. and Dower, S.K. 1995. The TNF ligand superfamily and its relevance for human diseases. *Cytokines and Molecular Therapy* 1(2), pp. 75–105.
- Gu, L. and Guo, Z. 2013. Alzheimer's Aβ42 and Aβ40 peptides form interlaced amyloid fibrils. *Journal of neurochemistry* 126(3), pp. 305–311. Available at: https://pubmed.ncbi.nlm.nih.gov/23406382/ [Accessed: 8 June 2022].
- Guillot-Sestier, M.V., Doty, K.R., Gate, D., Rodriguez, J., Leung, B.P., Rezai-Zadeh, K. and Town, T. 2015. Il10 deficiency rebalances innate immunity to mitigate Alzheimer-like pathology. *Neuron* 85(3), pp. 534–548. Available at: https://pubmed.ncbi.nlm.nih.gov/25619654/ [Accessed: 15 June 2022].
- Guo, C. et al. 2018. Tau Activates Transposable Elements in Alzheimer's Disease. *Cell reports* 23(10), pp. 2874–2880. doi: 10.1016/j.celrep.2018.05.004.
- Guo, T., Noble, W. and Hanger, D.P. 2017. Roles of tau protein in health and disease. *Acta neuropathologica* 133(5), pp. 665–704. doi: 10.1007/s00401-017-1707-9.
- Gutierrez, M.A., Dwyer, B.E. and Franco, S.J. 2019. Csmd2 Is a Synaptic Transmembrane Protein that Interacts with PSD-95 and Is Required for Neuronal Maturation. *eNeuro* 6(2). doi: 10.1523/ENEURO.0434-18.2019.
- H, T., S, K., M, N., M, I. and K, K. 2000. Junctophilins: a novel family of junctional membrane complex proteins. *Molecular cell* 6(1), pp. 11–22. Available at: https://pubmed.ncbi.nlm.nih.gov/10949023/ [Accessed: 26 May 2022].
- Halliday, M.R., Rege, S. v., Ma, Q., Zhao, Z., Miller, C.A., Winkler, E.A. and Zlokovic, B. v. 2016. Accelerated pericyte degeneration and blood–brain barrier breakdown in apolipoprotein E4 carriers with Alzheimer's disease. *Journal of Cerebral Blood Flow & Metabolism* 36(1), p. 216. Available at: /pmc/articles/PMC4758554/ [Accessed: 21 June 2022].

- Hammond, G.R.V. and Balla, T. 2015. Polyphosphoinositide binding domains: Key to inositol lipid biology. *Biochimica et Biophysica Acta (BBA) - Molecular and Cell Biology of Lipids* 1851(6), pp. 746–758. doi: 10.1016/J.BBALIP.2015.02.013.
- Hampel, H. et al. 2021. The Amyloid-β Pathway in Alzheimer's Disease. *Molecular Psychiatry 2021 26:10* 26(10), pp. 5481–5503. Available at: https://www.nature.com/articles/s41380-021-01249-0 [Accessed: 26 May 2022].
- Hansen, D. v., Hanson, J.E. and Sheng, M. 2018. Microglia in Alzheimer's disease. *J Cell Biol* 217(2), pp. 459–472. Available at: http://jcb.rupress.org/content/217/2/459 [Accessed: 7 May 2019].
- Hardie, R.C., Liu, C.H., Randall, A.S. and Sengupta, S. 2015. In vivo tracking of phosphoinositides in Drosophila photoreceptors. *Journal of Cell Science* 128(23), pp. 4328–4340. Available at: /pmc/articles/PMC4712823/ [Accessed: 29 April 2022].
- Hardy, J. and Allsop, D. 1991. Amyloid deposition as the central event in the aetiology of Alzheimer's disease. *Trends in pharmacological sciences* 12(10), pp. 383–8.
- Harold, D. et al. 2009. Genome-wide association study identifies variants at CLU and PICALM associated with Alzheimer's disease. *Nature genetics* 41(10), pp. 1088–1093. Available at: https://pubmed.ncbi.nlm.nih.gov/19734902/ [Accessed: 20 June 2022].
- Hawrylycz, M.J. et al. 2012. An anatomically comprehensive atlas of the adult human brain transcriptome. *Nature 2012 489:7416* 489(7416), pp. 391–399. Available at: https://www.nature.com/articles/nature11405 [Accessed: 2 April 2022].
- Haynes, L. 2020. Aging of the Immune System: Research Challenges to Enhance the Health Span of Older Adults. *Frontiers in Aging* 0, p. 2. doi: 10.3389/FRAGI.2020.602108.
- Hefendehl, J.K., Neher, J.J., Sühs, R.B., Kohsaka, S., Skodras, A. and Jucker, M. 2014. Homeostatic and injury-induced microglia behavior in the aging brain. *Aging Cell* 13(1), p. 60. Available at: /pmc/articles/PMC4326865/ [Accessed: 9 April 2022].

- Heigwer, F., Port, F. and Boutros, M. 2018. RNA Interference (RNAi) Screening in Drosophila. *Genetics* 208(3), p. 853. Available at: /pmc/articles/PMC5844339/ [Accessed: 12 July 2022].
- Hellwig, S., Masuch, A., Nestel, S., Katzmarski, N., Meyer-Luehmann, M. and Biber, K. 2015. Forebrain microglia from wild-type but not adult 5xFAD mice prevent amyloid-β plaque formation in organotypic hippocampal slice cultures. *Scientific Reports 2015 5:1* 5(1), pp. 1–9. Available at: https://www.nature.com/articles/srep14624 [Accessed: 20 June 2022].
- Heneka, M.T. et al. 2015. Neuroinflammation in Alzheimer's disease. *The Lancet. Neurology* 14(4), pp. 388–405. Available at: https://pubmed.ncbi.nlm.nih.gov/25792098/ [Accessed: 2 April 2022].
- Heneka, M.T., Kummer, M.P. and Latz, E. 2014. Innate immune activation in neurodegenerative disease. *Nature reviews. Immunology* 14(7), pp. 463–477. Available at: https://pubmed.ncbi.nlm.nih.gov/24962261/ [Accessed: 14 June 2022].
- Henry, R.M., Hoppe, A.D., Joshi, N. and Swanson, J.A. 2004. The uniformity of phagosome maturation in macrophages. *The Journal of cell biology* 164(2), pp. 185–194. Available at: https://pubmed.ncbi.nlm.nih.gov/14718518/ [Accessed: 26 May 2022].
- Hernandez, D., Egan, S.E., Yulug, I.G. and Fisher, E.M.C. 1994. Mapping the gene that encodes phosphatidylinositol-specific phospholipase C-gamma 2 in the human and the mouse. *Genomics* 23(2), pp. 504–507. Available at: https://pubmed.ncbi.nlm.nih.gov/7835906/ [Accessed: 13 April 2022].
- Hernández, F. and Avila, J. 2007. Tauopathies. *Cellular and Molecular Life Sciences* 64(17), pp. 2219–2233. doi: 10.1007/s00018-007-7220-x.
- Herzig, M.C., van Nostrand, W.E. and Jucker, M. 2006. Mechanism of Cerebral β-Amyloid Angiopathy: Murine and Cellular Models. *Brain Pathology* 16(1), p. 40. Available at: /pmc/articles/PMC8095938/ [Accessed: 22 June 2022].
- Herzog, C., Garcia, L.P., Keatinge, M., Greenald, D., Moritz, C., Peri, F. and Herrgen, L. 2019. Rapid clearance of cellular debris by microglia limits secondary neuronal cell death after brain injury in vivo. *Development (Cambridge)* 146(9). Available at: /pmc/articles/PMC6526721/ [Accessed: 13 June 2022].

- Hill, R.A., Li, A.M. and Grutzendler, J. 2018. Lifelong cortical myelin plasticity and age-related degeneration in the live mammalian brain. *Nature neuroscience* 21(5), pp. 683–695. Available at: https://pubmed.ncbi.nlm.nih.gov/29556031/ [Accessed: 20 June 2022].
- Hilu-Dadia, R., Hakim-Mishnaevski, K., Levy-Adam, F. and Kurant, E. 2018. Draper-mediated JNK signaling is required for glial phagocytosis of apoptotic neurons during *Drosophila* metamorphosis. *Glia* 66(7), pp. 1520–1532. Available at: http://www.ncbi.nlm.nih.gov/pubmed/29520845 [Accessed: 11 February 2019].
- Hinkovska-Galcheva, V. et al. 2008. Ceramide kinase promotes Ca2+ signaling near IgG-opsonized targets and enhances phagolysosomal fusion in COS-1 cellssâƒž. Available at: http://www.jlr.org [Accessed: 26 May 2022].
- Hippius, H. and Neundörfer, G. 2003. The discovery of Alzheimer's disease. *Dialogues in clinical neuroscience* 5(1), pp. 101–108. Available at: https://pubmed.ncbi.nlm.nih.gov/22034141/ [Accessed: 6 June 2022].
- Hirsch-Reinshagen, V. et al. 2005. The absence of ABCA1 decreases soluble ApoE levels but does not diminish amyloid deposition in two murine models of Alzheimer disease. *The Journal of biological chemistry* 280(52), pp. 43243–43256. Available at: https://pubmed.ncbi.nlm.nih.gov/16207707/ [Accessed: 26 July 2022].
- Hobert, O. 2010. Neurogenesis in the nematode Caenorhabditis elegans. *WormBook : the online review of C. elegans biology* , pp. 1–24. doi: 10.1895/WORMBOOK.1.12.2.
- Hodges, A.K., Piers, T.M., Collier, D., Cousins, O. and Pocock, J.M. 2021. Pathways linking Alzheimer's disease risk genes expressed highly in microglia. *Neuroimmunology and Neuroinflammation* 8, p. 245. Available at: https://nnjournal.net/article/view/3915 [Accessed: 15 June 2022].
- Hollingworth, P. et al. 2011. Common variants at ABCA7, MS4A6A/MS4A4E, EPHA1, CD33 and CD2AP are associated with Alzheimer's disease. *Nature Genetics* 43(5), pp. 429–436. Available at: http://www.ncbi.nlm.nih.gov/pubmed/21460840 [Accessed: 24 April 2020].
- Holmes, K., Williams, C.M., Chapman, E.A. and Cross, M.J. 2010. Detection of siRNA induced mRNA silencing by RT-qPCR: considerations for experimental

design. *BMC research notes* 3, p. 53. Available at: http://www.ncbi.nlm.nih.gov/pubmed/20199660 [Accessed: 8 September 2018].

- Hong, S. et al. 2016. Complement and microglia mediate early synapse loss in Alzheimer mouse models. *Science* 352(6286), pp. 712–716. Available at: http://science.sciencemag.org/content/352/6286/712 [Accessed: 23 January 2019].
- Hooli, B.V. et al. 2012. Role of common and rare APP DNA sequence variants in Alzheimer disease. *Neurology* 78(16), p. 1250. Available at: /pmc/articles/PMC3324321/ [Accessed: 12 July 2021].
- Hooli, B. v., Lill, C.M., Mullin, K., Qiao, D., Lange, C., Bertram, L. and Tanzi, R.E. 2015. PLD3 gene variants and Alzheimer's disease. *Nature* 520(7545), pp. E7–E8. Available at: https://pubmed.ncbi.nlm.nih.gov/25832413/ [Accessed: 2 April 2022].
- Hooper, N.M. 2005. Roles of proteolysis and lipid rafts in the processing of the amyloid precursor protein and prion protein. *Biochemical Society Transactions* 33(2), pp. 335–338. doi: 10.1042/BST0330335.
- Hopkins, B.D., Goncalves, M.D. and Cantley, L.C. 2020. Insulin–PI3K signalling: an evolutionarily insulated metabolic driver of cancer. *Nature Reviews Endocrinology 2020 16:5* 16(5), pp. 276–283. Available at: https://www.nature.com/articles/s41574-020-0329-9 [Accessed: 9 May 2022].
- Hoppe, A.D. and Swanson, J.A. 2004. Cdc42, Rac1, and Rac2 display distinct patterns of activation during phagocytosis. *Molecular biology of the cell* 15(8), pp. 3509–3519. Available at: https://pubmed.ncbi.nlm.nih.gov/15169870/ [Accessed: 10 May 2022].
- Hopperton, K.E., Mohammad, D., Trépanier, M.O., Giuliano, V. and Bazinet, R.P. 2017. Markers of microglia in post-mortem brain samples from patients with Alzheimer's disease: a systematic review. *Molecular Psychiatry 2018 23:2* 23(2), pp. 177–198. Available at: https://www.nature.com/articles/mp2017246 [Accessed: 15 June 2022].
- Houard, X. et al. 1998. The Drosophila melanogaster-related angiotensin-I-converting enzymes acer and ance - Distinct enzymic characteristics and alternative expression during pupal development. *European Journal of*

*Biochemistry* 257(3), pp. 599–606. Available at: https://pubmed.ncbi.nlm.nih.gov/9839949/ [Accessed: 6 May 2021].

- Hsiao, K. et al. 1996. Correlative memory deficits, Abeta elevation, and amyloid plaques in transgenic mice. *Science (New York, N.Y.)* 274(5284), pp. 99–102. Available at: http://www.ncbi.nlm.nih.gov/pubmed/8810256 [Accessed: 11 May 2019].
- Hsieh, C.L., Koike, M., Spusta, S.C., Niemi, E.C., Yenari, M., Nakamura, M.C. and Seaman, W.E. 2009. A role for TREM2 ligands in the phagocytosis of apoptotic neuronal cells by microglia. *Journal of neurochemistry* 109(4), pp. 1144–56. Available at: http://www.ncbi.nlm.nih.gov/pubmed/19302484 [Accessed: 11 May 2019].
- Hu, Z. et al. 2020. Shared Causal Paths underlying Alzheimer's dementia and Type 2 Diabetes. *Scientific Reports 2020 10:1* 10(1), pp. 1–15. Available at: https://www.nature.com/articles/s41598-020-60682-3 [Accessed: 26 May 2022].
- Huang, K.L. et al. 2017. A common haplotype lowers PU.1 expression in myeloid cells and delays onset of Alzheimer's disease. *Nature neuroscience* 20(8), pp. 1052–1061. Available at: https://pubmed.ncbi.nlm.nih.gov/28628103/ [Accessed: 13 June 2022].
- Huang, Y. and Mucke, L. 2012. Alzheimer Mechanisms and Therapeutic Strategies. *Cell* 148(6), pp. 1204–1222. doi: 10.1016/j.cell.2012.02.040.
- Hubler, M.J. and Kennedy, A.J. 2016. Role of lipids in the metabolism and activation of immune cells. *The Journal of nutritional biochemistry* 34, pp. 1–7. Available at: https://pubmed.ncbi.nlm.nih.gov/27424223/ [Accessed: 21 June 2022].
- Hughes, R.E. 2016. The role of MEGF10 in skeletal muscle myopathy.
- Hurst, D., Rylett, C.M., Isaac, R.E. and Shirras, A.D. 2003. The drosophila angiotensin-converting enzyme homologue Ance is required for spermiogenesis. *Developmental Biology* 254(2), pp. 238–247. doi: 10.1016/S0012-1606(02)00082-9.
- Husain, M.A., Laurent, B. and Plourde, M. 2021. APOE and Alzheimer's Disease: From Lipid Transport to Physiopathology and Therapeutics. *Frontiers in Neuroscience* 15, p. 85. doi: 10.3389/FNINS.2021.630502/BIBTEX.

- Hussain, B., Fang, C. and Chang, J. 2021. Blood–Brain Barrier Breakdown: An Emerging Biomarker of Cognitive Impairment in Normal Aging and Dementia. *Frontiers in Neuroscience* 15, p. 978. doi: 10.3389/FNINS.2021.688090/BIBTEX.
- Hussain, G. et al. 2019. Role of cholesterol and sphingolipids in brain development and neurological diseases. *Lipids in Health and Disease* 18(1), pp. 1–12. Available at: https://lipidworld.biomedcentral.com/articles/10.1186/s12944-019-0965-z [Accessed: 21 June 2022].
- I, G.-I., K, I., YC, T., M, Q., HM, W. and LI, B. 1986. Abnormal phosphorylation of the microtubule-associated protein tau (tau) in Alzheimer cytoskeletal pathology. *Proceedings of the National Academy of Sciences of the United States of America* 83(13), pp. 4913–4917. Available at: https://pubmed.ncbi.nlm.nih.gov/3088567/ [Accessed: 13 July 2021].
- Iba, M., Guo, J.L., McBride, J.D., Zhang, B., Trojanowski, J.Q. and Lee, V.M.Y. 2013. Synthetic Tau Fibrils Mediate Transmission of Neurofibrillary Tangles in a Transgenic Mouse Model of Alzheimer's-Like Tauopathy. *Journal of Neuroscience* 33(3), pp. 1024–1037. Available at: https://www.jneurosci.org/content/33/3/1024 [Accessed: 10 June 2022].
- Iijima-Ando, K. and Iijima, K. 2010. Transgenic Drosophila models of Alzheimer's disease and tauopathies. *Brain structure & function* 214(2–3), p. 245. Available at: /pmc/articles/PMC2849836/ [Accessed: 22 June 2022].
- Iqbal, K., Liu, F., Gong, C.-X. and Grundke-Iqbal, I. 2010. Tau in Alzheimer disease and related tauopathies. *Current Alzheimer research* 7(8), pp. 656–64.
- Iram, T. et al. 2016. Megf10 Is a Receptor for C1Q That Mediates Clearance of Apoptotic Cells by Astrocytes. *The Journal of Neuroscience* 36(19), pp. 5185–5192. Available at: http://www.ncbi.nlm.nih.gov/pubmed/27170117 [Accessed: 11 February 2019].
- Israel, M.A. et al. 2012. Probing sporadic and familial Alzheimer's disease using induced pluripotent stem cells. *Nature* 482(7384), pp. 216–220. Available at: https://pubmed.ncbi.nlm.nih.gov/22278060/ [Accessed: 22 June 2022].
- Iyer, S.S., Barton, J.A., Bourgoin, S. and Kusner, D.J. 2004. Phospholipases D1 and D2 coordinately regulate macrophage phagocytosis. *Journal of immunology (Baltimore, Md. : 1950)* 173(4), pp. 2615–2623. Available at: https://pubmed.ncbi.nlm.nih.gov/15294978/ [Accessed: 2 April 2022].

- J, de la T. 2018. The Vascular Hypothesis of Alzheimer's Disease: A Key to Preclinical Prediction of Dementia Using Neuroimaging. *Journal of Alzheimer's disease : JAD* 63(1), pp. 35–52. Available at: https://pubmed.ncbi.nlm.nih.gov/29614675/ [Accessed: 25 July 2021].
- Jack, C.R. et al. 2010. Hypothetical model of dynamic biomarkers of the Alzheimer's pathological cascade. *The Lancet. Neurology* 9(1), pp. 119–128. Available at: https://pubmed.ncbi.nlm.nih.gov/20083042/ [Accessed: 20 June 2022].
- Jackson, G.R., Wiedau-Pazos, M., Sang, T.-K., Wagle, N., Brown, C.A., Massachi, S. and Geschwind, D.H. 2002. Human wild-type tau interacts with wingless pathway components and produces neurofibrillary pathology in Drosophila. *Neuron* 34(4), pp. 509–19.
- Jackson, J.T., Mulazzani, E., Nutt, S.L. and Masters, S.L. 2021. The role of PLCγ2 in immunological disorders, cancer, and neurodegeneration. *Journal of Biological Chemistry* 297(2). Available at: http://www.jbc.org/article/S0021925821007055/fulltext [Accessed: 25 April 2022].
- Jäkel, S. and Dimou, L. 2017. Glial cells and their function in the adult brain: A journey through the history of their ablation. *Frontiers in Cellular Neuroscience* 11, p. 24. doi: 10.3389/FNCEL.2017.00024/BIBTEX.
- Janelsins, M.C. et al. 2008. Chronic neuron-specific tumor necrosis factor-alpha expression enhances the local inflammatory environment ultimately leading to neuronal death in 3xTg-AD mice. *The American journal of pathology* 173(6), pp. 1768–1782. Available at: https://pubmed.ncbi.nlm.nih.gov/18974297/ [Accessed: 15 June 2022].
- Jansen, I.E. et al. 2019. Genome-wide meta-analysis identifies new loci and functional pathways influencing Alzheimer's disease risk. *Nature Genetics* 51(3), pp. 404–413. Available at: http://www.nature.com/articles/s41588-018-0311-9 [Accessed: 11 May 2019].
- JC, de la T. 2004. Is Alzheimer's disease a neurodegenerative or a vascular disorder? Data, dogma, and dialectics. *The Lancet. Neurology* 3(3), pp. 184–190. Available at: https://pubmed.ncbi.nlm.nih.gov/14980533/ [Accessed: 25 July 2021].

- Jenkins, G.M. and Frohman, M.A. 2005. Phospholipase D: a lipid centric review. *Cellular and Molecular Life Sciences CMLS 2005 62:19* 62(19), pp. 2305–2316. Available at: https://link.springer.com/article/10.1007/s00018-005-5195-z [Accessed: 29 April 2022].
- Jensen, K. et al. 2013. Purification of Transcripts and Metabolites from Drosophila Heads. *Journal of Visualized Experiments : JoVE* (73), p. 50245. Available at: /pmc/articles/PMC3639516/ [Accessed: 5 July 2022].
- Jeon, Y., Lee, J.H., Choi, B., Won, S.Y. and Cho, K.S. 2020. Genetic Dissection of Alzheimer's Disease Using Drosophila Models. *International Journal of Molecular Sciences 2020, Vol. 21, Page 884* 21(3), p. 884. Available at: https://www.mdpi.com/1422-0067/21/3/884/htm [Accessed: 22 June 2022].
- Jho, Y.S., Zhulina, E.B., Kim, M.W. and Pincus, P.A. 2010. Monte Carlo Simulations of Tau Proteins: Effect of Phosphorylation. *Biophysical Journal* 99(8), p. 2387. Available at: /pmc/articles/PMC2955347/ [Accessed: 10 June 2022].
- Jiao, B. et al. 2014. Investigation of TREM2, PLD3, and UNC5C variants in patients with Alzheimer's disease from mainland China. *Neurobiology of aging* 35(10), pp. 2422.e9-2422.e11. Available at: https://pubmed.ncbi.nlm.nih.gov/24866402/ [Accessed: 2 April 2022].
- Johansson, L. 2014. Can stress increase Alzheimer's disease risk in women? *Expert review of neurotherapeutics* 14(2), pp. 123–125. Available at: https://pubmed.ncbi.nlm.nih.gov/24471710/ [Accessed: 23 March 2022].
- Jones, L. et al. 2015. Convergent genetic and expression data implicate immunity in Alzheimer's disease. *Alzheimer's and Dementia* 11(6), pp. 658–671. doi: 10.1016/j.jalz.2014.05.1757.
- Jonsson, T. et al. 2013. Variant of *TREM2* Associated with the Risk of Alzheimer's Disease. *New England Journal of Medicine* 368(2), pp. 107–116. Available at: http://www.ncbi.nlm.nih.gov/pubmed/23150908 [Accessed: 3 October 2018].
- Joshi, P. et al. 2014. Microglia convert aggregated amyloid-β into neurotoxic forms through the shedding of microvesicles. *Cell Death and Differentiation* . doi: 10.1038/cdd.2013.180.

- Joshi, T., Butchar, J.P. and Tridandapani, S. 2006. Fcγ receptor signaling in phagocytes. *International Journal of Hematology* 84(3), pp. 210–216. Available at: https://pubmed.ncbi.nlm.nih.gov/29349684/ [Accessed: 26 May 2022].
- Joung, S.M., Park, Z.-Y., Rani, S., Takeuchi, O., Akira, S. and Lee, J.Y. 2011. Akt contributes to activation of the TRIF-dependent signaling pathways of TLRs by interacting with TANK-binding kinase 1. *Journal of immunology (Baltimore, Md. : 1950)* 186(1), pp. 499–507. Available at: https://pubmed.ncbi.nlm.nih.gov/21106850/ [Accessed: 27 April 2022].
- Juang, J.-L. and Hoffmann, F.M. 1999. Drosophila Abelson interacting protein (dAbi) is a positive regulator of Abelson tyrosine kinase activity. *Oncogene* 18(37), pp. 5138–5147. Available at: http://www.nature.com/articles/1202911 [Accessed: 11 May 2019].
- Karch, C.M. and Goate, A.M. 2015. Alzheimer's disease risk genes and mechanisms of disease pathogenesis. *Biological Psychiatry* 77(1), pp. 43–51. doi: 10.1016/J.BIOPSYCH.2014.05.006.
- Karpanen, T. et al. 2017. An Evolutionarily Conserved Role for Polydom/Svep1 during Lymphatic Vessel Formation. *Circulation Research* 120(8), pp. 1263–1275. doi: 10.1161/CIRCRESAHA.116.308813.
- Kayali, A.G. et al. 1998. Association of the insulin receptor with phospholipase C-gamma (PLCgamma) in 3T3-L1 adipocytes suggests a role for PLCgamma in metabolic signaling by insulin. *The Journal of biological chemistry* 273(22), pp. 13808–13818. Available at: https://pubmed.ncbi.nlm.nih.gov/9593725/ [Accessed: 9 May 2022].
- Kehoe, P.G., Wong, S., al Mulhim, N., Palmer, L.E. and Miners, J.S. 2016. Angiotensin-converting enzyme 2 is reduced in Alzheimer's disease in association with increasing amyloid-β and tau pathology. *Alzheimer's Research and Therapy* 8(1), pp. 1–10. Available at: https://alzres.biomedcentral.com/articles/10.1186/s13195-016-0217-7 [Accessed: 6 May 2021].
- Kempuraj, D. et al. 2016. Neuroinflammation Induces Neurodegeneration. *Journal of neurology, neurosurgery and spine* 1(1). Available at: /pmc/articles/PMC5260818/ [Accessed: 13 June 2022].

- Keppler, A., Gendreizig, S., Gronemeyer, T., Pick, H., Vogel, H. and Johnsson, K. 2003. A general method for the covalent labeling of fusion proteins with small molecules in vivo. *Nature Biotechnology* 21(1), pp. 86–89. doi: 10.1038/nbt765.
- Kigerl, K.A., de Rivero Vaccari, J.P., Dietrich, W.D., Popovich, P.G. and Keane, R.W. 2014. Pattern recognition receptors and central nervous system repair. *Experimental neurology* 258, p. 5. Available at: /pmc/articles/PMC4974939/ [Accessed: 15 June 2022].
- Kim, J., Basak, J.M. and Holtzman, D.M. 2009. The Role of Apolipoprotein E in Alzheimer's Disease. *Neuron* 63(3), p. 287. Available at: /pmc/articles/PMC3044446/ [Accessed: 20 June 2022].
- Kim, J.-H., Seo, M. and Suk, K. 2013. Effects of therapeutic hypothermia on the glial proteome and phenotype. *Current protein & peptide science* 14(1), pp. 51–60. Available at: https://pubmed.ncbi.nlm.nih.gov/23441897/ [Accessed: 6 July 2022].
- Kim, Y.J., Sekiya, F., Poulin, B., Bae, Y.S. and Rhee, S.G. 2004. Mechanism of B-cell receptor-induced phosphorylation and activation of phospholipase C-gamma2. *Molecular and cellular biology* 24(22), pp. 9986–9999. Available at: https://pubmed.ncbi.nlm.nih.gov/15509800/ [Accessed: 13 April 2022].
- Kinchen, J.M. 2010. A model to die for: signaling to apoptotic cell removal in worm, fly and mouse. *Apoptosis : an international journal on programmed cell death* 15(9), pp. 998–1006. Available at: https://pubmed.ncbi.nlm.nih.gov/20461556/ [Accessed: 26 May 2022].
- Kinney, J.W., Bemiller, S.M., Murtishaw, A.S., Leisgang, A.M., Salazar, A.M. and Lamb, B.T. 2018. Inflammation as a central mechanism in Alzheimer's disease. *Alzheimer's & Dementia : Translational Research & Clinical Interventions* 4, p. 575. Available at: /pmc/articles/PMC6214864/ [Accessed: 15 June 2022].
- Kiral, F.R. et al. 2021. Brain connectivity inversely scales with developmental temperature in Drosophila. *Cell Reports* 37(12), p. 110145. doi: 10.1016/J.CELREP.2021.110145.
- Kitazawa, M., Medeiros, R. and LaFerla, F.M. 2012. Transgenic Mouse Models of Alzheimer Disease: Developing a Better Model as a Tool for Therapeutic Interventions. *Current pharmaceutical design* 18(8), p. 1131. Available at: /pmc/articles/PMC4437619/ [Accessed: 26 July 2022].

- Kleinberger, G. et al. 2014. TREM2 mutations implicated in neurodegeneration impair cell surface transport and phagocytosis. *Science translational medicine* 6(243), p. 243ra86. Available at: http://stm.sciencemag.org/cgi/doi/10.1126/scitranslmed.3009093 [Accessed: 11 May 2019].
- Kleinhesselink, K., Conway, C., Sholer, D., Huang, I. and Kimbrell, D.A. 2011. Regulation of hemocytes in Drosophila requires dappled cytochrome b5. *Biochemical Genetics* 49(5–6), pp. 329–351. doi: 10.1007/S10528-010-9411-7.
- Kokawa, A., Ishihara, S., Fujiwara, H., Nobuhara, M., Iwata, M., Ihara, Y. and Funamoto, S. 2015. The A673T mutation in the amyloid precursor protein reduces the production of β-amyloid protein from its β-carboxyl terminal fragment in cells. *Acta Neuropathologica Communications* 3, p. 66. Available at: /pmc/articles/PMC4632685/ [Accessed: 12 July 2021].
- Kolesnikov, Y.S., Nokhrina, K.P., Kretynin, S. v., Volotovski, I.D., Martinec, J., Romanov, G.A. and Kravets, V.S. 2012. Molecular structure of phospholipase D and regulatory mechanisms of its activity in plant and animal cells. *Biochemistry. Biokhimiia* 77(1), pp. 1–14. Available at: https://pubmed.ncbi.nlm.nih.gov/22339628/ [Accessed: 27 April 2022].
- Korvatska, O. et al. 2015. R47H Variant of TREM2 Associated With Alzheimer Disease in a Large Late-Onset Family: Clinical, Genetic, and Neuropathological Study. *JAMA neurology* 72(8), pp. 920–927. Available at: https://pubmed.ncbi.nlm.nih.gov/26076170/ [Accessed: 12 June 2022].
- Koss, H., Bunney, T.D., Behjati, S. and Katan, M. 2014. Dysfunction of phospholipase Cγ in immune disorders and cancer. *Trends in Biochemical Sciences* 39(12), pp. 603–611. doi: 10.1016/j.tibs.2014.09.004.
- Krasemann, S. et al. 2017. The TREM2-APOE Pathway Drives the Transcriptional Phenotype of Dysfunctional Microglia in Neurodegenerative Diseases. *Immunity* 47(3), pp. 566-581.e9. Available at: https://pubmed.ncbi.nlm.nih.gov/28930663/ [Accessed: 20 June 2022].
- Krasniak, C.S. and Ahmad, S.T. 2016. The role of CHMP2BIntron5 in autophagy and frontotemporal dementia. *Brain Research* 1649(Pt B), pp. 151–157. doi: 10.1016/j.brainres.2016.02.051.

- Kunda, P., Craig, G., Dominguez, V. and Baum, B. 2003. Abi, Sra1, and Kette control the stability and localization of SCAR/WAVE to regulate the formation of actin-based protrusions. *Current biology : CB* 13(21), pp. 1867–75. Available at: http://www.ncbi.nlm.nih.gov/pubmed/14588242 [Accessed: 11 May 2019].
- Kunkle, B.W. et al. 2019. Genetic meta-analysis of diagnosed Alzheimer's disease identifies new risk loci and implicates Aβ, tau, immunity and lipid processing. *Nature Genetics* 51(3), pp. 414–430. Available at: https://www.nature.com/articles/s41588-019-0358-2 [Accessed: 13 May 2021].
- Kurosaki, T., Maeda, A., Ishiai, M., Hashimoto, A., Inabe, K. and Takata, M. 2000. Regulation of the phospholipase C-gamma2 pathway in B cells. *Immunological reviews* 176, pp. 19–29. Available at: https://pubmed.ncbi.nlm.nih.gov/11043765/ [Accessed: 9 May 2022].
- Kusner, D.J., Hall, C.F. and Jackson, S. 1999. Fcγ Receptor-Mediated Activation of Phospholipase D Regulates Macrophage Phagocytosis of IgG-Opsonized Particles. *The Journal of Immunology* 162(4)
- Labbadia, J. and Morimoto, R.I. 2015. The biology of proteostasis in aging and disease. *Annual review of biochemistry* 84, pp. 435–464. Available at: https://pubmed.ncbi.nlm.nih.gov/25784053/ [Accessed: 26 July 2022].
- LaFerla, F.M. and Green, K.N. 2012. Animal models of Alzheimer disease. *Cold Spring Harbor perspectives in medicine* 2(11). Available at: https://pubmed.ncbi.nlm.nih.gov/23002015/ [Accessed: 22 June 2022].
- Lambert, J.-C. et al. 2013. Meta-analysis of 74,046 individuals identifies 11 new susceptibility loci for Alzheimer's disease. *Nature Genetics* 45(12), pp. 1452–1458. Available at: http://www.ncbi.nlm.nih.gov/pubmed/24162737 [Accessed: 3 October 2018].
- Lardenoije, R. et al. 2019. Alzheimer's disease-associated (hydroxy)methylomic changes in the brain and blood. *Clinical Epigenetics* 11(1), p. 164. Available at: https://clinicalepigeneticsjournal.biomedcentral.com/articles/10.1186/s13148-019-0755-5 [Accessed: 23 June 2020].
- Lawson, L.J., Perry, V.H., Dri, P. and Gordon, S. 1990. Heterogeneity in the distribution and morphology of microglia in the normal adult mouse brain. *Neuroscience* 39(1), pp. 151–170. Available at: https://pubmed.ncbi.nlm.nih.gov/2089275/ [Accessed: 26 July 2022].

- le Bras, A. 2021. A new mouse model to study late-onset Alzheimer's disease. *Lab Animal 2021 50:6* 50(6), pp. 151–151. Available at: https://www.nature.com/articles/s41684-021-00780-5 [Accessed: 22 June 2022].
- Lee, C.Y.D. and Landreth, G.E. 2010. The role of microglia in amyloid clearance from the AD brain. *Journal of neural transmission (Vienna, Austria : 1996)* 117(8), pp. 949–960. Available at: https://pubmed.ncbi.nlm.nih.gov/20552234/ [Accessed: 20 June 2022].
- Lee, V.M.-Y., Goedert, M. and Trojanowski, J.Q. 2001. Neurodegenerative Tauopathies. *Annual Review of Neuroscience* 24(1), pp. 1121–1159. doi: 10.1146/annurev.neuro.24.1.1121.
- Leech, T., Evison, S.E.F., Armitage, S.A.O., Sait, S.M. and Bretman, A. 2019. Interactive effects of social environment, age and sex on immune responses in Drosophila melanogaster. *Journal of evolutionary biology* 32(10), pp. 1082–1092. Available at: https://pubmed.ncbi.nlm.nih.gov/31313398/ [Accessed: 23 March 2022].
- Lein, E.S. et al. 2006. Genome-wide atlas of gene expression in the adult mouse brain. *Nature 2006 445:7124* 445(7124), pp. 168–176. Available at: https://www.nature.com/articles/nature05453 [Accessed: 25 April 2022].
- Lennon, M.J., Makkar, S.R., Crawford, J.D. and Sachdev, P.S. 2019. Midlife Hypertension and Alzheimer's Disease: A Systematic Review and Meta-Analysis. *Journal of Alzheimer's disease : JAD* 71(1), pp. 307–316. Available at: https://pubmed.ncbi.nlm.nih.gov/31381518/ [Accessed: 25 July 2022].
- Lenoir, G., D'Ambrosio, J.M., Dieudonné, T. and Čopič, A. 2021. Transport Pathways That Contribute to the Cellular Distribution of Phosphatidylserine. *Frontiers in Cell and Developmental Biology* 9, p. 2412. doi: 10.3389/FCELL.2021.737907/BIBTEX.
- Lenroot, R.K. and Giedd, J.N. 2008. The changing impact of genes and environment on brain development during childhood and adolescence: Initial findings from a neuroimaging study of pediatric twins. *Development and psychopathology* 20(4), p. 1161. Available at: /pmc/articles/PMC2892674/ [Accessed: 25 July 2022].

- Leonenko, G. et al. 2019. Genetic risk for Alzheimer's disease is distinct from genetic risk for amyloid deposition. *Annals of Neurology* , p. ana.25530. Available at: http://www.ncbi.nlm.nih.gov/pubmed/31199530 [Accessed: 18 June 2019].
- Lewis, J. et al. 2001. Enhanced neurofibrillary degeneration in transgenic mice expressing mutant tau and APP. *Science (New York, N.Y.)* 293(5534), pp. 1487–1491. Available at: https://pubmed.ncbi.nlm.nih.gov/11520987/ [Accessed: 22 June 2022].
- Li, C., Zhao, B., Lin, C., Gong, Z. and An, X. 2019a. TREM2 inhibits inflammatory responses in mouse microglia by suppressing the PI3K/NF-κB signaling. *Cell biology international* 43(4), pp. 360–372. Available at: https://pubmed.ncbi.nlm.nih.gov/29663649/ [Accessed: 21 June 2022].
- Li, J. et al. 2019b. Astrocyte-to-astrocyte contact and a positive feedback loop of growth factor signaling regulate astrocyte maturation. *Glia* 67(8), p. glia.23630. Available at: https://onlinelibrary.wiley.com/doi/abs/10.1002/glia.23630 [Accessed: 4 May 2020].
- Li, Q. et al. 2019c. Developmental Heterogeneity of Microglia and Brain Myeloid Cells Revealed by Deep Single-Cell RNA Sequencing. *Neuron* 101(2), pp. 207-223.e10. Available at: https://pubmed.ncbi.nlm.nih.gov/30606613/ [Accessed: 20 June 2022].
- Li, Q. and Barres, B.A. 2017. Microglia and macrophages in brain homeostasis and disease. *Nature Reviews Immunology* 18(4), pp. 225–242. Available at: http://www.nature.com/doifinder/10.1038/nri.2017.125 [Accessed: 27 February 2019].
- Li, Q.S., Sun, Y. and Wang, T. 2020a. Epigenome-wide association study of Alzheimer's disease replicates 22 differentially methylated positions and 30 differentially methylated regions. *Clinical Epigenetics 2020 12:1* 12(1), pp. 1–14. Available at: https://clinicalepigeneticsjournal.biomedcentral.com/articles/10.1186/s13148-020-00944-z [Accessed: 12 July 2021].
- Li, T. et al. 2016. Generation of induced pluripotent stem cells (iPSCs) from an Alzheimer's disease patient carrying an A79V mutation in PSEN1. *Stem cell research* 16(2), pp. 229–232. Available at: https://pubmed.ncbi.nlm.nih.gov/27345973/ [Accessed: 22 June 2022].

- Li, T.N., Chen, Y.J., Lu, T.Y., Wang, Y.T., Lin, H.C. and Yao, C.K. 2020b. A positive feedback loop between flower and pi(4,5)p2 at periactive zones controls bulk endocytosis in drosophila. *eLife* 9, pp. 1–33. doi: 10.7554/ELIFE.60125.
- Li, W. 2013. Phagocyte dysfunction, tissue aging and degeneration. *Ageing research reviews* 12(4), pp. 1005–1012. Available at: /pmc/articles/PMC3842398/ [Accessed: 25 July 2022].
- Li, W.X. 2005. Functions and Mechanisms of Receptor Tyrosine Kinase Torso Signaling: Lessons From Drosophila Embryonic Terminal Development. *Developmental dynamics : an official publication of the American Association of Anatomists* 232(3), p. 656. Available at: /pmc/articles/PMC3092428/ [Accessed: 9 May 2022].
- Li, Y. and Dulac, C. 2018. Neural coding of sex-specific social information in the mouse brain. *Current Opinion in Neurobiology* 53, pp. 120–130. doi: 10.1016/J.CONB.2018.07.005.
- Li, Z. et al. 2005. Regulation of PTEN by Rho small GTPases. *Nature cell biology* 7(4), pp. 399–404. Available at: https://pubmed.ncbi.nlm.nih.gov/15793569/ [Accessed: 9 May 2022].
- Liao, Q., Zhou, Y., Xia, L. and Cao, D. 2021. Lipid Metabolism and Immune Checkpoints. *Advances in experimental medicine and biology* 1316, pp. 191–211. Available at: https://pubmed.ncbi.nlm.nih.gov/33740251/ [Accessed: 21 June 2022].
- Lichtman, J.W. and Colman, H. 2000. Synapse elimination and indelible memory. *Neuron* 25(2), pp. 269–278. Available at: https://pubmed.ncbi.nlm.nih.gov/10719884/ [Accessed: 20 June 2022].
- Lin, T.-Y. et al. 2009. Abi plays an opposing role to Abl in Drosophila axonogenesis and synaptogenesis. *Development* 136(18), pp. 3099–3107. Available at: http://dev.biologists.org/cgi/doi/10.1242/dev.033324 [Accessed: 11 May 2019].
- Lin, X.P., Mintern, J.D. and Gleeson, P.A. 2020. Macropinocytosis in Different Cell Types: Similarities and Differences. *Membranes* 10(8), pp. 1–21. Available at: /pmc/articles/PMC7463864/ [Accessed: 29 April 2022].
- Lindquist, S.G., Brændgaard, H., Svenstrup, K., Isaacs, A.M. and Nielsen, J.E. 2008. Frontotemporal dementia linked to chromosome 3 (FTD-3) - Current

concepts and the detection of a previously unknown branch of the Danish FTD-3 family. *European Journal of Neurology* 15(7), pp. 667–670. doi: 10.1111/j.1468-1331.2008.02144.x.

- Linton, M.F. et al. 2019. The Role of Lipids and Lipoproteins in Atherosclerosis. *Science* 111(2877), pp. 166–186. Available at: https://www.ncbi.nlm.nih.gov/books/NBK343489/ [Accessed: 21 June 2022].
- Liu, C.H., Chen, Z., Oliva, M.K., Luo, J., Collier, S., Montell, C. and Hardie, R.C. 2020. Rapid Release of Ca2+ from Endoplasmic Reticulum Mediated by Na+/Ca2+ Exchange. *Journal of Neuroscience* 40(16), pp. 3152–3164. Available at: https://www.jneurosci.org/content/40/16/3152 [Accessed: 29 April 2022].
- Liu, K.A. and Dipietro Mager, N.A. 2016. Women's involvement in clinical trials: historical perspective and future implications. *Pharmacy Practice* 14(1). Available at: /pmc/articles/PMC4800017/ [Accessed: 9 April 2022].
- Livingston, G. et al. 2020. Dementia prevention, intervention, and care: 2020 report of the Lancet Commission. *The Lancet* 396(10248), pp. 413–446. Available at: http://www.thelancet.com/article/S0140673620303676/fulltext [Accessed: 25 July 2021].
- Löfgren, R., Serrander, L., Forsberg, M., Wilsson, Å., Wasteson, Å. and Stendahl, O. 1999. CR3, FcγRIIA and FcγRIIIB induce activation of the respiratory burst in human neutrophils: the role of intracellular Ca2+, phospholipase D and tyrosine phosphorylation. *Biochimica et Biophysica Acta (BBA) - Molecular Cell Research* 1452(1), pp. 46–59. doi: 10.1016/S0167-4889(99)00112-3.
- Logan, M.A. and Freeman, M.R. 2007. The scoop on the fly brain: glial engulfment functions in Drosophila. *Neuron glia biology* 3(1), p. 63. Available at: /pmc/articles/PMC2171361/ [Accessed: 9 May 2022].
- Logan, M.A., Hackett, R., Doherty, J., Sheehan, A., Speese, S.D. and Freeman, M.R. 2012a. Negative regulation of glial engulfment activity by Draper terminates glial responses to axon injury. *Nature neuroscience* 15(5), pp. 722–30. Available at: http://www.ncbi.nlm.nih.gov/pubmed/22426252 [Accessed: 11 February 2019].
- Lopategui Cabezas, I., Herrera Batista, A. and Pentón Rol, G. 2014. The role of glial cells in Alzheimer disease: potential therapeutic implications. *Neurología (English Edition)* 29(5), pp. 305–309. Available at:

https://www.sciencedirect.com/science/article/pii/S2173580814000625 [Accessed: 5 December 2018].

- Lord, J. and Cruchaga, C. 2014. THE EPIGENETIC LANDSCAPE OF ALZHEIMER'S DISEASE. *Nature neuroscience* 17(9), p. 1138. Available at: /pmc/articles/PMC5472058/ [Accessed: 12 July 2021].
- Lorenzo, M., Teruel, T., Hernandez, R., Kayali, A.G. and Webster, N.J.G. 2002. PLCγ Participates in Insulin Stimulation of Glucose Uptake through Activation of PKCζ in Brown Adipocytes. *Experimental Cell Research* 278(2), pp. 146–157. doi: 10.1006/EXCR.2002.5570.
- Lott, I.T. and Head, E. 2005. Alzheimer disease and Down syndrome: factors in pathogenesis. *Neurobiology of Aging* 26(3), pp. 383–389. doi: 10.1016/j.neurobiolaging.2004.08.005.
- Lu, T.Y., Doherty, J. and Freeman, M.R. 2014. DRK/DOS/SOS converge with Crk/Mbc/dCed-12 to activate Rac1 during glial engulfment of axonal debris. *Proceedings of the National Academy of Sciences of the United States of America* 111(34), pp. 12544–12549. Available at: www.pnas.org/cgi/doi/10.1073/pnas.1403450111 [Accessed: 2 April 2022].
- Lu, T.Y., MacDonald, J.M., Neukomm, L.J., Sheehan, A.E., Bradshaw, R., Logan, M.A. and Freeman, M.R. 2017. Axon degeneration induces glial responses through Draper-TRAF4-JNK signalling. *Nature Communications* 8(1), pp. 1–9. Available at: www.nature.com/naturecommunications [Accessed: 2 July 2020].
- Lundquist, M.R. et al. 2018. Phosphatidylinositol-5-phosphate 4-kinases regulate cellular lipid metabolism by facilitating autophagy. *Molecular cell* 70(3), p. 531. Available at: /pmc/articles/PMC5991623/ [Accessed: 25 July 2022].
- Lunnon, K. et al. 2014. Methylomic profiling implicates cortical deregulation of ANK1 in Alzheimer's disease. *Nature Neuroscience* 17(9), pp. 1164–1170. Available at: https://pubmed.ncbi.nlm.nih.gov/25129077/ [Accessed: 23 June 2020].
- Lyketsos, C.G. et al. 2011. Neuropsychiatric symptoms in Alzheimer's disease. *Alzheimer's & dementia : the journal of the Alzheimer's Association* 7(5), p. 532. Available at: /pmc/articles/PMC3299979/ [Accessed: 7 June 2022].

- Lystad, A.H. and Simonsen, A. 2016. Phosphoinositide-binding proteins in autophagy. *FEBS letters* 590(15), pp. 2454–2468. Available at: https://pubmed.ncbi.nlm.nih.gov/27391591/ [Accessed: 29 April 2022].
- M, G., MG, S., R, J., D, R. and RA, C. 1989. Multiple isoforms of human microtubule-associated protein tau: sequences and localization in neurofibrillary tangles of Alzheimer's disease. *Neuron* 3(4), pp. 519–526. Available at: https://pubmed.ncbi.nlm.nih.gov/2484340/ [Accessed: 13 July 2021].
- M. Isaacs, A., Johannsen, P., Holm, I., E. Nielsen, J. and Consortium, Fr. 2011. Frontotemporal Dementia Caused by CHMP2B Mutations. *Current Alzheimer Research* 8(3), pp. 246–251. doi: 10.2174/156720511795563764.
- M, S. and W, D. 2001. Chronic cerebral hypoperfusion in the rat enhances age-related deficits in spatial memory. *Journal of neural transmission (Vienna, Austria : 1996)* 108(12), pp. 1445–1456. Available at: https://pubmed.ncbi.nlm.nih.gov/11810407/ [Accessed: 25 July 2021].
- MacDonald, J.M., Beach, M.G., Porpiglia, E., Sheehan, A.E., Watts, R.J. and Freeman, M.R. 2006. The Drosophila Cell Corpse Engulfment Receptor Draper Mediates Glial Clearance of Severed Axons. *Neuron* 50(6), pp. 869–881. Available at: https://www.sciencedirect.com/science/article/pii/S0896627306003199?via%3Dihub#bib15 [Accessed: 22 January 2019].
- MacDonald, J.M., Doherty, J., Hackett, R. and Freeman, M.R. 2013. The c-Jun kinase signaling cascade promotes glial engulfment activity through activation of draper and phagocytic function. *Cell Death & Differentiation* 20(9), pp. 1140–1148. Available at: http://www.nature.com/articles/cdd201330 [Accessed: 28 February 2019].
- MacMillan, H.A., Knee, J.M., Dennis, A.B., Udaka, H., Marshall, K.E., Merritt, T.J.S. and Sinclair, B.J. 2016. Cold acclimation wholly reorganizes the Drosophila melanogaster transcriptome and metabolome. *Scientific Reports 2016 6:1* 6(1), pp. 1–14. Available at: https://www.nature.com/articles/srep28999 [Accessed: 23 March 2022].
- Magno, L. et al. 2019. Alzheimer's disease phospholipase C-gamma-2 (PLCG2) protective variant is a functional hypermorph. *Alzheimer's Research and Therapy* 11(1), pp. 1–11. Available at:

https://alzres.biomedcentral.com/articles/10.1186/s13195-019-0469-0 [Accessed: 13 April 2022].

- Magno, L., Bunney, T.D., Mead, E., Svensson, F. and Bictash, M.N. 2021. TREM2/PLCγ2 signalling in immune cells: function, structural insight, and potential therapeutic modulation. *Molecular Neurodegeneration 2021 16:1* 16(1), pp. 1–16. Available at: https://molecularneurodegeneration.biomedcentral.com/articles/10.1186/s13024-021-00436-5 [Accessed: 16 June 2022].
- Maguire, E. et al. 2020. The Alzheimer's disease protective P522R variant of PLCG2, consistently enhances stimulus-dependent PLCγ2 activation, depleting substrate and altering cell function. *bioRxiv* , p. 2020.04.27.059600. Available at: https://www.biorxiv.org/content/10.1101/2020.04.27.059600v1 [Accessed: 2 April 2022].
- Maguire, E. et al. 2021. PIP2 depletion and altered endocytosis caused by expression of Alzheimer's disease-protective variant PLCγ2 R522. *The EMBO journal* 40(17). Available at: https://pubmed.ncbi.nlm.nih.gov/34254352/ [Accessed: 10 May 2022].
- Mahajan, K. and Mahajan, N.P. 2012. PI3K-Independent AKT Activation in Cancers: A Treasure Trove for Novel Therapeutics. *Journal of Cellular Physiology* 227(9), p. 3178. Available at: /pmc/articles/PMC3358464/ [Accessed: 27 April 2022].
- Mahley, R.W., Weisgraber, K.H. and Huang, Y. 2006. Apolipoprotein E4: a causative factor and therapeutic target in neuropathology, including Alzheimer's disease. *Proceedings of the National Academy of Sciences of the United States of America* 103(15), pp. 5644–51. doi: 10.1073/pnas.0600549103.
- Mandal, K. 2020. Review of PIP2 in Cellular Signaling, Functions and Diseases. *International Journal of Molecular Sciences* 21(21), pp. 1–20. Available at: /pmc/articles/PMC7664428/ [Accessed: 18 July 2022].
- Mandrekar-Colucci, S. and Landreth, G.E. 2010. Microglia and inflammation in Alzheimer's disease. *CNS & neurological disorders drug targets* 9(2), pp. 156–67. Available at: http://www.ncbi.nlm.nih.gov/pubmed/20205644 [Accessed: 12 November 2019].

- Mankidy, R., Hastings, J. and Thackeray, J.R. 2003. Distinct phospholipase C-gamma-dependent signaling pathways in the Drosophila eye and wing are revealed by a new small wing allele. *Genetics* 164(2), pp. 553–563. Available at: https://pubmed.ncbi.nlm.nih.gov/12807776/ [Accessed: 30 March 2022].
- Manning, C.M., Mathews, W.R., Fico, L.P. and Thackeray, J.R. 2003. Phospholipase C-gamma contains introns shared by src homology 2 domains in many unrelated proteins. *Genetics* 164(2), pp. 433–442. Available at: https://pubmed.ncbi.nlm.nih.gov/12807765/ [Accessed: 2 April 2022].
- Marat, A.L. and Haucke, V. 2016. Phosphatidylinositol 3-phosphates—at the interface between cell signalling and membrane traffic. *The EMBO Journal* 35(6), p. 561. Available at: /pmc/articles/PMC4801949/ [Accessed: 29 April 2022].
- Marín-Teva, J.L., Dusart, I., Colin, C., Gervais, A., van Rooijen, N. and Mallat, M. 2004. Microglia promote the death of developing Purkinje cells. *Neuron* 41(4), pp. 535–547. Available at: https://pubmed.ncbi.nlm.nih.gov/14980203/ [Accessed: 20 June 2022].
- Martinkova, J. et al. 2021. Proportion of Women and Reporting of Outcomes by Sex in Clinical Trials for Alzheimer Disease: A Systematic Review and Meta-analysis. *JAMA Network Open* 4(9), pp. e2124124–e2124124. Available at: https://jamanetwork.com/journals/jamanetworkopen/fullarticle/2783983 [Accessed: 25 July 2022].
- Massoulié, J. 2002. The origin of the molecular diversity and functional anchoring of cholinesterases. *NeuroSignals* 11(3), pp. 130–143. doi: 10.1159/000065054.
- Mawuenyega, K.G. et al. 2010. Decreased clearance of CNS beta-amyloid in Alzheimer's disease. *Science (New York, N.Y.)* 330(6012), p. 1774. Available at: https://pubmed.ncbi.nlm.nih.gov/21148344/ [Accessed: 20 June 2022].
- Mayor, S., Parton, R.G. and Donaldson, J.G. 2014. Clathrin-Independent Pathways of Endocytosis. *Cold Spring Harbor Perspectives in Biology* 6(6). Available at: /pmc/articles/PMC4031960/ [Accessed: 25 July 2022].
- Mazaheri, F., Breus, O., Durdu, S., Haas, P., Wittbrodt, J., Gilmour, D. and Peri, F. 2014. Distinct roles for BAI1 and TIM-4 in the engulfment of dying neurons by microglia. *Nature Communications 2014 5:1* 5(1), pp. 1–11. Available at: https://www.nature.com/articles/ncomms5046 [Accessed: 20 June 2022].

- McGeer, P.L. and McGeer, E.G. 2002. Local neuroinflammation and the progression of Alzheimer's disease. *Journal of neurovirology* 8(6), pp. 529–538. Available at: https://pubmed.ncbi.nlm.nih.gov/12476347/ [Accessed: 15 June 2022].
- McGowan, E. et al. 2005. Abeta42 is essential for parenchymal and vascular amyloid deposition in mice. *Neuron* 47(2), pp. 191–199. Available at: https://pubmed.ncbi.nlm.nih.gov/16039562/ [Accessed: 22 June 2022].
- McGuire, S.E., Mao, Z. and Davis, R.L. 2004. Spatiotemporal gene expression targeting with the TARGET and gene-switch systems in Drosophila. *Science's STKE : signal transduction knowledge environment* 2004(220), p. pl6. Available at: http://stke.sciencemag.org/cgi/doi/10.1126/stke.2202004pl6 [Accessed: 26 March 2018].
- McQuade, A. and Blurton-Jones, M. 2019. Microglia in Alzheimer's Disease: Exploring How Genetics and Phenotype Influence Risk. *Journal of Molecular Biology* 431(9), pp. 1805–1817. doi: 10.1016/j.jmb.2019.01.045.
- MD, W., AH, L., SY, H. and MW, K. 1975. A protein factor essential for microtubule assembly. *Proceedings of the National Academy of Sciences of the United States of America* 72(5), pp. 1858–1862. Available at: https://pubmed.ncbi.nlm.nih.gov/1057175/ [Accessed: 13 July 2021].
- Melcarne, C., Lemaitre, B. and Kurant, E. 2019. Phagocytosis in Drosophila: From molecules and cellular machinery to physiology. *Insect Biochemistry and Molecular Biology* 109, pp. 1–12. doi: 10.1016/j.ibmb.2019.04.002.
- Melendez, A., Floto, R.A., Cameron, A.J., Gillooly, D.J., Harnett, M.M. and Allen, J.M. 1998. A molecular switch changes the signalling pathway used by the Fc gamma RI antibody receptor to mobilise calcium. *Current biology : CB* 8(4), pp. 210–222. Available at: https://pubmed.ncbi.nlm.nih.gov/9501983/ [Accessed: 26 May 2022].
- Melendez, A.J. and Allen, J.M. 2002. Phospholipase D and immune receptor signalling. *Seminars in Immunology* 14(1), pp. 49–55. doi: 10.1006/SMIM.2001.0341.
- Melendez, A.J. and Tay, H.K. 2008. Phagocytosis: a repertoire of receptors and Ca(2+) as a key second messenger. *Bioscience reports* 28(5), pp. 287–298.

Available at: https://pubmed.ncbi.nlm.nih.gov/18826374/ [Accessed: 26 May 2022].

- Melo, J.A. and Ruvkun, G. 2012. Inactivation of Conserved C. elegans Genes Engages Pathogen- and Xenobiotic-Associated Defenses. *Cell* 149(2), pp. 452–466. doi: 10.1016/J.CELL.2012.02.050.
- *Memantine: MedlinePlus Drug Information* [no date]. Available at: https://medlineplus.gov/druginfo/meds/a604006.html [Accessed: 22 June 2022].
- Meyer-Luehmann, M. et al. 2008. Rapid appearance and local toxicity of amyloid-beta plaques in a mouse model of Alzheimer's disease. *Nature* 451(7179), pp. 720–724. Available at: https://pubmed.ncbi.nlm.nih.gov/18256671/ [Accessed: 22 June 2022].
- Miquel, J., Lundgren, P.R., Bensch, K.G. and Atlan, H. 1976. Effects of temperature on the life span, vitality and fine structure of Drosophila melanogaster. *Mechanisms of ageing and development* 5(5), pp. 347–370. Available at: https://pubmed.ncbi.nlm.nih.gov/823384/ [Accessed: 25 March 2022].
- MIYAKAWA, T. 2010. Vascular pathology in Alzheimer's disease. *Psychogeriatrics* 10(1), pp. 39–44. doi: 10.1111/j.1479-8301.2009.00294.x.
- MN, R., NJ, G., AL, J., CQ, M., M, R. and LL, I. 1982. A post-mortem study of the cholinergic and GABA systems in senile dementia. *Brain : a journal of neurology* 105(Pt 2), pp. 313–330. Available at: https://pubmed.ncbi.nlm.nih.gov/7082992/ [Accessed: 25 July 2021].
- Mohamet, L., Miazga, N.J. and Ward, C.M. 2014. Familial Alzheimer's disease modelling using induced pluripotent stem cell technology. *World Journal of Stem Cells* 6(2), p. 239. Available at: /pmc/articles/PMC3999781/ [Accessed: 22 June 2022].
- Mol, M.O. et al. 2022. Mapping the genetic landscape of early-onset Alzheimer's disease in a cohort of 36 families. *Alzheimer's Research & Therapy 2022 14:1* 14(1), pp. 1–14. Available at: https://alzres.biomedcentral.com/articles/10.1186/s13195-022-01018-3 [Accessed: 12 June 2022].

- Moloney, A., Sattelle, D.B., Lomas, D.A. and Crowther, D.C. 2010. Alzheimer's disease: insights from Drosophila melanogaster models. *Trends in biochemical sciences* 35(4), pp. 228–35. doi: 10.1016/j.tibs.2009.11.004.
- Mondal, K., Vijayraghavan, K. and Varadarajan, R. 2007. Design and utility of temperature-sensitive Gal4 mutants for conditional gene expression in Drosophila. *Fly* 1(5), pp. 282–286. Available at: https://pubmed.ncbi.nlm.nih.gov/18836309/ [Accessed: 24 March 2022].
- Montagne, A. et al. 2015. Blood-Brain Barrier Breakdown in the Aging Human Hippocampus. *Neuron* 85(2), p. 296. Available at: /pmc/articles/PMC4350773/ [Accessed: 25 July 2021].
- Moore, Z., Taylor, J.M. and Crack, P.J. 2019. The involvement of microglia in Alzheimer's disease: a new dog in the fight. *British Journal of Pharmacology* 176(18), p. 3533. Available at: /pmc/articles/PMC6715787/ [Accessed: 9 April 2022].
- Morgan, B.P. 2018. Complement in the pathogenesis of Alzheimer's disease. *Seminars in Immunopathology* 40(1), pp. 113–124. doi: 10.1007/S00281-017-0662-9.
- Morris, G.P., Clark, I.A. and Vissel, B. 2014. Inconsistencies and Controversies Surrounding the Amyloid Hypothesis of Alzheimer's Disease. *Acta Neuropathologica Communications* 2(1), pp. 1–21. Available at: https://actaneurocomms.biomedcentral.com/articles/10.1186/s40478-014-0135-5 [Accessed: 7 June 2022].
- Morris, J.C., Storandt, M., Miller, J.P., McKeel, D.W., Price, J.L., Rubin, E.H. and Berg, L. 2001. Mild cognitive impairment represents early-stage Alzheimer disease. *Archives of neurology* 58(3), pp. 397–405. Available at: https://pubmed.ncbi.nlm.nih.gov/11255443/ [Accessed: 7 June 2022].
- Morrison, J.H. and Baxter, M.G. 2012. The ageing cortical synapse: hallmarks and implications for cognitive decline. *Nature reviews. Neuroscience* 13(4), pp. 240–250. Available at: https://pubmed.ncbi.nlm.nih.gov/22395804/ [Accessed: 20 June 2022].
- Mukadam, A.S., Breusegem, S.Y. and Seaman, M.N.J. 2018. Analysis of novel endosome-to-Golgi retrieval genes reveals a role for PLD3 in regulating endosomal protein sorting and amyloid precursor protein processing. *Cellular and*

*molecular life sciences : CMLS* 75(14), pp. 2613–2625. Available at: https://pubmed.ncbi.nlm.nih.gov/29368044/ [Accessed: 2 April 2022].

- Murillo-Maldonado, J.M., Bou Zeineddine, F., Stock, R., Thackeray, J. and Riesgo-Escovar, J.R. 2011. Insulin Receptor-Mediated Signaling via Phospholipase C-γ Regulates Growth and Differentiation in Drosophila. *PLOS ONE* 6(11), p. e28067. Available at: https://journals.plos.org/plosone/article?id=10.1371/journal.pone.0028067 [Accessed: 30 March 2022].
- Murrell, J., Farlow, M., Ghetti, B. and Benson, M.D. 1991. A mutation in the amyloid precursor protein associated with hereditary Alzheimer's disease. *Science (New York, N.Y.)* 254(5028), pp. 97–99. Available at: https://pubmed.ncbi.nlm.nih.gov/1925564/ [Accessed: 22 June 2022].
- Musashe, D.T., Purice, M.D., Speese, S.D., Doherty, J. and Logan, M.A. 2016. Insulin-like Signaling Promotes Glial Phagocytic Clearance of Degenerating Axons through Regulation of Draper. *Cell Reports* 16(7), pp. 1838–1850. Available at: http://www.ncbi.nlm.nih.gov/pubmed/27498858 [Accessed: 2 March 2019].
- Musiek, E.S. and Holtzman, D.M. 2015. Three Dimensions of the Amyloid Hypothesis: Time, Space, and "Wingmen." *Nature neuroscience* 18(6), p. 800. Available at: /pmc/articles/PMC4445458/ [Accessed: 7 June 2022].
- Muth, C., Hartmann, A., Sepulveda-Falla, D., Glatzel, M. and Krasemann, S. 2019. Phagocytosis of Apoptotic Cells Is Specifically Upregulated in ApoE4 Expressing Microglia in vitro. *Frontiers in cellular neuroscience* 13. Available at: https://pubmed.ncbi.nlm.nih.gov/31130847/ [Accessed: 26 May 2022].
- Nackenoff, A.G. et al. 2021. PLD3 is a neuronal lysosomal phospholipase D associated with β-amyloid plaques and cognitive function in Alzheimer's disease. *PLOS Genetics* 17(4), p. e1009406. Available at: https://journals.plos.org/plosgenetics/article?id=10.1371/journal.pgen.1009406 [Accessed: 31 March 2022].
- Naj, A.C. et al. 2011. Common variants at MS4A4/MS4A6E, CD2AP, CD33 and EPHA1 are associated with late-onset Alzheimer's disease. *Nature Genetics* 43(5), pp. 436–443. doi: 10.1038/ng.801.

- Naslavsky, N., Weigert, R. and Donaldson, J.G. 2003. Convergence of Non-clathrin- and Clathrin-derived Endosomes Involves Arf6 Inactivation and Changes in Phosphoinositides. *Molecular Biology of the Cell* 14(2), p. 417. Available at: /pmc/articles/PMC149982/ [Accessed: 25 July 2022].
- Nayak, D., Roth, T.L. and McGavern, D.B. 2014. Microglia development and function. *Annual review of immunology* 32, pp. 367–402. Available at: https://pubmed.ncbi.nlm.nih.gov/24471431/ [Accessed: 14 June 2022].
- Neary, D. et al. 1986. Alzheimer's disease: a correlative study. *Journal of Neurology, Neurosurgery, and Psychiatry* 49(3), p. 229. Available at: /pmc/articles/PMC1028720/?report=abstract [Accessed: 25 July 2021].
- Neher, J.J., Neniskyte, U., Zhao, J.-W., Bal-Price, A., Tolkovsky, A.M. and Brown, G.C. 2011. Inhibition of microglial phagocytosis is sufficient to prevent inflammatory neuronal death. *Journal of immunology (Baltimore, Md. : 1950)* 186(8), pp. 4973–4983. Available at: https://pubmed.ncbi.nlm.nih.gov/21402900/ [Accessed: 26 May 2022].
- Neukomm, L.J. et al. 2011. The phosphoinositide phosphatase MTM-1 regulates apoptotic cell corpse clearance through CED-5-CED-12 in C. elegans. *Development (Cambridge, England)* 138(10), pp. 2003–2014. Available at: https://pubmed.ncbi.nlm.nih.gov/21490059/ [Accessed: 26 May 2022].
- Neumann, H., Kotter, M.R. and Franklin, R.J.M. 2008. Debris clearance by microglia: an essential link between degeneration and regeneration. *Brain* 132(2), pp. 288–295. Available at: http://www.ncbi.nlm.nih.gov/pubmed/18567623 [Accessed: 16 January 2019].
- Ni, J.Q. et al. 2008. Vector and parameters for targeted transgenic RNA interference in Drosophila melanogaster. *Nature Methods* 5(1), pp. 49–51. doi: 10.1038/nmeth1146.
- Nimmerjahn, A., Kirchhoff, F. and Helmchen, F. 2005. Resting microglial cells are highly dynamic surveillants of brain parenchyma in vivo. *Science (New York, N.Y.)* 308(5726), pp. 1314–1318. Available at: https://pubmed.ncbi.nlm.nih.gov/15831717/ [Accessed: 20 June 2022].
- Niraula, A., Sheridan, J.F. and Godbout, J.P. 2016. Microglia Priming with Aging and Stress. *Neuropsychopharmacology 2017 42:1* 42(1), pp. 318–333. Available at: https://www.nature.com/articles/npp2016185 [Accessed: 9 April 2022].

- Nixon, R.A. 2020. The aging lysosome: an essential catalyst for late-onset neurodegenerative diseases. *Biochimica et biophysica acta. Proteins and proteomics* 1868(9), p. 140443. Available at: /pmc/articles/PMC7388076/ [Accessed: 19 May 2022].
- Nizami, S., Hall-Roberts, H., Warrier, S., Cowley, S.A. and di Daniel, E. 2019. Microglial inflammation and phagocytosis in Alzheimer's disease: Potential therapeutic targets. *British journal of pharmacology* 176(18), pp. 3515–3532. Available at: https://pubmed.ncbi.nlm.nih.gov/30740661/ [Accessed: 26 May 2022].
- NM, de W., J, V., A, K., J, H. and HE, de V. 2017. Inflammation at the blood-brain barrier: The role of liver X receptors. *Neurobiology of disease* 107, pp. 57–65. Available at: https://pubmed.ncbi.nlm.nih.gov/27659108/ [Accessed: 25 July 2021].
- Noris, M. and Remuzzi, G. 2013. Overview of Complement Activation and Regulation. *Seminars in Nephrology* 33(6), p. 479. Available at: /pmc/articles/PMC3820029/ [Accessed: 20 June 2022].
- Novikova, G. et al. 2021a. Integration of Alzheimer's disease genetics and myeloid genomics identifies disease risk regulatory elements and genes. *Nature communications* 12(1). Available at: https://pubmed.ncbi.nlm.nih.gov/33712570/ [Accessed: 13 June 2022].
- Novikova, G., Andrews, S.J., Renton, A.E. and Marcora, E. 2021b. Beyond association: successes and challenges in linking non-coding genetic variation to functional consequences that modulate Alzheimer's disease risk. *Molecular Neurodegeneration* 16(1), pp. 1–13. Available at: https://molecularneurodegeneration.biomedcentral.com/articles/10.1186/s13024-021-00449-0 [Accessed: 12 June 2022].
- NR, S., DM, B., SJ, A., CC, S., D, N., DJ, T. and AN, D. 1983. Presynaptic cholinergic dysfunction in patients with dementia. *Journal of neurochemistry* 40(2), pp. 503–509. Available at: https://pubmed.ncbi.nlm.nih.gov/6822833/ [Accessed: 25 July 2021].
- Nunes, P. and Demaurex, N. 2010. The role of calcium signaling in phagocytosis. *Journal of leukocyte biology* 88(1), pp. 57–68. Available at: https://pubmed.ncbi.nlm.nih.gov/20400677/ [Accessed: 10 May 2022].

- Nunes-Hasler, P., Kaba, M. and Demaurex, N. 2020. Molecular Mechanisms of Calcium Signaling During Phagocytosis. *Advances in Experimental Medicine and Biology* 1246, pp. 103–128. Available at: https://link.springer.com/chapter/10.1007/978-3-030-40406-2_7 [Accessed: 10 May 2022].
- Obst, J. et al. 2021. PLCγ2 regulates TREM2 signalling and integrin-mediated adhesion and migration of human iPSC-derived macrophages. *Scientific Reports 2021 11:1* 11(1), pp. 1–17. Available at: https://www.nature.com/articles/s41598-021-96144-7 [Accessed: 25 April 2022].
- Oddo, S. et al. 2003. Triple-transgenic model of Alzheimer's disease with plaques and tangles: intracellular Abeta and synaptic dysfunction. *Neuron* 39(3), pp. 409–421. Available at: https://pubmed.ncbi.nlm.nih.gov/12895417/ [Accessed: 22 June 2022].
- Oddo, S., Billings, L., Kesslak, J.P., Cribbs, D.H. and LaFerla, F.M. 2004. Abeta immunotherapy leads to clearance of early, but not late, hyperphosphorylated tau aggregates via the proteasome. *Neuron* 43(3), pp. 321–332. Available at: https://pubmed.ncbi.nlm.nih.gov/15294141/ [Accessed: 22 June 2022].
- Ojelade, S.A. et al. 2019. cindr, the Drosophila Homolog of the CD2AP Alzheimer's Disease Risk Gene, Is Required for Synaptic Transmission and Proteostasis. *Cell reports* 28(7), pp. 1799-1813.e5. Available at: https://pubmed.ncbi.nlm.nih.gov/31412248/ [Accessed: 22 June 2022].
- O'Keefe, L. and Denton, D. 2018. Using Drosophila Models of Amyloid Toxicity to Study Autophagy in the Pathogenesis of Alzheimer's Disease. *BioMed Research International* 2018. Available at: /pmc/articles/PMC5985114/ [Accessed: 22 June 2022].
- Oliveira, T.G. et al. 2010. Phospholipase D2 Ablation Ameliorates Alzheimer's Disease-Linked Synaptic Dysfunction and Cognitive Deficits. *The Journal of Neuroscience* 30(49), p. 16419. Available at: /pmc/articles/PMC3004537/ [Accessed: 13 April 2022].
- Oliveira-Pinto, A. v. et al. 2014. Sexual dimorphism in the human olfactory bulb: females have more neurons and glial cells than males. *PloS one* 9(11). Available at: https://pubmed.ncbi.nlm.nih.gov/25372872/ [Accessed: 6 July 2022].

- Osaki, M., Oshimura, M. and Ito, H. 2004. PI3K-Akt pathway: its functions and alterations in human cancer. *Apoptosis : an international journal on programmed cell death* 9(6), pp. 667–676. Available at: https://pubmed.ncbi.nlm.nih.gov/15505410/ [Accessed: 13 April 2022].
- Otani, Y., Yamaguchi, Y., Sato, Y., Furuichi, T., Ikenaka, K., Kitani, H. and Baba, H. 2011. PLD4 Is Involved in Phagocytosis of Microglia: Expression and Localization Changes of PLD4 Are Correlated with Activation State of Microglia. *PLOS ONE* 6(11), p. e27544. Available at: https://journals.plos.org/plosone/article?id=10.1371/journal.pone.0027544 [Accessed: 24 April 2022].
- Ou, J., He, Y., Xiao, X., Yu, T.M., Chen, C., Gao, Z. and Ho, M.S. 2014. Glial cells in neuronal development: Recent advances and insights from Drosophila melanogaster. *Neuroscience Bulletin* 30(4), pp. 584–594. doi: 10.1007/S12264-014-1448-2.
- Pająk, B., Kania, E. and Orzechowski, A. 2016. Killing Me Softly: Connotations to Unfolded Protein Response and Oxidative Stress in Alzheimer's Disease. *Oxidative medicine and cellular longevity* 2016. Available at: https://pubmed.ncbi.nlm.nih.gov/26881014/ [Accessed: 7 June 2022].
- Palmer, A.L. and Ousman, S.S. 2018. Astrocytes and Aging. *Frontiers in Aging Neuroscience* 10, p. 337. Available at: /pmc/articles/PMC6212515/ [Accessed: 7 July 2022].
- Pan, X.D., Zhu, Y.G., Lin, N., Zhang, J., Ye, Q.Y., Huang, H.P. and Chen, X.C. 2011. Microglial phagocytosis induced by fibrillar β-amyloid is attenuated by oligomeric β-amyloid: Implications for Alzheimer's disease. *Molecular Neurodegeneration* 6(1), pp. 1–18. Available at: https://molecularneurodegeneration.biomedcentral.com/articles/10.1186/1750-1326-6-45 [Accessed: 20 June 2022].
- Pandey, U.B. and Nichols, C.D. 2011. Human Disease Models in Drosophila melanogaster and the Role of the Fly in Therapeutic Drug Discovery. *Pharmacological Reviews* 63(2), p. 411. Available at: /pmc/articles/PMC3082451/ [Accessed: 22 June 2022].
- Paquet, D. et al. 2009. A zebrafish model of tauopathy allows in vivo imaging of neuronal cell death and drug evaluation. *The Journal of clinical investigation*

119(5), pp. 1382–1395. Available at: https://pubmed.ncbi.nlm.nih.gov/19363289/ [Accessed: 22 June 2022].

- Paquet, D. et al. 2016. Efficient introduction of specific homozygous and heterozygous mutations using CRISPR/Cas9. *Nature* 533(7601), pp. 125–129. Available at: https://pubmed.ncbi.nlm.nih.gov/27120160/ [Accessed: 22 June 2022].
- Paranjpe, M.D. et al. 2021. Sex-Specific Cross Tissue Meta-Analysis Identifies Immune Dysregulation in Women With Alzheimer's Disease. *Frontiers in Aging Neuroscience* 13, p. 622. doi: 10.3389/FNAGI.2021.735611/BIBTEX.
- Parekh, A., Fadiran, E.O., Uhl, K. and Throckmorton, D.C. 2011. Adverse effects in women: Implications for drug development and regulatory policies. *Expert Review of Clinical Pharmacology* 4(4), pp. 453–466. doi: 10.1586/ECP.11.29.
- Park, J. et al. 2018a. A 3D human triculture system modeling neurodegeneration and neuroinflammation in Alzheimer's disease. *Nature neuroscience* 21(7), pp. 941–951. Available at: https://pubmed.ncbi.nlm.nih.gov/29950669/ [Accessed: 22 June 2022].
- Park, S., Lee, J.H., Jeon, J.H. and Lee, M.J. 2018b. Degradation or aggregation: the ramifications of post-translational modifications on tau. *BMB reports* 51(6), pp. 265–273. Available at: https://pubmed.ncbi.nlm.nih.gov/29661268/ [Accessed: 10 June 2022].
- Pearson, J. V et al. 2007. Identification of the genetic basis for complex disorders by use of pooling-based genomewide single-nucleotide-polymorphism association studies. *American journal of human genetics* 80(1), pp. 126–39. doi: 10.1086/510686.
- Pelvig, D.P., Pakkenberg, H., Stark, A.K. and Pakkenberg, B. 2008. Neocortical glial cell numbers in human brains. *Neurobiology of aging* 29(11), pp. 1754–1762. Available at: https://pubmed.ncbi.nlm.nih.gov/17544173/ [Accessed: 26 July 2022].
- Peng, I.F., Berke, B.A., Zhu, Y., Lee, W.H., Chen, W. and Wu, C.F. 2007. Temperature-Dependent Developmental Plasticity of Drosophila Neurons: Cell-Autonomous Roles of Membrane Excitability, Ca2+ Influx, and cAMP Signaling. *The Journal of Neuroscience* 27(46), p. 12611. Available at: /pmc/articles/PMC6673343/ [Accessed: 24 March 2022].

- Peng, Q., Malhotra, S., Torchia, J.A., Kerr, W.G., Coggeshall, K.M. and Humphrey, M.B. 2010. TREM2- and DAP12-dependent activation of PI3K requires DAP10 and is inhibited by SHIP1. *Science signaling* 3(122). Available at: https://pubmed.ncbi.nlm.nih.gov/20484116/ [Accessed: 26 May 2022].
- Peri, F. and Nüsslein-Volhard, C. 2008. Live imaging of neuronal degradation by microglia reveals a role for v0-ATPase a1 in phagosomal fusion in vivo. *Cell* 133(5), pp. 916–927. Available at: https://pubmed.ncbi.nlm.nih.gov/18510934/ [Accessed: 20 June 2022].
- Perry, E.K., Tomlinson, B.E., Blessed, G., Bergmann, K., Gibson, P.H. and Perry, R.H. 1978. Correlation of cholinergic abnormalities with senile plaques and mental test scores in senile dementia. *British Medical Journal* 2(6150), p. 1457. Available at: /pmc/articles/PMC1608703/?report=abstract [Accessed: 25 July 2021].
- Perry, V.H. and Teeling, J. 2013. Microglia and macrophages of the central nervous system: the contribution of microglia priming and systemic inflammation to chronic neurodegeneration. *Seminars in Immunopathology* 35(5), p. 601. Available at: /pmc/articles/PMC3742955/ [Accessed: 13 June 2022].
- Peters, A. 2002. The effects of normal aging on myelin and nerve fibers: a review. *Journal of neurocytology* 31(8–9), pp. 581–593. Available at: https://pubmed.ncbi.nlm.nih.gov/14501200/ [Accessed: 20 June 2022].
- Peters, A., Moss, M.B. and Sethares, C. 2000. Effects of Aging on Myelinated Nerve Fibers in Monkey Primary Visual Cortex. *J. Comp. Neurol* 419, pp. 364–376.
- Petersen, E.N., Chung, H.W., Nayebosadri, A. and Hansen, S.B. 2016. Kinetic disruption of lipid rafts is a mechanosensor for phospholipase D. *Nature Communications* 7, pp. 13873–13873. Available at: https://europepmc.org/articles/PMC5171650 [Accessed: 27 April 2022].
- Pfaffl, M.W. 2001. A new mathematical model for relative quantification in real-time RT-PCR. *Nucleic acids research* 29(9), p. E45. Available at: https://pubmed.ncbi.nlm.nih.gov/11328886/ [Accessed: 5 July 2022].
- Phillips, A.E.M., Llerena, C. v, Piers, T.M., Cosker, K. and Hardy, J. 2018. Loss of Function of TREM2 Results in Cytoskeletal Malfunction in Microglia. *J Neurol*

*Neurobiol* 4(3). Available at: http://dx.doi.org/10.16966/2379-7150.152 [Accessed: 20 June 2022].

- Plesnila, N., Müller, E., Guretzki, S., Ringel, F., Staub, F. and Baethmann, A. 2000. Effect of hypothermia on the volume of rat glial cells. *The Journal of Physiology* 523(Pt 1), p. 155. Available at: /pmc/articles/PMC2269776/ [Accessed: 6 July 2022].
- Pluskota, E. et al. 2011. The integrin coactivator Kindlin-2 plays a critical role in angiogenesis in mice and zebrafish. *Blood* 117(18), pp. 4978–4987. doi: 10.1182/blood-2010-11-321182.
- Pohanka, M. 2011. Cholinesterases, a target of pharmacology and toxicology. *Biomedical Papers* 155(3), pp. 219–230. doi: 10.5507/BP.2011.036.
- Polvikoski, T. et al. 1995. Apolipoprotein E, Dementia, and Cortical Deposition of β-Amyloid Protein. *New England Journal of Medicine* 333(19), pp. 1242–1248. doi: 10.1056/NEJM199511093331902.
- Poon, R., Khanijow, K., Umarjee, S., Fadiran, E., Yu, M., Zhang, L. and Parekh, A. 2013. Participation of women and sex analyses in late-phase clinical trials of new molecular entity drugs and biologics approved by the FDA in 2007-2009. *Journal of Women's Health* 22(7), pp. 604–616. doi: 10.1089/JWH.2012.3753.
- Powe, A.C. et al. 1999. In vivo functional analysis of Drosophila Gap1: involvement of Ca2+ and IP4 regulation. *Mechanisms of development* 81(1–2), pp. 89–101. Available at: https://pubmed.ncbi.nlm.nih.gov/10330487/ [Accessed: 2 April 2022].
- Price, J.L. et al. 2009. Neuropathology of nondemented aging: presumptive evidence for preclinical Alzheimer disease. *Neurobiology of aging* 30(7), pp. 1026–36. Available at: http://www.ncbi.nlm.nih.gov/pubmed/19376612 [Accessed: 11 May 2019].
- PT, F., DM, B., SL, L., D, N., DM, M. and JS, S. 1987. Somatostatin content and release measured in cerebral biopsies from demented patients. *Journal of the neurological sciences* 78(1), pp. 1–16. Available at: https://pubmed.ncbi.nlm.nih.gov/3572446/ [Accessed: 25 July 2021].
- PT, F., NR, S., AW, P. and DM, B. 1993. Cortical pyramidal neurone loss may cause glutamatergic hypoactivity and cognitive impairment in Alzheimer's disease: investigative and therapeutic perspectives. *Journal of neurochemistry*

60(5), pp. 1589–1604. Available at: https://pubmed.ncbi.nlm.nih.gov/8473885/ [Accessed: 25 July 2021].

- Purice, M.D., Ray, A., Münzel, E.J., Pope, B.J., Park, D.J., Speese, S.D. and Logan, M.A. 2017. A novel Drosophila injury model reveals severed axons are cleared through a Draper/MMP-1 signaling cascade. *eLife* 6. Available at: http://www.ncbi.nlm.nih.gov/pubmed/28825401 [Accessed: 4 March 2019].
- Purice, M.D., Speese, S.D. and Logan, M.A. 2016. Delayed glial clearance of degenerating axons in aged Drosophila is due to reduced PI3K/Draper activity. *Nature communications* 7. Available at: https://pubmed.ncbi.nlm.nih.gov/27647497/ [Accessed: 2 April 2022].
- Putney, J.W. and Tomita, T. 2012. Phospholipase C Signaling and Calcium Influx. *Advances in biological regulation* 52(1), p. 152. Available at: /pmc/articles/PMC3560308/ [Accessed: 18 July 2022].
- Qiu, S., Adema, C.M. and Lane, T. 2005. A computational study of off-target effects of RNA interference. *Nucleic Acids Research* 33(6), pp. 1834–1847. Available at: https://academic.oup.com/nar/article-lookup/doi/10.1093/nar/gki324 [Accessed: 16 September 2018].
- Rafii, M.S. and Aisen, P.S. 2020. The search for Alzheimer disease therapeutics — same targets, better trials? *Nature Reviews Neurology 2020 16:11* 16(11), pp. 597–598. Available at: https://www.nature.com/articles/s41582-020-00414-3 [Accessed: 26 May 2022].
- Raj, T. et al. 2014. Polarization of the effects of autoimmune and neurodegenerative risk alleles in leukocytes. *Science (New York, N.Y.)* 344(6183), pp. 519–523. Available at: https://pubmed.ncbi.nlm.nih.gov/24786080/ [Accessed: 13 June 2022].
- Rajendran, L. and Paolicelli, R.C. 2018. Microglia-Mediated Synapse Loss in Alzheimer's Disease. *The Journal of neuroscience : the official journal of the Society for Neuroscience* 38(12), pp. 2911–2919. Available at: https://pubmed.ncbi.nlm.nih.gov/29563239/ [Accessed: 2 April 2022].
- Ramos-Cejudo, J., Wisniewski, T., Marmar, C., Zetterberg, H., Blennow, K., de Leon, M.J. and Fossati, S. 2018. Traumatic Brain Injury and Alzheimer's Disease: The Cerebrovascular Link. *EBioMedicine* 28, p. 21. Available at: /pmc/articles/PMC5835563/ [Accessed: 25 July 2022].

- Rao, Y.L., Ganaraja, B., Murlimanju, B. v., Joy, T., Krishnamurthy, A. and Agrawal, A. 2022. Hippocampus and its involvement in Alzheimer's disease: a review. *3 Biotech* 12(2), p. 55. Available at: /pmc/articles/PMC8807768/ [Accessed: 7 June 2022].
- Ray, A., Speese, S.D. and Logan, M.A. 2017. Glial Draper Rescues Aβ Toxicity in a *Drosophila* Model of Alzheimer's Disease. *The Journal of Neuroscience* 37(49), pp. 11881–11893. Available at: http://www.jneurosci.org/lookup/doi/10.1523/JNEUROSCI.0862-17.2017 [Accessed: 5 October 2018].
- Reitz, C. and Mayeux, R. 2014. Alzheimer disease: epidemiology, diagnostic criteria, risk factors and biomarkers. *Biochemical pharmacology* 88(4), pp. 640–51. Available at: http://www.ncbi.nlm.nih.gov/pubmed/24398425 [Accessed: 3 October 2018].
- Reitz, C., Rogaeva, E. and Beecham, G.W. 2020. Late-onset vs nonmendelian early-onset Alzheimer disease: A distinction without a difference? *Neurology: Genetics* 6(5). Available at: /pmc/articles/PMC7673282/ [Accessed: 7 June 2022].
- Reversi, A., Loeser, E., Subramanian, D., Schultz, C. and de Renzis, S. 2014. Plasma membrane phosphoinositide balance regulates cell shape during Drosophila embryo morphogenesis. *The Journal of Cell Biology* 205(3), p. 395. Available at: /pmc/articles/PMC4018783/ [Accessed: 29 April 2022].
- Richmond-Rakerd, L.S., D'Souza, S., Milne, B.J., Caspi, A. and Moffitt, T.E. 2022. Longitudinal Associations of Mental Disorders with Dementia: 30-Year Analysis of 1.7 Million New Zealand Citizens. *JAMA Psychiatry* 79(4), pp. 333–340. doi: 10.1001/JAMAPSYCHIATRY.2021.4377.
- Ries, M. and Sastre, M. 2016. Mechanisms of Aβ Clearance and Degradation by Glial Cells. *Frontiers in aging neuroscience* 8(JUN). Available at: https://pubmed.ncbi.nlm.nih.gov/27458370/ [Accessed: 20 June 2022].
- *Rivastigmine: MedlinePlus Drug Information* [no date]. Available at: https://medlineplus.gov/druginfo/meds/a602009.html [Accessed: 22 June 2022].
- Rocchi, A., Pellegrini, S., Siciliano, G. and Murri, L. 2003. Causative and susceptibility genes for Alzheimer's disease: a review. *Brain research bulletin* 61(1), pp. 1–24. Available at: https://pubmed.ncbi.nlm.nih.gov/12788204/ [Accessed: 26 May 2022].

- Rock, K.L. and Kono, H. 2008. The inflammatory response to cell death. *Annual review of pathology* 3, p. 99. Available at: /pmc/articles/PMC3094097/ [Accessed: 13 June 2022].
- Rolova, T., Zhang, F., Koskuvi, M. and Koistinaho, J. 2020. The role of ABI3 in human induced pluripotent stem cell-derived microglia. *Alzheimer's & Dementia* 16(S3), p. e047270. Available at: https://doi.org/10.1002/alz.047270 [Accessed: 6 May 2021].
- Roote, J. and Prokop, A. 2013. How to Design a Genetic Mating Scheme: A Basic Training Package for *Drosophila* Genetics. *G3: Genes|Genomes|Genetics* 3(2), pp. 353–358. Available at: http://www.ncbi.nlm.nih.gov/pubmed/23390611 [Accessed: 16 September 2018].
- Rossor, M. and Iversen, L.L. 1986. NON-CHOLINERGIC NEUROTRANSMITTER ABNORMALITIES IN ALZHEIMER'S DISEASE. *British Medical Bulletin* 42(1), pp. 70–74. Available at: https://academic.oup.com/bmb/article/42/1/70/330681 [Accessed: 25 July 2021].
- Ruijter, J.M., Ramakers, C., Hoogaars, W.M.H., Karlen, Y., Bakker, O., van den hoff, M.J.B. and Moorman, A.F.M. 2009. Amplification efficiency: linking baseline and bias in the analysis of quantitative PCR data. *Nucleic acids research* 37(6). Available at: https://pubmed.ncbi.nlm.nih.gov/19237396/ [Accessed: 5 July 2022].
- Ruiz, A. et al. 2014. Follow-up of loci from the International Genomics of Alzheimer's Disease Project identifies TRIP4 as a novel susceptibility gene. *Translational Psychiatry* 4. doi: 10.1038/tp.2014.2.
- S, F.-Z. and IA, N. 2018. Management of Measurable Variable Cardiovascular Disease' Risk Factors. *Current cardiology reviews* 14(3), pp. 153–163. Available at: https://pubmed.ncbi.nlm.nih.gov/29473518/ [Accessed: 25 July 2021].
- S, L. and JS, M. 2016. Cerebrovascular disease in ageing and Alzheimer's disease. *Acta neuropathologica* 131(5), pp. 645–658. Available at: https://pubmed.ncbi.nlm.nih.gov/26711459/ [Accessed: 25 July 2021].
- Sakamoto, S. et al. 2016. Individual risk alleles of susceptibility to schizophrenia are associated with poor clinical and social outcomes. *Journal of Human Genetics* 61(4), pp. 329–334. doi: 10.1038/jhg.2015.153.

- Salter, M.W. and Beggs, S. 2014. Sublime microglia: expanding roles for the guardians of the CNS. *Cell* 158(1), pp. 15–24. Available at: https://pubmed.ncbi.nlm.nih.gov/24995975/ [Accessed: 26 July 2022].
- Sanjuan, M.A. and Green, D.R. 2008. Eating for good health: Linking autophagy and phagocytosis in host defense. *Autophagy* 4(5), pp. 607–611. Available at: https://www.tandfonline.com/action/journalInformation?journalCode=kaup20 [Accessed: 24 April 2022].
- Satoh, J.I., Kino, Y., Yamamoto, Y., Kawana, N., Ishida, T., Saito, Y. and Arima, K. 2014. PLD3 is accumulated on neuritic plaques in Alzheimer's disease brains. *Alzheimer's Research and Therapy* 6(9), pp. 1–13. Available at: https://alzres.biomedcentral.com/articles/10.1186/s13195-014-0070-5 [Accessed: 2 April 2022].
- Scarpelli, E.M., Trinh, V.Y., Tashnim, Z., Krans, J.L., Keller, L.C. and Colodner, K.J. 2019. Developmental expression of human tau in Drosophila melanogaster glial cells induces motor deficits and disrupts maintenance of PNS axonal integrity, without affecting synapse formation. *PLoS ONE* 14(12). Available at: /pmc/articles/PMC6903755/ [Accessed: 22 June 2022].
- Schafer, D.P. and Stevens, B. 2013. Phagocytic glial cells: sculpting synaptic circuits in the developing nervous system. *Current opinion in neurobiology* 23(6), pp. 1034–1040. Available at: https://pubmed.ncbi.nlm.nih.gov/24157239/ [Accessed: 20 June 2022].
- Scheffer, S., Hermkens, D.M.A., Weerd, L. van der, Vries, H.E. de and Daemen, M.J.A.P. 2021. Vascular Hypothesis of Alzheimer Disease. *Arteriosclerosis, Thrombosis, and Vascular Biology* 41, pp. 1265–1283. Available at: https://www.ahajournals.org/doi/abs/10.1161/ATVBAHA.120.311911 [Accessed: 25 July 2021].
- Scheib, J.L., Sullivan, C.S. and Carter, B.D. 2012. Jedi-1 and MEGF10 Signal Engulfment of Apoptotic Neurons through the Tyrosine Kinase Syk. *The Journal of Neuroscience* 32(38), p. 13022. Available at: /pmc/articles/PMC3464495/ [Accessed: 2 April 2022].
- Schlesinger, A., Kiger, A., Perrimon, N. and Shilo, B.Z. 2004. Small Wing PLCγ Is Required for ER Retention of Cleaved Spitz during Eye Development in

Drosophila. *Developmental Cell* 7(4), pp. 535–545. doi: 10.1016/J.DEVCEL.2004.09.001.

- Schulte, E.C. et al. 2015. Excess of rare coding variants in PLD3 in late- but not early-onset Alzheimer's disease. *Human genome variation* 2(1). Available at: https://pubmed.ncbi.nlm.nih.gov/27081517/ [Accessed: 2 April 2022].
- Scott, C.C. et al. 2005. Phosphatidylinositol-4,5-bisphosphate hydrolysis directs actin remodeling during phagocytosis. *The Journal of cell biology* 169(1), pp. 139–149. Available at: https://pubmed.ncbi.nlm.nih.gov/15809313/ [Accessed: 10 May 2022].
- Sekino, S. et al. 2015. The NESH/Abi-3-based WAVE2 complex is functionally distinct from the Abi-1-based WAVE2 complex. *Cell Communication and Signaling* 13(1), p. 41. Available at: http://www.biosignaling.com/content/13/1/41 [Accessed: 11 May 2019].
- Sekiya, M. et al. 2018. Integrated biology approach reveals molecular and pathological interactions among Alzheimer's Aβ42, Tau, TREM2, and TYROBP in Drosophila models. *Genome Medicine* 10(1). Available at: /pmc/articles/PMC5875009/ [Accessed: 22 June 2022].
- Selkoe, D.J. and Hardy, J. 2016. The amyloid hypothesis of Alzheimer's disease at 25 years. *EMBO Molecular Medicine* 8(6), pp. 595–608. Available at: https://onlinelibrary.wiley.com/doi/full/10.15252/emmm.201606210 [Accessed: 7 June 2022].
- Seo, J.W., Kim, J.H., Kim, J.H., Seo, M., Han, H.S., Park, J. and Suk, K. 2012. Time-dependent effects of hypothermia on microglial activation and migration. *Journal of Neuroinflammation* 9(1), pp. 1–22. Available at: https://jneuroinflammation.biomedcentral.com/articles/10.1186/1742-2094-9-164 [Accessed: 6 July 2022].
- Seshadri, S. et al. 2010. Genome-wide analysis of genetic loci associated with Alzheimer disease. *JAMA - Journal of the American Medical Association* 303(18), pp. 1832–1840. Available at: http://www.ncbi.nlm.nih.gov/pubmed/20460622 [Accessed: 24 April 2020].
- Sevigny, J. et al. 2016. The antibody aducanumab reduces Aβ plaques in Alzheimer's disease. *Nature 2016 537:7618* 537(7618), pp. 50–56. Available at: https://www.nature.com/articles/nature19323 [Accessed: 9 June 2022].

- Shah, E.J., Gurdziel, K. and Ruden, D.M. 2020. Drosophila Exhibit Divergent Sex-Based Responses in Transcription and Motor Function After Traumatic Brain Injury. *Frontiers in Neurology* 11, p. 511. doi: 10.3389/FNEUR.2020.00511/BIBTEX.
- Shen, J., Ford, D., Landis, G.N. and Tower, J. 2009. Identifying sexual differentiation genes that affect Drosophila life span. *BMC Geriatrics* 9(1), pp. 1–13. Available at: https://bmcgeriatr.biomedcentral.com/articles/10.1186/1471-2318-9-56 [Accessed: 23 March 2022].
- Shi, Q. et al. 2017. Complement C3 deficiency protects against neurodegeneration in aged plaque-rich APP/PS1 mice. *Science translational medicine* 9(392). Available at: https://pubmed.ncbi.nlm.nih.gov/28566429/ [Accessed: 20 June 2022].
- Shi, Y. and Holtzman, D.M. 2018. Interplay between innate immunity and Alzheimer disease: APOE and TREM2 in the spotlight. *Nature Reviews Immunology* 18(12), pp. 759–772. Available at: http://www.nature.com/articles/s41577-018-0051-1 [Accessed: 18 June 2019].
- Shigemizu, D. et al. 2021. Ethnic and trans-ethnic genome-wide association studies identify new loci influencing Japanese Alzheimer's disease risk. *Translational Psychiatry* 11(1), pp. 1–10. Available at: https://doi.org/10.1038/s41398-021-01272-3 [Accessed: 4 May 2021].
- Shirey, J.K. et al. 2009. A selective allosteric potentiator of the M1 muscarinic acetylcholine receptor increases activity of medial prefrontal cortical neurons and restores impairments in reversal learning. *Journal of Neuroscience* 29(45), pp. 14271–14286. Available at: /record/2009-22017-030 [Accessed: 11 June 2022].
- Shirotani, K. et al. 2019. Aminophospholipids are signal-transducing TREM2 ligands on apoptotic cells. *Scientific Reports 2019 9:1* 9(1), pp. 1–9. Available at: https://www.nature.com/articles/s41598-019-43535-6 [Accessed: 15 June 2022].
- Shklyar, B., Levy-Adam, F. and Kurant, E. 2015. Drosophila Drosophila Model for Studying PhagocytosisPhagocytosis Following Neuronal Cell DeathNeuronal Cell Death. In: *Methods in molecular biology (Clifton, N.J.)*., pp. 359–368. Available at: http://www.ncbi.nlm.nih.gov/pubmed/25431078 [Accessed: 11 February 2019].
- Shulman, J.M. et al. 2014. Functional screening in Drosophila identifies Alzheimer's disease susceptibility genes and implicates Tau-mediated

mechanisms. *Human Molecular Genetics* 23(4), pp. 870–877. Available at: https://academic.oup.com/hmg/article/23/4/870/635149 [Accessed: 22 June 2022].

- Sigrist, S.J., Reiff, D.F., Thiel, P.R., Steinert, J.R. and Schuster, C.M. 2003. Experience-dependent strengthening of Drosophila neuromuscular junctions. *The Journal of neuroscience : the official journal of the Society for Neuroscience* 23(16), pp. 6546–6556. Available at: https://pubmed.ncbi.nlm.nih.gov/12878696/ [Accessed: 24 March 2022].
- Sims, R. et al. 2017. Rare coding variants in PLCG2, ABI3, and TREM2 implicate microglial-mediated innate immunity in Alzheimer's disease. *Nature Genetics* 49(9), pp. 1373–1384. Available at: http://www.nature.com/doifinder/10.1038/ng.3916 [Accessed: 16 October 2018].
- Sims, R., Hill, M. and Williams, J. 2020. The multiplex model of the genetics of Alzheimer's disease. *Nature Neuroscience 2020 23:3* 23(3), pp. 311–322. Available at: https://www.nature.com/articles/s41593-020-0599-5 [Accessed: 12 June 2022].
- Singh, J. and Aballay, A. 2020. Neuro-immune circuits in C. elegans. *Current opinion in neurobiology* 62, p. 34. Available at: /pmc/articles/PMC7272302/ [Accessed: 22 June 2022].
- Skibinski, G. et al. 2005. Mutations in the endosomal ESCRTIII-complex subunit CHMP2B in frontotemporal dementia. *Nature Genetics* 37(8), pp. 806–808. doi: 10.1038/ng1609.
- SL, L., DM, B., PT, F. and D, N. 1990. Ante mortem cerebral amino acid concentrations indicate selective degeneration of glutamate-enriched neurons in Alzheimer's disease. *Neuroscience* 38(3), pp. 571–577. Available at: https://pubmed.ncbi.nlm.nih.gov/1980143/ [Accessed: 25 July 2021].
- Slaby, O. and Lebiedz, D. 2009. Oscillatory NAD(P)H waves and calcium oscillations in neutrophils? A modeling study of feasibility. *Biophysical Journal* 96(2), pp. 417–428. doi: 10.1016/j.bpj.2008.09.044.
- Slanzi, A., Iannoto, G., Rossi, B., Zenaro, E. and Constantin, G. 2020. In vitro Models of Neurodegenerative Diseases. *Frontiers in Cell and Developmental Biology* 8, p. 328. doi: 10.3389/FCELL.2020.00328/BIBTEX.

- Sleegers, K. and van Broeckhoven, C. 2019. Novel Alzheimer's disease risk genes: exhaustive investigation is paramount. *Acta Neuropathologica* 138(2), pp. 171–172. doi: 10.1007/s00401-019-02041-9.
- Sloan, S.A. et al. 2017. Human Astrocyte Maturation Captured in 3D Cerebral Cortical Spheroids Derived from Pluripotent Stem Cells. *Neuron* 95(4), p. 779. Available at: /pmc/articles/PMC5890820/ [Accessed: 20 June 2022].
- Smith, A.D. 2002. Imaging the progression of Alzheimer pathology through the brain. *Proceedings of the National Academy of Sciences of the United States of America* 99(7), pp. 4135–4137. doi: 10.1073/PNAS.082107399/ASSET/18FC91BA-3BF4-45DA-B9A7-FE39EB0856A6/ASSETS/GRAPHIC/PQ0821073003.JPEG.
- Smith, A.R. et al. 2019. Parallel profiling of DNA methylation and hydroxymethylation highlights neuropathology-associated epigenetic variation in Alzheimer's disease. *Clinical epigenetics* 11(1). Available at: https://pubmed.ncbi.nlm.nih.gov/30898171/ [Accessed: 12 June 2022].
- Smith, R.G. et al. 2018. Elevated DNA methylation across a 48-kb region spanning the HOXA gene cluster is associated with Alzheimer's disease neuropathology. *Alzheimer's & dementia : the journal of the Alzheimer's Association* 14(12), pp. 1580–1588. Available at: https://pubmed.ncbi.nlm.nih.gov/29550519/ [Accessed: 12 June 2022].
- Soderling, T.R. 1999. The Ca-calmodulin-dependent protein kinase cascade. *Trends in biochemical sciences* 24(6), pp. 232–236. Available at: https://pubmed.ncbi.nlm.nih.gov/10366852/ [Accessed: 27 April 2022].
- Solé-Domènech, S., Cruz, D.L., Capetillo-Zarate, E. and Maxfield, F.R. 2016. The Endocytic Pathway in Microglia During Health, Aging and Alzheimer's Disease. *Ageing research reviews* 32, p. 89. Available at: /pmc/articles/PMC5127718/ [Accessed: 19 May 2022].
- Song, W.M., Joshita, S., Zhou, Y., Ulland, T.K., Gilfillan, S. and Colonna, M. 2018. Humanized TREM2 mice reveal microglia-intrinsic and -extrinsic effects of R47H polymorphism. *The Journal of Experimental Medicine* 215(3), p. 745. Available at: /pmc/articles/PMC5839761/ [Accessed: 26 July 2022].

- Soreq, L. et al. 2017. Major Shifts in Glial Regional Identity Are a Transcriptional Hallmark of Human Brain Aging. *Cell Reports* 18(2), p. 557. Available at: /pmc/articles/PMC5263238/ [Accessed: 7 July 2022].
- Spillantini, M.G. and Goedert, M. 2013. Tau pathology and neurodegeneration. *The Lancet. Neurology* 12(6), pp. 609–622. Available at: https://pubmed.ncbi.nlm.nih.gov/23684085/ [Accessed: 10 June 2022].
- Spittau, B. 2017. Aging Microglia—Phenotypes, Functions and Implications for Age-Related Neurodegenerative Diseases. *Frontiers in Aging Neuroscience* 9(JUN). Available at: /pmc/articles/PMC5469878/ [Accessed: 9 April 2022].
- Spletter, M.L. et al. 2015. The RNA-binding protein Arrest (Bruno) regulates alternative splicing to enable myofibril maturation in Drosophila flight muscle. *EMBO reports* 16(2), pp. 178–191. Available at: http://www.ncbi.nlm.nih.gov/pubmed/25532219 [Accessed: 11 May 2019].
- Spring, S., Lerch, J.P. and Henkelman, R.M. 2007. Sexual dimorphism revealed in the structure of the mouse brain using three-dimensional magnetic resonance imaging. *NeuroImage* 35(4), pp. 1424–1433. Available at: https://pubmed.ncbi.nlm.nih.gov/17408971/ [Accessed: 23 March 2022].
- Srinivasan, K. et al. 2016. Untangling the brain's neuroinflammatory and neurodegenerative transcriptional responses. *Nature Communications* 7(1), p. 11295. Available at: http://www.nature.com/articles/ncomms11295 [Accessed: 11 May 2019].
- ST, D., SW, S. and SD, S. 1996. Structural correlates of cognition in dementia: quantification and assessment of synapse change. *Neurodegeneration : a journal for neurodegenerative disorders, neuroprotection, and neuroregeneration* 5(4), pp. 417–421. Available at: https://pubmed.ncbi.nlm.nih.gov/9117556/ [Accessed: 25 July 2021].
- Steelman, Z.A., Tolstykh, G.P., Estlack, L.E., Roth, C.C. and Ibey, B.L. 2015. The role of PIP2 and the IP3/DAG pathway in intracellular calcium release and cell survival during nanosecond electric pulse exposures. *https://doi.org/10.1117/12.2079928* 9326, pp. 255–260. Available at: https://www.spiedigitallibrary.org/conference-proceedings-of-spie/9326/932611/The-role-of-PIP2-and-the-IP3-DAG-pathway-in/10.1117/12.2079928.full [Accessed: 9 May 2022].

- Stephan, A.H. et al. 2013. A dramatic increase of C1q protein in the CNS during normal aging. *The Journal of neuroscience : the official journal of the Society for Neuroscience* 33(33), pp. 13460–13474. Available at: https://pubmed.ncbi.nlm.nih.gov/23946404/ [Accessed: 20 June 2022].
- Stephan, A.H., Barres, B.A. and Stevens, B. 2012. The complement system: an unexpected role in synaptic pruning during development and disease. *Annual review of neuroscience* 35, pp. 369–389. Available at: https://pubmed.ncbi.nlm.nih.gov/22715882/ [Accessed: 20 June 2022].
- Stephan, Y., Sutin, A.R., Luchetti, M. and Terracciano, A. 2018. Subjective Age and Risk of Incident Dementia: Evidence from the National Health and Aging Trends Survey. *Journal of psychiatric research* 100, p. 1. Available at: /pmc/articles/PMC5866231/ [Accessed: 9 April 2022].
- Stevens, B. et al. 2007. The Classical Complement Cascade Mediates CNS Synapse Elimination. *Cell* 131(6), pp. 1164–1178. doi: 10.1016/J.CELL.2007.10.036.
- Stokin, G.B. et al. 2008. Amyloid precursor protein-induced axonopathies are independent of amyloid-beta peptides. *Human molecular genetics* 17(22), pp. 3474–86. doi: 10.1093/hmg/ddn240.
- Stork, T., Bernardos, R. and Freeman, M.R. 2012. Analysis of glial cell development and function in Drosophila. *Cold Spring Harbor protocols* 2012(1), pp. 1–17. doi: 10.1101/pdb.top067587.
- Stossel, T.P. 1973. Quantitative studies of phagocytosis. Kinetic effects of cations and heat-labile opsonin. *The Journal of Cell Biology* 58(2), pp. 346–356. Available at: https://europepmc.org/articles/PMC2109045 [Accessed: 26 May 2022].
- Straub, J. et al. 2020. Genetic interaction screen for severe neurodevelopmental disorders reveals a functional link between Ube3a and Mef2 in Drosophila melanogaster. *Scientific Reports* 10(1). doi: 10.1038/s41598-020-58182-5.
- Strittmatter, W.J., Saunders, A.M., Schmechel, D., Pericak-Vance, M., Enghild, J., Salvesen, G.S. and Roses, A.D. 1993. Apolipoprotein E: high-avidity binding to beta-amyloid and increased frequency of type 4 allele in late-onset familial Alzheimer disease. *Proceedings of the National Academy of Sciences of the United States of America* 90(5), pp. 1977–81. doi: 10.1073/pnas.90.5.1977.

- Su, T.T. 2019. Drug screening in Drosophila; why, when, and when not? *Wiley interdisciplinary reviews. Developmental biology* 8(6), p. e346. Available at: /pmc/articles/PMC6786905/ [Accessed: 22 June 2022].
- Sugimura, I. and Lilly, M.A. 2006. Bruno inhibits the expression of mitotic cyclins during the prophase I meiotic arrest of Drosophila oocytes. *Developmental cell* 10(1), pp. 127–35. Available at: http://www.ncbi.nlm.nih.gov/pubmed/16399084 [Accessed: 11 May 2019].
- Sullivan, K.M.C. and Rubin, G.M. 2002. The Ca(2+)-calmodulin-activated protein phosphatase calcineurin negatively regulates EGF receptor signaling in Drosophila development. *Genetics* 161(1), pp. 183–193. Available at: https://pubmed.ncbi.nlm.nih.gov/12019233/ [Accessed: 2 April 2022].
- Swanson, J.A. 2014. Phosphoinositides and engulfment. *Cellular Microbiology* 16(10), pp. 1473–1483. Available at: https://onlinelibrary.wiley.com/doi/full/10.1111/cmi.12334 [Accessed: 2 April 2022].
- Sweeney, M.D., Sagare, A.P. and Zlokovic, B. v. 2018. Blood–brain barrier breakdown in Alzheimer's disease and other neurodegenerative disorders. *Nature reviews. Neurology* 14(3), p. 133. Available at: /pmc/articles/PMC5829048/ [Accessed: 12 June 2022].
- T, M. et al. 2007. Expression of APP pathway mRNAs and proteins in Alzheimer's disease. *Brain research* 1161(1), pp. 116–123. Available at: https://pubmed.ncbi.nlm.nih.gov/17586478/ [Accessed: 13 July 2021].
- T, T., B, Z., JP, F. and H, K. 1991. In vitro effects of various cholinesterase inhibitors on acetyl- and butyrylcholinesterase of healthy volunteers. *Biochemical pharmacology* 41(1), pp. 139–141. Available at: https://pubmed.ncbi.nlm.nih.gov/1986738/ [Accessed: 25 July 2021].
- Tachida, Y. et al. 2008. Interleukin-1β up-regulates TACE to enhance α-cleavage of APP in neurons: Resulting decrease in Aβ production. *Journal of Neurochemistry* 104(5), pp. 1387–1393. doi: 10.1111/J.1471-4159.2007.05127.X.
- Takahashi, K., Rochford, C.D.P. and Neumann, H. 2005. Clearance of apoptotic neurons without inflammation by microglial triggering receptor expressed on myeloid cells-2. *The Journal of Experimental Medicine* 201(4), pp. 647–657.

Available at: http://www.jem.org/lookup/doi/10.1084/jem.20041611 [Accessed: 18 June 2019].

- Takalo, M. et al. 2020. The Alzheimer's disease-associated protective Plcγ2-P522R variant promotes immune functions. *Molecular Neurodegeneration* 15(1), pp. 1–14. Available at: https://molecularneurodegeneration.biomedcentral.com/articles/10.1186/s13024-020-00402-7 [Accessed: 16 June 2022].
- Takatori, S., Wang, W., Iguchi, A. and Tomita, T. 2019. Genetic Risk Factors for Alzheimer Disease: Emerging Roles of Microglia in Disease Pathomechanisms. In: *Advances in experimental medicine and biology*., pp. 83–116. Available at: http://www.ncbi.nlm.nih.gov/pubmed/30747419 [Accessed: 11 May 2019].
- Tan, M., Li, J., Ma, F., Zhang, X., Zhao, Q. and Cao, X. 2019. PLD3 rare variants identified in late-onset Alzheimer's disease affect amyloid-β levels in cellular model. *Frontiers in Neuroscience* 13(FEB), p. 116. doi: 10.3389/FNINS.2019.00116/BIBTEX.
- Tan, Z. and Boss, W.F. 1992. Association of Phosphatidylinositol Kinase, Phosphatidylinositol Monophosphate Kinase, and Diacylglycerol Kinase with the Cytoskeleton and F-Actin Fractions of Carrot (Daucus carota L.) Cells Grown in Suspension Culture : Response to Cell Wall-Degrading Enzymes. *Plant physiology* 100(4), pp. 2116–2120. Available at: https://pubmed.ncbi.nlm.nih.gov/16653250/ [Accessed: 10 May 2022].
- Tanikawa, S., Mori, F., Tanji, K., Kakita, A., Takahashi, H. and Wakabayashi, K. 2012. Endosomal sorting related protein CHMP2B is localized in Lewy bodies and glial cytoplasmic inclusions in α-synucleinopathy. *Neuroscience Letters* 527(1), pp. 16–21. doi: 10.1016/j.neulet.2012.08.035.
- Tansey, K.E., Cameron, D. and Hill, M.J. 2018. Genetic risk for Alzheimer's disease is concentrated in specific macrophage and microglial transcriptional networks. *Genome Medicine* 10(1), p. 14. Available at: http://www.ncbi.nlm.nih.gov/pubmed/29482603 [Accessed: 23 January 2019].
- Tasdemir-Yilmaz, O.E. and Freeman, M.R. 2014. Astrocytes engage unique molecular programs to engulf pruned neuronal debris from distinct subsets of neurons. *Genes & development* 28(1), pp. 20–33. doi: 10.1101/gad.229518.113.

- TCW, J. and Goate, A.M. 2017. Genetics of β-Amyloid Precursor Protein in Alzheimer's Disease. *Cold Spring Harbor Perspectives in Medicine* 7(6). Available at: /pmc/articles/PMC5453386/ [Accessed: 12 July 2021].
- Terry, R.D. et al. 1991. Physical basis of cognitive alterations in Alzheimer's disease: synapse loss is the major correlate of cognitive impairment. *Annals of neurology* 30(4), pp. 572–580. Available at: https://pubmed.ncbi.nlm.nih.gov/1789684/ [Accessed: 20 June 2022].
- Thackeray, J.R., Gaines, P.C.W., Ebert, P. and Carlson, J.R. 1998. small wing encodes a phospholipase C-(gamma) that acts as a negative regulator of R7 development in Drosophila. *Development (Cambridge, England)* 125(24), pp. 5033–5042. Available at: https://pubmed.ncbi.nlm.nih.gov/9811587/ [Accessed: 2 April 2022].
- Tito, A.J., Cheema, S., Jiang, M. and Zhang, S. 2016. A Simple One-step Dissection Protocol for Whole-mount Preparation of Adult Drosophila Brains. *Journal of Visualized Experiments : JoVE* 2016(118), p. 55128. Available at: /pmc/articles/PMC5226341/ [Accessed: 26 June 2022].
- Todt, J.C., Hu, B. and Curtis, J.L. 2004. The receptor tyrosine kinase MerTK activates phospholipase C γ2 during recognition of apoptotic thymocytes by murine macrophages. *Journal of Leukocyte Biology* 75(4), pp. 705–713. Available at: https://onlinelibrary.wiley.com/doi/full/10.1189/jlb.0903439 [Accessed: 25 July 2022].
- Tönnies, E. and Trushina, E. 2017. Oxidative Stress, Synaptic Dysfunction, and Alzheimer's Disease. *Journal of Alzheimer's Disease* 57(4), p. 1105. Available at: /pmc/articles/PMC5409043/ [Accessed: 25 July 2022].
- Tooley, U.A., Bassett, D.S. and Mackey, A.P. 2021. Environmental influences on the pace of brain development. *Nature Reviews Neuroscience 2021 22:6* 22(6), pp. 372–384. Available at: https://www.nature.com/articles/s41583-021-00457-5 [Accessed: 25 July 2022].
- Trapp, B.D., Nishiyama, A., Cheng, D. and Macklin, W. 1997. Differentiation and death of premyelinating oligodendrocytes in developing rodent brain. *The Journal of cell biology* 137(2), pp. 459–468. Available at: https://pubmed.ncbi.nlm.nih.gov/9128255/ [Accessed: 20 June 2022].

- Tridandapani, S., Lyden, T.W., Smith, J.L., Carter, J.E., Coggeshall, K.M. and Anderson, C.L. 2000. The adapter protein LAT enhances fcgamma receptor-mediated signal transduction in myeloid cells. *The Journal of biological chemistry* 275(27), pp. 20480–20487. Available at: https://pubmed.ncbi.nlm.nih.gov/10781611/ [Accessed: 10 May 2022].
- Tsai, A.P. et al. 2020. PLCG2 as a Risk Factor for Alzheimer's Disease. *bioRxiv* , p. 2020.05.19.104216. Available at: https://www.biorxiv.org/content/10.1101/2020.05.19.104216v1 [Accessed: 25 April 2022].
- Tsai, A.P. et al. 2022. PLCG2 is associated with the inflammatory response and is induced by amyloid plaques in Alzheimer's disease. *Genome Medicine* 14(1), pp. 1–13. Available at: https://genomemedicine.biomedcentral.com/articles/10.1186/s13073-022-01022-0 [Accessed: 13 April 2022].
- Turner, P.R., O'Connor, K., Tate, W.P. and Abraham, W.C. 2003. Roles of amyloid precursor protein and its fragments in regulating neural activity, plasticity and memory. *Progress in neurobiology* 70(1), pp. 1–32.
- Uddin, Md.S. et al. 2021. Molecular Genetics of Early- and Late-Onset Alzheimer's Disease. *Current gene therapy* 21(1), pp. 43–52. Available at: https://pubmed.ncbi.nlm.nih.gov/33231156/ [Accessed: 26 May 2022].
- Uffelmann, E. et al. 2021. Genome-wide association studies. *Nature Reviews Methods Primers 2021 1:1* 1(1), pp. 1–21. Available at: https://www.nature.com/articles/s43586-021-00056-9 [Accessed: 26 July 2022].
- v. DAVIES-COX, E., LAFFAFIAN, I. and B. HALLETT, M. 2001. Control of Ca2+ influx in human neutrophils by inositol 1,4,5-trisphosphate (IP3) binding: differential effects of micro-injected IP3 receptor antagonists. *Biochemical Journal* 355(Pt 1), p. 139. Available at: /pmc/articles/PMC1221721/ [Accessed: 26 May 2022].
- Vaqué, J.P. et al. 2014. PLCG1 mutations in cutaneous T-cell lymphomas. *Blood* 123(13), pp. 2034–2043. Available at: https://ashpublications.org/blood/article/123/13/2034/32600/PLCG1-mutations-in-cutaneous-T-cell-lymphomas [Accessed: 25 April 2022].

- Verfaillie, S.C.J. et al. 2015. Cerebral perfusion and glucose metabolism in Alzheimer's disease and frontotemporal dementia: two sides of the same coin? *European Radiology* 25(10), p. 3050. Available at: /pmc/articles/PMC4562004/ [Accessed: 25 July 2021].
- Verghese, P.B. et al. 2013. ApoE influences amyloid-β (Aβ) clearance despite minimal apoE/Aβ association in physiological conditions. *Proceedings of the National Academy of Sciences of the United States of America* 110(19). Available at: https://pubmed.ncbi.nlm.nih.gov/23620513/ [Accessed: 26 July 2022].
- Vermeulen, C.J. and Bijlsma, R. 2003. Changes in mortality patterns and temperature dependence of lifespan in Drosophila melanogaster caused by inbreeding. *Heredity 2004 92:4* 92(4), pp. 275–281. Available at: https://www.nature.com/articles/6800412 [Accessed: 25 March 2022].
- Vest, R.S. and Pike, C.J. 2013. Gender, sex steroid hormones, and Alzheimer's disease. *Hormones and behavior* 63(2), p. 301. Available at: /pmc/articles/PMC3413783/ [Accessed: 23 March 2022].
- Vieira, O. v. et al. 2001. Distinct roles of class I and class III phosphatidylinositol 3-kinases in phagosome formation and maturation. *The Journal of cell biology* 155(1), pp. 19–25. Available at: https://pubmed.ncbi.nlm.nih.gov/11581283/ [Accessed: 26 May 2022].
- Vilalta, A. and Brown, G.C. 2018. Neurophagy, the phagocytosis of live neurons and synapses by glia, contributes to brain development and disease. *The FEBS Journal* 285(19), pp. 3566–3575. Available at: http://doi.wiley.com/10.1111/febs.14323 [Accessed: 6 May 2019].
- von Bernhardi, R. 2007. Glial cell dysregulation: a new perspective on Alzheimer disease. *Neurotoxicity research* 12(4), pp. 215–32. Available at: http://www.ncbi.nlm.nih.gov/pubmed/18201950 [Accessed: 14 November 2018].
- von Stein, W., Ramrath, A., Grimm, A., Müller-Borg, M. and Wodarz, A. 2005. Direct association of Bazooka/PAR-3 with the lipid phosphatase PTEN reveals a link between the PAR/aPKC complex and phosphoinositide signaling. *Development (Cambridge, England)* 132(7), pp. 1675–1686. Available at: https://pubmed.ncbi.nlm.nih.gov/15743877/ [Accessed: 9 May 2022].

- Vosshall, L.B., Wong, A.M. and Axel, R. 2000. An olfactory sensory map in the fly brain. *Cell* 102(2), pp. 147–159. Available at: https://pubmed.ncbi.nlm.nih.gov/10943836/ [Accessed: 26 June 2022].
- Wakselman, S., Béchade, C., Roumier, A., Bernard, D., Triller, A. and Bessis, A. 2008. Developmental neuronal death in hippocampus requires the microglial CD11b integrin and DAP12 immunoreceptor. *The Journal of neuroscience : the official journal of the Society for Neuroscience* 28(32), pp. 8138–8143. Available at: https://pubmed.ncbi.nlm.nih.gov/18685038/ [Accessed: 20 June 2022].
- Waldemar, G. et al. 2007. Recommendations for the diagnosis and management of Alzheimer's disease and other disorders associated with dementia: EFNS guideline. *European journal of neurology* 14(1). Available at: https://pubmed.ncbi.nlm.nih.gov/17222085/ [Accessed: 7 June 2022].
- Walker, L.C. and Jucker, M. 2015. Neurodegenerative diseases: expanding the prion concept. *Annual review of neuroscience* 38, pp. 87–103. Available at: https://pubmed.ncbi.nlm.nih.gov/25840008/ [Accessed: 26 July 2022].
- Wang, C. et al. 2015a. Common Variants in PLD3 and Correlation to Amyloid-Related Phenotypes in Alzheimer's Disease. *Journal of Alzheimer's disease : JAD* 46(2), p. 491. Available at: /pmc/articles/PMC6312181/ [Accessed: 2 April 2022].
- Wang, M.-M., Miao, D., Cao, X.-P., Tan, L. and Tan, L. 2018. Innate immune activation in Alzheimer's disease. *Annals of Translational Medicine* 6(10), pp. 177–177. Available at: /pmc/articles/PMC5994517/ [Accessed: 13 June 2022].
- Wang, S. et al. 2020. Anti-human TREM2 induces microglia proliferation and reduces pathology in an Alzheimer's disease model. *The Journal of experimental medicine* 217(9). Available at: https://pubmed.ncbi.nlm.nih.gov/32579671/ [Accessed: 15 June 2022].
- Wang, S.H., Simcox, A. and Campbell, G. 2000. Dual role for Drosophila epidermal growth factor receptor signaling in early wing disc development. *Genes & Development* 14(18), p. 2271. Available at: /pmc/articles/PMC316934/ [Accessed: 13 July 2022].
- Wang, W.Y., Tan, M.S., Yu, J.T. and Tan, L. 2015b. Role of pro-inflammatory cytokines released from microglia in Alzheimer's disease. *Annals of translational*

*medicine* 3(10). Available at: https://pubmed.ncbi.nlm.nih.gov/26207229/ [Accessed: 15 June 2022].

- Wang, Y. et al. 2015c. TREM2 lipid sensing sustains the microglial response in an Alzheimer's disease model. *Cell* 160(6), pp. 1061–1071. Available at: https://pubmed.ncbi.nlm.nih.gov/25728668/ [Accessed: 15 June 2022].
- Wang, Y. and Mandelkow, E. 2015. Tau in physiology and pathology. *Nature Reviews Neuroscience 2015 17:1* 17(1), pp. 22–35. Available at: https://www.nature.com/articles/nrn.2015.1 [Accessed: 13 July 2021].
- Waring, S.C. and Rosenberg, R.N. 2008. Genome-Wide Association Studies in Alzheimer Disease. *Archives of Neurology* 65(3), pp. 329–34. Available at: http://www.ncbi.nlm.nih.gov/pubmed/18332245 [Accessed: 7 May 2019].
- Watanabe, K., Taskesen, E., van Bochoven, A. and Posthuma, D. 2017. Functional mapping and annotation of genetic associations with FUMA. *Nature Communications 2017 8:1* 8(1), pp. 1–11. Available at: https://www.nature.com/articles/s41467-017-01261-5 [Accessed: 26 July 2022].
- Watson, C.T. et al. 2016. Genome-wide DNA methylation profiling in the superior temporal gyrus reveals epigenetic signatures associated with Alzheimer's disease. *Genome medicine* 8(1). Available at: https://pubmed.ncbi.nlm.nih.gov/26803900/ [Accessed: 12 June 2022].
- Watson, D. et al. 2005. Physicochemical characteristics of soluble oligomeric Abeta and their pathologic role in Alzheimer's disease. *Neurological research* 27(8), pp. 869–881. Available at: https://pubmed.ncbi.nlm.nih.gov/16354549/ [Accessed: 26 May 2022].
- Weavers, H., Evans, I.R., Martin, P. and Wood, W. 2016. Corpse Engulfment Generates a Molecular Memory that Primes the Macrophage Inflammatory Response. *Cell* 165(7), pp. 1658–1671. Available at: https://pubmed.ncbi.nlm.nih.gov/27212238/ [Accessed: 26 May 2022].
- Weavers, H., Wood, W. and Martin, P. 2019. Injury Activates a Dynamic Cytoprotective Network to Confer Stress Resilience and Drive Repair. *Current Biology* 29(22), p. 3851. Available at: /pmc/articles/PMC6868510/ [Accessed: 26 July 2022].
- Whitelaw, B.S. 2018. Microglia-mediated synaptic elimination in neuronal development and disease. *Journal of Neurophysiology* 119(1), pp. 1–4. Available

at: https://www.physiology.org/doi/10.1152/jn.00021.2017 [Accessed: 5 December 2018].

- Wilcock, D.M. et al. 2008. Progression of amyloid pathology to Alzheimer's disease pathology in an amyloid precursor protein transgenic mouse model by removal of nitric oxide synthase 2. *The Journal of neuroscience : the official journal of the Society for Neuroscience* 28(7), pp. 1537–1545. Available at: https://pubmed.ncbi.nlm.nih.gov/18272675/ [Accessed: 22 June 2022].
- Williamson, A.P. and Vale, R.D. 2018. Spatial control of Draper receptor signaling initiates apoptotic cell engulfment. *The Journal of Cell Biology* 217(11), p. 3977. Available at: /pmc/articles/PMC6219719/ [Accessed: 10 May 2022].
- Wittmann, C.W., Wszolek, M.F., Shulman, J.M., Salvaterra, P.M., Lewis, J., Hutton, M. and Feany, M.B. 2001. Tauopathy in Drosophila: Neurodegeneration Without Neurofibrillary Tangles. *Science* 293(5530), pp. 711–714. doi: 10.1126/science.1062382.
- Wong, S.H., Robbins, P.D., Knuckey, N.W. and Kermode, A.G. 2006. Cerebral amyloid angiopathy presenting with vasculitic pathology. *Journal of Clinical Neuroscience* 13(2), pp. 291–294. doi: 10.1016/J.JOCN.2005.03.025.
- Wood, W. and Jacinto, A. 2007. Drosophila melanogaster embryonic haemocytes: masters of multitasking. *Nature Reviews Molecular Cell Biology 2007 8:7* 8(7), pp. 542–551. Available at: https://www.nature.com/articles/nrm2202 [Accessed: 13 April 2022].
- Woodward, M. 2013. Aspects of communication in Alzheimer's disease: clinical features and treatment options. *International Psychogeriatrics* 25(6), pp. 877–885. Available at: https://www.cambridge.org/core/journals/international-psychogeriatrics/article/abs/aspects-of-communication-in-alzheimers-disease-clinical-features-and-treatment-options/9335C41F99EB4869158D86EBE0242902 [Accessed: 7 June 2022].
- *World Alzheimer Report 2015* | *Alzheimer's Disease International (ADI)* [no date]. Available at: https://www.alzint.org/resource/world-alzheimer-report-2015/ [Accessed: 6 June 2022].
- *World Alzheimer Report 2021* | *Alzheimer's Disease International (ADI)* [no date]. Available at: https://www.alzint.org/resource/world-alzheimer-report-2021/ [Accessed: 6 June 2022].

- Worth, R.G., Kim, M.K., Kindzelskii, A.L., Petty, H.R. and Schreiber, A.D. 2003. Signal sequence within FcγRIIA controls calcium wave propagation patterns: Apparent role in phagolysosome fusion. *Proceedings of the National Academy of Sciences of the United States of America* 100(8), pp. 4533–4538. Available at: www.pnas.orgcgidoi10.1073pnas.0836650100 [Accessed: 26 May 2022].
- Wu, J.S. and Luo, L. 2006. A protocol for dissecting Drosophila melanogaster brains for live imaging or immunostaining. *Nature protocols* 1(4), pp. 2110–2115. Available at: https://pubmed.ncbi.nlm.nih.gov/17487202/ [Accessed: 26 June 2022].
- Wyss-Coray, T. and Mucke, L. 2002. Inflammation in neurodegenerative disease--a double-edged sword. *Neuron* 35(3), pp. 419–432. Available at: https://pubmed.ncbi.nlm.nih.gov/12165466/ [Accessed: 22 June 2022].
- Xi, Z., Gavotte, L., Xie, Y. and Dobson, S.L. 2008. Genome-wide analysis of the interaction between the endosymbiotic bacterium Wolbachia and its Drosophila host. *BMC Genomics* 9. Available at: https://pubmed.ncbi.nlm.nih.gov/18171476/ [Accessed: 6 May 2021].
- Xie, Y., Li, J., Kang, R. and Tang, D. 2020. Interplay Between Lipid Metabolism and Autophagy. *Frontiers in Cell and Developmental Biology* 8, p. 431. doi: 10.3389/FCELL.2020.00431/BIBTEX.
- Xin, T., Xuan, T., Tan, J., Li, M., Zhao, G. and Li, M. 2013. The Drosophila putative histone acetyltransferase Enok maintains female germline stem cells through regulating Bruno and the niche. *Developmental Biology* 384(1), pp. 1–12. Available at: https://www.sciencedirect.com/science/article/pii/S0012160613005320?via%3Dihub [Accessed: 11 May 2019].
- Xiong, W.C., Okano, H., Patel, N.H., Blendy, J.A. and Montell, C. 1994. repo encodes a glial-specific homeo domain protein required in the Drosophila nervous system. *Genes & development* 8(8), pp. 981–994. Available at: https://pubmed.ncbi.nlm.nih.gov/7926782/ [Accessed: 25 March 2022].
- Xu, H.J. et al. 2015. Two insulin receptors determine alternative wing morphs in planthoppers. *Nature* 519(7544), pp. 464–467. Available at: https://pubmed.ncbi.nlm.nih.gov/25799997/ [Accessed: 9 May 2022].

- Yagi, T. et al. 2011. Modeling familial Alzheimer's disease with induced pluripotent stem cells. *Human molecular genetics* 20(23), pp. 4530–4539. Available at: https://pubmed.ncbi.nlm.nih.gov/21900357/ [Accessed: 22 June 2022].
- Yamamoto, K., Pardee, J.D., Reidler, J., Stryer, L. and Spudich, J.A. 1982. Mechanism of interaction of Dictyostelium severin with actin filaments. *The Journal of cell biology* 95(3), pp. 711–719. Available at: https://pubmed.ncbi.nlm.nih.gov/6897549/ [Accessed: 10 May 2022].
- Yang, F., Uéda, K., Chen, P.P., Ashe, K.H. and Cole, G.M. 2000. Plaque-associated alpha-synuclein (NACP) pathology in aged transgenic mice expressing amyloid precursor protein. *Brain research* 853(2), pp. 381–383. Available at: https://pubmed.ncbi.nlm.nih.gov/10640638/ [Accessed: 22 June 2022].
- Yasojima, K., Schwab, C., McGeer, E.G. and McGeer, P.L. 1999. Up-regulated production and activation of the complement system in Alzheimer's disease brain. *The American journal of pathology* 154(3), pp. 927–936. Available at: https://pubmed.ncbi.nlm.nih.gov/10079271/ [Accessed: 20 June 2022].
- Yeh, F.L., Wang, Y., Tom, I., Gonzalez, L.C. and Sheng, M. 2016. TREM2 Binds to Apolipoproteins, Including APOE and CLU/APOJ, and Thereby Facilitates Uptake of Amyloid-Beta by Microglia. *Neuron* 91(2), pp. 328–340. Available at: https://pubmed.ncbi.nlm.nih.gov/27477018/ [Accessed: 20 June 2022].
- Yesavage, J.A., Brooks, J.O., Taylor, J. and Tinklenberg, J. 1993. Development of aphasia, apraxia, and agnosia and decline in Alzheimer's disease. *The American journal of psychiatry* 150(5), pp. 742–747. Available at: https://pubmed.ncbi.nlm.nih.gov/8480819/ [Accessed: 7 June 2022].
- Yiannopoulou, K.G. and Papageorgiou, S.G. 2020. Current and Future Treatments in Alzheimer Disease: An Update. *Journal of Central Nervous System Disease* 12, p. 117957352090739. Available at: /pmc/articles/PMC7050025/ [Accessed: 4 July 2022].
- Younan, N.D., Chen, K.-F., Rose, R.-S., Crowther, D.C. and Viles, J.H. 2018. Prion protein stabilizes amyloid-β (Aβ) oligomers and enhances Aβ neurotoxicity in a *Drosophila* model of Alzheimer's disease. *Journal of Biological Chemistry* 293(34), pp. 13090–13099. doi: 10.1074/jbc.RA118.003319.

- Zeisel, A. et al. 2015. Brain structure. Cell types in the mouse cortex and hippocampus revealed by single-cell RNA-seq. *Science (New York, N.Y.)* 347(6226), pp. 1138–1142. Available at: https://pubmed.ncbi.nlm.nih.gov/25700174/ [Accessed: 26 July 2022].
- Zhang, D.F., Fan, Y., Wang, D., Bi, R., Zhang, C., Fang, Y. and Yao, Y.G. 2016a. PLD3 in Alzheimer's Disease: a Modest Effect as Revealed by Updated Association and Expression Analyses. *Molecular neurobiology* 53(6), pp. 4034–4045. Available at: https://pubmed.ncbi.nlm.nih.gov/26189833/ [Accessed: 2 April 2022].
- Zhang, J., Chen, S., Zhang, S., Lu, Z., Yang, H. and Wang, H. 2009. [Over-expression of phospholipase D3 inhibits Akt phosphorylation in C2C12 myoblasts]. *Sheng wu Gong Cheng xue bao = Chinese Journal of Biotechnology* 25(10), pp. 1524–1531. Available at: https://europepmc.org/article/med/20112697 [Accessed: 25 April 2022].
- Zhang, M.S. et al. 2022. Hypoxia-induced macropinocytosis represents a metabolic route for liver cancer. *Nature Communications 2022 13:1* 13(1), pp. 1–19. Available at: https://www.nature.com/articles/s41467-022-28618-9 [Accessed: 25 July 2022].
- Zhang, Q.Y. et al. 2016b. FERMT2 rs17125944 polymorphism with Alzheimer's disease risk: A replication and meta-analysis. *Oncotarget* 7(26), pp. 39044–39050. doi: 10.18632/oncotarget.9679.
- Zhang, Y. et al. 2016c. Purification and Characterization of Progenitor and Mature Human Astrocytes Reveals Transcriptional and Functional Differences with Mouse. *Neuron* 89(1), pp. 37–53. Available at: https://pubmed.ncbi.nlm.nih.gov/26687838/ [Accessed: 2 April 2022].
- Zhao, N., Liu, C.C., Qiao, W. and Bu, G. 2018. Apolipoprotein E, Receptors, and Modulation of Alzheimer's Disease. *Biological psychiatry* 83(4), pp. 347–357. Available at: https://pubmed.ncbi.nlm.nih.gov/28434655/ [Accessed: 21 June 2022].
- Zhao, T. et al. 2013. Kindlin-2 promotes genome instability in breast cancer cells. *Cancer Letters* 330(2), pp. 208–216. doi: 10.1016/j.canlet.2012.11.043.

- Zhao, T., Hu, Y., Zang, T. and Wang, Y. 2019. Integrate GWAS, eQTL, and mQTL Data to Identify Alzheimer's Disease-Related Genes. *Frontiers in Genetics* 10, p. 1021. Available at: www.frontiersin.org [Accessed: 13 May 2021].
- Zhao, Z. et al. 2015. Central role for PICALM in amyloid-β blood-brain barrier transcytosis and clearance. *Nature neuroscience* 18(7), pp. 978–987. Available at: https://pubmed.ncbi.nlm.nih.gov/26005850/ [Accessed: 26 July 2022].
- Zheng, H. and Koo, E.H. 2006. The amyloid precursor protein: beyond amyloid. *Molecular Neurodegeneration* 1(1), p. 5. Available at: /pmc/articles/PMC1538601/ [Accessed: 13 July 2021].
- Zheng, Q., Ma, A.Y., Yuan, L., Gao, N., Feng, Q., Franc, N.C. and Xiao, H. 2017. Apoptotic cell clearance in Drosophila melanogaster. *Frontiers in Immunology* 8(DEC), p. 1881. doi: 10.3389/FIMMU.2017.01881/BIBTEX.
- Zhou, Z., Hartwieg, E. and Horvitz, H.R. 2001. CED-1 is a transmembrane receptor that mediates cell corpse engulfment in C. elegans. *Cell* 104(1), pp. 43–56. Available at: https://pubmed.ncbi.nlm.nih.gov/11163239/ [Accessed: 21 June 2022].
- Zhu, X.C., Dai, W.Z. and Ma, T. 2020. Impacts of CR1 genetic variants on cerebrospinal fluid and neuroimaging biomarkers in alzheimer's disease. *BMC Medical Genetics* 21(1), pp. 1–8. Available at: https://bmcmedgenet.biomedcentral.com/articles/10.1186/s12881-020-01114-x [Accessed: 20 June 2022].
- Ziegenfuss, J.S. et al. 2008. Draper-dependent glial phagocytic activity is mediated by Src and Syk family kinase signalling. *Nature* 453(7197), pp. 935–939. Available at: http://www.nature.com/articles/nature06901 [Accessed: 5 October 2018].
- Ziegenfuss, J.S., Doherty, J. and Freeman, M.R. 2012. Distinct molecular pathways mediate glial activation and engulfment of axonal debris after axotomy. *Nature neuroscience* 15(7), p. 979. Available at: /pmc/articles/PMC4976689/ [Accessed: 2 April 2022].
- Zou, W., Reeve, J.L., Liu, Y., Teitelbaum, S.L. and Ross, F.P. 2008. DAP12 couples c-Fms activation to the osteoclast cytoskeleton by recruitment of Syk. *Molecular cell* 31(3), pp. 422–431. Available at: https://pubmed.ncbi.nlm.nih.gov/18691974/ [Accessed: 21 June 2022].

– Zumerle, S., Calì, B., Munari, F., Angioni, R., di Virgilio, F., Molon, B. and Viola, A. 2019. Intercellular Calcium Signaling Induced by ATP Potentiates Macrophage Phagocytosis. *Cell Reports* 27(1), pp. 1-10.e4. doi: 10.1016/J.CELREP.2019.03.011.